



Going with the flow: Assessing
the impact of a milli-fluidic
flow-through system and
probiotic bacteria on intestinal
cell lines

PhD (Doctor of Philosophy)

2021

Kyle Robert Murphy

Summary

When attempting to model the human gut, cell culture research has traditionally employed a reductionist approach to encapsulate the nuanced behaviours of these cells *in situ*. However, as these studies almost exclusively employ static cell culture methodologies, the biological relevance of such research could be disputed, as many of the complex factors that influence the gut's behaviour and responsiveness to external stimuli are omitted. From host-microbial interactions to dynamic flow, such factors are omnipresent within the gut and, in the case of the host microbiome, have been historically proven to induce considerable behavioural changes. This thesis aims to examine the impact of both dynamic flow – which is regularly absent from cell culture studies – and bacteria, specifically probiotics, on four intestinal cell lines used commonly within cell culture studies.

By introducing a dynamic flow element to cell culture via the Kirkstall Quasi Vivo® QV500 milli-fluidic flow-through system, it was hypothesised that an alteration in cellular behaviour would be observed, although whether such changes would pose a positive or negative influence remained unknown. Following verification of any observed behavioural changes, bacteria – both probiotic and pathogenic – were introduced to the QV500 to enable co-exposure of flow and bacteria to cell lines.

Ultimately, this study has concluded that the presence of dynamic flow and the co-culturing of cell lines with both flow and bacteria is beneficial for improving current gut methodologies. While this study has provided a preliminary insight into the importance of flow in modelling the production of pro-inflammatory cytokines from human cells to bacterial stimuli, further research is required to optimise flow systems for application in wider studies and to overcome the limitations of systems such as the QV500, as this study has proposed that flow may be invaluable in furthering the current understanding surrounding the gut and its essential factors.

Contents

Summary	i
List of figures.....	ix
List of tables	xii
List of abbreviations.....	xiii
Acknowledgements.....	xv
1 Introduction	1
1.1 Cell culture within research	2
1.1.1 Animal modelling and their role in modelling methodologies	3
1.1.2 The use of cell culture models as “models” of the human gut epithelium	5
1.1.2.1 The physiology of the gut.....	7
1.1.2.2 Biological parameters of the gut.....	8
1.1.2.2.1 The microbiome.....	9
1.1.2.2.2 The mucus layer of the gut	11
1.1.2.2.2.1 Transmembrane mucins	11
1.1.2.2.2.2 Gel-forming mucins	12
1.1.2.2.2.3 Using cell culture to assess mucin production	12
1.1.2.2.3 pH of the gut.....	13
1.1.2.2.4 The inflammatory response of the gut.....	14
1.1.3 The intrinsic benefits of cell culture	15
1.1.4 The limitations present within cell culture research	16
1.1.4.1 The emergence of 3D cell culture and its utility as an <i>in situ</i> -like model	17
1.2 What is 3D cell culture?	18
1.2.1 Parameters that are used in 3D culture and example systems for incorporating them	19
1.2.1.1 Hypoxia within cell culture.....	19
1.2.1.2 Biological pressure within the gut and its application <i>in vitro</i>	20
1.2.1.3 Flow within the gut	21
1.2.1.3.1 Fluidic systems.....	21
1.2.1.3.2 Currently employed fluidic systems	22
1.2.1.3.3 The current limitations of 3D fluidic culture	23
1.2.2 The required parameters for emulating the gut <i>in vitro</i>	24
1.3 Probiotics and their use in cell culture studies	25
1.3.1 Commonly used probiotic strains in research	26

1.3.2	Lactic acid bacteria and the Lab4 probiotic consortia	27
1.4	General aims of the study	28
2	Materials and methods.....	30
2.1	Human gut epithelial cell lines selected for the study.....	30
2.2	Cell culture maintenance	31
2.2.1	Medium preparation and selection	31
2.2.2	Cultivating human cells from frozen stock	31
2.3	Initialising the JuLI™ Br system	32
2.3.1	Measuring the percentage confluence of a sample	33
2.3.2	Live cell monitoring using the JuLI™ Br.....	33
2.4	Maintaining and preserving cell samples.....	33
2.4.1	Continued maintenance of cell lines via sub-culturing.....	34
2.5	Using and maintaining the Muse® cell analyser apparatus	35
2.6	Preparing cells for use in experiments.....	36
2.6.1	Analysing cellular viability and cell health using the Muse® cell analyser	36
2.6.2	Seeding coverslips with intestinal cell lines.....	37
2.7	Processing and assembly of the Kirkstall QV500 system	38
2.7.1	Components of the QV500 system and pre-processing required prior to assembly	38
2.7.2	Assembling the QV500 system	39
2.7.3	Calibrating the QV500 system flow rates and synchronising systems for future experiments	41
2.7.4	Preparing the QV500 system for experiments	42
2.7.5	Maintaining the QV500 systems.....	43
2.8	Experimental setup	43
2.9	Measuring cellular proliferation as a proxy of cellular viability via Tetrazolium 3-(4,5-dimethylthiazol-2-yl)-2,5-diphenyltetrazolium bromide (MTT) assay	44
2.10	Measuring cellular viability via the LDH-Glo™ assay.....	45
2.10.1	Preparing reagents.....	45
2.10.2	Collecting and preparing cell culture medium for LDH analysis.....	45
2.10.3	LDH assay protocol.....	46
2.11	Image formatting.....	46
2.12	Statistical analysis software.....	46

3	Exploring the incorporation of the QV500 dynamic flow-through system in cell culture research	48
3.1	Introduction.....	48
3.1.1	Exploring the introduction of a dynamic flow as an essential component in cell culture practices	48
3.1.2	Utilising the QV500 to introduce flow to cell culture	49
3.1.3	The aims of the chapter	50
3.2	Materials and methods	50
3.2.1	Cells utilised for experiments	50
3.2.1.1	Monitoring cell growth rates on glass and plastic coverslips	50
3.2.1.2	Cellular adherence on coverslips exposed to dynamic flow	52
3.2.1.3	Assessing the production of pro-inflammatory cytokine IL-8 and the cellular proliferation of HT29MTX cells under serum-starved and serum-supplemented conditions	53
3.2.1.3.1	Formulating serum-supplemented and serum-free media.....	53
3.2.1.3.2	Assessing HT29MTX under various serum exposure conditions.....	54
3.2.2	MTT analysis of cells exposed to periods of dynamic flow.....	54
3.2.3	LDH analysis of cells exposed to dynamic flow.....	55
3.2.3.1	Alcian blue glycoprotein assay	55
3.2.3.1.1	Preparing cells for alcian blue staining.....	55
3.2.3.1.2	Assessing stain exposure duration	56
3.2.3.1.3	Optimising alcian blue stain release.....	56
3.2.3.1.4	Attempting to develop a standard curve methodology for the alcian blue glycoprotein production assay.....	57
3.2.3.1.5	Finalised alcian blue glycoprotein assay.....	58
3.2.3.2	Measuring glycoprotein production via alcian blue (absorbance measurement).....	59
3.2.3.3	Assessing the production of glycoproteins via light microscopy	60
3.2.3.3.1	Visualising glycoprotein via microscopy	61
3.2.3.3.2	Extracting RNA from experimental samples for qPCR analysis.....	61
3.2.3.3.3	Measuring RNA concentration using the Qubit™ 3.0 fluorometer	62
3.2.3.3.4	cDNA synthesis	63
3.2.3.3.5	Identifying primers for MUC qPCR analysis.....	63
3.2.3.3.6	RT-qPCR protocol.....	64
3.3	Results	65

3.3.1	Cellular adherence and growth rates of cell lines Caco-2 and HT29MTX on solid substrates.....	65
3.3.2	Identifying the optimal media formulation and the impact of FBS in prolonged experimental exposure via MTT assay.....	68
3.3.3	Measuring the cellular proliferation of intestinal cell lines following exposure to dynamic flow via MTT assay.....	71
3.3.4	Measuring cellular viability of cell lines exposed to dynamic flow via LDH Glo™ cytotoxicity assay.....	74
3.3.5	Developing a qAlcian blue standard curve.....	77
3.3.6	Measuring the production of glycoprotein by intestinal cells via qAlcian blue analysis following exposure to dynamic flow.....	77
3.3.7	Glycoprotein production in HT29MTX cells monitored via light microscopy....	80
3.3.8	MUC gene expression in cell lines exposed to a trio of experimental conditions	81
3.4	Discussion.....	83
4	Exploring the use of bacteria-conditioned medium and live bacterial cells within a dynamic flow cell culture system.....	89
4.1	Introduction.....	89
4.1.1	The impact of probiotics on immortalised cell lines.....	89
4.1.2	The importance of cytokines within the gut.....	90
4.1.3	Cell lines and their known response to pro-inflammatory stimuli.....	92
4.1.4	Concepts of interest.....	93
4.1.5	The aims of the chapter.....	94
4.2	Materials and methods.....	94
4.2.1	The Lab4 and Lab4B bacterial communities.....	94
4.2.2	Establishing active cultures of <i>Escherichia coli</i> strains.....	95
4.2.3	Medium and agar selected for bacterial growth and maintenance.....	96
4.2.4	Reviving bacterial cultures from frozen stocks.....	96
4.2.5	Maintaining bacterial cultures throughout the study.....	97
4.2.6	Generating anaerobic media for probiotic growth.....	97
4.2.6.1	Generating growth curves for Lab4 and Lab4B probiotic bacteria and for <i>E. coli</i> strains E69, MP1 and Nissle 1917.....	98
4.2.7	Generating conditioned media using Lab4, Lab4B and <i>E. coli</i>	99
4.2.8	Identifying the impact of probiotics and pathogenic <i>E. coli</i> E69 on intestinal cell lines under flow.....	100

4.2.8.1	Establishing cell lines.....	100
4.2.8.2	Optimising the Lab4 and Lab4B probiotic consortia for direct cellular exposure	101
4.2.8.2.1	<i>E. coli</i> exposure optimisation assay.....	102
4.2.8.3	Cell infection protocol using <i>E. coli</i> strain E69.....	102
4.2.9	Understanding the impact of flow on the pH of cell culture medium with no additives or cells	103
4.2.9.1	Metabolite profiling bacteria-only pH analysis medium	104
4.2.9.2	Assessing the impact of pH on cellular viability via the LDH assay.....	104
4.2.9.3	Preparing endotoxins for cellular exposure.....	105
4.2.10	Utilising ELISA to detect the pro-inflammatory markers IL-8, RANTES and TNF- α	105
4.2.10.1	Collecting growth medium samples for ELISA-based analyses.....	105
4.2.10.2	Preparing ELISA reagents	106
4.2.10.3	ELISA protocols for measuring the production of IL-8, RANTES and TNF- α	106
4.2.11	RT-qPCR protocol for cellular IL-8 production following exposure to Lab4- and Lab4B-conditioned medium.....	108
4.2.12	Statistical analysis	110
4.3	Results	110
4.3.1	Probiotic bacterial growth curves.....	110
4.3.2	<i>E. coli</i> growth curves	111
4.3.3	Cellular proliferation of cell lines Caco-2 and HT29MTX following a 48-hour exposure to Lab4- and Lab4B-conditioned medium	112
4.3.3.1	Glycoprotein production observed in Caco-2 and HT29MTX samples following exposure to Lab4- and Lab4B-conditioned medium	114
4.3.4	The impact of flow on the pH of cell culture medium supplemented with Lab4 and Lab4B live bacteria.....	115
4.3.5	Assessing the impact of pH on cellular viability via LDH assay.....	118
4.3.5.1	Monitoring the LDH production of Caco-2 cells exposed to pH adjusted medium	118
4.3.5.2	Monitoring the LDH production of HT29MTX cells exposed to pH adjusted medium	119
4.3.6	The impact of dynamic flow on the production of pro-inflammatory cytokines and chemokines	123
4.3.6.1	Monitoring the production of IL-8, RANTES and TNF- α in Caco-2 cells stimulated with Lab4 and Lab4B.....	125

4.3.6.2	Monitoring the production of IL-8, RANTES and TNF- α in HT29MTX cells stimulated with Lab4 and Lab4B.....	126
4.3.6.3	The impact of <i>E. coli</i> strains E69, MP1 and Nissle 1917 on the production of pro-inflammatory cytokines	130
4.3.6.3.1	The impact of <i>E.coli</i> exposure on the production of IL-8 and RANTES in Caco-2 cultures	130
4.3.6.3.2	The impact of <i>E.coli</i> exposure on the production of IL-8, RANTES and TNF- α in HT29MTX cultures	131
4.3.6.4	Modelling the prophylactic effect of probiotic communities Lab4 and Lab4B in response to bacterial endotoxin alone and in the presence of a gastrointestinal pathogen	135
4.3.6.4.1	Assessing the role of LPS and LTA in the stimulation of pro-inflammatory cytokines	135
4.3.6.4.2	Pre-treatment of cell lines with the Lab4 and Lab4B probiotics and the subsequent effect on the response to the bacterial endotoxin LPS	135
4.3.6.5	Pre-treatment and post-pathogen exposure of Caco-2 cells to Lab4 and Lab4B probiotics and the impact on the production of IL-8.....	138
4.3.6.6	Pre-treatment and post-pathogen exposure of HT29MTX to Lab4 and Lab4B probiotics and the impact on the production of IL-8	138
4.3.6.7	RT-qPCR analysis of cytokine IL-8 in HT29MTX cells exposed to varying concentrations of probiotic conditioned medium.....	147
4.4	Discussion.....	150
5	Metabolite analysis of probiotic and pathogenic bacteria-conditioned media	158
5.1	Introduction.....	158
5.1.1	The importance of bacterial metabolites	158
5.1.2	Understanding the impact of growth medium on the metabolic profiles of the Lab4 and Lab4B probiotic consortia	160
5.1.3	The aims of the chapter	162
5.2	Materials and methods	162
5.2.1	Preparing conditioned medium	162
5.2.2	Nuclear magnetic resonance (NMR) analysis of conditioned medium for metabolite identification	163
5.2.2.1	Preparing samples for NMR analysis.....	163
5.2.2.2	Identification of metabolites in conditioned medium samples via multivariate analysis and the use of metabolite identification software	164
5.2.3	Analysis of Lab4- and Lab4B-conditioned medium metabolite profiles in four distinct cell culture media.....	164

5.2.4	Metabolite presence-absence analysis and function identification in Lab4 and Lab4B consortia-conditioned, single-species-conditioned and <i>E. coli</i> -conditioned medium	165
5.2.4.1	Metabolite presence-absence analysis	165
5.2.4.2	Identifying metabolite functions, and metabolic pathways influenced	165
5.2.5	Data visualisation	166
5.3	Results	167
5.3.1	The importance of medium selection in the production of bacterial metabolites in conditioned medium assays	167
5.3.1.1	Metabolite variations in Lab4-conditioned cell culture media	167
5.3.1.2	Metabolite variations in Lab4B-conditioned cell culture media	167
5.3.2	Impact of glucose levels on metabolite production in conditioned media	171
5.3.3	Bacterial metabolite composition following growth in MRS and high glucose DMEM	171
5.3.4	Metabolite production in single-species- and dual-species-conditioned medium	174
5.3.5	Metabolic analysis of enteropathogenic <i>E. coli</i> E69-conditioned media generated using both LB broth and high glucose DMEM	176
5.3.6	The metabolic pathways influenced by the Lab4 and Lab4B probiotics and the pathogenic <i>E. coli</i> EPEC E69	177
5.4	Discussion	178
6	General discussion	184
6.1	Future work	189
6.2	Conclusion	190
	References	192
	Appendices	211

List of figures

Figure 1-1: Total publications with research focusing on 3D cell culture between the years 2000 and 2020	19
Figure 2-1: Assembled QV500 system attached to a twin mechanism pump.....	40
Figure 2-2: Example calibration curve for a single QV500 system generated from three experimental cycles	42
Figure 3-1: Schematic of an assembled QV500 chamber with cell-seeded coverslips	53
Figure 3-2: Absorbance scan of alcian blue in 96-well plate for method optimisation	59
Figure 3-3: Caco-2 and HT29MTX growth on plastic and glass coverslips over a 48 hour period.....	67
Figure 3-4: Assessing the impact of serum on the cellular proliferation of HT29MTX cells via MTT assay.....	70
Figure 3-5: Cellular proliferation of intestinal cell lines following periods of exposure to increased medium volume and a physiological flow element.	73
Figure 3-6: LDH production in HT29MTX cells following experimental exposure to flow and static conditions.....	75
Figure 3-7: LDH production in Caco-2 cells following experimental exposure to flow and static conditions.....	76
Figure 3-8: Glycoprotein production in cell lines following exposure to flow and static conditions for 48 hours measured via the qAlcian blue methodology	79
Figure 3-9: Monitoring the production of glycoproteins in the cell line HT29MTX via alcian blue and nuclear fast red staining and subsequent microscopy	80
Figure 3-10: qPCR analysis on MUC gene expression in HT29MTX cell lines following exposure to dynamic flow and static conditions	82
Figure 4-1: Cellular proliferation of HT29MTX and Caco-2 cells following 48-hour exposure to various concentrations of probiotic-conditioned media via MTT assay	113
Figure 4-2: Glycoprotein production in cell lines Caco-2 and HT29MTX following 48-hour exposure to Lab4 and Lab4B probiotic-conditioned media, measured via the qAlcian blue assay.....	116
Figure 4-3: The impact of flow on the pH of media supplemented with Lab4 an Lab4B products	117

Figure 4-4: LDH production in Caco-2 cells exposed to static and flow conditions at pH 6.5, 7.0 and 7.4 monitored over a 48-hour period	121
Figure 4-5: LDH production in HT29MTX cells exposed to static and flow conditions at pH 6.5, 7.0 and 7.4 monitored over a 48-hour period	122
Figure 4-6: Monitoring the inflammatory response of Caco-2 and HT29MTX following exposure to static and flow conditions.....	124
Figure 4-7: Monitoring the production of pro-inflammatory molecules IL-8, RANTES and TNF- α in Caco-2 cells following exposure to Lab4 and Lab4B probiotics under flow and static conditions.....	128
Figure 4-8: Monitoring the production of pro-inflammatory molecules IL-8, RANTES and TNF- α in HT29MTX cells following exposure to Lab4 and Lab4B under flow and static conditions for a 48-hour period.....	129
Figure 4-9: The impact of E. coli strains E69, Nissle 1917 and MP1 on the production of IL-8 and RANTES in Caco-2 cells exposed to flow and static conditions for 48 hours.....	133
Figure 4-10: The impact of E. coli strains E69, Nissle 1917 and MP1 on the production of IL-8, RANTES and TNF- α in HT29MTX cells exposed to flow and static conditions for 48 hours ..	134
Figure 4-11: The impact of LPS and LTA on the production of IL-8, and subsequent impact of probiotic pre-treatment on the production of IL-8 in cell lines Caco-2 and HT29MTX.....	137
Figure 4-12: IL-8 production in Lab4- and Lab4B-treated Caco-2 cells exposed to EPEC E69 under flow and static conditions	140
Figure 4-13: IL-8 production in Lab4- and Lab4B-treated HT29MTX cells exposed to EPEC E69 under flow and static conditions	141
Figure 4-14: IL-8 gene expression in HT29MTX cells exposed to various concentrations of Lab4- and Lab4B-conditioned media, and conditioned media generated from single-species bacteria under static conditions as measured via qPCR.....	149
Figure 5-1: Identified metabolites and relative concentration profile of Lab4 probiotic-conditioned medium made from four distinct cell culture medium bases (McCoy's 5A, RPMI 1640, low glucose DMEM and high glucose DMEM)	169
Figure 5-2: Identified metabolites and relative concentration profile of Lab4B probiotic-conditioned medium made from four distinct cell culture medium bases (McCoy's 5A, RPMI 1640, low glucose DMEM and high glucose DMEM)	170

Figure 5-3: Metabolite profiles of the individual bacteria that comprise the Lab4 and Lab4B probiotics prepared using both MRS Broth and high glucose DMEM.....173

Figure 5-4: Metabolite profiles of the constituent bacteria found in the Lab4 and Lab4B probiotics, generated using high glucose DMEM175

Figure 5-5: Metabolite profiles of enteropathogenic E. coli strain E69 (EPEC E69)-conditioned medium generated using both LB broth and high glucose DMEM176

List of tables

Table 2-1: Information regarding cell lines selected for study	30
Table 2-2: Experimental medium preparations	31
Table 3-1: Primer sequences for MUC qPCR.	64
Table 4-1: Bacterial composition of commercial probiotic products	95
Table 4-2:Primer Sequences for IL-8 qPCR	109
Table 4-3: Summary of results from sections 4.3.6	142
Table 5-1: Metabolic pathways influenced by both probiotic and pathogenic single- species/dual-species- conditioned media.	178

List of abbreviations

ATCC – American Type Culture Collection

BSA – bovine serum albumin

CCL5 – chemokine ligand 5

CD – Crohn's disease

CM – conditioned medium

csFBS – charcoal-stripped foetal bovine serum

CT – threshold cycle

DMEM – Dulbecco's Modified Eagle Medium

DMSO – dimethyl sulphoxide

dNTP – deoxyribonucleotide triphosphate

dPBS – Dulbecco's phosphate-buffered saline

ECACC – European Collection of Authenticated Cell Cultures

ELISA – enzyme-linked immunosorbent assay

EPEC – enteropathic *E. coli*

FBS – foetal bovine serum

GAPDH – glyceraldehyde 3-phosphate dehydrogenase

GI – gastrointestinal

HIF – hypoxia-induced factors

HRP – horseradish peroxidase

IBD – inflammatory bowel disease

IBS – irritable bowel syndrome

IL-8 – interleukin 8

KEGG – Kyoto Encyclopedia of Genes and Genomes

LAB – lactic acid bacteria

LB – lysogeny broth

LDH – lactate dehydrogenase

LEE – locus of enterocyte effacement

LPS – lipopolysaccharide

LTA – lipoteichoic acid

MMI – Microbiomes, Microbes and Informatics

MRI – magnetic resonance imaging
MRS – De Man, Regosa and Sharpe
NADPH – nicotinamide adenine dinucleotide phosphate
NCBI – National Center for Biotechnology Information
NCCIH – National Center for Complementary and Integrative Health
NEAA – non-essential amino acids
NHS – National Health Service
NMR – nuclear magnetic resonance
PBS – phosphate-buffered saline
PCR – polymerase chain reaction
PPV – positive predictive value
qPCR – quantitative polymerase chain reaction
QV – Quasi Vivo®
RANTES – Regulated on Activation, Normal T Cell Expressed and Secreted
RT – reverse transcriptase
SCFA – short-chain fatty acids
TMB – tetramethylbenzidine
TNF α – tumour necrosis factor alpha
TSP – trisodium phosphate
UC – ulcerative colitis
WHO – World Health Organisation
WHOCC – World Health Organisation Collaborating Centre

Acknowledgements

The process of completing a PhD is far from an easy one, and as challenging as the whole process was, the hardest part to write has to be this. That's because it would never have been possible to reach this point without the help of many fantastic people, and there are so many people I need to thank that I wouldn't want to miss anyone out!

Firstly, I need to thank the funders of this project, KESS2. Next, I have to thank my supervisory team: Prof. Julian Marchesi and Dr Lee Parry of Cardiff University, and Dr Daryn Michael, Dr Tom Webberley and Dr Sue Plumber of Cultech Ltd. Throughout the entire PhD, they've been there, offering guidance and advice wherever possible and be it discussing potential research avenues or working through the more head-scratching moments, their help has been invaluable. I would also like to especially thank Julian and Daryn, as it was thanks to working previously with them that led to me wanting to pursue a PhD in the first place, and they have been just as great throughout the process as they were in my previous experiences with them.

Then, there are the staff and students in the Cardiff University MMI division, and while I could list them all here for being a great group, there are a few in particular that I need to thank as they provided invaluable help and assistance throughout the project as well as sharing reagents and knowhow throughout these past few years. In particular, I need to thank Dr Laura Rushton, Dr Jane Mikhail, Dr Laura Osborne, Dr Gordon Webster, Dr Beky Weiser, Dr Cedric Berger, Dr Giulia Masetti and Teresa Paradell Gil for their advice and for providing methodologies and reagents that were used at specific points in the study.

I also would like to thank Aimee Bettridge for being an amazing friend throughout the PhD. Whether it was talking through potential experiments, troubleshooting ideas or our many stress-fuelled coffee trips throughout the years that really helped take the edge off a long day, thank you so much. Also, thank you for providing the base R script used in generating the final colour plots seen in Chapter 5 (Figures 5-3 through 5-5) – it really helped add a much-needed splash of colour to the final thesis!

I also need to thank Jesús Miguéns Blanco of Imperial College London for all his help with the metabolite chapter and for performing the metabolite profiling and initial identification of metabolites present in each sample. His patience when it came to dealing with my many questions, his guidance and help overall was invaluable for the creation of Chapter 5. I also need to thank Josh Kerry of Cultech Ltd. for him performing the qPCR experiments for IL-8 production seen in Chapter 4 of this thesis, and for allowing me to present that data here, and Martyn Allen, also from Cultech Ltd., for meeting and discussing potential collaborations between both Cultech Ltd. and Cardiff University. While these ideas never bore the fruit of a publication, it was thanks to the meetings with both him and Tom Webberley, and the ideas and concepts discussed in those meetings that resulted in my performing the work seen in Figure 3-4.

Now, though, I need to send my thanks to my nearest and dearest.

To Bry and Sally, whether it was the best day ever or the worst, you always had a lasagne and coffee waiting and a compassionate ear to help laugh through the tough times. You also always had some great story of wonder and woe on hand that helped make the toughest moments just melt away. Plus, with our DnD sessions, we could always escape for a night to tame some Kobolds or slay some killer butterflies – you know, just work through some of those suppressed frustrations!

To my Mam, Nan and Bampa, you helped foster in me my love of science from a very young age – I mean, mixing bubble baths to make magic potions at bath time is both the coolest childhood memory every and also goes a long way in explaining my love of both science and my general obsession with all things magical and fantastical! But seriously, my family have been there for me through thick and thin, and without their endless support (even when times were particularly rough), I can honestly say I'd never have made it to where I am now, and I owe them everything. But also, how could I talk about my family without mentioning the best pooch in the world – Bertie! Always there with a wet nose and a *lot* of barking, I couldn't forget to mention him (I'd never live it down if didn't!).

Finally, to my dear Josh, who has been there through the good and bad, made endless cups of tea (because keeping me caffeinated has been an essential factor throughout this whole endeavour) and talked me down from that metaphoric ledge when nothing was going right. Thank you for loving me as I am and for being my anchor when the world threatened to spin out of control. I guess I have to admit now that you were right, I really could do it after all – I kept fighting and I finally made it happen. It's been an interesting few years, but I'm glad that it was you who was there beside me through it all – I wouldn't have had it any other way!

I think that I've thanked everyone, but I'd finally like to make one final thank you to everyone I've interacted with throughout the PhD, you've certainly made it an experience I'll never forget!

1 Introduction

Given the importance of cell culture models in the wider field of gastrointestinal modelling, the extensive evolution of cell culture methodologies from 2D to 3D systems over the past 20 years has proven invaluable in expanding upon existing methodologies where a cell line is assessed for its response to a given stimulus through introducing a myriad of biologically relevant stimuli. Furthermore, while the combined analysis of probiotic products with cell culture has enabled a considerably improved understanding of the effects induced by specific strains of bacteria, and artificially combined bacterial consortia found in commercial probiotic formulations, the combination of these probiotics and cell lines has led to results that on occasion conflict with what is seen in studies conducted on mice, or human impact studies.

This thesis seeks to address the impact of a commercially available dynamic flow through system on four commonly utilised cell lines, how the response of these cell lines varies under flow conditions compared to static conditions, and how the introduction of probiotic bacteria influences the cellular response under flow. The aims of the thesis, which will be outlined in finer detail in the following chapters, could be broadly stated as testing the effect of physiological flow in cell culture, and whether the observed results can be stated as providing results that better represents what would be expected *in situ*, despite the limitations inherent in cell lines.

In the following chapter, the key features of cell culture research, cellular parameters, 3D cell culture and probiotic research will be outlined, with particular emphasis on how these contribute to this study.

1.1 Cell culture within research

Cell culture is the scientific practice of utilising human cells to replicate the biological response of a specific tissue/cell type following exposure to a given stimulus by controlling the physiochemical environment (Philippeos et al. 2012). This method of conducting human research generally seeks to exploit the physiological characteristics of cancer, and immortalised cells, including their ability to extensively reproduce, due to a reactivated telomerase (Blagoev 2009), or artificially manipulated cell lines (Kaur and Dufour 2012) that express general characteristics of interest, such as de novo mucin production. Making use of these cell lines allows for a high throughput and relatively consistent means of assessing the human response to a given stimulus. Primary cell culture is also a commonly employed branch of cell culture that utilises a collection of human cells directly cultured from the organ or region of interest (Stacey 2006). The use of primary cell lines can provide the unique benefit of greater biological accuracy and improved relevancy when compared to immortalised cell lines, as primary cells typically express characteristics of their tissue of origin (Pastor et al. 2010). However, due to the difficulty in isolating primary cells, and the finite number of replication cycles these cells may undertake, most preliminary research will revolve around the implementation of readily established immortalised cell lines for optimisation prior to the introduction of primary cells.

However, whilst cell culture is considered both highly effective and comparably simple to implement (Masters and Stacey 2007), one must consider additional limiting factors when designing a cell culture experiment, with particular focus on the cell lines selected and the conditions to which the cells are exposed. While cell culture is widely employed, the limited comparability of immortalised cells to healthy functionality will inevitably limit the scope of the study, requiring the eventual use of primary cell lines – cells directly extracted from biopsies or direct-from-source, and that have yet to undergo a subculturing procedure (Geraghty et al. 2014), or ideally the use of methodologies *in vivo*. Despite this, immortalised cell lines provide an invaluable tool, providing considerable insight, upon which future research and concepts can be built.

1.1.1 Animal modelling and their role in modelling methodologies

While cell culture has proven an invaluable tool in assessing the response of a cell line to a given stimulus, animal models have historically provided an effective means of assessing both disease development and the physiological response of an organism to a given stimulus (Barré-Sinoussi and Montagutelli 2015). One of the greatest benefits to animal research is the ability to utilise a varied number of species (Andersen and Winter 2019), exploiting the benefits of each in an attempt to circumvent the limitations present within different animal model systems. While there are a number of ethical concerns regarding the continued implementation of animal models into wide-scale human studies, the application of these animal models in attempting to unravel the underlying mechanisms of disease to improve disease diagnosis, prognosis and treatment remains an invaluable tool that, at present, prevents the total removal of animal models from research due to a lack of a viable yet comparable system.

The most commonly observed species used as part of animal modelling in research is *Mus musculus*, having become ingrained within a number of research fields, ranging from psychology to cancer biology. However, the use of mice as a means of predicting the human response within these fields is highly contested (Pound et al. 2004), as while animal models provide invaluable predictive models, they ultimately lack the human-like response element essential for *in situ* biological relevancy, as much of the data generated does not translate when applied to humans. The use of this species has become such common practice, in fact, mouse-centric research constitutes an approximate 95% of all current animal-focused research (Vandamme 2014).

However, despite the benefits that accompany animal modelling, primarily being that these animal systems enable *in vivo* analysis of a given mechanism or disease state that otherwise would remain impossible to assess, they still present a limited means of assessing the response of human cells or environments. One of the major limitations of animals within research is that these models often lack the insight required to understand the human response required to accurately depict the progression of disease or the efficacy of a given therapeutic agent *in situ*. One such example of this is the well documented limitations

in drug safety testing. Animal models do not provide sufficient clinical relevance for potential drug-related side effects, due to distinct drug metabolism pathways being present that will distinguish between species, particularly due to species differences in cytochrome P450s that will confer a variable response to drugs between species (Cheung and Gonzalez 2008), thus limiting the overall reliability of these models.

Furthermore, it must be stated that animal models are a somewhat difficult topic to address, as despite the inherent benefits that animal models have provided to research, the limitations and emotional and ethical aspects of employing such, the area remains a divisive one, both within research communities and beyond. As a result, numerous organisations have emerged in an attempt to remedy the issues in animal research, the most prolific of which being the NC3R, responsible for furthering the implementation of the now widely known Three Rs tenet (Fenwick et al. 2009).

The tenet pertains to the handling and usage of animals within scientific research, with The Three Rs title referencing the following guidelines: to Reduce the number of animals used in experiments wherever possible, to Refine the methods to limit any undue stress or harm to the animals and to Replace animal usage where possible, be that partially or fully depending on the method in question (NC3R). Furthermore, the tenet acknowledges the historical and present-day importance of animal modelling as an intrinsic aspect of biological research and advancement. It is this statement that remains essential and core for those attempting to address the goals of the NC3Rs, as it acknowledges that the concept of removing animal models from research is not one so easily achieved, and instead alternative methodologies might better assist in complimenting animal research, while simultaneously reducing the overall reliance on such systems.

It is here, then, that the implementation of cell culture systems has found its niche. By providing a means of developing exploratory models that aim to assess the response of cell lines to specific stimuli, alternative cell culture systems have become ingrained within human research and have presented an attractive means of analysing specific regions of the human body, including the gut, the primary focus of this study. In the following section, the use of cell lines as “models” of the human gut will be explored, including further details of

the essential biological parameters that are becoming ever more ingrained in cell culture methodologies.

1.1.2 The use of cell culture models as “models” of the human gut epithelium

Cell lines have played an integral role in assessing the response of human-like cells to specific stimuli and in contextualising what might be expected *in situ*. One such “model” is that of the human gut epithelium, a site of considerable interest within this study. The ability of cell culture methodologies to replicate complex environments *in vitro* stems from the unique characteristics of these cell lines. As such, there are often a large number of available cell lines when designing experiments, and a number of studies that have historically employed the use of such cell lines. The four cell lines used in this study, Caco-2, HCT116, HT29 and HT29MTX, have each been utilised expansively within cell culture research that focuses on the gut, albeit the niche applications of each allow them to provide intrinsic benefits that the other cell lines lack.

The Caco-2 cell line is one of the more commonly utilised cell lines in gut-centred research thanks to its specific characteristics. Originally sourced from a colorectal adenocarcinoma, the cell line expresses an epithelial cell-like physiology, allowing for a niche model of the gut (Public Health England 2021a). Characteristics of particular interest expressed by this cell line are its unique ability to spontaneously polarise at 14 to 21 days post confluence. This polarisation into a clearly defined apical and basolateral orientation has been well characterised and can be noted by the formation of tight junctions between adjacent cells and the formation of a brush border thanks to the presence of microvilli at the cellular apex (Lea 2015a). Unfortunately, the Caco-2 cell line does possess a few select limitations. As this cell line requires continuous maintenance over a prolonged period to allow for its characteristic polarisation, it can become time and resource intensive. When coupled with the reduced expression of the TLR4 membrane receptor (Sodhi et al. 2012), responsible for the recognition of the bacterial endotoxin LPS, Caco-2 could be viewed as a cell line that, while invaluable under the correct circumstances, should be carefully considered in relation

to the experimental setup as opposed to a cell line that is an automatic inclusion within cell culture studies.

HCT116 is also a commonly utilised cell line when modelling the gut, isolated originally from a colorectal carcinoma (Public Health England 2021b). This cell line, similar to Caco-2, has acted as a commonly used epithelial model of the gut, as its source from the colon/rectum provides an alternative tissue type in gut modelling. This cell line has a select number of unique traits that are beneficial within gut-modelling research – those being its use as a metastasis model (Lee et al. 2014), or its unique niche within 3D-centric cell culture research thanks to its ability to form viable spheroids when cultured under the correct environmental conditions (Shaheen et al. 2016). Unfortunately, while this cell line possesses a number of beneficial traits that cell culture studies might wish to exploit, HCT116 lacks the capacity to differentiate, a feature that is highly desirable within cell culture research (Yeung et al. 2010). As such, while this cell line is flexible in its use and applications, care should be taken when selecting this cell line if cellular differentiation is a feature of interest within a given study.

The cell line HT29 has a historic use in cell culture research thanks to the numerous biological applications it is capable of performing and shares a number of traits with Caco-2, including its site of isolation, that being from a colorectal adenocarcinoma (Public Health England 2021c). HT29's extensive usage is somewhat tied to the shared characteristics it has with the commonly utilised Caco-2, as this cell line is capable of expressing an altered brush border and forming tight junctions when appropriately differentiated. Furthermore, the differentiation of this cell line, and its innate potential for differentiating differently if exposed to a correct specific agent, has enabled HT29 to carve a niche within cell culture alongside Caco-2. However, despite the utility of this cell line, and its expression of its biologically relevant brush border-associated hydrolases (Martínez-Maqueda et al. 2015), HT29 still lacks the biological relevancy to that seen *in situ*. Despite this, the functionality and extensive use of these cells *in vitro* makes them an attractive prospect for studies aiming to incorporate cell lines into their research.

Finally, HT29MTX is a cell line unique within the context of those cell lines selected for use in this study, as its origin is that of an artificially induced cell line, mutated from a common

HT29 cell (Public Health England 2020). The synthesis of this cell line occurred when an active culture of HT29 cells were treated with methotrexate, a drug commonly utilised as an immunosuppressant and in cancer treatments. Following the mutation process, cells were selected according to desirable traits, one of which being increased mucin production observed in the HT29MTX cell line. Furthermore, HT29MTX provides an alternative cell model to the other cells used in this study, as they mimic goblet cell behaviours as opposed to epithelial cells. While this cell line can provide an invaluable model of the gut, particularly when combined with the cell line Caco-2 (Chen et al. 2010; Kleiveland 2015), the cell line lacks a responsiveness to bacterial endotoxin, similar to that seen with Caco-2, meaning that in those experiments that seek to examine the inflammatory potential of a given stimulus, this cell line may return a diminished response.

Ultimately, the selection of cell line is integral to a given study, as the aims and objectives should shape the selection of cell lines used. Due to the complexity of the gut, it is important that those seeking to assess a gut-like response within cell culture additionally understand the physiology of the gut and the parameters that govern it, features that are outlined in the following sections.

1.1.2.1 The physiology of the gut

When it comes to modelling the gut, one of the greatest barriers faced by researchers comes when aiming to replicate the physiology of the gut *in vitro*. The gastrointestinal tract is a complex collection of biological layers, consisting of multiple layers of tissue, muscle and cellular protrusions.

While the outer layers of the GI tract, including the serosa and sub-serosa, are important in providing muscular lubrication, aiding in blood flow and providing structural support, it is the inner layers, primarily the mucosa and muscular layers, that are of particular interest to this study, the reasons for which will be described in the following segment.

The mucosal layer is a blanket term that encapsulates the biological layers within the GI tract closest to the luminal space. The three primary layers include the epithelium, the cell

layer in direct contact with the contents of the lumen; the lamina propria, a thin layer of connective tissue, and a thin layer of muscle. This region is often the site where physiological abnormalities manifest, including tumours, both malignant and benign, and inflammatory diseases, including CD (Hendrickson et al. 2002).

The epithelial layer is typically organised into protrusions and form crypts where the mucus layer is generated by goblet cells, resulting in an increased surface area. Furthermore, the epithelial layer is in continued contact with the mucus layer, which provides an adhesion site for the microbial constituents of the gut and provides a protective layer between both the luminal contents and the epithelium. Additionally, this is the site most directly impacted by external stimuli due to being in direct contact with the contents of the GI tract, which is particularly important when considering the rapid cellular turnover rate within this region and the organisation of the gut, in which villi and microvilli are prominent features that maximise nutrient and water absorption by increasing the surface area within the gut (Kiela and Ghishan 2016)

While the behaviour of cells found in this region of the gut is important in understanding the behaviour of the gut, as much of the complexity of this region is omitted within a cell culture experiment, it is important to consider these features to assess the biological relevance of both the experiments in question and the results generated. Finally, while the epithelia are essential, particularly within the context of this study, so too is the environmental influence afforded to the gut by the muscle layers present within it. With both rounded and straight musculature found in the gut, the movement of substances through the GI tract is enabled via peristaltic mediated flow, a feature essential for understanding the function of the gut, and a factor that will play a key role in this study, despite its often-overlooked nature within the confines of modelling methodologies.

1.1.2.2 Biological parameters of the gut

The GI tract could be considered as one of the more complex environments within the human body due to the sheer number of physiological and environmental factors contributing both to the behaviour and functionality of the gut. Each of these factors could

become subject to interference by the interplay that occurs within the host, including factors such as water content and pH (Redondo et al. 2015; Hansen et al. 2018), bacterial community composition and disease state, among others, and those factors external to the host, including general behaviours such as diet (Conlon and Bird 2015) and medication habits of the patient (Maier et al. 2018). As such, utilising cell culture as a proxy for assessing the cellular response of gut cells, whilst somewhat reductionist by nature, also requires that these factors be considered, both to better represent the complex environment *in situ*, and to inform how these parameters are incorporated so as to not unintentionally introduce bias. In the following sections, the key parameters of the gut considered within this study will be discussed, outlining the roles that these environmental factors play in maintaining the general wellbeing of the gut, and their importance in a cell culture context.

1.1.2.2.1 The microbiome

A term first defined by Burge in 1988, the human microbiome is one of the largest areas of microbial research to have emerged within the past 50 years (Burge 1988). The human microbiome could be broadly defined as a distinct yet diverse bacterial community inhabiting a specific niche within the human body (Ursell et al. 2012). These bacteria are typically symbiotic in nature, conferring benefits to their host in exchange for an exclusive suite of host-conferred benefits. These interactions include the breakdown of ingested materials, more specifically indigestible sugars and fibre – often referred to as prebiotics – that can aid in digestion and host health through the release of metabolites (Lustri et al. 2017). These interactions include the production of chain fatty acids (SCFA), which can be used in signalling pathways or as useful metabolites to aid in cellular function by the host. Additionally, the constituents of the host's microbiota perform a key role by physically inhibiting the colonisation of a given niche by pathogenic bacteria through the formation of densely populated poly-microbial biofilms and the synthesis of anti-microbial compounds to form a biochemical defence barrier (Ubeda et al. 2017).

An important facet in further understanding the human microbiome is dysbiosis, a controversial facet of microbiome research (Olesen and Alm 2016), but remains a feature that cannot be overlooked when assessing the combined effect of the microbiota on host health. Dysbiosis is defined as the state where the host microbiome is altered following a physical trauma or antibiotic therapy, which results in reduced bacterial diversity and simplified species composition within a given niche (Petersen and Round 2014). The characteristic simplification of bacterial communities has been observed in some cases as resulting in a reduction in host immunity, which can increase susceptibility to a range of diseases.

This further emphasises the role of the host microbiome in protecting its host and preventing disease development, and how the loss of bacterial diversity can result in the development of specific disease states. Interestingly, there has also been much discussion as to whether dysbiosis is a cause or effect within certain diseases. IBD, for example, has been observed as having a reduced bacterial diversity when compared to healthy patients (Gong et al. 2016). However, this reduction in diversity has been noted as often co-occurring with an increased host inflammatory response, raising the question of whether dysbiosis is a driver for inflammatory diseases, or if these diseases are induced as a by-product of said dysbiosis (Buttó and Haller 2016).

Within cell culture studies, much microbial research utilising cell lines sourced from the gut has been undertaken to aid in understanding the impact of specific bacteria within a gut environment. Due to the nature of cell culture, however, the complexity of the microbiome cannot be fully encapsulated using such methods, instead allowing for targeted studies examining the impact of bacteria on these cells. Particular interest has been directed towards specific probiotic bacteria, including those belonging to the genera *Lactobacillus* and *Bifidobacterium* and their interactions not only within the cells, but with mucin, another key component of the gut that is discussed in greater detail in the following section.

1.1.2.2.2 The mucus layer of the gut

The mucus layer within the gut is an important factor to consider when examining cells *in vitro*, as it provides a physiological barrier between the epithelium and luminal content. This barrier is composed of a series of high molecular weight glycoproteins referred to as mucins (Cornick et al. 2015). Mucins are a set of glycoprotein substances that are carbohydrate-dominated in their composition (Thornton and Sheehan 2004), whereby a protein core dominated by the amino acids proline, serine and threonine tandem repeats, often referred to as a PTS-rich, is extensively O-glycosylated (Paone and Cani 2020) to form a unique structure which has been referred to as a “bottle brush” conformation. Mucins have been recorded as providing a multitude of protective functions, ranging from inhibiting the establishment of pathogens to immune modulation essential for the health and protection of the gut (Cornick et al. 2015). Additionally, the mucin present provides a nutritional source and adhesion site for the complex microbial communities that inhabit the gut, enabling the formation and establishment of everyone’s gut microbiome (Corfield 2018), further enhancing the host’s innate defence against pathogens within the GI tract.

Broadly, mucins can be classified into two unique subgroups, those being transmembrane mucins, and gel-forming mucins, which can also be referred to as secreted mucins. While gel-forming mucins were the primary focus within this thesis, in the following section, both subgroups will be discussed in greater depth.

1.1.2.2.2.1 Transmembrane mucins

Transmembrane mucins are those mucins involved primarily in cell protection, and do not contribute to the formation of the mucus barrier (Paone and Cani 2020). The composition of these mucins consists of an extracellular N-terminal, a number of mucin domains, and an intracellular C-terminal tail. Many of these mucins are upregulated during infection and cancer and not via other methods. Within the context of this study, while the mucus barrier is something of particular interest, it is important to consider that membrane-bound mucins are often retained during staining methodologies as opposed to gel-forming mucins, which

are typically difficult to retain. Many common transmembrane mucins are expressed within the GI tract, those being MUC1 /3/4/12/13/15/17/20, and 21 (Paone and Cani 2020).

1.1.2.2.2.2 Gel-forming mucins

Gel-forming mucins are a subset of mucins that are synthesised and secreted by goblet cells within the gut (Paone and Cani 2020). These mucins are generally seen in large quantities within the gut as they compromise the mucus layer. Three primary gel-forming mucins are found within the gut, those being MUC2, 6 and 5B (Grondin et al. 2020). Due to the nature of the gut's mucus barrier, consisting of two layers of mucus, mucins are continuously synthesised and secreted within the GI tract to best ensure that the epithelial cells are protected from direct contact with bacteria that inhabit the gut, or ingested lumina contents. As mentioned in section 1.1.2.2.2.1, the difficulty when attempting to monitor the production of secreted mucins is the fact that binding mucins for staining or microscopy is a difficult challenge, requiring a specific set of binding solutions to prevent loss of the mucins of interest. When combined with the addition of a dynamic flow system, such as in this study, the challenge of measuring the abundance of secreted mucins is apparent. However, as other glycoproteins can be found within the gut, including membrane-bound mucins, it is these that are targeted primarily within this thesis, rather than mucins directly, and in turn, we can examine how these alternative methodologies can work in tandem with molecular based techniques to explore the impact of flow on mucin production.

1.1.2.2.2.3 Using cell culture to assess mucin production

One of the key considerations within a cell culture context is the fact that many commonly used cell lines lack the expression of mucins found within the gut, primarily that of MUC2, the key component of the mucus barrier (Paone and Cani 2020). Instead, certain cell lines, such as HT29MTX, are utilised due to their de novo expression of a common mucin subgroup. While mucins such as MUC5AC and MUC5B are typically expressed in the stomach (Grondin et al. 2020) and salivary glands respectively (Frenkel and Ribbeck 2015),

the expression of these mucins enables cell culture to be used to examine the impact of a given stimulus on mucin production *in vitro* in hopes of applying the findings to an *in situ*-like context. It should be stated that these considerations were addressed throughout the thesis, and as such, the selected targets for mucin production acknowledges the limitations in this methodology.

1.1.2.2.3 pH of the gut

The gut is often subject to external influences, both from within the host and due to by-products of host behavioural patterns, and this is most apparent when examining the pH of the GI tract. To expand further, the gut is also highly complex with regard to its pH modulation, with the optimal pH within the gut being region dependent. For example, the optimal pH of the small intestine varies somewhat, with the mean pH varying between 6.6 and 7.5 between the proximal small intestine and the terminal ileum (Evans et al. 1988), and these optimal pH profiles are subject to constant flux due to host dietary practices and disease states (Nugent et al. 2001).

Dietary influx, in addition to its nutritional composition, are primary influencers for environmental pH within the GI tract, although within the gut the impact is somewhat minimised due to the neutralisation of luminal pH within the gut. The importance of an individual's dietary habits is hardly a novel concept, however, with poor diet having been associated with numerous diseases ranging from diabetes to obesity (Hu et al. 2001) and some even linking poor nutrition to Alzheimer's disease (Hu et al. 2013).

As already alluded to, something that must be considered is the delicate balance between beneficial and deleterious substances and micronutrients on the host, as microbial composition is heavily dependent on the pH of the gut (Ilhan et al. 2017). Foods whose composition includes probiotics, dietary fibre (prebiotics) (Lin et al. 2014) and antioxidants (Pizzino et al. 2017) have long since been associated with health benefits to the host.

A key issue to consider therefore within the confines of this study is the impact of pH in a cell culture context. Previous studies have revealed that alterations in ambient pH, resulting in either acidic or alkaline conditions can influence cell lines *in vitro*, limiting cellular

functions, or potentially inducing a mild to severe stress response (Li et al. 2020), including an instance where the cell line Caco-2 exposed to an acidic environment displayed an upregulation of genes relating to endoplasmic reticulum (ER) stress, a key cellular component in both pH homeostasis and inflammation within IBD (Maeyashiki et al. 2020).

As such, it could be noted that even minor fluctuations in pH might result in a cellular response that might otherwise impact the reliability of the observed data. Furthermore, as this study aims to explore the impact of dynamic flow on intestinal cell lines, further considerations should be made regarding pH, as through introducing flow, the issues identified in 2D cell culture may be further compounded, or mitigated entirely, a theory that without additional investigation should be approached with caution.

1.1.2.2.4 The inflammatory response of the gut

The inflammatory response characteristically observed in diseases of the GI tract is a complex one to encapsulate fully, as it has been implicated in a large number of disease states, both as a symptom and as a contributing factor to disease progression and cancer development in patients (Itzkowitz and Yio 2004). While many would be quick to suggest that an inflammatory response is negative, it remains an important component of the host immune system, limiting the incidence of infection through inducing an inhospitable microenvironment for invading pathogens.

The human gut is far from a continuously inflamed microenvironment, however, instead providing a system that could be stated as being in a constant state of minor flux when faced with a potential antagonistic agent. Due to the rapid passing of luminal contents through the GI tract, one could conclude that an inflamed environment could, in part, be attributed to the physiological conditions present within the gut, be that externally influenced factors such as pH and dietary input (Valdes et al. 2018) or internally influenced factors, including the host microbiome and the presence of liquid flow through the GI tract (Cremer et al. 2017). When considering the inflammatory response of the gut *in situ*, how then does this compare to what has been observed within cell culture?

When examining the inflammatory response of cell culture systems, considerations must be given to the experimental model selected for this task and, in particular, the inflammatory potential of the selected cell lines. Caco-2, despite its dissemination within the field of intestinal cell culture thanks to the distinct physiological characteristics outlined previously, comes with a distinct set of limitations that impact its potential as a cell culture tool. The most impactful of these limitations, when considering the implications of the study, is the poor response of Caco-2 cells to pro-inflammatory stimuli, including LPS, and its diminished responsiveness as a result of excessive passaging, and medium composition (Huang et al. 2003). Caco-2's lack of response following exposure to pro-inflammatory stimuli has been well characterised in many publications, with attention directed at the response, or rather the lack of response, from Caco-2 cells following LPS exposure.

HT29MTX, however, provides an alternative perspective on intestinal response to pro-inflammatory stimuli. Due to the mutation in this cell line promoting the expression of mucin, HT29MTX has an additional physiological factor that could influence the ability of a given stimulus through the introduction of a physiological mucin barrier, considered to protect the host as a "first line of defence" in infection (Kim and Khan 2013). However, as has been recorded with Caco-2, HT29MTX has also been noted as responding poorly to LPS exposure (Böcker et al. 2003); thus, the potential responsiveness of these cell lines to conditioned medium may suggest that the metabolic activities of these probiotic bacteria may contribute a greater influence on cell behaviour and host health than initially realised.

Ultimately, the key feature of understanding the response of cell lines to proinflammatory stimuli lies in selectivity and understanding the cell lines used within a given context, a feature that will further be explored throughout this thesis.

1.1.3 The intrinsic benefits of cell culture

Through exploiting the intrinsic characteristics of cell lines whose origins stem from a cancerous origin or from viral manipulation, and combining this with a high throughput methodology via the use of multi-well plate systems, it is possible to assess an incredibly large number of variables simultaneously, each of which with a large number of biological

and technical replicates. The diversity and range of cell lines, origins and traits present within cell repositories provides a unique advantage to cell culture methodologies, where the European Collection of Authenticated Cell Cultures (ECACC) maintains a collection of over 1,100 cell lines from over 45 species (Public Health England 2018), and the American Type Culture Collection (ATCC) possesses a repository of nearly 4,000 cell lines from humans alone, to say nothing of the other species (ATCC 2019).

One must also consider the intrinsic benefits exclusively conferred by cell lines when undertaking cell culture research, including the immortalised nature of these cells. The perceived immortality of these cell lines is either due to their origins as cancer cells or comes as a result of genetic or viral manipulation, thus gifting these cell lines with the potential to propagate extensively, given the correct environmental conditions (Mouriaux et al. 2016). While this ability to propagate infinitely can prove as much of a hindrance as it does a benefit, cell lines can prove invaluable in rapidly generating large volumes of cells for large-scale experiments. Additionally, due to the rapid growth and propagation speed of many immortalised cell lines, the invaluable ability to cryopreserve cells provides minimal issue, and along with the aforementioned ability to generate large quantities of cells, there is a considerably reduced concern regarding revival (Bahari et al. 2018) – allowing for cell maintenance within a given passage range for both short-term and long-term research.

When considering all of these factors, cell culture would, at first glance, appear as an ideal prospect for human research. However, there are some inherent drawbacks present in the use cell lines, which must be considered both when designing experiments and when considering the applicability of results generated through cell culture.

1.1.4 The limitations present within cell culture research

As previously alluded to, the human gut is a highly complex microenvironment, where both those physiological factors and environmental conditions present within the host, alongside external, behavioural factors contribute significantly to general health and wellbeing of the host. However, it is these very factors that limit the overall application of cell culture within

research, preventing this methodology from standing as a true potential replacement for animal models. Cell culture has typically been performed using 2D methodologies, with little consideration for the general physiology of the cells in question, or the considerable external impact the microenvironment of the gut contributes *in situ*. As noted by Knight and Przyborski in their 2015 study, cells cultured in two-dimensional cell culture systems, such as in multi-well cell culture plates or cell culture inserts, display an altered cellular morphology, with cells cultured under these conditions becoming flattened and spread, thus presenting an alternative model to that seen *in situ*, where cells would typically display a three-dimensional morphology with additional intercellular signalling between different cell types (Knight and Przyborski 2015).

These systems are also most commonly mono-cellular in nature, and by ignoring the incredible cellular diversity present within the gut, further remove such models from the desired environment found *in situ*. Many findings observed in cell culture systems do little to explore the true impact of examining these cells in a vacuum, where excluding those factors essential in capturing the complexity of the gut, such as the aforementioned dynamic flow, pH and host microbiome, may, in truth, introduce significant bias to such studies. Bearing this in mind, it could be said that by omitting these environmental factors from cell culture research, we are presented with a far less robust model as a result.

1.1.4.1 The emergence of 3D cell culture and its utility as an *in situ*-like model

Despite the potential drawbacks addressed in section 1.1.4, it must be stated that great strides are being taken to expand current 2D methodologies and evolve conventions through accommodating for the limitations inherent within cell culture. Whether it is the use of organoid/ spheroid culture, which enable a 3D orientation of cells, the incorporation of primary cell lines and tissue samples to assess a more physiologically accurate and relevant response, the number and complexity of systems that seek to challenge convention and improve current modelling technologies through the incorporation of physiologically relevant conditions is ever increasing within research. As such, as these methodologies become more commonplace within research and systems become more readily available to

research groups, the prospect is that these 3D systems might assist in better representing an *in situ*-like environment, and thus the physiological relevance of generated results. This study seeks to further explore this concept through the use of a commercially available milli-fluidic flow system, and in the following section will outline the wider aspects of 3D cell culture, with particular focus on milli-fluidic culture, its benefits and potential limitations.

1.2 What is 3D cell culture?

As mentioned previously, one of the potential limitations of 2D cell culture is the omission of biologically relevant parameters and a loss of physiological relevancy compared to what is seen *in situ*. It is therefore logical that methodologies have evolved to account for this, the primary of these being 3D cell culture, which can broadly be defined as cell culture that allows cells to grow and interact with their environment in a 3D space, using extracellular matrices (Huh et al. 2011). The benefits of 3D cell culture has proven so attractive to potential investors and researchers that research focusing on 3D cell culture methodologies has increased annually between 2001 and 2020 (Figure 1-1). However, while 3D cell culture can be considered as focusing on morphological changes at a cellular level, other definitions for 3D cell culture exist, in which culture methods incorporates parameters and features found within a given microenvironment to better replicate that setting *in vitro*. In the following section, some of these parameters will be further expanded upon, including some insight into their importance within the context of this study, and their relation to the gut.

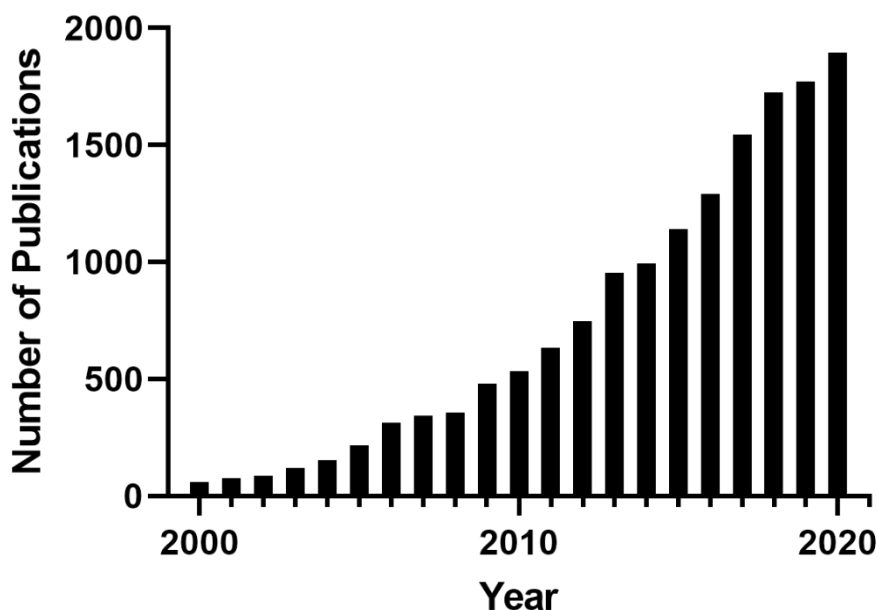


Figure 1-1: Total publications with research focusing on 3D cell culture between the years 2000 and 2020. The above figure was generated from metadata gathered from PubMed using the search term “3D cell culture” (<https://pubmed.ncbi.nlm.nih.gov/?term=3d+cell+culture&filter=years.2000-2020>). [Last Accessed: 28 March 2021]

1.2.1 Parameters that are used in 3D culture and example systems for incorporating them

1.2.1.1 Hypoxia within cell culture

Oxygen availability in cell culture has been explored in detail, due in part to the fact that cell culture uses non-biological oxygen concentrations, i.e. normoxia (18.6% – 21% oxygen) (Pavlacky and Polak 2020) to favour simplicity over biological accuracy. However, cells *in situ* are exposed to considerably more hypoxic environments. While the oxygen levels are tissue dependent, with some regions receiving significantly less oxygen than others, it is believed that approximately 3% – 5% oxygen is what cells would experience in a typical gut, depending on the region examined (Zeitouni et al. 2016).

Hypoxia-induced factors (HIF) are a subset of genes that regulate the production of erythropoietin (Eckardt and Kurtz 2005), in addition to numerous genes involved in cell division (Carrera et al. 2014). These genes are typically inactivated at higher oxygen

concentrations and yet have been well documented as important moderators of cellular behaviour. If this sub-family of genes is inactivated at ambient oxygen levels, such as those used in cell culture, it must be asked what other genes or behaviours are being artificially altered as a result of this methodology.

To address this, companies have invested in the development of specific, bespoke hypoxic chambers to control the oxygen levels of cell culture. Many of these systems, such as those produced by Biospherix, have been designed specifically to fit comfortably in cell culture incubators allowing for tightly controlled assays conducted at the optimal temperature. For this study, the impact of hypoxia was not considered due to the incompatibility with the selected milli-fluidic flow system. However, it remains an important caveat to consider in 3D methodologies aiming for improved biological relevancy.

1.2.1.2 Biological pressure within the gut and its application *in vitro*

Similarly to the aforementioned hypoxia, biological pressure was not a factor that was explored within this study; however, it remains an important factor to consider in studies examining the impact of such systems. Hydrostatic pressure has been implicated in several different cellular behaviours, including differentiation, apoptosis and proliferation (Liu et al. 2019). Furthermore, hydrostatic pressure varies by region, and requires careful modulation *in vitro* if incorporating into a given study. The impact of even minute changes in pressure, as low as 10 mmHg in some instances, has been shown to influence the response of cell culture systems, although this topic is a somewhat debated one due to the issue of reproducibility (Tworkoski et al. 2018).

Incorporating hydrostatic pressure is often a result of bespoke equipment designed to induce a specific pressurised environment to monitor cell morphological changes and variations that may occur as a result of direct cellular expose. However, biological pressure is commonly coupled with a biological flow element to induce shear stress within a given environment, and it is this aspect that is of greater interest within this study.

1.2.1.3 Flow within the gut

Characterising the concept of “flow” within the gut is a somewhat complex undertaking, as there are different varieties of flow that occur within the gut. While laminar and turbulent flow within the gut have been examined in previous studies, in which animal models have suggested that the balance of viscous forces and inertial forces will dictate the nature of the flow observed (Janssen et al. 2007), peristalsis and subsequent peristaltic mixing of luminal contents has been implicated in the general health of an individual by exerting significant influence over the microbial composition of the GI tract (Cremer et al. 2016; Arnoldini et al. 2018). While the function of peristalsis has been well associated with the maintenance of a healthy GI tract, the inhibition of peristaltic movement is often noted as resulting in the development of a disease phenotype (Bassotti et al. 2014). Peristalsis is of particular importance within this study, as the milli-fluidic system introduces a dynamic flow environment stimulated by a peristaltic pump mechanism.

It has been estimated that approximately 1.5 – 2 L of fluids pass along the luminal surface of the gut within any given 24-hour period (Cremer et al. 2017). It could therefore be assumed that the luminal surface is always subject to a form of flow, suggesting that continued contact of cells with a given substance or molecule for prolonged periods is highly unlikely, and thus providing an additional attractive prospect for those considering incorporating flow into their cell culture methodologies. With the desire to incorporate flow into cell culture, a new field of research emerged – referred to as fluidics – that has evolved to encompass the key fields of milli-fluidics, micro-fluidics and organ-on-a-chip, all of which being discussed in the following sections.

1.2.1.3.1 Fluidic systems

Fluidics is a field that broadly aims to incorporate a biologically relevant liquid flow element into cell culture systems through the cycling of cell culture medium through closed systems to simulate the flow seen *in situ*. Often referred to as shear stress flow models, these systems are typically developed as bespoke pieces of equipment, either as exclusive tools

for individual teams of cell culture researchers or as more accessible products sold by companies, allowing for widespread dissemination of dynamic flow within the general cell culture research community.

These systems are incredibly diverse in both their structure and complexity with some enabling the use of larger volumes of medium and sample sizes, often being referred to as milli-fluidic systems, or bioreactors, due to their larger size (Berger et al. 2018); and micro-fluidics, which are often considerably smaller in size and scale, allowing assays to be performed at the level of single cells in some instances (Luo et al. 2019) while still providing a large surface area for stimulation and analysis. Organ-on-a-chip is a further expansion on microfluidic technologies in which cells are exposed to a tightly controlled environment within the chip that mimics the organ in question from the perspectives of a tissue interface and mechanical stimulation (Wu et al. 2020). While both system types allow for flow exposure to cells, the function and research prospects vary considerably, examples of which will be outlined in the followings section.

1.2.1.3.2 Currently employed fluidic systems

Two recent examples of milli-fluidic systems that have sought to emulate the gut include the Quasi Vivo® (QV) range of systems developed by Kirkstall Ltd., and the similarly conceptualised bioreactor system presented by Lindner and colleagues (Lindner et al. 2021). Both systems allow for solid, cell-seeded surfaces to be inserted into a reaction chamber for exposure to dynamic flow within a closed, inter-connected chamber system (McGinty et al. 2017), therefore presenting a system that can incorporate both physiological factors and human cells into a single system. Both the speed and medium composition in these systems can be calibrated and altered by the user, and this system provides a user-friendly and relatively inexpensive means of assessing cells under dynamic flow. Additionally, due to the extensive hydrodynamic modelling that took place during their development, the QV systems ensure that any cells inserted into the Quasi Vivo® reaction chambers will be subject to a flow element (Mattei et al. 2014). Most importantly, these systems allow for continued use thanks to the ability to clean and reuse them, be that via autoclaving or a

more direct cleaning methodology, making it a promising long-term investment. The speed settings of the QV range are also fully customisable, and, additionally, speed modulation devices are available to enable a given flow speed capable of replicating that seen in most regions within the human body, thus making it a robust device with a wide degree of potential applications. Due to this level of customisation, coupled with a compact nature, the QV range by Kirkstall provides a tempting offer thanks to considerable customisation with regard to medium, stimuli and even oxygen levels, given the appropriate available equipment and the invaluable multi-use nature as opposed to commonly observed single use plastic items, while also being a system that is commercially available, a feature not shared by the one used by Lindner and colleagues.

Micro-fluidic systems, such as the HuMiX system and the Hele-shaw chip, allow for greater customisation than their milli-fluidic counterparts. The HuMiX system, a modular micro-fluidic system, enables the use of three individual layers, custom formulated for a given function (Shah et al. 2016). Typically, the system incorporates a microbial layer, a perfusion layer and a cell culture layer sandwiched between. This enables the system to tightly control the parameters of each layer while allowing for interactions to occur between the cells and additional stimuli. Furthermore, these systems allow for real-time monitoring, either via fluorescent methods or electrical resistance, thus enabling for long-term studies to be performed without the risk of contamination or need for assays that might disrupt the cells. Micro-fluidics, while not utilised within this study, present an option far more diverse in scope than the milli-fluidic counterparts; however, additional resources and investment is required to best utilise these systems.

1.2.1.3.3 The current limitations of 3D fluidic culture

While flow systems possess the potential for improving current research methodologies, and present numerous potential benefits for investors, one of the limitations found in almost all instances is the comparably small sample size per experimental cycle. To firstly consider the Quasi Vivo® range of flow systems yet again, due to their commercial availability, these systems typically reduce the quantity of assayable compartments

considerably to enable a consistent flow rate and replicable hydrodynamics within the confines of each flow chamber (Mazzei et al. 2010; Mattei et al. 2014). In both the QV500 and QV600 systems, assays are generally limited to the three chambers supplied in each commercial kit. While this limits the sample size considerably, this imposes an additional burden on those attempting to conduct higher throughput experiments – thus requiring the purchase of multiple system kits and pumps, without which the maximum sample size would be fixed at three samples.

As such, the limited sample number per experimental cycle presents a considerable issue for those aiming to step into the world of 3D cell culture and adopt its methodologies, as this low sample number undermines the greatest advantage of cell culture research, that being the high throughput. Despite this, many research teams are now shifting focus towards improving upon and counteracting this currently limiting and unappealing caveat of 3D cell culture (Astashkina et al. 2012). Another potential issue could be the lack of reusability within these systems. Particularly when considering micro-fluidic systems, many of the currently available systems that enable analysis at the level of a single cell are offered as merely self-contained, single-use materials (Mimetas 2020). While these systems can be relatively high throughput, the issue of single use does impose some complications while contributing to the already considerable requirement for single-use plastics within cell culture methodologies to maintain sterility at all times, as well as incurring a considerable and continuous investment of materials into these systems.

1.2.2 The required parameters for emulating the gut *in vitro*

Ultimately, when attempting to emulate an artificial intestinal system, a few key parameters are essential, those being: human derived cells, a shear stress/flow system to induce mechanophysical stress, a microbial element to mimic the microbiome and a 3D structural substrate (Costa and Ahluwalia 2019). With the exception of a 3D structure, these were core parameters in this study aiming to assess the impact of flow and probiotics on human epithelial cells. In the following section, as the shear stress/flow systems and cell culture elements have been previously discussed in sections 1.2.1.3 and 1.1.3 respectively, the

importance of probiotic bacteria and their relevancy to this project and gut modelling methodologies will be explored.

1.3 Probiotics and their use in cell culture studies

Probiotics can be defined as “live microorganisms that, when administered in adequate amounts, confer a health benefit to the host” (Michael et al. 2021), such as a reduced incidence and risk of disease development (Verna and Lucak 2010). One of the most fundamental issues currently faced by the probiotic industry is a lack of a distinct classification to allow probiotics to become known as either a medicinal product or a health supplement. While probiotics have received a number of classifications dependent on the region in question, as a health supplement (NHS 2018), a prophylactic (Varankovich et al. 2015), a functional food (Syngai et al. 2016) or a complimentary medicine (Australian Government 1990), they have struggled to receive recognition as a therapeutic due to a number of issues. Furthermore, the European Food Safety Authority (EFSA) does not easily accept the term probiotics, thus further emphasising the discrepancy in probiotic acceptance and uptake between regions (de Simone 2019).

A primary issue facing probiotic producers is that, according to the WHO Collaborating Centre, a therapeutic must be classified according to the function of its main active ingredient (WHOCC 2018). However, the applications of probiotics have expanded in recent years. With certain disease states, such as antibiotic-associated diarrhoea (Draper et al. 2017), probiotics are more likely to be prescribed by general practitioners as a means of lessening the impact of diseases that might otherwise prove fatal. Furthermore, probiotics in Australia have received some recognition as a potential therapeutic, and have received the classification of complimentary medicines, which can be broadly defined as an agent that is often prescribed alongside a conventional treatment and that provides some additional benefit to a patient while also “consisting wholly or principally of 1 or more designated active ingredients, each of which has a clearly established identity and a traditional use” (Australian Government 2021b). Due to this definition, probiotics classified

as complementary medicines in Australia are subject to further scrutiny, and are required to adhere to the Therapeutic Goods Act 1989 (Australian Government 2013,2021a).

Furthermore, while the opinions of governments and regulatory bodies is somewhat divided, one cannot overlook the sheer financial impact of the probiotic industry. As of 2018, it was estimated that the worldwide probiotic market was valued at approximately 49.4 billion USD, with the projected value set to increase to 69.3 billion USD by 2023 (Markets 2019). As such, the use of alternative models to explore these products may prove invaluable.

1.3.1 Commonly used probiotic strains in research

Many lactic acid-producing bacteria, in particular those of the genus *Lactobacillus* and *Bifidobacterium*, have historically been utilised as probiotic health supplements and play a key role in both the health-food industry and the field of food microbiology. The species *Lactobacillus acidophilus* is considered one of the most commonly consumed beneficial microbes thanks, in part, to its potential role as a health supplement and wider role in the food industry at large (Sanders and Klaenhammer 2001). As of 2020, a number of commonly utilised lactobacilli were reclassified, with species *Lactobacillus paracasei* and *Lactobacillus salivarius*, two probiotic species used extensively within this project being reclassified as *Lactocaseibacillus paracasei* and *Ligilactobacillus salivarius* respectively (Zheng et al. 2020).

Furthermore, within a cell culture context, it is important to note that, as cell culture research practices use a wide range of immortalised cell lines, these cells are typically derived from biopsies extracted from cancer patients. In a study conducted in 2017 by Motevaseli and colleagues, it was revealed that numerous *Lactobacillus* species, including *L. acidophilus* and *L. casei*, display the potential to exert an anti-cancer effect, impacting both the metastatic ability and proliferation of these cell lines (Motevaseli et al. 2017). These findings were further validated using other lactobacilli, with significant effects being observed in both HeLa and HT29 cell lines – cell lines that are commonly implemented in cell culture research (Nouri et al. 2016).

Additional probiotic strains of interest have been identified that are external to the usual lactobacilli and bifidobacterial species, particularly within cell culture studies that seek to emulate the gut. The bacterial strain *E. coli* Nissle 1917 has been recorded as being effective in combating gastrointestinal inflammation, including inflammation associated with ulcerative colitis (Fábrega et al. 2017). However, recent data suggests that this strain is effective in combating foodborne illnesses that stem from shigatoxin and lambda phages (Bury et al. 2018). Another key example of probiotic bacteria of interest within the gut is that of *Fecalibacterium prausnitzii*. This bacterium is a well-established resident of healthy gut microbiomes, and the loss of this bacterium from the gut microbiome has been associated with a disease phenotype including those linked to inflammatory disorders (Martín et al. 2017). However, much research has revealed that *Fecalibacterium prausnitzii* has the potential to also function as a second-generation probiotic if administered adequately, as it has been shown to confer a number of desirable effects, including anti-inflammatory effects, improved gut barrier function and the production of desirable metabolites such as butyrate (He et al. 2021). While these additional probiotics are abundant and well examined, within the context of this study, it is the lactic acid bacteria that are of greater interest, due in part to the expansive use of the Lab4 and Lab4B consortia throughout this study, which are discussed further in the following section.

1.3.2 Lactic acid bacteria and the Lab4 probiotic consortia

A commonly utilised probiotic in both cell culture studies and human intervention studies are the Lab4 range of products developed by Cultech Ltd. Lab4 probiotics contain four unique strains of lactic acid bacteria (LAB), consisting of two *Lactobacillus* strains and two *Bifidobacterium* strains (Smith et al. 2016). Subsequent formulations have been developed by expanding upon the Lab4 groundwork, enabling the development of products and formulations that are suitable for adults, children and babies, including the commonly used Lab4B, where the two strains of *Lactobacillus* present in the Lab4 formulation are substituted for two unique strains of *Lactobacillus*.

Despite the varied consensus by some regarding the efficacy of probiotics, the Lab4 range has established a solid foundation of research since its inception showcasing the potential benefits and impact that probiotics can exert within a biological system, both in research and, more specifically, human intervention studies. Those human intervention studies conducted on patients suffering with gastrointestinal syndromes, such as IBS, have shown that patients experience considerable improvements when ingesting the Lab4 probiotics, with the symptoms experienced by those patients being noted as improving (Williams et al. 2009), a trend that has been seen in other studies conducted using different probiotic formulations to the Lab4 consortium (Dale et al. 2019). Furthermore, the Lab4 and Lab4B formulations have shown to impact the general wellbeing of an individual and have the potential to modulate key factors in the development of disease states, including cholesterol transport and assimilation (Michael et al. 2017), which play a key role in cardiovascular disease.

While the studies conducted utilising the Lab4 and Lab4B probiotics are varied in range and scope, often utilising both live probiotic- and conditioned medium-based approaches, the number of studies conducted utilising these products, and the efficacy of these products in said studies, showcases the promise of Lab4 in alternative modelling methodologies, such as those using flow.

1.4 General aims of the study

To re-iterate the key points outlined above, cell culture systems have provided an impactful alternative to animal models; however, these systems present their own suite of limitations that 3D culture seeks to address. This study aims to investigate whether the inclusion of 3D culture methodologies in the form of milli-fluidic flow can address the limitations of 2D culture, to provide an environment that better represents that seen *in situ* via the hybridisation of cell culture with a physiologically relevant flow element.

This study will further aim to explore the impact and efficacy of probiotic products within cell culture research. Additionally, this study will begin by exploring the similarities and differences observed in four commonly used intestinal cell lines (Caco-2, HT29, HT29MTX and HCT116) when exposed to various experimental conditions, thus assessing the comparability of results observed within distinct cell lines and whether current methods of selecting cell lines for experiments translate well or poorly under physiologically relevant conditions, including that of flow, which will be an omnipresent factor within this study

2 Materials and methods

2.1 Human gut epithelial cell lines selected for the study

Four commonly utilised human intestinal cell lines were selected for the initial study: Caco-2, HT29, HT29MTX and HCT116. These cell lines were selected from among commonly utilised cell lines due to their unique characteristics and status among human intestinal cell line studies. The characteristics, origins and notable functions of these four cell lines are noted in Table 2-1 below. All cell lines used in the study were provided by Cultech Ltd. (Port Talbot, UK). Each of the cell lines used in this study was maintained within a 15-passage range, as also noted in Table 2-1, to limit the impact of passage number on the overall study.

Table 2-1: Information regarding cell lines selected for study. All cell lines were maintained in 5% CO₂ conditions at 37 °C within a humidified incubator. All information was gathered from ATCC and Public Health England culture collection databases.

Cell line	Medium	Origin	Notable characteristics	Passage range
Caco-2	DMEM	72-year-old Caucasian male, isolated from primary colonic tumour	Spontaneous polarisation, formation of tight junctions	55 – 70
HCT116	DMEM	Male, isolated from a colonic carcinoma	Used in metastasis models and for 3D cell culture	19 – 34
HT29	McCoys5A	44-year-old Caucasian female, isolated from a primary tumour	Capable of forming tight junctions and an altered brush border	77 – 92
HT29MTX	DMEM/McCoy's 5A	HT29 (treated with methotrexate and phenotypically selected for mucin-secreting properties (Lesuffleur et al. 1990))	Mucin producing	66 – 81

2.2 Cell culture maintenance

2.2.1 Medium preparation and selection

Two cell culture medium preparations were used throughout the study: a general growth medium and an experimental medium (Table 2-2). The cell culture medium bases used during the study – those being high glucose Dulbecco’s modified eagle medium (DMEM) and McCoy’s 5A medium – were selected in accordance with guidelines outlined on The European Collection of Authenticated Cell Cultures (ECACC) and American Type Culture Collection (ATCC) online databases for each individual cell line.

Table 2-2: Experimental medium preparations

Medium type/purpose	Components
Growth medium	Base medium (high glucose DMEM or McCoy’s 5A), 10% FBS, 1% non-essential amino acids (NEAA), 1% Penicillin/Streptomycin (P/S)
Experimental medium	Base medium, 1% NEAA, 1% HEPES buffer

Foetal bovine serum (FBS) and penicillin/streptomycin (10,000 units/mL) solutions (Sigma Aldrich, Poole, UK) were aliquoted and stored at -20 °C. Both the penicillin/streptomycin and FBS were thawed out prior to medium preparation using a water bath set to 37 °C. A fresh medium stock was prepared weekly throughout the study to ensure continued sterility of culture medium and to limit the introduction of any potential contaminants.

2.2.2 Cultivating human cells from frozen stock

Frozen cell stocks were utilised to maintain a constant stock of available cells throughout the course of the study, where cells were stored at -80 °C in a 1:10 dimethyl sulphoxide (DMSO)/FBS mixed solution. Cells were initially frozen at -20 °C for 24 hours in cotton wool

and blue roll before being transferred to -80 °C to limit the formation of ice crystals that might otherwise compromise cellular integrity.

Cells were revived from frozen as necessary and by rapidly thawing in a water bath set to 37 °C, following which cells were re-suspended in the appropriate cell culture medium for a given cell line before centrifugation at 262 rcf for 5 minutes at 21 °C to form a cell culture pellet. Cells were re-suspended using 10 mL of fresh cell culture growth medium, which was transferred to T25 flasks fitted with a filter cap (Greiner Bio One, UK).

Cell culture vessels were stored in a 37 °C, 5% CO₂, BINDER C 170 humidified incubator (Binder Inc., USA) with a relative humidity of 90 – 95% for the duration of the study in order to maintain optimal cell culture conditions. These cultures were visually inspected using the JuLI™ Br cell monitoring system (NanoEnTek, Seoul, Korea) 24 hours post revival to ensure cell adherence. If adherent cells were observed, the cell culture medium was replaced with 10 mL of the appropriate cell culture medium, and the cell culture vessel returned to the incubator. In instances where cells were non-adherent at the 24-hour timepoint, the flask was returned to the incubator and allowed a further 48 hours to adhere, with adherence monitored at 24-hour intervals. If cultures remained non-adherent after this time, a fresh frozen culture was established following the above procedure, and the non-adherent culture would be observed daily for one week, following which the culture would be discarded if no adherent cells could be observed when using the JuLI™ Br system.

2.3 Initialising the JuLI™ Br system

In all instances where the JuLI™ Br system was utilised, it was required that the system software be initialised. In each instance, a flask or multi-well plate was placed on the camera stage surface. A system image focus was performed prior to each assay, using the autofocus function, where the system software would automatically adjust white balance, brightness and focus to monitor cell confluence optimally and accurately.

2.3.1 Measuring the percentage confluence of a sample

When attempting to monitor confluence, a cell culture vessel was placed on the camera of the JuLI™ Br cell monitoring system and, on the Focus tab of the system, the confluence command was selected. Following this step, the system would return a confluence percentage for a given field of view. This process was repeated for three areas of a given cell culture vessel to ensure comparable confluence throughout, and values averaged.

2.3.2 Live cell monitoring using the JuLI™ Br

The detachable camera stage was sterilised via cleaning with 70% w/v ethanol prepared using deionised water (dH₂O) before being transferred into the BINDER CO₂ incubator. The cell culture vessel of interest was placed upon the detachable camera stage in the incubator, and the incubator was sealed. A system focus was performed in the manner outlined in section 2.3.1, and the “monitoring” software accessed on the main system. Monitoring parameters were set to capture an image and record the confluence at 5-minute intervals for a desired duration. The CO₂ incubator containing the JuLI™ Br camera and sample of interest was sealed for the duration of the monitoring procedure to ensure that no accidental movement of the cell culture vessel occurred that may otherwise impede the monitoring.

2.4 Maintaining and preserving cell samples

Cell culture medium was changed regularly at 2 – 3-day intervals or if the phenol red indicator present in all cell culture media became orange or yellow in colour, thus indicating an acidic environment. Any cell culture medium removed from cells was treated with Virkon™ solution prior to discarding.

Fresh cell culture medium was warmed to 37 °C in a water bath prior to use and transferred aseptically from the cell culture vessel to the actively growing cells using a pipette boy and

serological pipettes, taking care that the cell monolayer remained undisturbed. Should the cell monolayer become dislodged, cells were resuspended in cell culture medium by pipetting up and down using a sterile serological pipette and centrifuged at 262 rcf for 5 minutes at 21 °C to reform a pellet. Cells were re-plated in an appropriate T25 or T75 cell culture vessel with fresh cell culture medium and returned to the CO₂ incubator to adhere for 48 hours. If no adherent cells were observable following this period, a fresh cell stock was started from a frozen vial of cells and the non-adherent cells discarded.

2.4.1 Continued maintenance of cell lines via sub-culturing

Cell confluence was monitored daily using the JuLI™ Br cell imaging system (NanoEnTek, Seoul, Korea). Cells were sub-cultured when confluence was observed as occupying an average of between 75 – 90% of the culture flask's surface area as noted by three JuLI™ Br system confluence reads from different areas of the cell culture vessel.

During the sub-culturing procedure, expended cell culture medium was removed using a sterile serological pipette and discarded. The confluent monolayers were rinsed with Dulbecco's Phosphate Buffered Saline (dPBS) (Merck, UK) that had been warmed in a water bath set to 37 °C to ensure that any remnants of the DMEM and FBS were removed, before being treated with a 0.25% v/v trypsin/EDTA solution to promote detachment.

Trypsin/EDTA-treated cells were returned to the humidified CO₂ incubator to allow for cell detachment and, following a 5-minute incubation period, cell detachment would be observed via the use of the JuLI™ Br cell-imaging software. In cases where cells remained adherent, flasks were gently tapped against the palm of the hand, if necessary, to aid in detachment. Warmed cell culture growth medium was added to the cell suspension to neutralise the trypsin, prior to centrifugation at 262 rcf for 5 minutes at 21 °C to re-form a pellet, and expended cell culture medium was discarded while ensuring that the pellet remain undisturbed. Cell pellets were re-suspended in an appropriate volume of cell culture growth medium before being transferred to a trio of T75 cell culture vessels. If sub-culturing from a T25 flask, a single T75 flask would be generated during the sub-culturing procedure, whereas subsequent sub-culturing procedures would proceed as noted above.

2.5 Using and maintaining the Muse® cell analyser apparatus

In order to ensure the apparatus remained operational, regular cleaning cycles were required and performed in accordance with the manufacturer's guidance notes. The manufacturer-provided Guava® instrument cleaning solution was utilised every 14 days to ensure the sterility of the apparatus during experiments, where the manufacturer-supplied cleaning solution would be loaded into a sterile, non-lidded 1.5 mL microcentrifuge tube, which in turn was loaded into the Muse® system. The "system clean" option was selected from the system menu, where the system would be subjected to a system flush, whereby the cleaning solution would be passed through the internal tubing and flushed into the waste receptor to remove any trace particles, residual dye solution or other potential contaminants from the system. A subsequent "quick rinse" cycle with sterile dH₂O was also required to remove remaining traces of the cleaning solution and avoid damage to the internal mechanisms as a result of prolonged exposure to the cleaning solution.

A dH₂O quick rinse was performed prior to and following each experiment to ensure that the system's pipes remained obstruction free and that no particulates remained as a contaminant in the system, while additionally providing the function of preventing the Muse® system from drying out.

Manufacturer-supplied system check beads were also used at regular intervals to calibrate the system and ensure the system's internal scanners remained accurate and operational during the course of the study, further strengthening the reliability of the assays.

2.6 Preparing cells for use in experiments

2.6.1 Analysing cellular viability and cell health using the Muse® cell analyser

To prepare cells for downstream experimental challenging and conditional exposure, confluent T75 (75 cm³) cell culture flasks were treated with a 0.25% v/v trypsin/EDTA solution and pelleted using the same method as outlined in the sub-culturing protocol seen in section 2.4.1. Cell numbers were estimated utilising the Muse® cell count and viability reagent kit and Muse® cell analyser system following the manufacturer's protocol for both (Luminex, USA).

Cells were initially treated with a 0.25% v/v trypsin/EDTA solution and pelleted following the methodology outlined in section 2.4.1. Cell pellets were resuspended using a supplemented DMEM, ensuring the pellet was resuspended fully prior to staining. To a fresh Muse® compatible microcentrifuge tube, 450 µL of the Muse® cell count and viability reagent was added, in addition to 50 µL of the cell suspension. The cell suspension and staining solution were mixed via gentle pipetting and allowed to rest at room temperature for 5 minutes to allow for staining to occur. Following the staining period, the solution was pipetted gently to ensure that cells remained in suspension. The unused cell suspension was transferred to a 37 °C incubator for the duration of the staining protocol to ensure cells remained viable.

Prior to performing the cell count, a system check and capillary rinse were performed, ensuring that no blockage was present within the Muse® system. Utilising the preinstalled software, a total count and viability assay was selected and experimental parameters maintained at the pre-set values for both the "Viability vs Cell Size Index" and "Viability vs Nucleated Cells" plots. The cell count and viability reagent treated sample was loaded into the system and the assay performed by selecting the appropriate assay and following the on-screen instructions noted on the Muse® system. In instances where the cell number (count) was low in the assessed suspension, as noted by the system timing out, a secondary dilution was performed at a dye-to-cell suspension ratio of 1:1.

Upon successful acquisition of a total viable cell count, a system readout was generated that would disclose the viable cells per mL, viability percentage and total cells per mL. The above assay was repeated three times for each cell sample, and the average values across all three reads was used. A sample was deemed fit for use in experiments where the viability percentage was noted as being 65% or higher across all three experimental reads, and when the total cell number was above 1.5×10^4 viable cells/mL. If either of these prerequisites was not achieved, the sample was discarded and not utilised in any downstream application.

2.6.2 Seeding coverslips with intestinal cell lines

Cell suspensions were diluted to $1.5 - 2 \times 10^4$ viable cells/mL working concentration, and this suspension was transferred to 24-well plates, with each well containing a 13 mm glass coverslip (Pyramid, USA). Cell-seeded coverslips were transferred to a humidified CO₂ incubator for an overnight incubation at 37 °C in 5% CO₂.

Coverslips were visualised using both light microscopy and the JuLI™ Br system to ensure the presence of adherent cells on individual coverslips to monitor cell growth and adherence. Coverslips observed as having adherent cells were transferred to a fresh 24-well plate, where 1 mL of fresh medium was added to each well prior to coverslip transferral to limit cell loss and maximise the number of adherent cells.

The coverslips were re-visualised using the JuLI™ Br imaging system, following the transfer of coverslips to a fresh 24-well plate to re-affirm the presence of adherent cells. These coverslips were returned to the CO₂ incubator and monitored daily via light microscopy. The cell culture medium was changed at two-day intervals until each coverslip was observed as having grown to confluence.

Caco-2 cells were allowed to differentiate for 21 days prior to experimental use to allow for the characteristic differentiation observed in the Caco-2 cell line to occur. All other cell lines were monitored as above and were experimentally challenged immediately when observed to be at 100% confluence.

2.7 Processing and assembly of the Kirkstall QV500 system

The QV500 system was not pre-assembled for use out of the box. As such, assembly was required for the system, as noted in the following section.

2.7.1 Components of the QV500 system and pre-processing required prior to assembly

The QV500 system starter kit included the following items for use in assembling the system: one media reservoir; three QV500 experimental chambers; 1.6 mm and 2.4 mm tubing; luer locks in both a male and female configuration, with one set of male/female luer locks per tubing diameter. Each item in the starter kit was individually packaged ensuring that each piece of equipment was sterile upon initial assembly. However, the tubing and luer locks were packaged together in bulk.

To each tubing segment required for assembling the complete QV500 system, a male and female luer lock was added to each end and, to ensure the sterility of both the luer locks and tubing, these assembled tubing segments were placed into autoclavable vessels. These vessels were autoclaved to sterilise the tubing and allowed to cool prior to assembly.

Manifold tubing was provided with the Parker QV-PF22X0103 Dual-Head Polyflex Peristaltic Pumps used in the study and, as such, was absent from the QV500 starter kits. This section of tubing was sterilised by submerging in 70% v/v ethanol for 2 hours followed by 3 washes in sterile PBS to remove any traces of the ethanol that may prove detrimental to the longevity of the system or the cells incubated therein. Manifold tubing was air-dried in a laminar flow cabinet prior to assembly.

Due to the proximity of the manifold tubing to the peristaltic pump mechanism, this tubing was regularly monitored after each use to ensure the system remained operational and uncompromised during experimental challenging.

2.7.2 Assembling the QV500 system

The QV500 systems were assembled under sterile conditions in accordance with the assembly instructions provided by the manufacturer and can be seen in Figure 2-1.

Each QV500 starter kit was provided with two sizes of specialised tubing, with an internal diameter of 1/16" and 3/32" respectively. To construct the QV500, appropriately sized luer locks were added to a single piece of 3/32" tubing, with a male and female luer placed at either end of a given piece of specialised tubing. This process was also conducted for two pieces of 1/16" tubing; however, only a male or a female luer was added to each piece of tubing, leaving the other side luer free.

To the lid of the media reservoir bottle, a 0.2 µm air filter was fitted to the corresponding pre-fitted luer, as noted by a blue colouration. To the 1/16" sized pre-installed tubing connected to the reservoir bottle, a section of 1/16" tubing was attached using the appropriate luer configuration. To the end of the tubing that lacked a luer, the above noted manifold tubing was attached, and this was repeated for the additional piece of 1/16" tubing. Both the 1/16" and 3/32" tubing was attached together using the appropriate luers, and the 3/32" tubing was additionally attached to the 1/16" tubing attached to the first experimental chamber, where all three chambers were attached in sequence. Finally, the 1/16" tubing attached to the final chamber in the sequence was attached to the media reservoir using the luer locks and the circuit completed.

To ensure the system was correctly assembled, a 15 mL volume of sterile water was cycled through the system at room temperature to monitor for leaks or structural instabilities prior to use. If systems were deemed to be structurally sound, the assembled QV500 systems were subjected to an additional sterilisation protocol prior to use as noted in section 2.7.4.

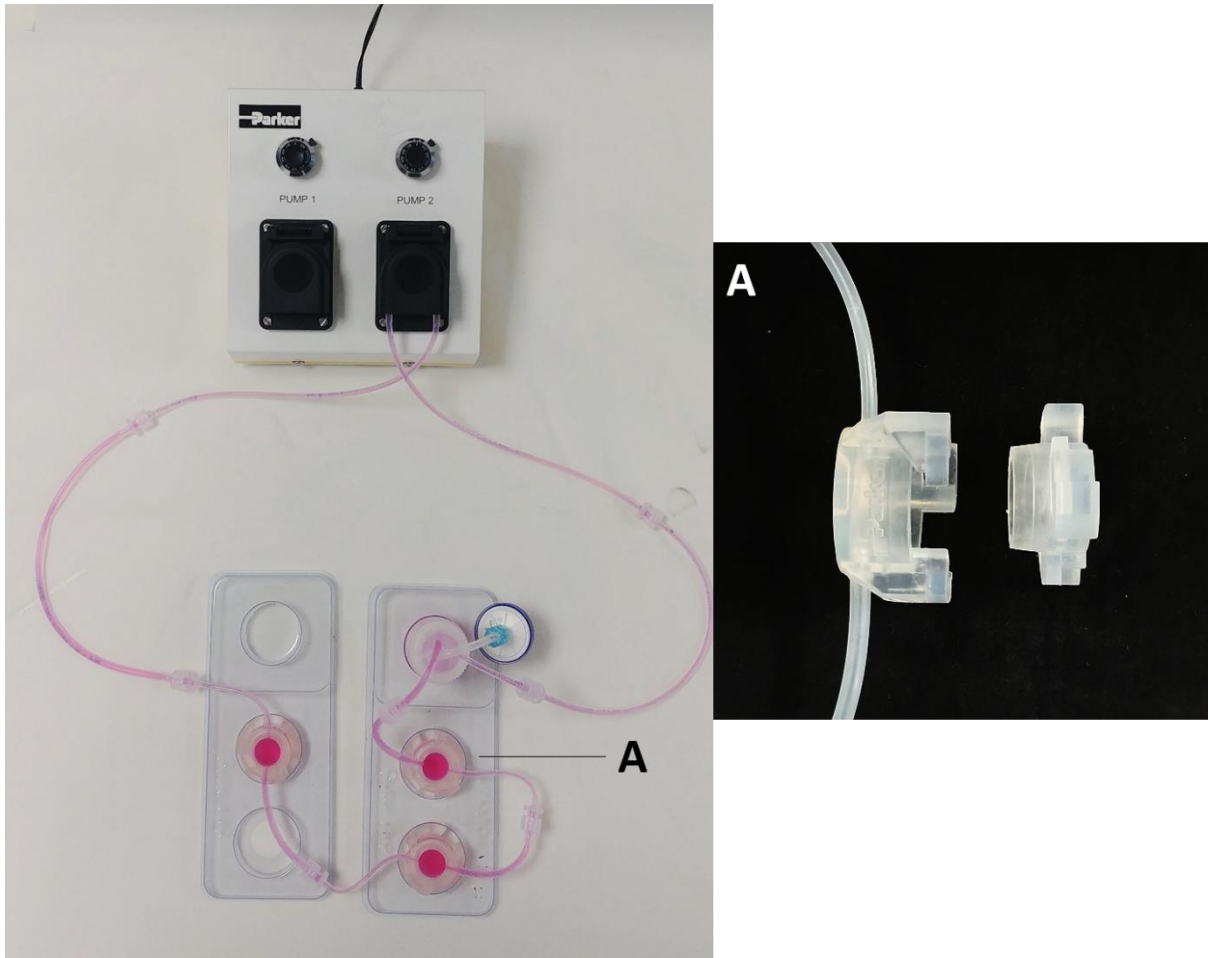


Figure 2-1: Assembled QV500 system attached to a twin mechanism pump. The pictured QV500 system is complete with three experimental chambers, a single medium reservoir, and is filled with cell culture medium. A) QV500 experimental chamber, disassembled. Chambers are composed of two interlocking silicone halves that, when interlocked, provide a gas-permeable, water-tight seal, protecting samples from external influence. Up to three experimental chambers can be used in sequence per experimental cycle.

2.7.3 Calibrating the QV500 system flow rates and synchronising systems for future experiments

An initial calibration of the QV500 systems was performed upon first assembly and every 6 months subsequently to ensure flow rates remained constant throughout the study.

Firstly, the fully constructed QV500 systems were connected to a pump and their media reservoirs filled with sterile PBS. A set of empty weighing vessels were weighed, and their weight recorded.

The pumps were set to full speed to allow the PBS to rapidly fill every section of tubing and every experimental chamber. Once filled with PBS, the final section of tubing responsible for returning the PBS to the reservoir bottle was removed, and the tubing connected to the final experimental chamber was placed into one of the weighing vessels. The system was run for one minute at full speed, at which time the pumps were stopped, the weight of the filled weighing vessel measured, and the process repeated a further two times, totalling three runs in all. After each run cycle, the expended PBS was replaced to ensure the systems would not exhaust their supply of PBS. This process was repeated for each speed setting on the pump ranging from 1 – 10 (maximum speed), and the weights were measured.

The acquired volume of liquid per run was utilised to generate a standard curve expressing $\mu\text{L}/\text{min}$, an example of which can be seen in Figure 2-2. The process noted above was repeated for each QV500 system and a standard curve generated for each. Following the successful generation of a standard curve, each system was assigned an identifier and the speed settings standardised for each system to ensure approximately equal flow speeds to eliminate any potential sources of variation in the study, and ensure the desired flow rate of 1.5 – 2 L/day was achieved in all instances.

Additional calibration cycles were performed in instances where tubing was replaced, be that due to a technical fault or as a result of general maintenance, in order to ensure the replaced tubing did not affect the flow rate of the system in downstream applications.

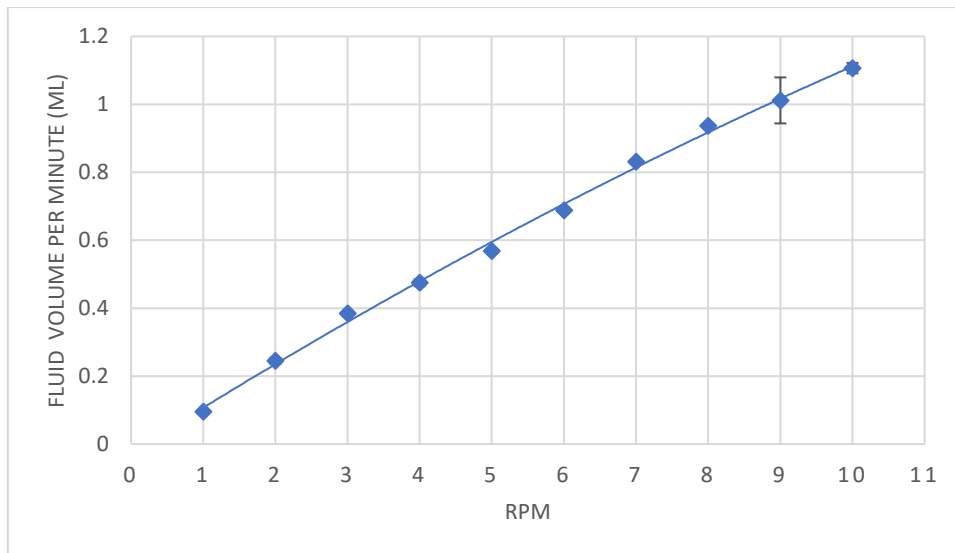


Figure 2-2: Example calibration curve for a single QV500 system generated from three experimental cycles. Maximum speed recorded from a QV500 system was 1.2033 mL/min. The highest speed settings were utilised on every pump system, as it was at this speed where all QV500 systems showed the desired flow rate decided for this project (1.5 – 2 L/day).

2.7.4 Preparing the QV500 system for experiments

The QV500 systems would receive an internal wash with a 70% v/v ethanol solution in dH₂O prior to each experimental cycle. This solution would be loaded into the media reservoir and cycled through the system for 2 hours at room temperature to remove any trace particulates. The system flow would then be reversed, with the spent ethanol returning to the media reservoir to be discarded.

A second wash cycle was subsequently performed using a 10% v/v penicillin/streptomycin solution (pre-mixed and supplied by Sigma Aldrich) in dPBS for 24 hours at room temperature to eradicate any potential contaminating bacteria from the system. The antibiotic solution was also drained from the system and discarded in the same manner as the ethanol solution.

Following this, a non-supplemented cell culture medium – either high glucose DMEM or McCoy's 5A – was passed through the system to remove any traces of ethanol and antibiotic and prolong the lifespan of the QV500 systems by limiting degradation. If

additional sterilisation was required, the QV500 systems were first 24-hour cleaned as outlined above, prior to autoclaving, and finally subjected to an additional cleaning cycle.

2.7.5 Maintaining the QV500 systems

Once monthly, the QV500 would be cleaned internally following the same protocol as outlined above in section 2.7.4, with an ethanol pre-wash followed by a prolonged penicillin-streptomycin clean. An additional secondary 2-hour wash cycle using a 10% v/v amphotericin B solution in PBS was also performed to remove any fungal contaminants.

Following this, the QV500 systems were drained and disassembled before being submerged in a Virkon™ cleaning solution for 10 minutes to perform a deep clean. Each component would then be removed from the Virkon™ solution and submerged in sterile water to remove traces of the Virkon™, preventing lasting damage to the QV500 system.

Following the Virkon™ clean cycle, the systems were reassembled and a final, non-supplemented, high glucose DMEM was flushed through the system to remove any residual traces of Virkon™.

The systems were drained, and experimental chambers inspected visually to check for any remaining residue from experiments. In instances where residue was observed, the system would receive a manual clean before being placed into a large autoclavable vessel and autoclaved. Cleaned systems were stored in full accordance with manufacturer's guidance as per the manufacturer-supplied instructions.

2.8 Experimental setup

Prior to use in experiments, coverslips firstly must have been observed as having a confluent monolayer in the case of intestinal cell lines HCT116, HT29MTX and HT29 using the JuLI™ Br. In the case of Caco-2, as noted above, 21 additional days from confluence must have passed

to have ensured spontaneous differentiation and formation of the characteristic tight junctions and microvilli at the cells' apical surfaces.

Coverslips were transferred to one of the three conditional exposure vessels: a 24-well plate for 1 mL static exposure, a petri dish for 15 mL static exposure or the QV500 dynamic flow-through system for 15 mL flow exposure, using metal tweezers sterilised with 70% v/v ethanol.

To both the 15 mL static and QV500 flow systems, 3 coverslips were added to enable direct comparison between the equivalent volume assays. To each system, an appropriate volume of experimental cell culture medium was added, and the vessels returned to a humidified CO₂ incubator for the duration of the assay.

In instances where additives, conditioned medium or bacteria were added, a non-supplemented cell culture medium was selected as opposed to the experimental supplemented medium noted in Table 2-2.

2.9 Measuring cellular proliferation as a proxy of cellular viability via Tetrazolium 3-(4,5-dimethylthiazol-2-yl)-2,5-diphenyltetrazolium bromide (MTT) assay

Cells were grown on glass 13 mm coverslips as outlined in section 2.6.2 and exposed to flow or static conditions in the manner outlined in section 2.8 above.

Following conditional exposure, cell-coated coverslips were removed from the QV500 experimental flow chambers, or static equivalent, and transferred to a sterile 24-well plate. To each coverslip, 500 µL of a 2.5 mg/mL 3-[4,5-dimethylthiazole-2-yl]-2,5-diphenyltetrazolium bromide (MTT) solution was added and diluted 1:1 in the relevant serum-free cell culture medium.

The cell-treated coverslips submerged in MTT solution were returned to a CO₂ incubator and allowed to develop for 1.5 hours, allowing for the formation of formazan crystals. Following

incubation, excess MTT solution was removed, and coverslips were rinsed gently with warm dPBS to remove traces of MTT solution while ensuring that cells remain adherent.

To each well containing a cell-seeded coverslip, 500 μ L of DMSO was added to solubilise the formazan crystals, and each plate was rocked gently by hand for 2 minutes to aid in the solubilisation process.

Following this, the multi-well plates were transferred to a Tecan multi-well plate reader, and the absorbance was monitored at 490 nm wavelength using installed Magellan software. Each well was read from 16 regions within the well, and the average generated.

For subsequent data analysis and visualisation, R, RStudio and the associated R packages were selected as noted below in section 2.12.

2.10 Measuring cellular viability via the LDH-Glo™ assay

2.10.1 Preparing reagents

Prior to performing the assay, the manufacturer-supplied LDH reductase substrate and LDH detection enzyme mix were removed from -80 °C storage and thawed at room temperature. Having thawed, the substrate solution was stored on ice, while the detection enzyme was allowed to reach room temperature. For each individual reaction, 50 μ L of the detection enzyme was mixed with 0.25 μ L of reagent in a microcentrifuge tube by gently inverting 5 times. Remaining enzyme and substrate solutions were returned to a -80 °C freezer, and the prepared LDH assay solution was stored on ice until ready for use in experiments.

2.10.2 Collecting and preparing cell culture medium for LDH analysis

Cells were prepared for experiments and seeded on coverslips in the manner noted in section 2.6.2 and exposed to the three conditions of interest for this study, those being a 1 mL static

culture, a 15 mL increased media volume static culture and a flow culture in which the QV500 was used. At the designated timepoints, each experiment was transferred from the BINDER CO₂ incubator to a sterile laminar flow cell culture cabinet, ensuring that the coverslips remained undisturbed. From each condition, a 10 µL aliquot of cell culture medium was extracted and transferred to a microcentrifuge tube. In instances where a time course experiment was performed, each experiment was re-sealed and returned to the CO₂ incubator until the next sampling time. Experimental cell culture medium was diluted as recommended by the manufacturer prior to experiments and stored on ice prior to use.

2.10.3 LDH assay protocol

To each well of a white 96-well plate, 50 µL of the diluted cell culture medium was added to 50 µL of the LDH reaction solution. The plate was incubated at room temperature for 45 minutes in the dark, following which it was transferred to the Tecan multi-well plate reader, and luminescence was measured using the luminescence function of the system. This process was repeated for each condition at each desired time-point. For subsequent data analysis and visualisation, GraphPad Prism 8 and its associated t-test and boxplot functions were utilised as noted in section 2.12.

2.11 Image formatting

Where required, figures and images were composited into a single figure/image using the open-source image-editing program Krita ver. 4.0.1, which was selected due to its flexibility and the added ability to export high-quality images.

2.12 Statistical analysis software

Microsoft Excel 365 was utilised for the generation of datasets and for data handling and manipulation prior to statistical analysis. Data was statistically analysed and visualised using GraphPad Prism 8 version 8.4.2.679, R version 3.4.3 and RStudio version 1.1.423 as the analysis software in each instance.

Data was formatted using Excel into .csv format for compatibility with R software packages. R packages Ggplot2 ver. 2.2.1 and dplyr ver. 0.7.4. were utilised for the generation and visualisation of boxplots observed in the following experimental chapters in instances where R was selected as the analysis software of choice.

3 Exploring the incorporation of the QV500 dynamic flow-through system in cell culture research

3.1 Introduction

3.1.1 Exploring the introduction of a dynamic flow as an essential component in cell culture practices

In recent years, numerous systems have been developed with the ultimate aim of addressing the issue of incorporating dynamic flow into cell culture. Despite there being several novel flow models, the high initial investment and continued maintenance costs, coupled with the intensive technical knowledge required to maintain such systems, often poses a barrier to entry, thus limiting the accessibility and subsequent uptake of such systems. As the true impact of flow remains under-explored within the confines of cell culture, it is important to assess the impact that flow might exert on biological parameters.

The majority of cell culture practices are performed using a solid surface to which cells can be applied and adhere to – be that round coverslips (Koh and Lorsch 2013) or cell culture inserts (Lea 2015b) – with the substrate surface varying in accordance with the methodology. It has also been previously discussed that the material used for this adhesive surface plays a vital role in dictating the physiology and growth rates of cell lines in the preparation of cell culture models (Ryan 2008; Scholz 2010).

One could additionally argue that the presence of flow may dictate that the adherence of cells be considered of greater importance due to the risk of these cells becoming dislodged by the flow, which may promote physiological and molecular changes in the cells to ensure successful adherence, as would be found *in situ*.

While the approximate volume of liquid known to flow through the gut varies on a person-by-person basis, in the 2016 study by Cremer and colleagues, it was estimated that the

volume of liquid that passes through the GI tract totals approximately 1.5 – 2 L/day (Cremer et al. 2016). While this is only a general approximation of the liquid that passes through the human gut within a 24-hour period, it inarguably provides valuable insight for flow models when seeking to calibrate systems to equate to that seen *in situ*. Therefore, to accurately understand the impact of flow within a cell culture system, one must compare the effectiveness of flow against the most utilised current practice, that being 2D-static methodologies, as used in most cell culture studies.

3.1.2 Utilising the QV500 to introduce flow to cell culture

As previously mentioned in this thesis, the Kirkstall QV500 cell culture chamber system was selected for this study due to its ease of use coupled with its reusability, and, as such, it was also important to select a number of parameters for monitoring the response of cells and to observe the impact of this system's induced flow on these parameters. Given the many potential stimuli naturally present within the gut, from the wide array of cell types (Quante and Wang 2009), hormone- and metabolite-mediated interactions and the host-specific microbiome interactions (Martin et al. 2019), it must first be noted that modelling the true complexity of the human gut is far beyond the scope of this study and, as such, is not the goal of this study.

The utility of cell culture, as previously described, comes in its ability to provide insight into otherwise difficult-to-access regions of the human body. However, these expansive studies often lack the omnipresent physiological factors seen *in situ* (Kapałczyńska et al. 2018). It could therefore be stated that incorporating dynamic flow into cell culture methodologies via milli- and micro-fluidic methodologies is of great importance when undertaking cell culture studies. Furthermore, the inclusion of dynamic flow and the optimisation of the QV500 for this study stands as the bedrock for the following chapter, particularly with focus given to understanding the impact of a dynamic flow element on measured cellular parameters of health. The primary goal of this chapter is to assess whether the presence of physiological flow significantly alters the behavioural response of cell lines, and if this varies

by passage number or medium composition, to validate the continued use of a dynamic flow-through system in the subsequent study.

3.1.3 The aims of the chapter

1. To optimise the QV500 flow through system for use in conjunction with cell culture.
2. To optimise experimental parameters (including flow rate, experimental coverslip material and serum supplementation) for downstream applications.
3. To assess the impact of flow on the viability of commonly used cell lines.
4. To assess the impact of flow on the cell lines' production of glycoproteins, including mucin via gene expression methodologies.

3.2 Materials and methods

3.2.1 Cells utilised for experiments

Cell lines were all prepared for experiments in the manner outlined in section 2.6. Caco-2, HCT116, HT29 and HT29MTX cell lines were all selected for use throughout the initial aspects of the study, the unique defining characteristics of which can all be seen in Table 2-1.

3.2.1.1 Monitoring cell growth rates on glass and plastic coverslips

Cell lines HT29MTX and Caco-2 were sub-cultured following the protocol outlined in section 2.4.1 and centrifuged at 262 rcf for 5 minutes at 20 °C to allow for the formation of a cell pellet. The waste medium was discarded appropriately and treated with Virkon™, ensuring the pellet remained undisturbed and, following which, the pellet was resuspended using 10 mL of cell culture medium warmed in a water bath set to 37 °C.

Live-dead cell counts were performed on each cell suspension using the Guava® Muse® cell count and analyser apparatus following the protocol outlined in section 2.6.1, and using the total cell counts, a $1.5 - 2 \times 10^4$ live cell/mL density of cells was generated by diluting the initial cell stock in warmed DMEM. A 1 mL volume of the cell suspension was pipetted onto either glass or plastic coverslips housed in a sterile 24-well plate (Greiner Bio One, UK), and the plate was gently rocked by hand by slowly moving the multi-well plate on a solid surface to ensure that the coverslip surface became totally submerged.

The coverslips submerged in cell suspensions were transferred to a humidified CO₂ incubator set to 37 °C for 8 hours to allow for some cellular adherence. Coverslips were visually inspected for adherent cells using the JuLI™ Br cell-imaging system (NanoEnTek, Seoul, Korea). Following this, a single coverslip was selected and placed into a clean well within the same plate, and fresh warmed cell culture supplemented in accordance with the growth medium composition outlined in Table 2-2, which was gently added to the coverslip, ensuring that the adhered cells remain undisturbed.

The JuLI™ Br system camera was transferred to a humidified CO₂ incubator and the coverslip placed into the camera field of view. Camera visuals were adjusted using the auto-focus feature of the JuLI™ Br system and the accuracy of the system assessed using the confluence feature, in which the confluence of the cell monolayer is assessed from a single captured image. In instances where the auto-focus was insufficient, exposure, focus and brightness were manually adjusted and reassessed until the confluence function returned three accurate reads, which were defined by visual assessment of the system's ability to recognise adhered cells. The system was programmed to perform a growth rate analysis over a 72-hour period, with an image captured to assess confluence at 5-minute intervals. These images were analysed by the JuLI™ Br system software and assigned a numeric value relating to the confluence percentage of the image, which was recorded in a separate information sheet. The incubator was sealed for 72 hours and left undisturbed to not impact the final footage by introducing any movement of the coverslip. Following the recording period, the data was collected and formatted using Microsoft Excel 365 before using GraphPad Prism 8 to generate a growth curve for both cell lines on each coverslip type, and

a growth rate was generated. The above process was completed for both Caco-2 and HT29MTX cells on both glass and plastic coverslips.

3.2.1.2 Cellular adherence on coverslips exposed to dynamic flow

Each of the four initial cell lines was grown to confluence on both the glass and plastic coverslips as outlined in section 2.6.2, with Caco-2 allowed to further differentiate for 21 days.

Cell-seeded coverslips were observed prior to experiments at three distinct regions on the coverslip and the confluence ascertained using the JuLI™ Br apparatus. In all instances prior to exposure to dynamic flow, coverslips were observed as being 100% confluent in each of the four regions observed. The cell-seeded coverslips were transferred to the QV500 dynamic flow system, as shown in Figure 3-1 and exposed to a flow environment for 72 hours in a humidified CO₂ incubator.

Following flow exposure, the QV500 systems were drained and coverslips harvested, all while ensuring that the monolayer remain as undisturbed as possible. Cells were re-examined under light microscopy and confluence reassessed to assess cellular adherence following dynamic flow.

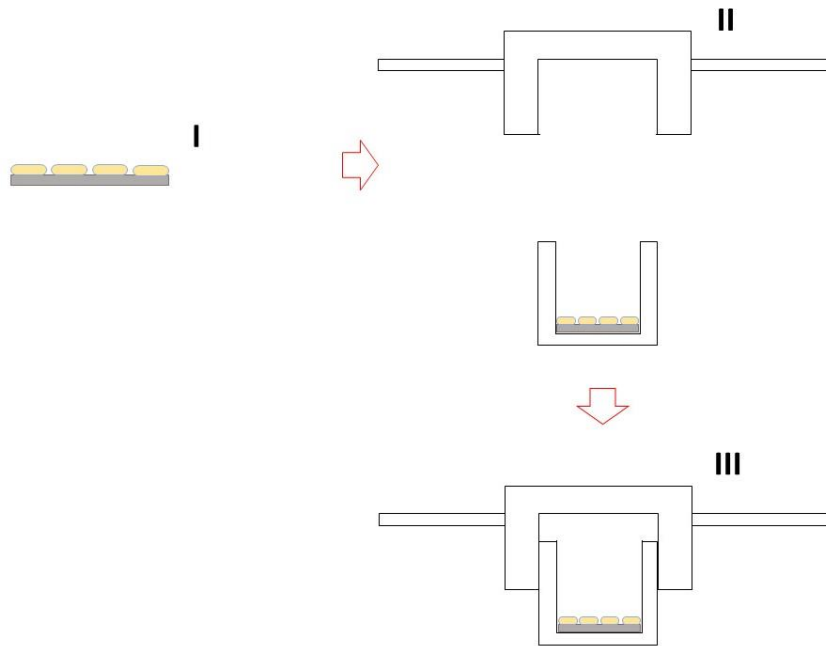


Figure 3-1: Schematic of an assembled QV500 chamber with cell-seeded coverslips. Cell-seeded coverslips (I) were transferred into the bottom component of a QV500 reaction chamber separated into its two halves (II), following which the two halves of the QV500 reaction chamber were re-assembled and sealed to form a water-tight reaction chamber complete with a cell-seeded coverslip (III).

3.2.1.3 Assessing the production of pro-inflammatory cytokine IL-8 and the cellular proliferation of HT29MTX cells under serum-starved and serum-supplemented conditions

3.2.1.3.1 Formulating serum-supplemented and serum-free media

FBS (Sigma Aldrich, UK) and charcoal-stripped FBS (Labtech, USA) were both utilised to prepare a 10% v/v, 1% v/v and 0.1% v/v serum medium for use in the assay, where the relevant serum was thawed using a water bath set to 37 °C, prior to being added to the cell culture medium using a sterile serological pipette. Additionally, a control medium lacking supplemented material (serum-free) was prepared. All media was prepared 24 hours prior to experimental exposure.

3.2.1.3.2 Assessing HT29MTX under various serum exposure conditions

Cells were prepared and grown on glass coverslips following the protocol outlined in section 2.6.2. All cell-coated coverslips were serum starved for 24 hours prior to experimental challenging. Serum starving was achieved 24 hours prior to experimental challenging by removing the growth medium and washing the cell layer with dPBS warmed in a water bath set to 37 °C for at least an hour, before replacing the medium with the appropriate experimental medium, as noted in Table 2-2, in an attempt to acclimatise the cells to the new environment.

Cells were subsequently exposed to a static model, an increased medium volume static model and the QV500-induced flow model for 24 hours, following which the QV500 systems were drained and cell culture medium collected, frozen at -20 °C and stored for any potential future applications. Coverslips were removed from the exposure vessel and transferred to a fresh multi-well plate for analysis via MTT assay.

MTT analysis was performed following the method outlined in section 2.9, and absorbance measured at a 490 nm wavelength using the Tecan multi-well plate reader apparatus as noted in section 2.9. Statistical analysis was performed using GraphPad Prism 8 version 8.4.2.679, using the t-test functionality and visualised with the software's boxplot function.

3.2.2 MTT analysis of cells exposed to periods of dynamic flow

Cells were prepared and maintained in adherence to the protocol outlined in section 2.4 and plated onto glass 13 mm coverslips and prepared for experimental exposure in the manner noted in section 2.6.2 with an initial seeding density of $1.5 - 2 \times 10^4$ live cells/mL.

Cell-seeded coverslips were transferred to the relevant condition, be that the static, increased medium static or flow model, and exposed to flow for 24 hours. Coverslips were collected and exposed to MTT solution (Sigma Aldrich, Poole, UK) following the protocol outlined in section 2.9. Coverslips were collected and the stain solubilised using DMSO in

the same manner as outlined in section 2.9, before having the absorbance read in a Tecan multi-well plate reader set to a wavelength of 490 nm.

3.2.3 LDH analysis of cells exposed to dynamic flow

In an identical manner to that noted in the above section 3.2.2, coverslips were seeded with HT29MTX and Caco-2 cells and maintained until confluent. Cells were exposed to the relevant experimental model: static, increased medium static or flow. Cells were returned to a humidified CO₂ incubator for 72 hours. At 24-hour intervals, a small quantity of the cell culture media was collected from each experimental condition and prepared following the protocol outlined in section 2.10 before mixing with an LDH assay solution. Supernatant and reaction mixes were incubated at room temperature for 45 minutes before luminescence was measured using the luminometer function of a Tecan multi-well plate reader. Data was exported to Microsoft Excel and formatted before being statistically analysed and visualised using GraphPad Prism 8.

3.2.3.1 Alcian blue glycoprotein assay

3.2.3.1.1 Preparing cells for alcian blue staining

HT29MTX cells were grown as outlined in section 2.4 and sub-cultured in a similar manner to that outlined in section 2.4.1 until the formation of a pellet.

Cells were resuspended in cell culture medium warmed to 37 °C in a water bath. Cells were subsequently assayed for viability and live-dead percentage by utilising the Guava® Muse® cell analyser methodology outlined in section 2.6.1, before being diluted to $1.5-2 \times 10^4$ live cells/mL.

The diluted cell suspensions were plated into 96-well plates, with 100 µL of the cell suspension added per well. Cell-seeded microplates were returned to the humidified CO₂

incubator for 24 hours before removing the media and visually observing the monolayer using the JuLI™ Br cell imaging system. Cell-seeded microplates were monitored daily via the JuLI™ Br and the medium was replaced every 1 – 2 days until confluent monolayers were observed. As noted previously, Caco-2 samples were allowed to differentiate over a 21-day period prior to experimental challenging, while being monitored daily to ensure monolayer integrity.

3.2.3.1.2 Assessing stain exposure duration

Cells were first washed using dPBS warmed to 37 °C in a water bath, ensuring the monolayer remained undisturbed. Following this, 100 µL of the 1% w/v alcian blue solution, prepared using 3% v/v acetic acid (Sigma Aldrich, Poole, UK), was added to each well and allowed to develop for one of the following durations: 1 minute, 5 minutes, 10 minutes, 30 minutes, 1 hour and 2 hours. Additionally, a separate control plate was treated with dPBS only in place of alcian blue for the duration of the staining period.

Following the desired exposure period, excess alcian blue stain solution was removed, and wells were gently washed with warm dPBS containing 0.05% w/v Tween-20 (Sigma Aldrich) 5 times to remove excess stain, taking care to avoid disrupting the monolayer. Tween-20 supplementation in dPBS was added following consultation with Prof. Nathalie Juge (pers. comm.) to ensure the glycoproteins remained undisturbed during the extensive wash process. Wells were visually observed post-wash to assess colour development (data not included).

3.2.3.1.3 Optimising alcian blue stain release

Stained cells were submerged in multi-well plates containing a range of potential solvents, those being dimethyl sulphoxide (DMSO), absolute ethanol and 10% v/v solutions of acetic acid and hydrochloric acid prepared using 1 M stocks. Cells were submerged for 3 hours and visually inspected following 5 minutes exposure to the solvents and subsequently at 30-minute intervals for monitoring of the stain release from the cells into the assessed solvents.

Following the initial optimisation, an additional cycle was performed using the perceived optimal solvent, acetic acid, in which the plates shaken gently for 5 minutes at initial exposure (T0) and again at 30 minutes. A trio of controls were also performed, where cells were shaken at T0 only, at 30 minutes only and with no shaking. Shaking was performed by placing the multi-well plate containing the cells and acetic acid on a flat surface and moving the plates in a circular motion for 5 minutes. Shaking was performed rapidly enough to allow for agitation of the solubilising agent, thus promoting stain release, while simultaneously being gentle enough so that the liquid remained in the relevant wells, thus ensuring that all experiments remained bias free. At each stage, cells were visually inspected to assess the impact of shaking in conjunction with exposure to acetic acid.

3.2.3.1.4 Attempting to develop a standard curve methodology for the alcian blue glycoprotein production assay

Porcine mucin (Sigma Aldrich, Poole, UK) was first solubilised to a concentration of 1 mg/mL in PBS by continuously stirring using a magnetic stirrer at room temperature for 2 hours. Solubilised mucin suspensions were visually assessed to ensure complete solubilisation prior to performing dilutions. If mucin was not successfully solubilised, the solution was returned to a magnetic stirrer and assessed visually at 30-minute intervals until solubilised. Mucin solutions were diluted by a factor of 2 until a final concentration of 7.8125 µg/mL of mucin was achieved. The exact concentrations used for this experiment were as follows: 1000 µg/mL, 500 µg/mL, 250 µg/mL, 125 µg/mL, 62.5 µg/mL, 31.25 µg/mL, 15.625 µg/mL and 7.8125 µg/mL.

The above-noted mucin concentrations were plated in a 96-well high-bind microplate and placed into a fridge set to 4 °C overnight to promote adhesion of the mucin to the treated cell surface.

Following the adhesion period, the microplate was removed from the fridge and excess mucin solution removed and discarded, following which plates were washed twice gently using Tween-20 supplemented dPBS to remove residual unbound mucin. Mucin-treated microplates were exposed to the 1% v/v alcian blue solution as noted above in section

3.2.3.1.2 for 5 minutes before any excess stain solution was removed. Microplates were rinsed using warm dPBS to remove residual stain and allowed to air-dry. Stained microplates were finally exposed to a 10% v/v acetic acid as also noted in section 3.2.3.1.3.

Prior to assessing the microplates, the optimal absorbance wavelength for the qAlcian blue was first estimated using an absorbance scan method using the Tecan multi-well plate reader. A scan range between the wavelengths of 230 nm and 1000 nm was selected, and the alcian blue solution was assayed in triplicate at each wavelength, resulting in the generation of an alcian blue absorbance profile (Figure 3-2). Following initial analysis, it was decided that 580 nm was the optimal absorbance for this method due to the high absorbance peak recorded and its positioning following a number of reduced absorbance wavelengths. As such, 580 nm absorbance was utilised in any subsequent experiment utilising alcian blue.

3.2.3.1.5 Finalised alcian blue glycoprotein assay

Cells were grown to confluence on glass coverslips in the same manner as noted in section 2.6.2, with Caco-2 cells allowed to differentiate for 21 days prior to experimental challenging. When confluent, cell-coated coverslips were transferred to one of three experimental conditions, those being 1 mL static, 15 mL static and 15 mL QV500-mediated flow, with the exact details outlined in section 2.8, each containing a supplemented experimental medium, the formulation of which can be seen in Table 2-2. Cells were exposed to the relevant condition for both 48 hours and 72 hours before the medium was removed and the coverslips were gently transferred to a fresh multi-well plate, ensuring that no damage occurred to the coverslip and that the cell monolayer remained undisturbed.

To each coverslip, 500 μ L of 1% w/v alcian blue solution (Sigma Aldrich, Poole, UK) was added before recovering the plate with its lid and allowing stain development for 30 minutes at room temperature. Excess alcian blue solution was removed and coverslips transferred to a fresh multi-well plate, in which the coverslips were washed 5 times with a

warm dPBS solution supplemented with 0.05% w/v Tween-20 to remove any residue alcian blue. The rinsed coverslips were transferred to a final multi-well plate ensuring that the coverslips and monolayer remained undisturbed and that cells were allowed to air-dry for 1 hour. To the dried coverslips, 500 μ L of 10% v/v acetic acid in dH₂O were added and incubated at room temperature for 30 minutes. Following the incubation period, the multi-well plate was shaken gently for 5 minutes to aid with stain solubilisation.

3.2.3.2 Measuring glycoprotein production via alcian blue (absorbance measurement)

Multi-well plates were placed into a Tecan multi-well plate reader and absorbance was measured at a 580 nm wavelength with four reads per well. The above process was repeated for each cell line at the 72-hour timepoint.

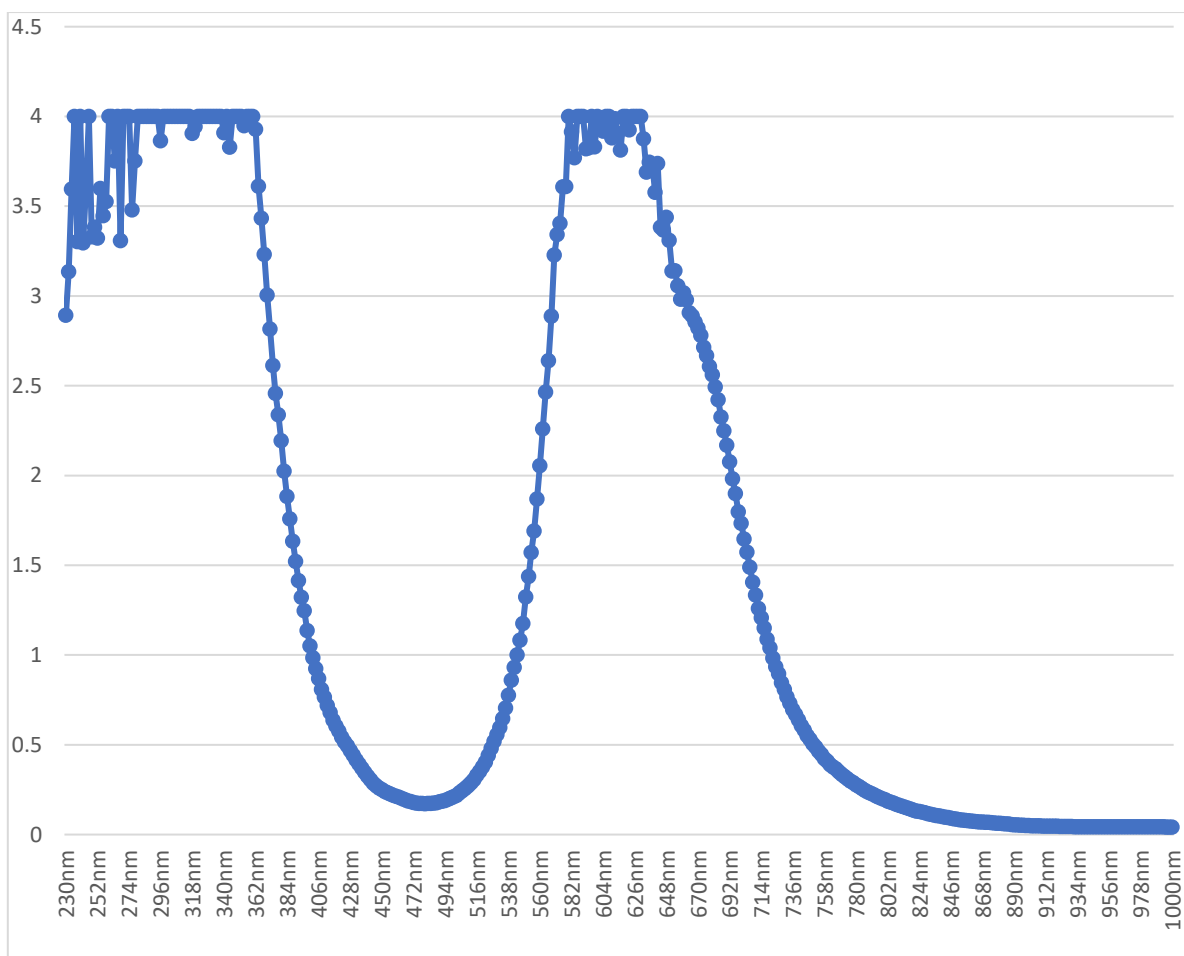


Figure 3-2: Absorbance scan of alcian blue in 96-well plate for method optimisation. Absorbance was recorded twice for each well with the average absorbance estimated for each wavelength between 230 and 1000 nm.

3.2.3.3 Assessing the production of glycoproteins via light microscopy

Cell-seeded coverslips were prepared following the protocol outlined in section 2.6.2 and experimentally challenged in the same manner as outlined in section 2.8, before being collected and transferred to a multi-well plate.

Coverslips were inspected visually to ensure that monolayers remained undisturbed via light microscopy prior to the fixation process. If cells were observed as adhered, coverslips were submerged in a 4% v/v paraformaldehyde solution (Sigma Aldrich, Poole, UK) for 15 minutes at room temperature before aspirating the paraformaldehyde solution and discarding appropriately. Coverslips were subsequently treated with 1% w/v alcian blue solution at room temperature, before being washed gently with dPBS supplemented with 0.05% w/v Tween-20 5 times to ensure removal of residual staining. Cells were additionally stained with a nuclear fast red counterstain (Sigma Aldrich, Poole, UK) for 5 minutes at room temperature before once again being washed 5 times with dPBS with 0.05% w/v Tween-20. Stained cells were stored in dPBS at 4 °C prior to mounting to maintain cellular integrity and prevent fixed cells from drying out.

Coverslips were mounted on glass microscope slides, with the cell-adhered surface placed away from the glass coverslip. To the cell-treated surface, 100 µL of DPX mounting solution were added, following which a 13 mm square coverslip was placed above the cell-adhered coverslip and pressed gently to disperse any air bubbles. The cells and mounting solution were left at room temperature for 5 minutes, following which mounted cells were bound in place using clear nail polish, which was placed at the edges of the square 13 mm coverslip and allowed to air-dry. Prepared coverslips were stored for up to 48 hours in the dark prior to visualisation via light microscopy to limit potential degradation.

3.2.3.3.1 Visualising glycoprotein via microscopy

Microscopy was performed using the Leica DMRB brightfield photomicroscope equipped with a Jenoptik ProgRes® SpeedXT core 3 colour digital camera (Jenoptik, Germany). A 20× objective was utilised for the acquisition of the images, and the ProgRes® CapturePro software was utilised to perform white balance and image optimisation prior to image capturing. Images were exported in .JPEG format and composited together using Krita ver. 4.0.1 (KDE Community 2020).

3.2.3.3.2 Extracting RNA from experimental samples for qPCR analysis

Following an experimental cycle in which cell-seeded coverslips were prepared according to the protocol outlined in section 2.6.2 and exposed to the experimental conditions outlined in section 2.8, coverslips were collected and transferred to a fresh 24-well plate, while ensuring that there was no disruption to the cell monolayer or damage incurred by the coverslip.

Coverslips were washed gently with warm dPBS to remove any trace medium before submerging the coverslip in 500 µL of TRIzol® solution. Cells were incubated at room temperature for 5 minutes in the TRIzol® solution before the TRIzol® was triturated several times to aid with extraction of nucleic acid material. Following the incubation and titration, the TRIzol® solution was removed from the cells and stored in an appropriate volume cryovial. Due to the small cell number present on the coverslips, TRIzol® samples from three coverslips were pooled in each instance. TRIzol®-treated samples were stored at -80 °C for up to one month before use in cDNA synthesis.

TRIzol® samples were collected from -80 °C and brought to room temperature before 0.2 µL of chloroform was added for every 1 mL of TRIzol®. The chloroform-TRIzol® mixture was inverted continuously for approximately 15 seconds until a clear, colourless region was observable at the top of the solution when allowed to settle.

The solution was centrifuged for 15 minutes at 17,000 rcf at 4 °C to allow phase separation. Following this step, the clear RNA phase was extracted from the top of the microcentrifuge tube, taking care not to contaminate the sample with genomic DNA, and transferred to a fresh microcentrifuge tube and the remaining pink protein and genomic phases were disposed of.

To the collected RNA phase, 0.5 mL of isopropanol was added for each 1 mL of TRIzol® present in the initial stages, and this mixture was inverted by hand continuously for 10 seconds. The isopropanol mix was transferred to a -80 °C freezer for one hour, as this method had been noted as having an increased yield compared to that seen from extractions conducted following the on-ice method recommended by the manufacturer.

Having conducted the long -80 °C incubation, the microcentrifuge tube was thawed at room temperature and centrifuged for 10 minutes at 17,000 rcf to form a pellet. Ensuring that the pellet was not lost, the isopropanol was removed and the microcentrifuge tube blotted dry using paper towels. To each microcentrifuge tube, 1 mL of ethanol was added before being rapidly vortexed for 10 seconds, and the microcentrifuge tube was re-centrifuged at 7,500 rcf for 5 minutes. The above step was repeated a further three times with fresh ethanol, and on the final wash, the ethanol was removed, and the pellet allowed to air-dry. The pellets were resuspended in 20 µL of nuclease-free water and stored for a maximum of 24 hours at -20 °C prior to cDNA synthesis due to reduced stability of mRNA compared to cDNA.

3.2.3.3.3 Measuring RNA concentration using the Qubit™ 3.0 fluorometer

Prior to undertaking cDNA synthesis, the RNA concentrations of each solution were acquired using the Qubit™ High Sensitivity RNA kit (ThermoFisher, UK). The standards for the Qubit™ 3.0 Fluorometer were pre-performed prior to the assay and, as such, were not performed. RNA samples were thawed and stored on ice for the duration of the assay to minimise RNA degradation.

Qubit™ reagents were brought to room temperature prior to undertaking the assay, which was performed in accordance with the manufacturer's guidelines. A final volume of 20 µL was selected for each assay, and the RNA sample was diluted in Qubit™ working solution and allowed to rest at room temperature for 2 minutes prior to reading in the Qubit™ apparatus. Each sample tube was inserted into the chamber before closing the lid and running the assay. The concentration was recorded in each instance and the process repeated for each sample.

3.2.3.3.4 cDNA synthesis

Using the concentrations produced by the Qubit™ 3.0 fluorometer, the required volume for a working concentration of 1 ng/mL RNA was calculated. To conduct the cDNA synthesis, the High Capacity cDNA Reverse Transcription Kit (Life Technologies, Paisley, UK) was utilised. Following the manufacturer's guidelines, nuclease-free H₂O, reverse transcriptase (RT), random primers, dNTPs, an RT buffer and 1 ng of the prepared RNA sample were added to a sterile PCR tube. Tubes were appropriately labelled and transferred to a thermal cycler programmed to undertake amplification. Following the completion of the cycle, cDNA samples were transferred to an appropriate storage vessel and stored at -20 °C until required. This process was repeated for each sample as required.

3.2.3.3.5 Identifying primers for MUC qPCR analysis

To prepare primers for MUC genes, previously utilised qPCR primers from a number of academic publications were selected and analysed using the NCBI primer-BLAST tool (NCBI 2020) to identify the specificity of the primers. In instances where the primers lacked specificity, these primers were discarded and alternative primers sought and the process repeated. The online primer repository oliGO! (oliGO! 2018) was ultimately utilised as the primary source of many primer sequences due to returning a high binding specificity percentage and producing accurate targeting for the genes of interest.

The housekeeping gene glyceraldehyde 3-phosphate dehydrogenase (GAPDH) was selected to aid in normalising the qPCR MUC gene counts, and primers were generated using the primers found on the online primer repository oliGO!

All primers used in the study were synthesised by Eurofins Genomics (Germany). Primer sequences used for the MUC qPCR can be seen in Table 3-1.

Table 3-1: Primer sequences for MUC qPCR.

Primer name	Primer sequence (5' – 3')	Source
MUC2 (Forward)	CAGCACCGATTGCTGAGTTG	(Cobo et al. 2017)
MUC2 (Reverse)	GCTGGTCATCTCAATGGCAG	(Cobo et al. 2017)
MUC5AC (Forward)	TCCACCATATAACGCCACAGA	(Matull et al. 2008)
MUC5AC (Reverse)	TGGACGGACAGTCACTGTCAAC	(Matull et al. 2008)
MUC5B (Forward)	ACGTCAAGGCCACAGCTATT	(Kumar et al. 2016)
MUC5B (Reverse)	AGGTGGGAGGCTCCTCTG	(Kumar et al. 2016)
GAPDH (Forward)	CTTTTGCCTGCCAGCCGAG	(oliGO! 2018)
GAPDH (Reverse)	GCCCAATACGACCAAATCCGTTGACT	(oliGO! 2018)

3.2.3.3.6 RT-qPCR protocol

Real-time qPCR amplification was performed using the iTaq Universal SYBR Green SuperMix (Bio-Rad, Hemel Hempstead, UK) in accordance with the manufacturer's guidelines. To each well of a skirted 96-well qPCR plate (Bio-Rad, Hemel Hempstead, UK) 10 µL SYBR green, 50 mM of the forward and reverse primers, 1 µL cDNA and 8 µL nuclease-free H₂O were added. Plates were sealed using a sealing film and transferred to a CFX Connect™ Real-Time Instrument (Bio-Rad), in which an initial melting cycle at 95 °C for 5 minutes, followed by 40 cycles of melting (94 °C for 15 seconds), annealing (60 °C for 15 seconds) and extension (72 °C for 30 seconds) were performed. Fold changes were calculated following the methodology outlined in (Michael et al. 2016) where "fold changes in transcript level were

determined using $2^{-(\Delta Ct1 - \Delta Ct2)}$, where ΔCt represents the difference between the threshold cycle (CT) for each target gene" (those being MUC2, MUC5AC and MUC5B in this instance) and the GAPDH housekeeping gene.

A control sample for each gene lacking the reverse transcriptase was utilised in each experiment to ensure the accuracy of each sample and that the observed trends were not induced by the presence of contaminating DNA.

Generated data was exported to Microsoft Excel 365 for initial analysis and data processing prior to statistical analysis using the software R and RStudio associated packages, all of which are as noted in section 2.12.

3.3 Results

3.3.1 Cellular adherence and growth rates of cell lines Caco-2 and HT29MTX on solid substrates

Prior to introducing cells to the experimental challenge, it was essential to optimise cell growth and adherence to the desired coverslips, as these would play an important role in the upcoming study. The final growth rates for Caco-2 and HT29MTX cells seeded onto 13 mm circular glass coverslips and 13 mm cell culture treated Nunc.™ Thermanox™ plastic coverslips that were monitored over a 48-hour period can be seen in Figure 3-3.

In the case of HT29MTX, samples seeded on Thermanox™ coverslips were observed as having a slower growth rate when compared to the equivalent cell line plated on a glass coverslip of equal size. In the case of Caco-2, while initial confluence was higher in Thermanox™ seeded samples compared to glass, confluence was noted as having decreased over the observed 48 hours. However, in glass seeded samples, while initially a lower adherence was observed, cell growth over the observed period was consistent. Additionally, the final confluence percentage at the final timepoint of 48 hours in HT29MTX samples was

considerably lower in Thermanox™ coverslip-plated samples compared to glass coverslips, suggesting that Thermanox™ coverslips are a sub-optimal surface for this cell line. While the final confluence percentage of Caco-2 cells plated to glass coverslips was lower than that of the Thermanox™ plated samples, the negative trend observed in the Thermanox™ samples made them an undesirable prospect for use in downstream applications in this study.

With regard to the adherence of cells to the assessed coverslip materials, a slight variation was observed in overall cellular adherence upon visual examination (data not included). In the case of HCT116, some cells were lost across both coverslip materials, with a reduced confluence observed following exposure to dynamic flow. However, in the case of the glass coverslips, an increased retention was observed compared to the plastic, where, in each instance, all cells were lost under flow. HT29, HT29MTX and Caco-2 showed a slight reduction in adherent cells when grown on treated plastic coverslips following exposure to flow, whereas with the glass coverslips, in all instances, each cell line showed no visible reduction in cell adherence following a period of flow exposure (data not included).

Having identified that plastic coverslips resulted in a slower growth rate of the cell lines of interest, in conjunction with the improved cellular adherence and retention rate of glass coverslips under flow conditions, in spite of their fragility, glass coverslips were selected in favour of the more durable plastic due to the significantly increased speed at which confluence was reached that might, in turn, help in balancing the time limitations imposed by the QV500 system.

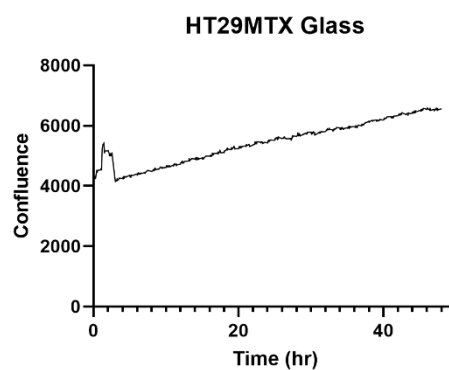
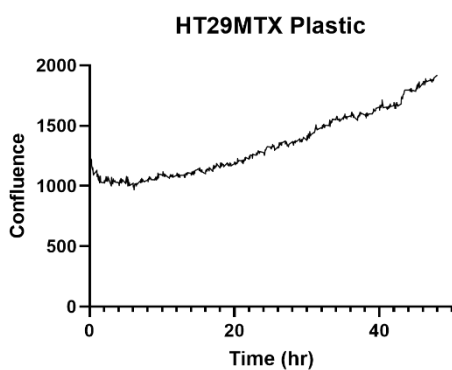
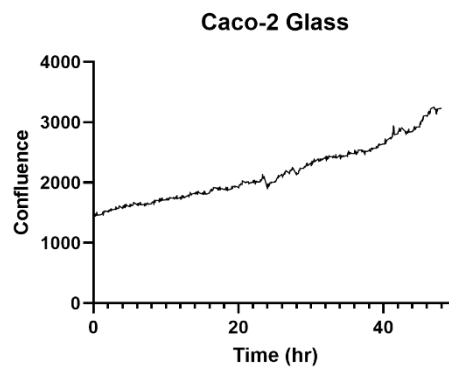
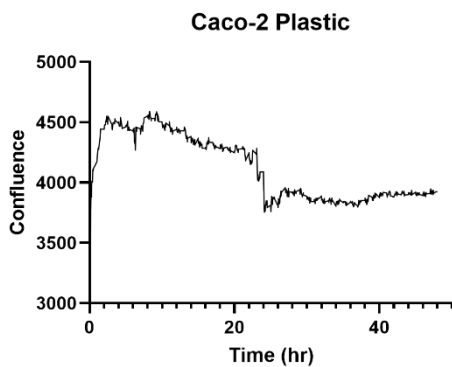
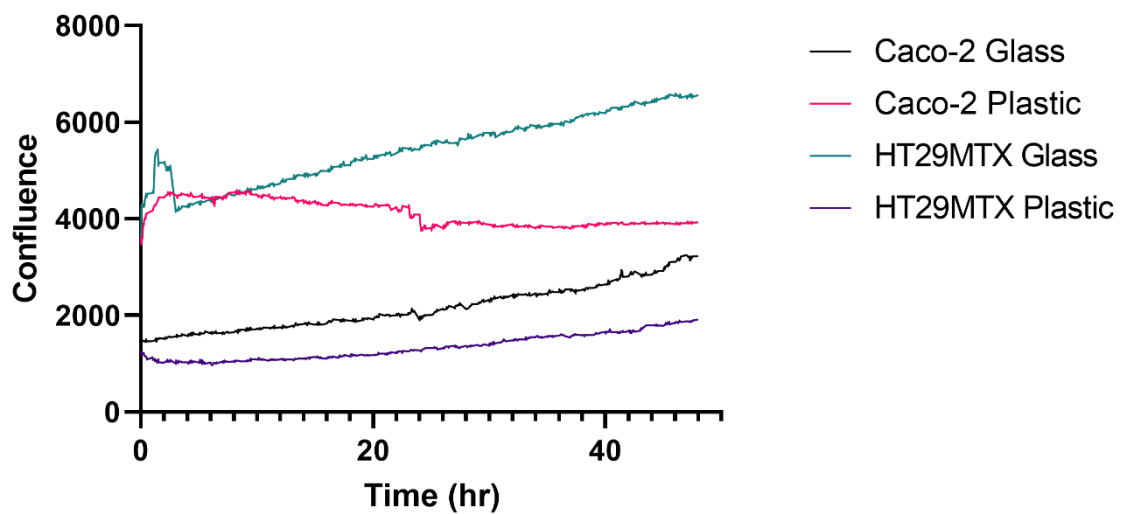


Figure 3-3: Caco-2 and HT29MTX growth on plastic and glass coverslips over a 48 hour period. Due to inter-sample variation in initial confluence recorded following coverslip seeding, the above results represent a single run on each coverslip material for each cell line. Trends observed were consistent across all experimental runs, only varying as a result of initial adherent cell density. "Confluence" relates to confluence percentage $\times 100$.

3.3.2 Identifying the optimal media formulation and the impact of FBS in prolonged experimental exposure via MTT assay

It was decided that, to assess the optimal experimental medium to proceed with the study, three experimental conditions would be examined, those being the commonly utilised FBS and serum-free conditions, and a third alternative, a charcoal-stripped FBS, produced by Labtech (USA). HT29MTX cells displayed alterations in cellular viability in all assessed conditions following a 24-hour exposure period to the media formulations containing various concentrations of FBS and csFBS (Figure 3-4).

Samples exposed to charcoal-stripped FBS displayed a dose-dependent increase in cellular proliferation all experimental conditions, with the highest concentrations of csFBS showing the highest viability of the three concentrations tested, although no significance was observed between the three csFBS concentrations under any condition. Additionally, it was noted that, in the case of csFBS, HT29MTX cells showed a reduced viability at lower concentrations compared to the serum-starved control samples, with the sole exception being those samples exposed to 10% csFBS under flow conditions (Figure 3-4). This reduction in viability, compared to serum-starved samples, was statistically significant in the following 15 mL static and flow-exposed samples: 15 mL static 0.1% and 1% csFBS samples and flow-exposed 0.1% csFBS samples (15 mL static: 0.1% csFBS $p < 0.001$, 1% csFBS $p < 0.05$; Flow: 0.1% csFBS $p < 0.05$). Although the trend observed in all three samples was similar, the degree of this trend varied by exposure condition. As such, as csFBS was observed as having a consistent reduction in cellular proliferation across all exposure conditions compared to the serum-free control, csFBS-centred medium composition was discarded from future experiments.

FBS-challenged samples displayed a somewhat more varied response across all conditions, with 1 mL static samples showcasing a slight dose-dependent increase in viability, and both 15 mL static and flow samples displaying a somewhat more variable trend. No significant differences in viability were observed when comparing FBS concentrations.

As there were no statistically significant benefits observed at any concentration of FBS when compared to the serum-starved control, it was decided that serum-starved medium would instead be utilised for any downstream assays. The use of serum-free conditions in future experiments was additionally reinforced as, in a serum-free experimental medium, there would be no growth factors, hormones or inflammatory molecules present from the FBS that might otherwise influence cellular behaviour or cellular response to a given stimulus, and as the influence of these additional factors introduced by FBS could not be verified at this time, serum-free medium was selected.

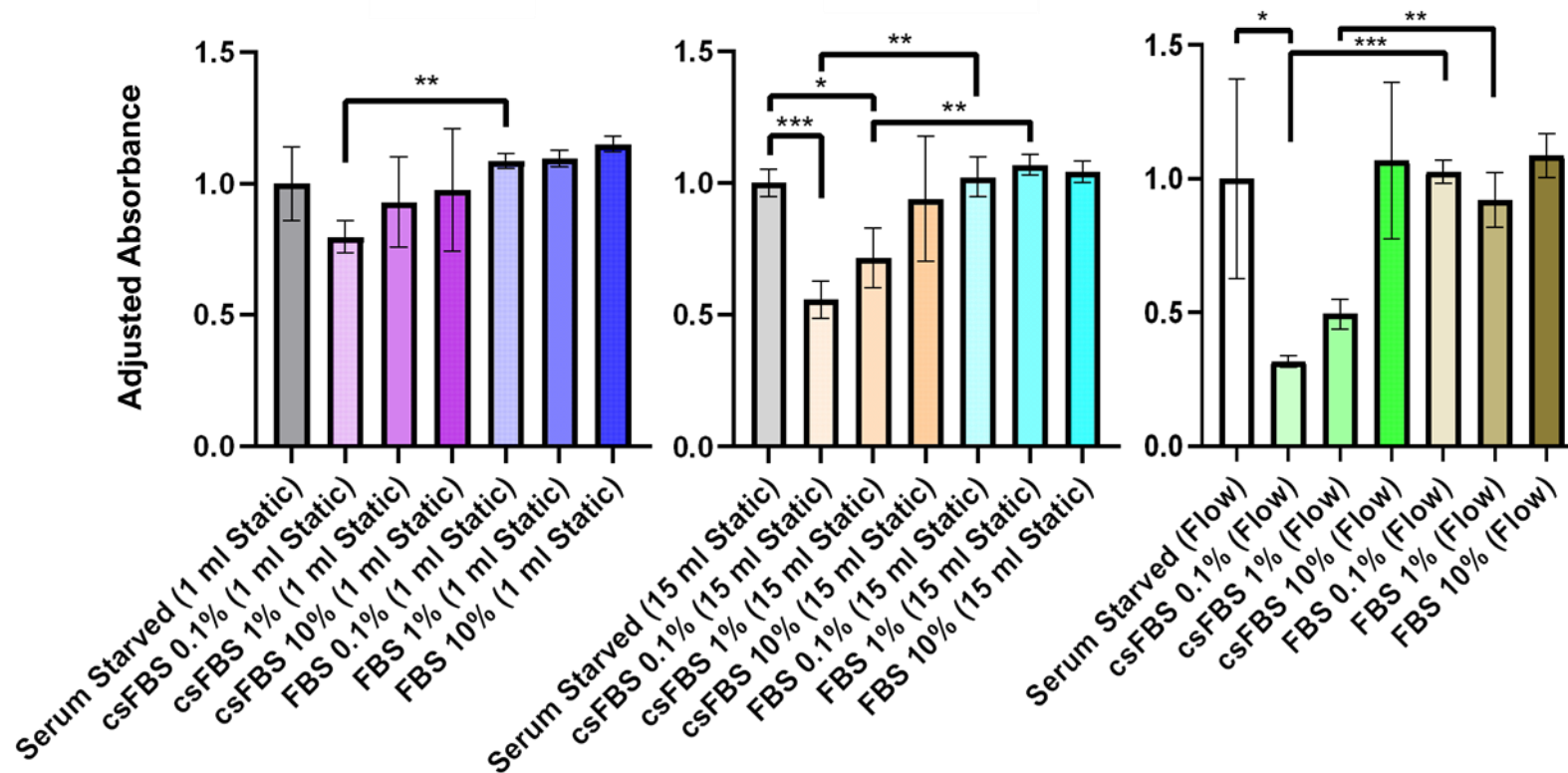


Figure 3-4: Assessing the impact of serum on the cellular proliferation of HT29MTX cells via MTT assay. HT29MTX cells were exposed to serum-free, csFBS- and FBS-supplemented DMEM for 24 hours under either 1 mL static, 15 mL static or flow conditions, following which cellular proliferation was measured via the MTT assay. The data represent the mean ± standard deviation (SD) of 3 independent experiments and are presented as fold-change compared to the serum-starved control that has been arbitrarily set as 1. Statistical analysis was performed using unpaired t-test where * p < 0.05, ** p < 0.01, *** p < 0.001.

3.3.3 Measuring the cellular proliferation of intestinal cell lines following exposure to dynamic flow via MTT assay

As time had not previously been observed as significantly impacting cellular viability, it was important to first ascertain whether the exposure time exerted an additional effect on the cell lines. Cell samples within the study were all noted as being within the passage window recorded in Table 2-1, to additionally assess the impact of passage on cellular behaviour *in vitro*.

While some variation was observed with cells of a different passage number, no significant difference was noted between passage, inferring that the results generated were a consequence of the conditional exposure.

No significant difference was observed in any cell line at the 24-hour timepoint when comparing experimental conditions (Figure 3-5). A minor increase in cellular proliferation was observed in the flow-exposed cells at the 24-hour timepoint in cell lines Caco-2, HT29 and HT29MTX, and in all cell lines, cellular proliferation was elevated in increased medium volume (15 mL) experiments, though no significance was noted in any cell line.

Caco-2 exhibited significant increases in cellular proliferation following 48-hour exposure to experimental conditions (Figure 3-5). A significant change in MTT cellular proliferation was observed in both increased media (15 mL) and flow experiments when compared to cell culture methods, with the greatest significance noted in the flow cohort ($p < 0.05$).

Following exposure to experimental conditions for 72 hours, it was noted that in cell lines HT29 and HCT116, there was significantly increased cellular proliferation at 72 hours. HCT116 cell lines showed significantly increased cellular proliferation when exposed to flow conditions when compared to both the 15 mL increased medium static ($p < 0.05$) and static methodologies ($p < 0.01$). HT29, however, displayed an inverse behaviour. A general trend of reduced cellular proliferation in both the 15 mL increased medium static samples and flow-exposed samples when compared to the 1 mL static samples was seen in the assessed

HT29 samples, with a significant reduction in cellular proliferation recorded in the static 15 mL increased medium samples compared to the 1 mL static exposed samples ($p < 0.05$).

Cell lines Caco-2, HT29MTX and HCT116 displayed similar trends at each timepoint, with elevated cellular proliferation observed in flow samples compared to static methodologies. However, HT29 displayed a varied response, although a general trend of decreased cellular proliferation over time could be seen, with a significantly negative impact noted at 72 hours (Figure 3-5). Cell lines should, therefore, be noted as having a cell-line-distinct response to specific stimuli, and variation is also noted to be induced by temporal variation across individual cell lines. Additionally, cell lines could be noted as being either well suited or incompatible for use within a physiologically representative environment – thus suggesting a need for a preliminary evaluation of cell lines when adjusting established cell culture protocols to incorporate a flow or other physiologically relevant condition.

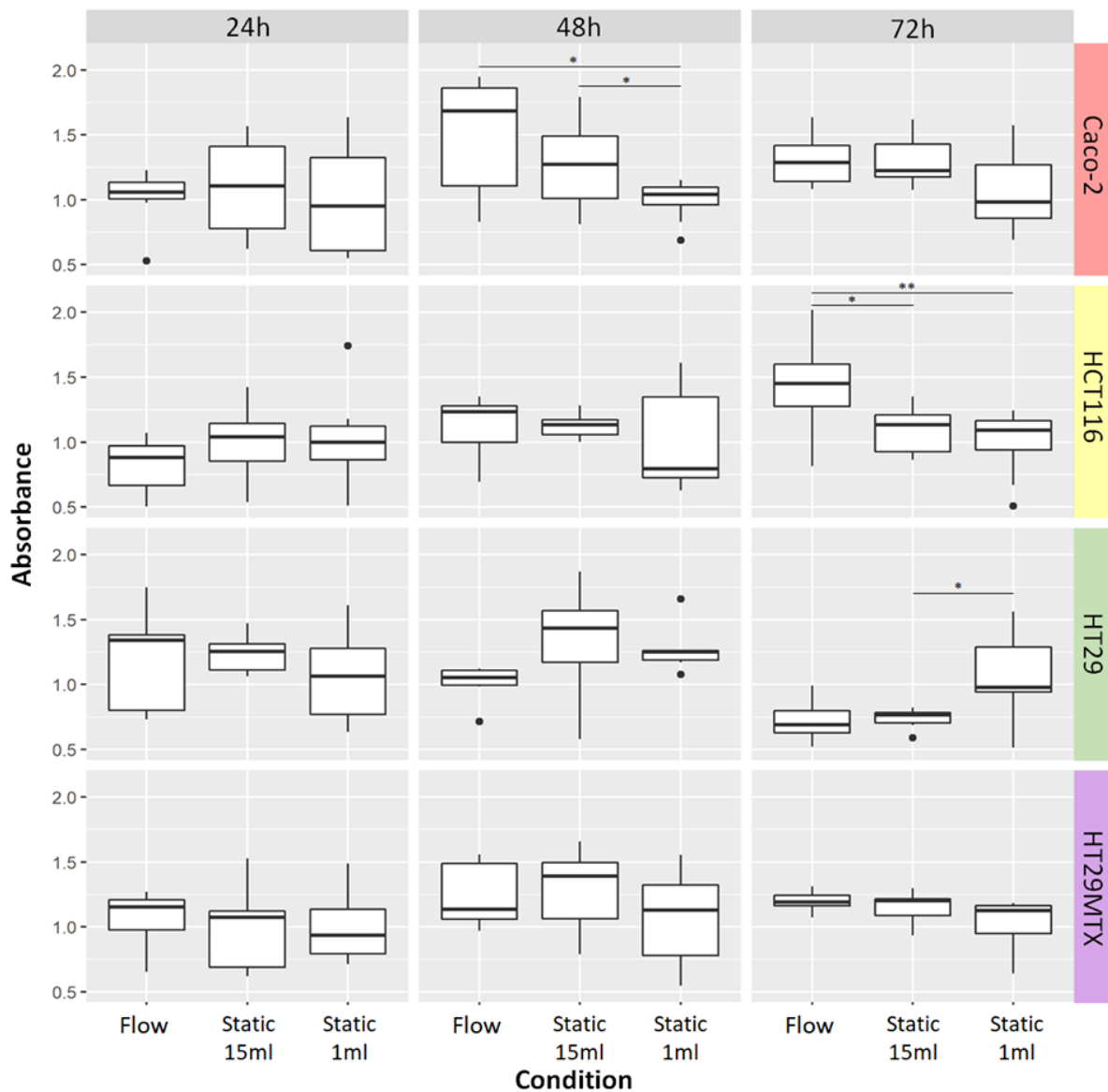


Figure 3-5: Cellular proliferation of intestinal cell lines following periods of exposure to increased medium volume and a physiological flow element. Cell lines Caco-2, HCT116, HT29 and HT29MTX seeded glass coverslips were exposed to either static (1 mL or 15 mL) or flow conditions and assessed at either 24-, 48- or 72-hours exposure for cellular proliferation using the MTT assay. The data represent the mean±standard deviation (SD) of 3 independent experiments (containing triplicate samples of each condition) and are presented as fold-change compared to the control at each timepoint that has been arbitrarily set as 1. Statistical analysis was performed using the unpaired t-test where * $p < 0.05$, ** $p < 0.01$.

3.3.4 Measuring cellular viability of cell lines exposed to dynamic flow via LDH Glo™ cytotoxicity assay

Lactate dehydrogenase assays for both cell lines exhibited similar yet distinct trends, further exemplifying the variation in behaviour that is observed between cell lines.

HT29MTX held a similar trend at all timepoints. Cells that were exposed to an increased medium volume, but no flow element, exhibited lower production levels of LDH compared to other conditions at all timepoints ($p < 0.001$). Interestingly, however, 1 mL static samples exhibited comparatively low LDH production at 24 hours, but as time progressed to 48 hours, LDH production increased significantly, even surpassing those levels seen in flow samples ($p < 0.01$). As such, it could be concluded that prolonged exposure to low medium volumes may introduce a stressful microenvironment for cell culture, resulting in a cellular stress response, potentially due to a build-up of waste products and changes in pH over time.

While the addition of dynamic flow to HT29MTX induced a significant increase in LDH production compared to the 1 mL and 15 mL equivalents, no significant changes occurred between the 24-hour and 72-hour timepoints (Figure 3-6). The above results led to the conclusion that the initial exposure of cell lines to dynamic flow induces a stress response in the cells – a response that, once acclimatised, the cells do not continue to exhibit.

Interestingly, when examining the LDH production by Caco-2 cells, a different pattern of behaviour is observed. At all timepoints, static 1 mL samples are observed as having a trend of increased LDH production, with significantly reduced LDH produced at all timepoints in 15 mL static experiments (24h: $p < 0.01$; 48h and 72h: $p < 0.001$) and in flow experiments (24hr and 48hr: $p < 0.01$; 72hr: $p < 0.001$) as is seen in Figure 3-7. Additionally, while all conditions display significant increases in LDH production between 24 and 48 hours, 15 mL static samples show no significant changes between 48 and 72 hours. While the trends remained consistent throughout, the previously mentioned stress response induced by flow in HT29MTX appears to be cell line specific.

HT29MTX LDH Viability Timecourse

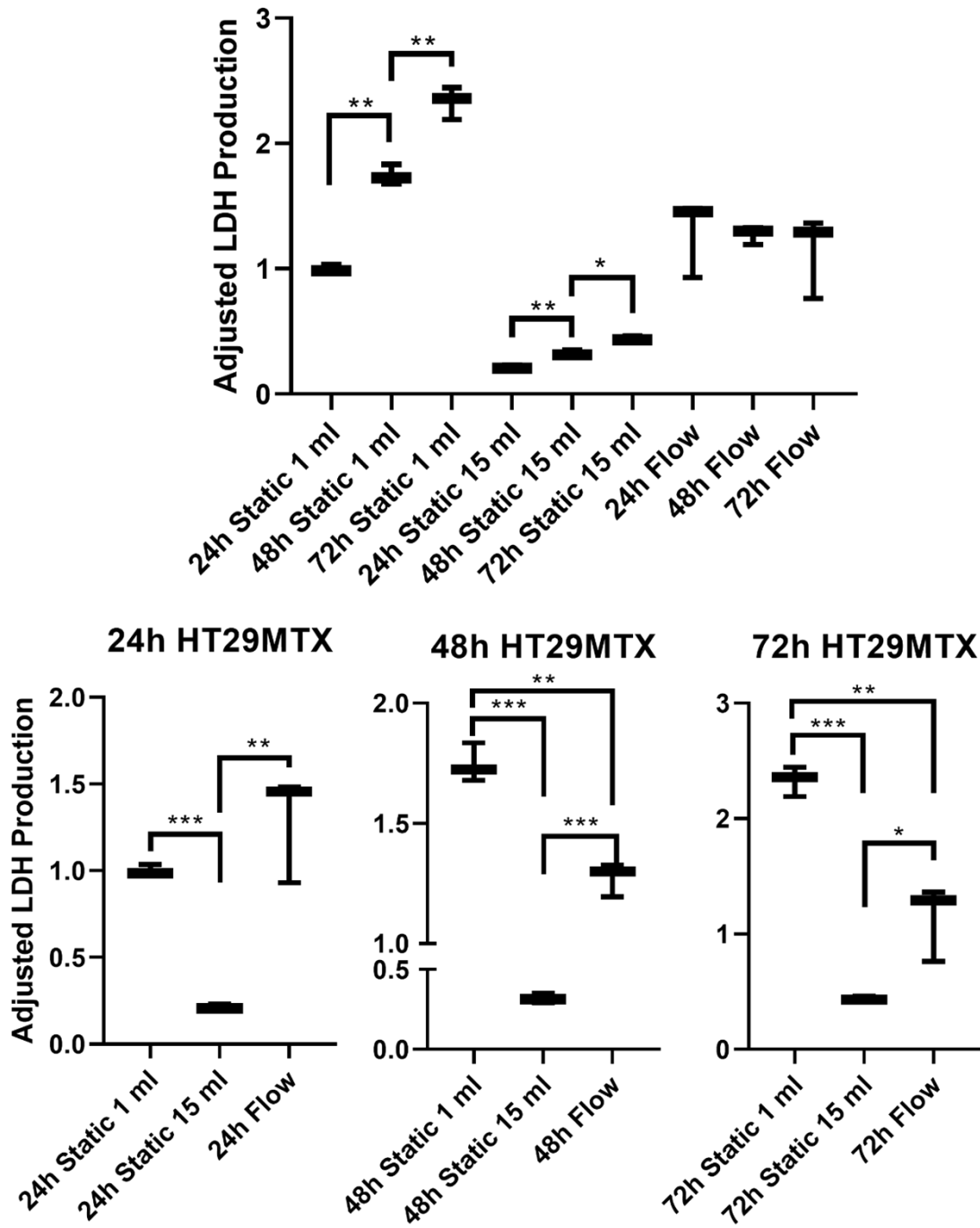


Figure 3-6: LDH production in HT29MTX cells following experimental exposure to flow and static conditions. HT29MTX cell-seeded coverslips were exposed to either static (1 mL or 15 mL) or flow conditions for a period of 72 hours, where medium samples were collected and analysed at 24-hour intervals via the LDH-Glo™ assay. The data represent the mean±standard deviation (SD) of 3 independent experiments and are presented as fold-change compared to the 1 mL static control at 24 hours that has been arbitrarily set as 1. Unpaired t-test was used when comparing experimental conditions 1 mL static, 15 mL and flow; paired t-test was used when comparing values across a given time period. Statistical analysis was performed using the paired or unpaired t-test where * $p < 0.05$, ** $p < 0.01$, *** $p < 0.001$).

Caco-2 LDH Viability Timecourse

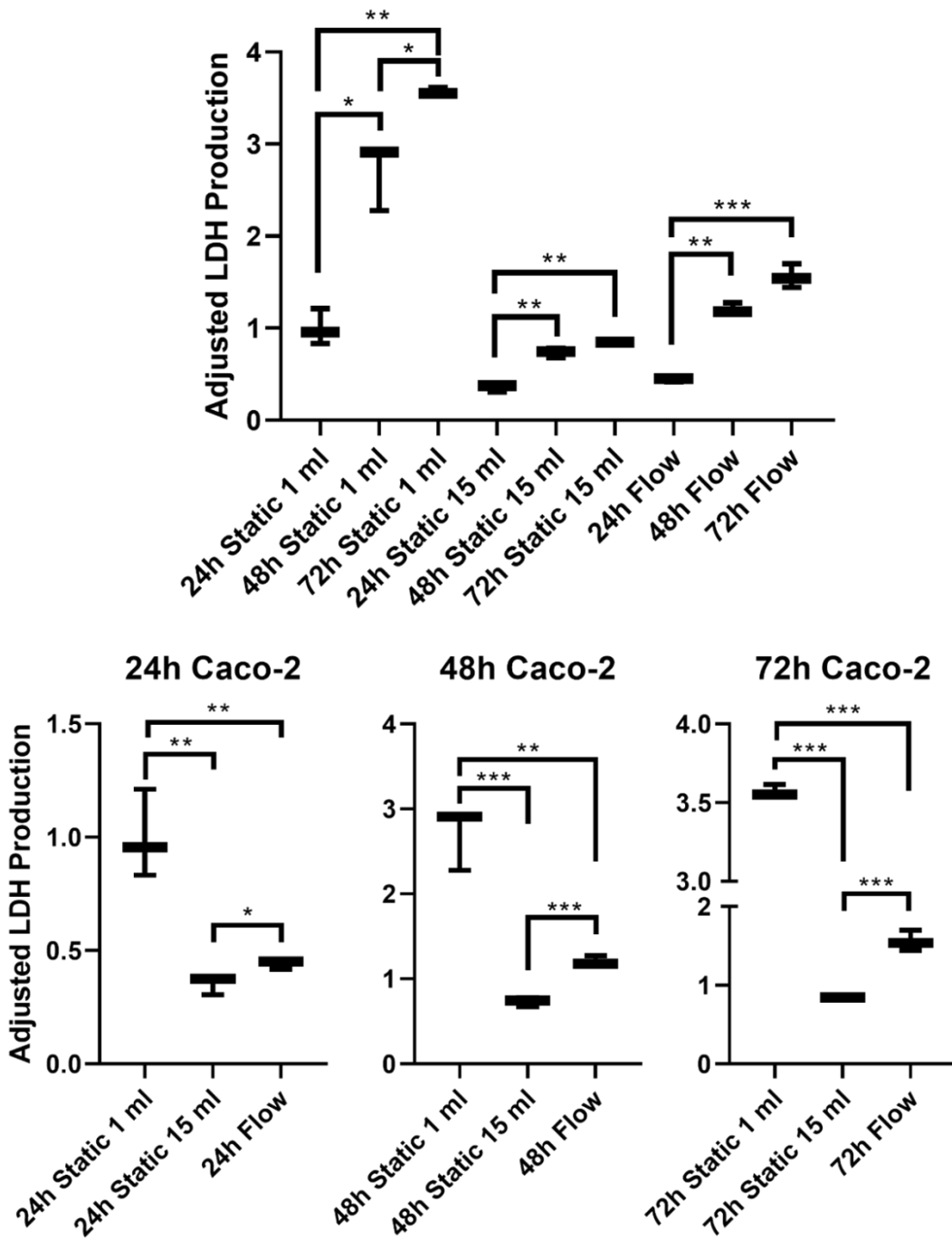


Figure 3-7: LDH production in Caco-2 cells following experimental exposure to flow and static conditions. Caco-2 cell-seeded coverslips were exposed to either static (1 mL or 15 mL) or flow conditions for a period of 72 hours, where media samples were collected and analysed at 24-hour intervals via the LDH-Glo™ assay. The data represent the mean±standard deviation (SD) of 3 independent experiments and are presented as fold-change compared to the 1 mL static control at 24 hours that has been arbitrarily set as 1. Unpaired t-test was used when comparing experimental conditions 1 mL static, 15 mL and flow; paired t-test was used when comparing values across a given time period. Statistical analysis was performed using the paired or unpaired t-test where *p < 0.05, **p < 0.01, ***p < 0.001.

3.3.5 Developing a qAlcian blue standard curve

Upon assessing the coated microplates, the data recorded in those instances was revealed to be inconclusive and variable, suggesting sub-optimal mucin binding (data not included). The process was repeated, adjusting for binding time, and adjusting starting mucin concentration; however, additional issues were still observed at lower concentrations of mucin due to a low degree of sensitivity at lower concentrations.

Despite this, some differentiation could be observed at higher concentrations. Due to the technical issues and lack of consistency, the standard curve methodology for assigning exact mucin concentrations was discarded, but the alcian blue assay proceeded due to observable differentiation when using this method.

3.3.6 Measuring the production of glycoprotein by intestinal cells via qAlcian blue analysis following exposure to dynamic flow

Alcian blue staining of glycoproteins was successful in all cell lines assessed in this study, albeit to different degrees.. Post-wash and solubilisation of alcian blue resulted in detection of glycoprotein in all assayed cell lines.

Significant increases in glycoprotein production were noted in Caco-2 sample exposed to increased medium static and flow when comparing them to the 1 mL static samples ($p < 0.001$) (Figure 3-8). HT29MTX exhibited a similar general trend of increased glycoprotein production in other assessed parameters when compared to the static equivalents, although significance was only noted in HT29MTX increased medium static samples ($p < 0.001$).

When considering the remaining cell lines HCT116 and HT29, both display a general trend of decreased glycoprotein production in the increased medium static samples and flow samples. Significant reductions can be noted in flow samples compared to the 1 mL static samples in HCT116 ($p < 0.01$). In the case of HT29, while both increased medium samples

(static and flow) displayed significant decreases in glycoprotein production compared to the static 1 mL samples (15 mL static: $p < 0.001$; flow: $p < 0.05$), flow samples display a significant increase in glycoprotein production between flow and increased medium static samples ($p < 0.001$).

The qAlcian blue methodology, therefore, was believed to be capable of differentiating between cell lines exposed to different conditions and could therefore be considered a novel, semi-quantitative means of differentiating glycoprotein production in cell culture, but may require further optimisation with regard to the generation of a quantifiable method complete with standard curve.

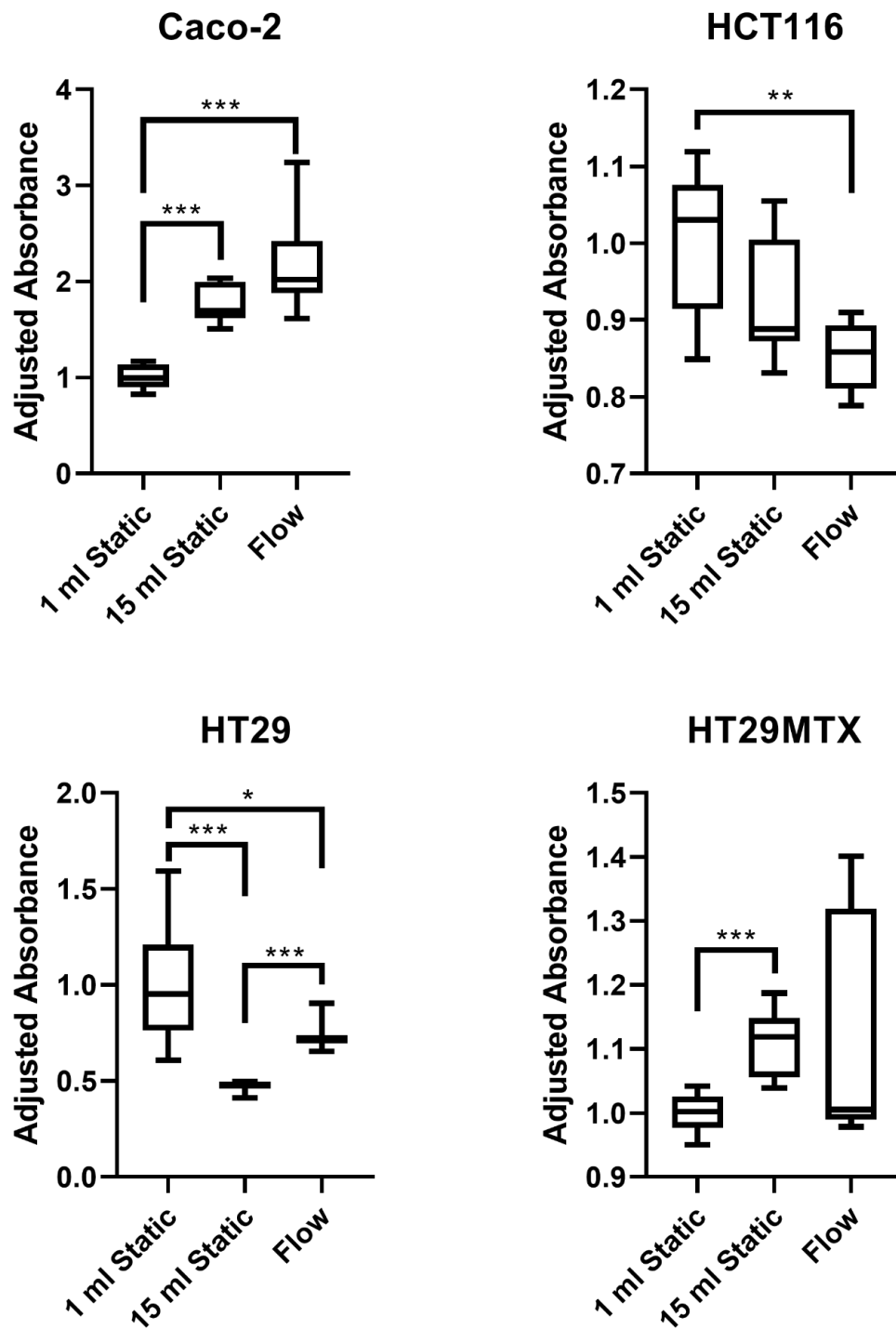


Figure 3-8: Glycoprotein production in cell lines following exposure to flow and static conditions for 48 hours measured via the qAlcian blue methodology. Cell-seeded coverslips of either Caco-2, HCT116, HT29 or HT29MTX were exposed to either static (1 mL or 15 mL) or flow conditions for 48 hours, following which glycoprotein production was assessed via the qAlcian blue methodology. The data represent the mean±standard deviation (SD) of 4 independent experiments (containing duplicate samples of each condition) and are presented as fold-change compared to the 1 mL static control that has been arbitrarily set as 1. Statistical analysis was performed using the unpaired t-test where * $p < 0.05$, ** $p < 0.01$, *** $p < 0.001$).

3.3.7 Glycoprotein production in HT29MTX cells monitored via light microscopy

HT29MTX cells were observed within one day of being fixed to the coverslip to limit any potential impact incurred from coverslips drying out. Increased medium static-exposed cells and dynamic flow-exposed cells, respectively, display considerable increases in glycoprotein production, which can be observed via the increase in blue staining in Figure 3-9. While glycoprotein production is increased in these samples, there is a considerable shift in cellular morphology in both 15 mL increased medium static samples and in the dynamic flow exposed samples in comparison with those samples exposed to 1 mL static cell culture conditions (Figure 3-9(A)). The largest morphological changes can be observed in Figure 3-9(C)), whereby cellular morphology has shifted to become more rounded or spherical compared to the other samples, which is characteristic of cells under stress or entering apoptosis.

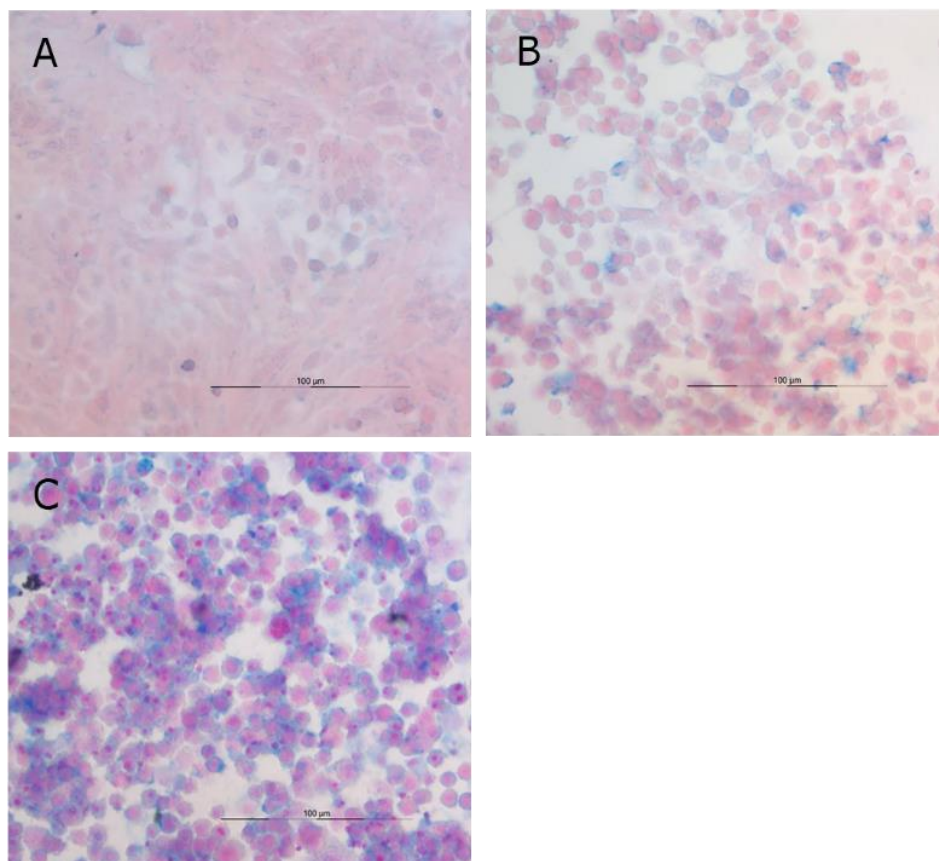


Figure 3-9: Monitoring the production of glycoproteins in the cell line HT29MTX via alcian blue and nuclear fast red staining and subsequent microscopy. HT29MTX cells were exposed to either A) 1 mL static, B) 15 mL static or C) flow conditions for 48 hours before being stained using alcian blue and nuclear fast red for monitoring of glycoprotein production.

3.3.8 MUC gene expression in cell lines exposed to a trio of experimental conditions

As a final measure of glycoprotein production, qPCR for mucin gene expression was performed as a molecular method to compliment already generated data. It was observed that, in all instances, the gene expression of MUC2, MUC5AC and MUC5B was undetectable in the cell line Caco-2, a cell line documented as having relatively low mucin production rate. The above trend was observed from samples collected from all three experimental models, and thus no data can be recorded here.

In the case of HT29MTX, some changes in MUC gene expression were measured between experimental conditions for each gene of interest, although the pattern varied somewhat between genes, as can be seen in Figure 3-10. MUC2 saw those samples collected from flow and increased medium static models display a reduction in gene expression compared to the 1 mL static method. While no significant changes were observed in the expression levels of MUC2, the trend remains that through increasing the medium volume, MUC2 expression levels were decreased in HT29MTX.

For the gene expression of MUC5B and MUC5AC, there appeared to be no significant modulation in gene expression levels as a direct result of increasing the medium volume under static conditions (Figure 3-10). As such, it could be stated that the significant changes observed in both MUC5B and MUC5AC flow model samples compared to their 1 mL static model samples (in which $p < 0.05$ and $p < 0.001$ was observed for both MUC5B and MUC5AC respectively) were indeed due to the presence of flow – a promising result for the exploration of the impact of flow in cell culture research.

Additionally, the results recorded here, in addition to those observed in microscopy-based mucin assay, further aid in corroborating those results observed in the qAlcian blue assay. Unfortunately, the validity of the assay when utilising the cell line Caco-2 is less conclusive at this stage. However, for those cell lines known for expressing mucin, the qAlcian blue method may prove an effective addition to the currently utilised methodologies.

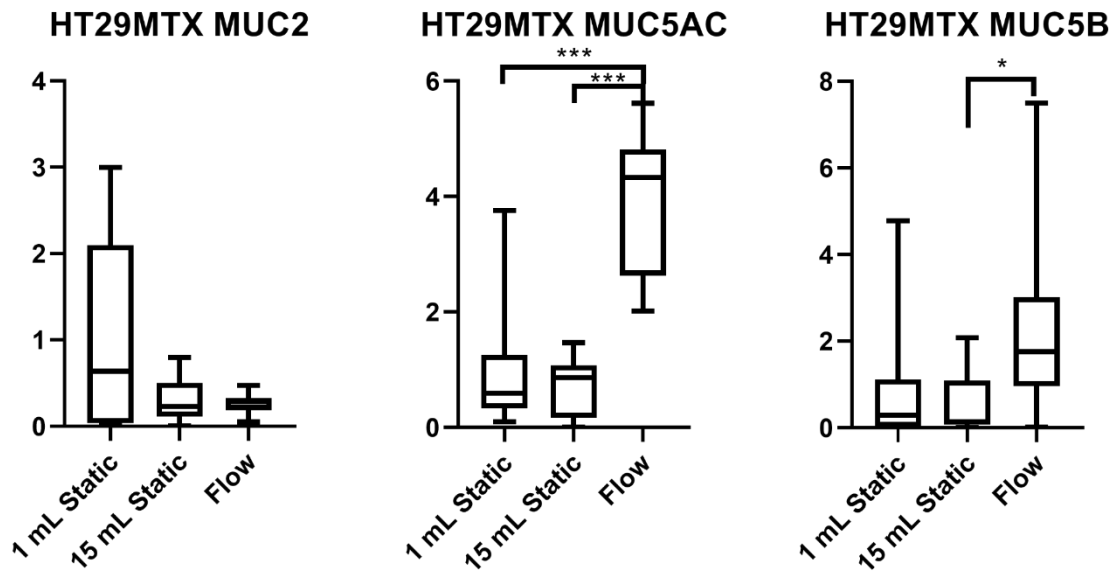


Figure 3-10: qPCR analysis on MUC gene expression in HT29MTX cell lines following exposure to dynamic flow and static conditions. HT29MTX cells exposed to static (1 mL or 15 mL) or flow conditions were harvested and assessed via qPCR for the production of 3 unique mucins, MUC2, MUC5AC and MUC5B. The data represent the mean±standard deviation (SD) of 5 independent experiments (containing triplicate samples of each condition) and are presented as fold-change compared to the 1 mL static control that has been arbitrarily set as 1. Statistical analysis was performed using the unpaired t-test where * $p < 0.05$, ** $p < 0.01$, *** $p < 0.001$).

3.4 Discussion

The investigatory stages of the study presented several interesting preliminary findings, particularly when focusing on the wider goal of the study – that being the impact of dynamic flow on cell culture and the implications for the wider field of cell culture. Cell culture has received widespread adoption due to the comparatively low investment required in terms of both time and money. Furthermore, it often mitigates issues that may arise in some studies as it allows for a large sample number, which can lead to an impressive number of technical replicates.

The inherent limitation of the QV500 system's small sample number required further analysis of multiple cell lines rather than a single cell line to provide a wider understanding of the impact of flow, while simultaneously attempting to circumvent any issues that may arise because of the comparatively low sample number. While the issues in the QV500 system were noted as limiting, the benefit of the system on the overall efficacy of the study was somewhat greater than initially expected. However, when combined with the additional unforeseen issues faced regarding the cell lines selected for the study, a re-assessment was required for downstream applications.

While it was initially planned to implement several cell lines in this study, the number of cell lines was ultimately reduced due to unforeseen technical issues. Even so, these cell lines still provided some invaluable insight into currently employed cell culture methodologies. It was believed at the beginning of the study that, with the exception of those distinct biological and behavioural differences in the selected cell lines (such as elevated mucin production in HT29MTX cells and tight junction formation in the Caco-2 cell line), similar trends would be observed in each of the cell lines when exposed to flow conditions. The above belief of shared trends among the selected cells was formed as a result of each of the four selected cell lines being cultured under similar conditions, using similar medium formulations. The concept was further strengthened as, with the exception of specific studies that focus on the unique behavioural characteristics of a cell line, the cell lines share a number of

comparable behavioural characteristics and are widely used within cell culture (Cencič and Langerholc 2010).

However, previous studies have suggested that certain cell lines, thanks to their unique biological traits, present a small niche that researchers can exploit to better assess a given environment. In turn, this implies that exposure to flow might influence cells inhabiting other biological niches in unique ways, as was exemplified in this study. The research conducted in this chapter revealed that cells exposed to *in situ* factors respond in a distinct manner, dependent on their source and unique set of behavioural and morphological characteristics. This concept was revealed to be one of merit within the preliminary assays of the study – particularly within the confines of the MTT, LDH and glycoprotein production assays.

When examining the data generated in the MTT assay, one aspect is immediately apparent: while similar trends can be observed in HT29MTX, HCT116 and Caco-2, where viability was either nominally impacted or improved, HT29 shows a contrasting behaviour. HT29, following exposure to flow conditions, shows reduced viability, a trend that worsens over time. Additionally, the trends seen in each of the three remaining cell lines, while similar, were behaviourally distinct, further emphasising the importance regarding cell line selection in the preliminary planning stages of a given study.

While many cell culture-focused gut studies draw from a comparatively small selection of cell lines, typically two to three cell lines – for example, Caco-2 and HT29MTX – it is common to see cell culture studies incorporating only a single cell line that expresses a phenotype or behavioural characteristic of interest, with no additional cell line that might offer a behavioural comparison. From what was observed in this chapter, where each cell line exhibited distinct behavioural characteristics under the various selected experimental conditions, one must consider the potential necessity of incorporating multiple cell lines into a study, not only for the improved robustness of a model, but also to ensure that those findings retain the reliability and applicability when modelling health and disease *in vitro* and comparing those findings to studies *in vivo*.

Furthermore, initial findings in this chapter lead to the conclusion that dynamic flow does indeed induce a behavioural change in the four cell lines selected for the study. While many studies have already confirmed the relevance of the QV500 system in modelling the blood-brain barrier (Miranda-Azpiazu et al. 2018) and in improving cardiac tissue maturation in 3D cultures (Pagliari et al. 2014), the incorporation and application of intestinal cell lines remains, as mentioned previously, an underexplored niche, particularly in those studies incorporating the Quasi Vivo® range of products. The results showcased in this chapter do however align with research undertaken in 2021 using a similar, if bespoke, milli-fluidic chamber system developed by Lindner and colleagues (Lindner et al. 2021), which is promising. Much of the published research using milli- and micro-fluidic methodologies rely on bespoke pieces of equipment, rather than commercially available systems. As such, the shared trends relating to cellular viability, proliferation and mucin production only acts to further strengthen the robustness of the system moving forward, as a similar system has yielded similar data to that seen here.

However, despite producing a number of promising preliminary findings, upon further examination, it must be noted that there is some ambiguity within the data of this chapter, although it should also be said that the deviations observed in cells under flow compared to static conditions indicate a behavioural shift towards a potentially biologically relevant system, as, in all instances, cellular behaviour was altered, albeit not always significantly. However, with such considerable inter-cell line variation, further analysis would be required to ascertain the impact of flow on cell culture modelling, yet it can still be noted that changes in behaviour are consistently observed when cell lines are exposed to flow, further strengthening the argument that cell culture research, when omitting those biologically relevant factors found *in situ* could be considered as having limited biological relevance. Furthermore the inclusion of flow and other biological parameters should be considered if attempting to improve the biological relevancy of cell culture systems, however, the limitations of the system and needs of a given study should inform whether flow is necessary or if traditional methodologies would better suit the study at hand.

Returning to the ambiguity of the current findings, this is particularly exemplified when considering those responses observed in the glycoprotein production assays. While mucin

production can be noted as a feature of behaviourally normal cells within the gut, the rapid production of mucins and other glycoproteins has additionally been linked to a stress response *in vitro*, where misfolded mucin induces apoptosis by the accumulation of reactive oxygen species (Tawiah et al. 2018).

In this study, flow consistently resulted in an increase in glycoprotein production in the cell line HT29MTX. The microscopic analysis of the HT29MTX cells indicated a potential negative response of the cells to flow, as seen by the morphological change in the HT29MTX cells in that they became rounded – a characteristic response of cells entering an apoptotic state (Elmore 2007). While this morphological change might come as a direct result of exposure to dynamic flow, it might also be explained by an increased growth rate, whereby cells are dividing at an increased rate compared to that observed in the other samples. However, without further investigation, this remains only speculation at this stage, as no apoptosis assay was performed. It should also be noted that due to the methods selected for glycoprotein measurement, only acidic glycoproteins were measured using alcian blue, which in turn would have failed to capture any other glycoproteins present. While this behavioural shift in glycoprotein production could be viewed as a positive indicator of changes in cellular glycoprotein production, without additional insight and further analysis, all that could be stated at this stage is that the behaviour of the cells is altered following the addition of flow, and that cells exposed to dynamic flow may face an acclimation period in which cells exhibit a stress response.

Additionally, when the above data is coupled with the observed decrease in glycoprotein production seen in both the HCT116 and HT29 cells, the disparity in response between cell lines provides a further discussion point as to the importance of selecting appropriate cell lines and conditions for a given study, as the inverse behavioural trends seen in these cell lines may act to bias a study in one direction or another if approached in isolation rather than as a collective.

Unfortunately, further microscopic analysis of the cell lines was not possible due to the technical limitations of the QV500 system and subsequent preparation of samples for microscopy. However, to further address some of the concepts explored in this chapter,

subsequent experiments were proposed to explore the production of proinflammatory cytokines by the remaining cell lines under flow to address the key research questions of whether cell lines exposed to flow are subject to a stressful environment, and also how important the utilisation of multiple cell lines is in understanding the response of a given stimulus.

Regarding the aims raised at the beginning of this chapter, following the successful integration of flow, it was suggested in this chapter that medium volume and the presence of flow alter cellular behaviour. Furthermore, the choice of cell line was shown as being a significant factor regarding the response induced by physiological factors, as the select cell lines used in this study responded in a distinct, cell line-specific manner – a concept that will, for the remainder of this thesis, stand as a key foundation of the research conducted.

It must be noted that certain limitations in the QV500 apparatus and the protocols selected may have introduced an element of bias into the study. For example, to account for the time investment required per experiment, numerous QV500 systems were utilised to circumvent the issues of time lost during system preparation and cleaning cycles, and the low sample number per experimental cycle, an issue previously highlighted in this study.

However, it could be speculated that the utilisation of multiple systems may have introduced minute flow variations into the study. While studies exploring the flow rates and flow perfusion within the Quasi Vivo® range of systems have taken great care in modelling and understanding the hydrodynamics of their reaction chambers (Mazzei et al. 2010), the flow rates of the same QV500 apparatus were seen to vary in accordance with which pump mechanism the system was connected to, thus inferring that further optimisation is required of the external pump apparatus to ensure a consistent flow rate throughout a given study. Furthermore, the use of glass coverslips, while shown to be the most time-efficient surface for the study in the preliminary experiments, may, in truth, provide a sub-optimal surface for any future experiments, as glass is often deemed undesirable for cell culture practices due to the inherent fragility of the material. Despite this, the accommodations made in this study for the experimental procedures with medium optimisation and experimental surface optimisation under all three experimental conditions

in the study, in addition to the incorporation of numerous commonly utilised cell lines to accommodate for potential variations, were performed to mitigate the potential bias in experimental design and sampling to further improve the overall robustness of the study.

As such, to summarise the findings of this chapter, it should first be stated that the initial aims of the chapter were achieved, as dynamic flow was seen to be an integral element in modulating the behaviour of intestinal cell lines, particularly those biological factors innately linked to cell health. However, despite the results reported in this chapter regarding cellular viability and glycoprotein production, the nature of the behavioural modulation, be that positive or negative, at this stage cannot be concluded. Additionally, it should be noted that the cell lines utilised in a given study are of greater importance than initially believed. The importance of cell line selection was further emphasised as it was consistently observed that the cellular response to a given stimulus could vary significantly under flow conditions, resulting in a series of diverse responses that ultimately displayed a cell line-specific stimulation under flow – a trend that might act to otherwise influence a cell line's behavioural response when exposed to a compound or stimulus of interest. As such, additional analysis is required to understand the role that both dynamic flow and the selected cell lines might play within cell culture research – two aspects that are explored in greater detail in the coming chapters.

4 Exploring the use of bacteria-conditioned medium and live bacterial cells within a dynamic flow cell culture system

4.1 Introduction

Direct exposure of lactic acid-producing bacteria to human cell lines *in vitro*, while beneficial *in situ*, may provide a hazardous microenvironment due to the optimum pH of human-derived cell lines typically residing within the neutral region of the pH spectrum, at a pH of 7.4 (Arora 2013). In addition, the impact of direct bacterial exposure on human-derived cell lines may induce a negative response due to the unique structure and composition of the bacterial cell wall, which includes compounds such as lipoteichoic acid (LTA), the Gram-positive counterpart to lipopolysaccharides (LPS), a well reported endotoxin believed to facilitate the adhesion of *Lactobacillus* sp. to the mucin layers produced by the cells within the gut (Lightfoot and Mohamadzadeh 2013). When considering the proinflammatory potential of bacterially derived molecules, combined with the immune responsiveness of cell lines such as Caco-2 and HT29MTX, both of which are documented as poor responders to LPS (Böcker et al. 2003), a pre-exposure stage is important in probiotic exposure methodologies within cell culture systems, particularly when utilising alternative methodologies such as those employed in this study. In this chapter, the use of bacteria-conditioned media, a commonly utilised method in probiotic-coupled cell culture studies (Davies et al. 2018; Michael et al. 2019), as a probiotic proxy, will additionally explore the impact of probiotic-derived metabolites on human cells and whether these metabolites are of a beneficial or detrimental nature to intestinal cell lines.

4.1.1 The impact of probiotics on immortalised cell lines

It has been previously showcased that probiotic bacteria can exert an anti-cancer effect on immortalised cell lines (Motevaseli et al. 2017). As such, the use of probiotic bacteria within the limited confines of cell culture must also be subject to additional optimisation to ensure

that neither bacteria nor metabolites prove toxic to the cell lines at the selected working concentration.

To explore the statements above, a series of bacteria-conditioned media were generated, and a selection of concentrations were exposed to human cells. The pH was adjusted to limit the impact of lactic acid within the sample, allowing for any potential impacts induced by bacterial metabolites to be observed under a more controlled set of conditions. Combining both the adjusted pH and the conditioned cell culture medium allowed for the optimal concentration of conditioned medium to be estimated for future exposure experiments, while observing whether cytotoxicity was induced by these probiotic products at elevated conditions.

4.1.2 The importance of cytokines within the gut

Cytokines and chemokines are a series of pro-inflammatory molecules produced by a wide range of cell types throughout the human body and are well established as being linked both to the host immune response and the recruitment of immune cells in instances of infection, allergy and disease (Justiz Vaillant and Qurie 2019). Unsurprisingly, the extracellular concentrations of these molecules have also been observed to be significantly elevated in cases where patients are suffering from an inflammatory disease, with particular increases noted in those diseases localised to the GI tract, such as IBD and its derivatives, CD and UC (Sanchez-Muñoz et al. 2008).

When considering the human inflammatory response, one of the most studied and well-understood molecules related not only to inflammatory diseases of the gut, but to the general functionality of the human system, is interleukin 8 (IL-8). IL-8 is a molecule well characterised as being present in elevated levels in IBD patients, often as a result of a bacterial agents, which was noted due to the required presence of bacterial commensals in IBD models in order to induce inflammation *in vitro* (Subramanian et al. 2008).

Additionally, IL-8 is a chemokine with a varied and diverse set of roles within the human body. While the majority of these roles have been mapped to the inflammatory response, this is far from its sole function. However, one of the more interesting roles of IL-8 is its association with the production of the biogenic amine and pro-inflammatory molecule, histamine, responsible for inflammation induction both as a key player in the allergic response, and as a response to combat infection (Smuda and Bryce 2011). The connection of IL-8 with histamine is due to IL-8's associated role as an intercellular signalling molecule (cytokine), which has led to some referring to IL-8 as a histamine release factor (Liao and Hsieh 1992). Simultaneously, however, histamine has been noted in many studies to influence the synthesis of many interleukins, including that of IL-8 (Li et al. 2001), which in turn suggests that IL-8 acts to influence its own production. As such, the abundance of IL-8 within a given environment could be an indicator as to the inflammatory potential of a given environment, and the behaviour/composition of its microbial inhabitants, thanks to the ability of histamine coupled with IL-8, alongside other interleukins, to produce an inflammatory or stress-response feedback loop.

Similar, to IL-8, RANTES, also known as CCL5, is a chemokine whose functions are diverse in modulating the body's innate immunity to infection. Typically, RANTES is mostly associated with biological functions allowing for the recruitment of T-helper cells and monocytes to combat infection, in which it acts as a chemotactic compound. Additionally, like many chemokines, RANTES is responsible for stimulating the production of histamine from basophiles and is, therefore, implicated in the general inflammatory immune response (Kuna et al. 2002), providing a secondary, distinct measure of the inflammatory feedback loop that is of considerable interest within this study.

A somewhat different inflammatory target compared to those chemokines listed above, is tumour necrosis factor alpha (TNF- α), a cytokine also associated with inflammatory diseases (Monaco et al. 2015). It should be noted that a number of therapeutic agents, commonly used in the treatment of gastrointestinal inflammatory diseases, including CD and UC, target TNF- α . Anti-TNF- α agents are a means of moderating the inflammatory response of the recipient (Adegbola et al. 2018).. Interestingly, however, TNF- α has been implemented in the dampening of response to other pro-inflammatory stimuli, including a study in which

mice exposed to TNF- α were reported having a dampened immune response to elevated levels of LPS (Kallioli and Ivashkiv 2016). As such, TNF- α could be considered a measure of cellular health, as elevated levels of TNF- α may suggest that the system is adapting to the toxin to avoid inflammatory induced cell damage.

It is important to note at this stage that the modelling of the inflammatory response is not the goal in this chapter, as the cell lines used in this study are not immune cells. Instead, the focus of this chapter is to examine the response of the Caco-2 and HT29MTX cell lines to a bespoke number of bacterial stimuli and the subsequent production of pro-inflammatory molecules, whose roles include the activation or suppression of the immune system *in situ*.

4.1.3 Cell lines and their known response to pro-inflammatory stimuli

Caco-2, despite its dissemination within the field of intestinal cell culture thanks to the distinct physiological characteristics outlined previously, comes with a distinct set of limitations that impact its potential as a cell culture tool. The most impactful of these limitations, when considering the implications of the study, is the poor response of Caco-2 cells to pro-inflammatory stimuli, including LPS, and its diminished responsiveness as a result of excessive passaging, and medium composition (Huang et al. 2003). Caco-2's lack of response following exposure to pro-inflammatory stimuli has been well characterised in many publications, with attention directed at the response, or rather the lack of response, from Caco-2 cells following LPS exposure.

HT29MTX, however, provides an alternative perspective on intestinal response to pro-inflammatory stimuli. Due to the mutation in this cell line promoting the expression of mucin, HT29MTX has an additional physiological factor that could influence the ability of a given stimulus through the introduction of a physiological mucin barrier, considered to protect the host as a "first line of defence" in infection (Kim and Khan 2013). However, as has been recorded with Caco-2, HT29MTX has also been noted as responding poorly to LPS exposure (Böcker et al. 2003); thus, the potential responsiveness of these cell lines to conditioned

medium may suggest that the metabolic activities of these probiotic bacteria may contribute a greater influence to cell behaviour and host health than initially realised. To reiterate, an issue encountered widely with intestinal or gut cell lines, particularly those aiming to model colonocytes, is a comparatively poor inflammatory potential, particularly when challenged with bacterial LPS. While the cell line HT29 has been documented as responding strongly following stimulation from LPS, it was shown to have a negative response when exposed to flow (see Chapter 3). As such, it was decided that the cell line HT29 would not be used in the following experiments, despite being a cell line of considerable interest for modelling the production of pro-inflammatory molecules.

Furthermore, gastrointestinal pathogens, such as enteropathogenic *E. coli* (EPEC) have been shown to induce an inflammatory response from cell lines in vitro (Edwards et al. 2011), with Caco-2 showcasing the importance of direct epithelial contact regarding the production of pro-inflammatory molecules such as IL-8. Certain considerations were therefore made to account for pathogenic stimulation, both using conditioned medium and direct bacterial exposure, and how this would compare with those trends seen in the probiotic exposed samples.

4.1.4 Concepts of interest

Firstly, this chapter seeks to assess the cellular response of intestinal cell lines to probiotic metabolites, and whether the probiotic metabolites produced by the probiotic consortia Lab4 and Lab4B prove toxic to intestinal cell lines. Achieving this aim will enable further downstream assays to be performed through optimisation of both a probiotic consortium and, later, pathogenic species.

Secondly, this chapter aims to understand the effect of both probiotic and pathogenic bacterial metabolites (conditioned media) and physiological flow conditions on the production of pro-inflammatory markers within the cell lines Caco-2 and HT29MTX, and whether the observed response is similar to those observed within static cell culture.

4.1.5 The aims of the chapter

1. To optimise the experimental conditions for the exposure of Lab4 and Lab4B probiotics to the selected cell lines under static cell culture conditions, and to ascertain the optimal dose for each probiotic so that cells retain viability and glycoprotein production when exposed to flow and static conditions.
2. To assess and implement three strains of *E. coli* of the same phylogenetic group into both flow and static cell culture conditions to compare the changes in cellular behaviour induced by probiotic and pathogenic bacteria.
3. To analyse the inflammatory potential of probiotic and pathogenic bacteria in cell culture and how those responses vary under flow conditions.
4. To observe and compare the inflammatory response of cell lines exposed to pathogenic bacteria both prior to and following treatment with probiotic bacteria, under both flow and static cell culture conditions.

4.2 Materials and methods

4.2.1 The Lab4 and Lab4B bacterial communities

All probiotic products used in the study were supplied and manufactured by Cultech Ltd. (Port Talbot, UK). Two of the probiotic products produced commercially by Cultech Ltd. were selected for use throughout the study, those being BC Bioacidophilus Powder and Proven Baby Breastfed, containing the Cultech-formulated Lab4 and Lab4B bacterial communities respectively.

The bacterial composition of Lab4 and Lab4B including the bacterial cell counts can be seen in Table 4-1.

All bacterial products were stored at -20 °C as lyophilised powders throughout the study. Bacterial counts were adjusted accordingly to allow for inter-sample comparability. All bacteria used in this study were sourced from the same commercial batch in which all

additives and/or prebiotics found within the product were disclosed by Cultech Ltd. prior to the study (data not included).

Table 4-1: Bacterial composition of commercial probiotic products

Product	Total bacterial cell count/ g	Bacterial strains comprising probiotic products
BC Bioacidophilus Powder (Lab4)	1.55×10^{10}	<i>Lactobacillus acidophilus</i> – CUL60* <i>Lactobacillus acidophilus</i> – CUL21* <i>Bifidobacterium bifidum</i> – CUL20* <i>Bifidobacterium animalis</i> sub sp. <i>lactis</i> – CUL34*
Proven Baby Breastfed (Lab4B)	6.15×10^{10}	<i>Lactobacillus salivarius</i> – CUL61* <i>Lactobacillus paracasei</i> – CUL08* <i>Bifidobacterium bifidum</i> – CUL20* <i>Bifidobacterium animalis</i> sub sp. <i>lactis</i> – CUL34*

* CUL refers to Cultech-specific strain.

4.2.2 Establishing active cultures of *Escherichia coli* strains

Three strains of *E. coli* from phylogenetic sub-group B2 (Lasaro et al. 2014; Hazen et al. 2017) were selected for the study: a pathogenic strain (Enteropathogenic *E. coli* (EPEC) strain E69), a probiotic strain (*E. coli* strain Nissle 1917) and a mutualistic strain (*E. coli* strain MP1).

E. coli strains E69 and MP1 were provided by Dr Cedric Berger and Teresa Paradell Gil (MMI Division of Organisms and Environment, Cardiff University School of Biosciences), whereas *E. coli* strain Nissle 1917 was revived from a previous -80 °C frozen stock sourced from the MMI Division, Cardiff University.

4.2.3 Medium and agar selected for bacterial growth and maintenance

Two bacterial media compositions were selected for the study. De Man, Regosa and Sharpe (MRS) agar and broth was used to culture both the Lab4 and Lab4B probiotics throughout the study, whereas a low-salt Lysogeny Broth (LB) agar and broth was used for the continued cultivation of the *E. coli* strains. Both media compositions were selected according to guidelines found on the ATCC website in addition to the advice of colleagues who had previously worked with the various strains.

MRS broth (Sigma Aldrich, Poole, UK) was prepared following manufacturer's instructions, using Tween-80 (Sigma Aldrich, Poole, UK) and ultrapure Type 1 (polished) water, while LB broth (Sigma Aldrich, Poole, UK) was also prepared following manufacturer's instructions using ultrapure Type 1 (polished) water and Tween-20 (Sigma Aldrich, Poole, UK).

Autoclaved MRS and LB broths were stored at room temperature away from direct sunlight for up to one month before discarding to ensure that medium purity was maintained throughout the study.

4.2.4 Reviving bacterial cultures from frozen stocks

Frozen bacterial stocks were removed from the -80 °C freezer, and utilising a disposable plastic loop, a small amount of the frozen stock was aseptically transferred to an LB agar plate for *E. coli* strains. Samples were stored on ice while in use to prevent samples from thawing.

When reviving probiotic products Lab4 and Lab4B from frozen, a small quantity of a given lyophilised powder was transferred to 10 mL of MRS broth before being vortexed to ensure resuspension of the bacteria. Using a sterile plastic loop, a small amount of the bacterial suspension of both Lab4 and Lab4B probiotics was transferred aseptically to a fresh MRS agar plate to confirm successful growth and reconstitution of the lyophilised powders.

Lab4 and Lab4B probiotics were revived from frozen lyophilised powder stocks as required for use in the study and were not maintained on agar plates. In the case of the probiotic single species where a lyophilised powder alternative was not available, frozen cryogenic bead stocks supplied by Cultech Ltd. were rapidly thawed in a water bath set to 37 °C and the entire contents transferred to an MRS agar plate to maximise growth. The above protocol was adapted due to poor revival potential observed when attempting to revive the bacterial species from a single cryogenic bead.

The above-listed processes were repeated for each bacterial species before transferring to a 37 °C incubator to allow for the formation of colonies. The probiotics were grown under anaerobic conditions due to the oxygen-sensitive nature of the bacterial constituents.

Following the incubation period, agar plates were inspected and, if bacterial colonies were observed, the bacterial cultures were stored at 4 °C for an extended period.

4.2.5 Maintaining bacterial cultures throughout the study

All *E. coli* strains were maintained on LB agar at 4 °C throughout the study and sub-cultured monthly using sterile plastic loops following a similar protocol to that outlined in section 4.2.4. Active cultures were inspected twice weekly to ensure cultures remained contamination free.

A fresh culture was initiated from the frozen stock every two months to avoid any potential contamination or issues that might arise from prolonged storage on agar.

4.2.6 Generating anaerobic media for probiotic growth

An MRS broth and an untreated high glucose DMEM were selected for optimisation and use, with the MRS broth being prepared as noted in section 4.2.3. High glucose DMEM and MRS broth were aliquoted in 10 mL volumes and transferred to an anaerobic cabinet, in which

the lids of each medium vessel were opened to allow for the equilibration of the medium with the anaerobic atmosphere in the anaerobic cabinet. Medium aliquots were degassed for 1 week under anaerobic conditions, following which the medium was re-sealed and stored under anaerobic conditions for up to a further 1 month.

To investigate the use of this medium, a single colony of *Bifidobacterium bifidum* and *Bifidobacterium animalis* sub sp. *lactis* were transferred to a 10 mL aliquot of aerobic and anaerobic (degassed) MRS broth for growth in an overnight culture in anaerobic conditions. Additionally, a small sample of each MRS suspension was transferred to a 96-well plate and a 24-hour growth curve performed at ambient oxygen levels.

Overnight cultures displayed some additional biomass in all recorded anaerobic samples compared to the aerobic growth medium. Additionally, while no growth was observed in the aerobic MRS samples, some growth could be observed in anaerobic medium samples when conducted at ambient oxygen concentrations. Following these findings, anaerobic medium was adopted for any subsequent assays involving probiotics to maximise growth while attempting to limit any potential negative impact from ambient oxygen.

4.2.6.1 Generating growth curves for Lab4 and Lab4B probiotic bacteria and for *E. coli* strains E69, MP1 and Nissle 1917

Lyophilised powders of the Lab4 and Lab4B probiotics were first diluted 1:1,000 in anaerobic MRS broth before vortex mixing to ensure resuspension of the bacterial products. To 10 mL of sterile LB broth, a single colony of *E. coli* was added and vortexed to ensure resuspension, and the process repeated for each individual strain.

A 100 μ L aliquot of the bacterial suspensions was transferred to a 96-well microplate and a growth curve generated over a 24-hour period using the Tecan multi-well plate reader utilising the Magellan™ 900 pro software, set to 37 °C, 600 nm absorbance with a shaking amplitude of 1, with a measurement recorded at 30-minute intervals.

This process was repeated for each bacterial probiotic pre-mix powder, single-species

powder and strain of *E. coli*. Raw data was log₁₀-transformed and the blank values deducted at each timepoint prior to generation of the growth curves using Microsoft Excel 365.

4.2.7 Generating conditioned media using Lab4, Lab4B and *E. coli*

Probiotics powders were diluted 1:1,000 in MRS broth (Sigma Aldrich, UK), as noted above, and transferred to an anaerobic environment overnight, ensuring the bacteria remained in the exponential phase – as estimated via the growth curves. In the instance of *E. coli* species, a single colony was suspended in LB broth (Sigma Aldrich, UK) and vortexed for 30 seconds. Cultures were transferred to a shaking incubator set to 37 °C and 100 rpm overnight, ensuring, as noted above, that cells remained in the exponential phase of growth as estimated by the growth curves generated previously.

Overnight bacterial suspensions were centrifuged at 1638 rcf for 10 minutes at 4 °C to form a pellet, following which the MRS was discarded. The bacteria were re-suspended in dPBS warmed using a water bath set to 37 °C and centrifuged again at 1638 rcf for 10 minutes at 4 °C to ensure the removal of any trace of the MRS/LB. Lab4B suspensions were additionally diluted using warmed dPBS to adjust the bacterial count to equal that of its Lab4 equivalent following advice provided by staff at Cultech Ltd., as Lab4B had previously been observed as producing 1.5 times the colony forming units (cfu) as Lab4. A base cell culture medium (lacking any additives) was used to re-suspend the bacteria, which was returned to anaerobic conditions for 5 hours.

Following the additional incubation, the bacterial cell culture medium suspension was checked for signs of bacterial growth. This was performed by visually inspecting the medium for turbid suspensions and pH change. If the phenol red indicator present in the DMEM had changed to a yellow/orange colouration, this indicated an acidic environment. Both features were taken as markers of bacterial growth due to production of lactic acid by the probiotic bacteria, or rapid growth by the *E. coli*. Following the visual checks, the

bacterial suspensions were centrifuged (1638 rcf for 10 minutes at 4 °C) and the medium collected. Bacterial pellets generated via centrifugation were discarded.

Conditioned medium was filter-sterilised using a sterile 0.2 µm filter, and the pH was re-adjusted to a neutral pH using a 1 M sodium hydroxide (NaOH) solution until the phenol red indicator returned to red, following which the pH was assessed using the Mettler Toledo pH meter AH#E124, and was further adjusted as required. The pH-adjusted conditioned medium was aliquoted and stored at 4 °C until required for a maximum of 1 week. If the conditioned medium remained unused after that period, old stock was discarded, and fresh conditioned medium was prepared as outlined above.

4.2.8 Identifying the impact of probiotics and pathogenic *E. coli* E69 on intestinal cell lines under flow

4.2.8.1 Establishing cell lines

Human cell lines HT29MTX and Caco-2 were sub-cultured and cell numbers were estimated using the Guava® Muse® cell count and analyser system (Merck, Livingston, UK) as described in section 2.6.1. Using the estimated cell counts generated by the Guava® Muse® system, cells were diluted to a concentration of 10^4 viable cells per mL using unsupplemented high glucose DMEM, and 100 µL of the cell suspensions were added to each well of a 96-well system. Cells were monitored daily using the JuLI™ Br cell analyser system, and cell culture medium was changed every 2 days until confluent (HT29MTX), or until 21 days had passed (Caco-2) to allow for spontaneous differentiation.

Probiotic-conditioned medium was generated using the method noted in section 4.2.7 above and was diluted with unsupplemented high glucose DMEM to form 10 concentrations for use in the assay, those being: 100%, 75%, 50%, 25%, 20%, 15%, 10%, 5%, 1% and 0.1% v/v. A 0% conditioned medium control, consisting of non-supplemented high glucose DMEM only, was utilised for each cell line. The above-mentioned conditioned medium concentrations were added to the 96-well plates seeded with intestinal cell lines, and

monolayer integrity was visually assessed using the JuLI™ Br (NanoEnTek, Seoul, Korea) before being returned to the CO₂ incubator for 48 hours. Following this 48-hour incubation period, all conditioned medium was gently removed from the cell monolayers using a pipette, ensuring the monolayer integrity remained preserved, and discarded. Both an MTT and qalcian blue assay were performed on the cell lines following the protocols outlined in sections 2.9 and 3.2.3.1.5 respectively. This protocol was repeated using both Lab4- and Lab4B-conditioned medium to establish a comparable measure of concentration-based toxicity in both probiotics.

4.2.8.2 Optimising the Lab4 and Lab4B probiotic consortia for direct cellular exposure

In preliminary assays, probiotic cell counts were assessed following a brief growth period in MRS broth for 1 hour, conducted to promote cell growth and revival from frozen lyophilised powder stock. This method was ultimately discarded, however, due to the number of uncontrollable variables introduced when undertaking the initial growth in MRS, including the inherent unpredictability of the samples' growth rates and the potential for variable bacterial cell counts across multiple experimental repeats that might introduce an element of undesirable bias into the study.

Following consultation with Research Director Dr Sue Plummer of Cultech Ltd., (Port Talbot, UK), a 24-hour experiment was proposed where a 10⁴ and a 10⁵ bacterial cells/mL suspension of the lyophilised powders would be incubated with HT29MTX cells under static cell culture methods (1 mL static in a multi-well plate) to observe the impact on cellular integrity and cell health using the JuLI™ Br cell stage cellular recording apparatus.

This assay was performed by adding the required amount of lyophilised powder to non-supplemented high glucose DMEM to produce a suspension corresponding to the required bacterial cell count before vortex mixing. The bacterial suspensions were added to coverslips coated with a confluent monolayer of HT29MTX cells in a 24-well multi-well plate, before being returned to a humidified CO₂ incubator set to 37 °C.

Following the initial 24-hour period, no visible impact on the cellular integrity or integrity of the monolayer was observed, and the experiment was extended for a further 24 hours. Again, at the 48-hour timepoint, cells were observed utilising the JuLI™ Br cell imaging stage (NanoEnTek, Seoul, Korea), and no detrimental impact was observed visually to the cells (data not included).

4.2.8.2.1 *E. coli* exposure optimisation assay

To a non-supplemented aliquot of high glucose DMEM, a single bacterial colony of *E. coli* E69 was added and the sample vortexed. The sample was diluted from a neat suspension by a factor of 10, forming a dilution series to ranging from 10^0 to 10^{-4} . This suspension was incubated with HT29MTX- and Caco-2-coated coverslips for 48 hours, with visual observations recorded at 24-hour intervals (data not included).

Following 48 hours of incubation, it was identified that at all concentrations below 10^{-4} bacteria/ mL, cellular integrity was compromised. Samples treated with bacterial suspensions that were diluted to a final concentration of 10^{-4} also had a mildly acidic environment, with evident bacterial growth. However, the integrity of the cell monolayer was preserved at this concentration when visually inspected. As such, a dilution of 10^{-4} was selected for all subsequent assays utilising *E. coli* strains.

4.2.8.3 Cell infection protocol using *E. coli* strain E69

E. coli E69 was grown aerobically in LB broth overnight at 37 °C at 100 rpm before being centrifuged at 1638 rcf for 10 minutes at 4 °C and washed using dPBS in the manner outlined in section 4.2.7. The washed bacterial pellet was resuspended in non-supplemented high glucose DMEM warmed to 37 °C in a water bath and diluted 1:100 using warmed antibiotic-supplemented high glucose DMEM to encourage the expression of locus of enterocyte effacement (LEE)-encoded virulence factors, including the Type III secretion system essential for achieving bacterial infection (Edwards et al. 2011).

The diluted *E. coli* suspension was plated on to the Caco-2- and HT29MTX-coated coverslips and allowed to incubate for 3 hours in a 37 °C humidified CO₂ incubator. Following bacterial exposure, coverslips were washed 3 times with dPBS warmed in a water bath set to 37 °C, and a 1:100 dilution of EPEC E69 in antibiotic-free high glucose DMEM was added to each well. The coverslips were further incubated for an additional hour. Coverslips that had been incubated with *E. coli* E69 were rinsed a further 5 to 10 times to remove any non-adherent bacteria and exposed to a 100 µg/mL gentamicin-supplemented dPBS for 20 minutes to remove any remaining live bacteria.

Antibiotic solutions were removed from all cells, and the coverslips were washed twice more with dPBS warmed to 37 °C using a water bath to remove any residual traces of the antibiotic. Coverslips were examined using both light microscopy and the JuLI™ Br (NanoEnTek, Seoul, Korea) apparatus to ensure a maintained monolayer integrity before transferring to the relevant experimental condition.

4.2.9 Understanding the impact of flow on the pH of cell culture medium with no additives or cells

The pH of a non-supplemented high glucose DMEM was measured using a Mettler Toledo pH meter AH#E124 to establish the starting pH of the medium. The non-supplemented medium was cycled through the system for a period of 72 hours with the pH recorded at 24-hour intervals.

Therefore, it was decided that the Lab4 and Lab4B bacterial consortia should additionally receive exposure to the flow model in the absence of human cells to monitor whether any behavioural changes were induced following exposure to a dynamic flow element when no human cells were present.

A suspension of 10⁴ cells/mL of both Lab4 and Lab4B probiotic was prepared using the methodology outlined in section 4.2.8.2 and the pH measured prior to exposing the suspensions to flow conditions. As with the bacteria-free media, the bacterial suspension

was cycled through the QV500 system for 72 hours, and the pH was probed at 24-hour intervals and the medium pH recorded.

4.2.9.1 Metabolite profiling bacteria-only pH analysis medium

The final experimental media for both probiotic consortia used in section 4.2.9 were collected following the 72-hour exposure to flow and frozen at -80 °C to preserve the metabolites found therein. Samples were subsequently stored on ice and transferred to Imperial College, London for metabolite analysis. However, due to time constraints, metabolite profiles for this assay were unable to be generated prior to the completion of the project and, as such, are omitted from the study.

4.2.9.2 Assessing the impact of pH on cellular viability via the LDH assay

Three pH points were selected for analysis: pH 7.4, similar to the pH of high glucose DMEM (Merck 2020); pH 7, and pH 6.5. Ten 1 µL droplets of 1 M acetic acid were added to 30 mL aliquots of non-supplemented high glucose DMEM while mixing the medium gently by hand-swirling after each addition of the acid to aid in the distribution of the acid throughout the solution and to aid with stabilising the pH. The pH was measured using the Mettler Toledo pH meter AH#E124. When the desired pH was achieved, the medium was left to equilibrate at room temperature for 30 minutes before being measured again. If the pH had altered in that time, further acetic acid was added, and the process was repeated until the pH was noted as having stabilised. Should the pH be below the desired values, a 1 M NaOH solution was utilised to increase pH to the level desired. In these instances, the medium was left again for 30 minutes at room temperature to allow the pH to stabilise, following which the pH was once again measured. Once stable, the exact finalised pH values were recorded, and the medium was used immediately.

4.2.9.3 Preparing endotoxins for cellular exposure

Freeze-dried LPS and LTA were obtained from Sigma Aldrich (Poole, UK) and for *E. coli* O55:B5 and *B. subtilis* respectively. *E. coli* O55:B5 was selected due to its common use within LPS-based studies seeking to activate the TLR4 receptors and induce an immune response, while *B. subtilis*-sourced LTA was selected for the study as *B. subtilis* has been documented as being a naturally occurring organism commonly found within the GI tract (Hong et al. 2009), making it an ideal candidate for gut-modelling methodologies. Freeze-dried endotoxin was prepared to the recommended concentrations provided by the manufacturer using dH₂O and aliquoted prior to freezing at -20 °C for a maximum of 6 months.

Prior to use in assays, LPS and LTA aliquots were thawed to room temperature and diluted to a final working concentration of 10 ng/mL using supplemented high glucose DMEM. Endotoxin suspensions were stored at 4 °C for up to 24 hours prior to use. Following experimental exposure, LPS/LTA endotoxin suspensions were collected and frozen if required for ELISA assays, or were discarded appropriately.

4.2.10 Utilising ELISA to detect the pro-inflammatory markers IL-8, RANTES and TNF- α

4.2.10.1 Collecting growth medium samples for ELISA-based analyses

Post-experimental medium was collected from three separate experimental runs for non-probiotic and both Lab4- and Lab4B-exposed Caco-2 and HT29MTX cells under flow and 15 mL static conditions. These samples were aliquoted individually and stored at -20 °C prior to analysis via ELISA. In instances where live bacteria were present in the medium, medium was collected and centrifuged at 1638 rcf for 10 minutes at 4 °C to pellet the bacteria, before being aliquoted and stored at -20 °C. The collection process was repeated for each experimental condition used for this study.

4.2.10.2 Preparing ELISA reagents

The ELISA mini prep kits (Peprotech, USA) were prepared in accordance with manufacturer's protocol, in which the reagents were re-constituted using nuclease-free H₂O or PBS supplemented with 0.1% v/v bovine serum albumin (BSA), as appropriate, and stored at -20 °C.

All buffer solutions were purchased pre-mixed from Peprotech, USA and stored at 4 °C. The buffer solutions that required preparation and diluting to a working concentration of ×1 were prepared a maximum of 24 hours prior to each ELISA using ultrapure type 1 (polished) water. These buffers were sterile-filtered (0.2 µm) in accordance with the manufacturer's instructions and stored at 4 °C until use. If these buffers were not utilised within a 24-hour period of preparation, they were discarded to ensure the sterility and integrity of the ELISAs performed.

4.2.10.3 ELISA protocols for measuring the production of IL-8, RANTES and TNF-α

ELISAs were performed in accordance with the manufacturer's protocol, with the sole exception being that the IL-8 standard concentrations were modified to a range of 600 pg/mL – 0.58 pg/mL, following a dilution range of 1:2 in manufacturer-supplied diluent to accurately capture the concentrations of all inflammatory markers found in the samples.

The relevant capture antibodies were diluted to the working concentration for each given target and transferred to a Corning® 96-well clear polystyrene microplate. The plates were sealed using manufacturer-supplied plate-sealing strips and covered in aluminium foil to limit light exposure overnight to allow for binding of the capture antibody to the plates.

Following the incubation period, excess capture antibody solution was discarded, and plates were washed using a wash buffer solution containing 1% w/v Tween-20 in PBS, where 300 µL of the wash buffer were added to each well before rocking the plate gently back and forth on the bench by hand and removing the wash buffer. The wash step was repeated a

further three times and the plate blotted dry on absorbent tissue. To the dried plates, 300 μL of blocking buffer (Peprotech, USA) containing 1% w/v BSA in PBS were added to each well and allowed to incubate at room temperature for at least 1 hour in the dark. During this incubation period, a range of protein standards for IL-8 (600 pg/mL – 0.58 pg/mL), RANTES (2,000 pg/mL – 1.95 pg/mL) or TNF- α (300 pg/mL – 0.29 pg/mL) were prepared to pre-defined concentrations following a dilution range of 1:2 using manufacturer-supplied diluent.

Blocking buffer was removed following the period of incubation at room temperature, and plates were washed as described above and blotted dry. To each well, the pre-prepared protein standards were added in duplicate, and nine 100 μL aliquots of an experimental sample were added until the plate was filled. The plate was re-sealed using manufacturer-supplied sealing strips, and these samples and protein standards were incubated in the dark at room temperature for a further 2 hours.

Following the 2-hour incubation, plates were once again emptied, and any excess sample or protein standard solutions were discarded. Plates were once again washed 4 times in the manner outlined above, only with a more rigorous rocking step between each wash to ensure all residual sample/standard was removed. To each well, a detection antibody solution prepared using manufacturer supplied diluent was added and allowed to incubate for a further 2 hours in the dark.

Plates were once again emptied following the incubation, washed 4 times using the wash buffer solution as noted above and blotted dry before 100 μL of either avidin-horseradish peroxidase (avidin-HRP) for TMB-based ELISA (RANTES targeted ELISA), or streptavidin-horseradish peroxidase (streptavidin-HRP) were added to each well for ABTS-based ELISA. Plates were re-sealed and allowed to incubate at room temperature for 30 minutes.

For the RANTES ABTS-based ELISA, following incubation at room temperature, excess avidin-HRP was discarded and plates were washed 4 additional times in the manner outlined previously and blotted dry before 100 μL of a ABTS liquid substrate (Peprotech, USA) were added to each well. These plates were re-sealed using the plastic sealing strips and returned

to the dark to incubate for 40 minutes, with the progress of colour development checked visually at 10-minute intervals. Following the incubation, plates were transferred to a Tecan multi-well plate reader, and absorbance was measured at 405 nm with a wavelength correction set to 650 nm.

In the case of IL-8 and TNF- α , where both the ELISA kits were TMB-based, excess streptavidin-HRP was discarded, and plates were washed as noted above and blotted dry. To each well, 100 μ L of TMB liquid substrate were added (Peprotech, USA) and the plates re-sealed before being incubated at room temperature in the dark for 20 minutes. Following the final incubation, 100 μ L of a hydrochloric acid (HCl) stop solution (Peprotech, USA) were added to each well to stop the enzymatic reaction. The addition of a HCl stop solution was accompanied by a distinct colour change from blue to yellow. The absorbance of the IL-8 and TNF- α ELISA plates were read using a Tecan multi-well plate reader set to 450 nm with a wavelength correction set to 620 nm.

Protein concentrations were calculated using the Myassays.com 4 parameter logistic curve assay with the protein standard concentration curves present in each plate (MyAssays Ltd 2020).

4.2.11 RT-qPCR protocol for cellular IL-8 production following exposure to Lab4- and Lab4B-conditioned medium

The following RT-qPCR analysis was performed on the cell line HT29MTX by staff at Cultech Ltd.

HT29MTX cells were grown in multi-well plates to confluence and serum-starved prior to exposure assays. Cell-coated surfaces were subsequently exposed to one of three conditions – medium-only negative controls (a formulation lacking any bacterial cells), Lab4 exposure and Lab4B exposure. Following exposure, RNA was harvested from the cell coverslips utilising TRIzol[®] as outlined in section 3.2.3.3.2 and stored at -20 °C prior to being converted

to cDNA utilising the High Capacity cDNA Reverse Transcription Kit (Life Technologies, Paisley, UK).

These assays were performed on samples from 24- and 48-hour timepoints to assess whether those results viewed at 48 hours in the ELISA-based analyses were mirrored at an earlier timepoint or whether reduced exposure resulted in a different cellular response. Additionally, samples were exposed to a range of conditioned medium concentrations to further assess the impact of conditioned medium on cellular inflammation pathways. The selected concentrations were 10%, 25% and 50% to coincide with the data acquired in section 4.2.8, where 10% – 50% conditioned media were noted as having the most positive impact on the cell lines without inducing a reduction in cell viability.

A second stage analysis was performed using only single-strain conditioned medium to further scrutinise the Lab4 and Lab4B product line and identify which of bacterial constituents present in these pre-mixes were making the most significant impact.

The qPCR was conducted using the method described in section 3.2.3.3.6 in which a SYBR green master mix was utilised to allow for the measurement of the amplicon of interest, that being for IL-8 in this instance. The primers used in this assay are as seen in Table 4-2, and were sourced from the online repository oligo! and verified using the NCBI primer BLAST tool as described in section 3.2.3.3.5.

Table 4-2:Primer Sequences for IL-8 qPCR

Primer name	Primer sequence (5' – 3')	Source
IL-8 (Forward)	GAAGTTTTTGAAGAGGGCTGAGA	(oligo! 2018)
IL-8 (Reverse)	TTTGCTTGAAGTTTCACTGGCA	(oligo! 2018)
Actin (Forward)	ACTCTCCAGCCTTCCTCC	(oligo! 2018)
Actin (Reverse)	CGTACAGGTCTTTGCGGATG	(oligo! 2018)

Statistical analysis was performed using GraphPad Prism version 8.4.2.679, utilising installed analysis software packages, and data was visualised utilising the pre-installed Prism GraphPad boxplot functionality.

4.2.12 Statistical analysis

Statistics were performed using R version 3.4.3, and RStudio version 1.1.423. Paired and unpaired t-test were performed to analyse results and assess significance in all instances. R package GGplot 2 was utilised for visualising and colouring viability assay boxplots, whereas subsequent boxplots were generated using GraphPad Prism 8 and its associated boxplot functionality.

Significance was assigned according to the following thresholds as: ° $p < 0.10$, * $p < 0.05$, ** $p < 0.01$, *** $p < 0.001$.

4.3 Results

4.3.1 Probiotic bacterial growth curves

Due to the technical limitations of conducting growth curves under anaerobic conditions, both single-species and mixed-community growth curves for Lab4- and Lab4B-derived bacteria were performed in an aerobic environment. These growth curves were conducted using an anaerobically treated MRS media to maximise the initial growth potential of these bacterial communities.

The growth curves for the single-species, dual mixes and multi-species consortia for both the probiotic and *E. coli* species are shown in Appendix 1. The exponential phase for each situation was observed as ranging between hour 1 and 10 in each instance.

It was observed that the growth of the *Bifidobacterium* species was hindered in this assay, as the *Bifidobacterium* dual mix (consisting of *B. bifidum* and *B. animalis* sub sp. *lactis*) was noted as having a short stationary phase following exponential growth, which was followed by a rapid death phase, while neither of the *Bifidobacterium* was able to grow as single species in isolation. When compared to the other bacterial growth curves conducted in this study, this trend was uncharacteristic. In the growth curves generated for each *Lactobacillus*

species (*L. acidophilus* (premix), *L. paracasei*, *L. salivarius*), no death phase was observed within the assayed 24 hours, thus leading to the conclusion that nutrients were not a limiting factor in this instance. As such, it could be concluded that the ambient oxygen within the Tecan plate reader may have acted as the limiting factor for the growth of the *Bifidobacterium* in this instance.

The proposed impact of ambient oxygen on the growth of the bifidobacteria in this study corresponds to characteristic behaviours of the genus, where *Bifidobacterium* genus typically display low tolerance to oxygen, which in turn might act to limit the growth potential of these species when under sub-optimal conditions.

The data presented within these growth curves was utilised to ensure that all conditioned media used throughout the study were generated using bacteria residing within the exponential phase of growth, thus maximising the bacterial metabolite production and efficacy of conditioned media within subsequent experiments.

4.3.2 *E. coli* growth curves

Unlike the issues encountered when assaying the growth of the probiotics, each of the selected *E. coli* strains grew well under aerobic conditions, and, as such, growth curves were conducted at ambient oxygen levels with untreated growth medium using the Tecan multi-well plate reader apparatus.

Each bacterial strain was assessed over a 24-hour period, and *E. coli* strains E69, MP1 and Nissle 1917 were observed as entering the exponential phase between hour 1 and hour 10, similar to that observed in the probiotics. Additionally, from the *E. coli* strains selected for the study, none displayed evidence of entering the death phase during the observed 24-hour period, further suggesting that any detrimental impact or slow growth observed was unlikely due to nutrient availability.

Both Lab4 and Lab4B showed similar growth curves to the assessed *E. coli* reported above, with the exponential phase of growth occurring between approximately 1 and 10 hours. As such, an identical conditioned medium protocol was adapted for the synthesis of bacteria-conditioned medium in both the probiotic and pathogenic bacterial samples.

4.3.3 Cellular proliferation of cell lines Caco-2 and HT29MTX following a 48-hour exposure to Lab4- and Lab4B-conditioned medium

All cell monolayers were first inspected by light microscopy, post growth, to ensure that there was no disruption, and an intact confluent monolayer was in place for subsequent downstream applications and experiments. Neither Caco-2 nor HT29MTX exhibited significant increases in cellular proliferation at any concentration when compared to the 0% conditioned medium control (Figure 4-1), whereas cellular proliferation significantly decreased when incubated with 100% Lab4B-conditioned medium ($p < 0.001$). An additional trend was observed, however, in the cell line HT29MTX. With 100% conditioned medium, from Lab4- and Lab4B-treated samples, a decreased cellular proliferation was observed, thus leading to the conclusion that at higher concentrations of conditioned medium, cellular proliferation is negatively impacted.

Caco-2, however, displayed no major changes in cellular proliferation. Some minor increases to cellular proliferation were observed at 25% and 50% in both Lab4- and Lab4B-exposed samples for Caco-2 and HT29MTX cell lines, although there were no significant changes to cellular proliferation noted at any concentration across both cell lines.

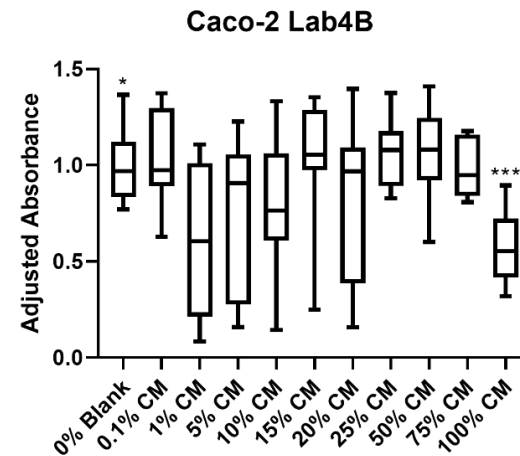
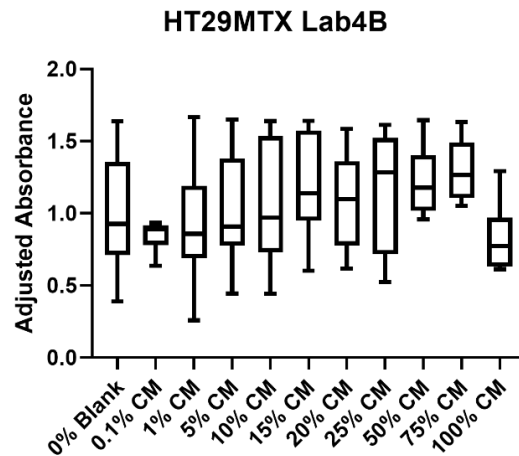
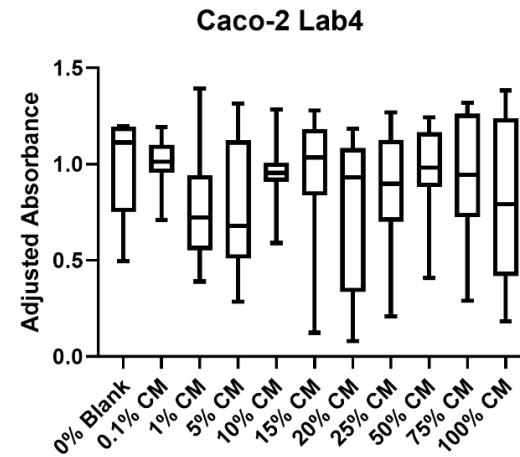
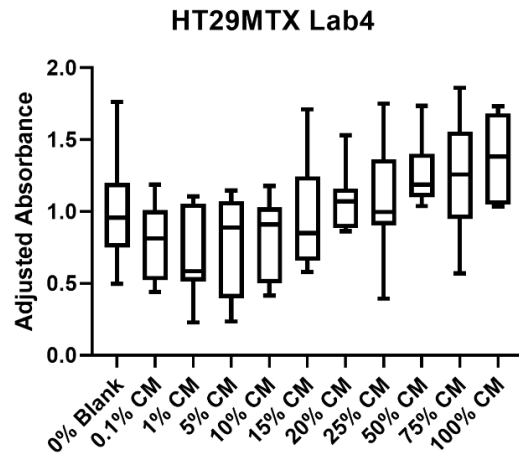


Figure 4-1: Cellular proliferation of HT29MTX and Caco-2 cells following 48-hour exposure to various concentrations of probiotic-conditioned media via MTT assay. HT29MTX and Caco-2 cells exposed to either Lab4 or Lab4B conditioned medium of various concentrations for 48 hours were assessed for cellular proliferation using the MTT assay. The data represent the mean±standard deviation (SD) of 4 independent experiments (containing duplicate samples of each condition) and are presented as fold-change compared to the blank control that has been arbitrarily set as 1. Statistical analysis was performed using the unpaired t-test where *** $p < 0.001$.

4.3.3.1 Glycoprotein production observed in Caco-2 and HT29MTX samples following exposure to Lab4- and Lab4B-conditioned medium

Unlike the findings observed in the cellular proliferation assays noted above, both cell lines exhibited significant changes in glycoprotein production following prolonged exposure to probiotic-conditioned medium at specific concentrations, although these changes varied according to both the cell line of choice and probiotic-conditioned medium (Figure 4-2).

Additionally, Caco-2 exhibited a generally positive response to both Lab4 and Lab4B probiotic-conditioned media, with a dose-dependent response observed in Lab4-exposed cells, where, with 25%, 50%, 75% and 100% conditioned media, Caco-2 showed significant increases in glycoprotein production ($p < 0.01$). In Lab4B-exposed cells, however, only 20%, 25% and 75% conditioned medium-exposed cells displayed any significant increases in glycoprotein production compared to the blank medium control (20% and 25% conditioned media: $p < 0.01$; 75% conditioned medium: $p < 0.05$). However, it should be noted that any concentration assayed above 25% Lab4B-conditioned medium returned reduced glycoprotein production, thus leading to the conclusion that, in the case of Caco-2 cells, glycoprotein production was optimal at 25% conditioned medium and, at elevated concentrations of Lab4B, a potentially negative impact was experienced by those cells.

HT29MTX, however, varied considerably compared to Caco-2. No significant changes in glycoprotein production were observed at any concentration in Lab4-exposed cells when compared to the blank control samples. However, when examining the Lab4B-exposed cells, HT29MTX was observed as producing lower quantities of glycoprotein, even at lower levels of Lab4B, and this trend was significant at all concentrations except for 10% and 100% conditioned media (0.1%, 20%, 25% and 75% conditioned media: $p < 0.5$; 1%, 5% and 50% conditioned media: $p < 0.01$), an inverse trend from that seen in Caco-2 samples.

Due to the variable results observed across both cell lines and concentrations, a dilution of 25% conditioned medium was selected for subsequent experiments due to the observed trend of increased cellular proliferation in the 25% – 50% conditioned medium assays for both Lab4- and Lab4B-exposed cells in both cell lines, and the significant influence of both

Lab4 and Lab4B on the glycoprotein production of the cell line Caco-2 at this concentration. Additionally, the selected concentration was further corroborated by protocols used by staff at Cultech Ltd. (Port Talbot, UK), where 25% conditioned medium is considered an acceptable standard for probiotic-conditioned media experiments (Davies et al. 2018; Michael et al. 2019).

4.3.4 The impact of flow on the pH of cell culture medium supplemented with Lab4 and Lab4B live bacteria

To accurately assess the impact of bacterial products on intestinal cells, it was important to assess the impact of pH on intestinal cells exposed to both static and flow environments. In both the Lab4 and Lab4B assayed samples, it was observed that prolonged exposure to the QV500 system induced significant changes in pH. However, it was not in a manner that had been expected. Due to the fermentative nature of the lactobacilli and bifidobacteria that comprise the Lab4 and Lab4B products utilised in the study, it was initially proposed that the pH would become somewhat more acidified as a result of exposure to a biological element like that induced by the QV500 dynamic flow-through system.

However, in both Lab4 and Lab4B samples exposed to dynamic flow, the pH was observed as having become more alkaline (Figure 4-3). The uncharacteristic change in pH was observed as being significant compared to that observed in an equivalent non-flow control with an equivalent medium volume.

It was noted that the medium from this assay was collected and used for further metabolic analysis. However, as previously stated, due to unforeseen time constraints, analysis of the metabolites present in the sample was not possible in time for the completion of this study, and, therefore, those results are not included.

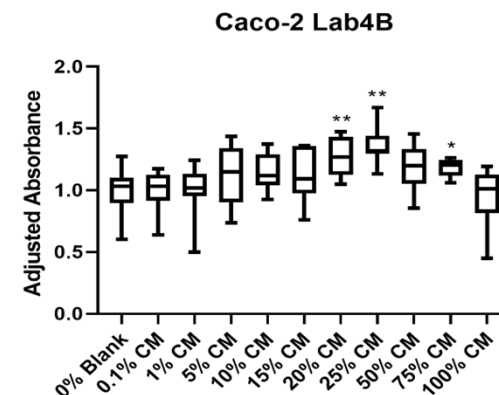
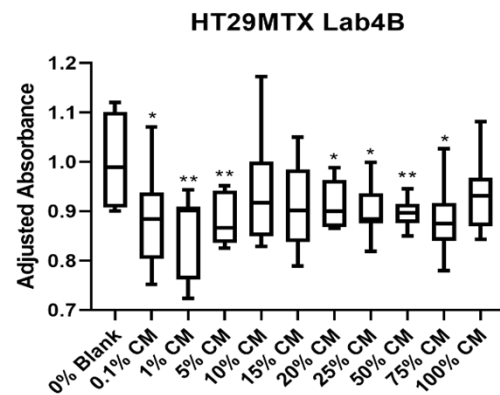
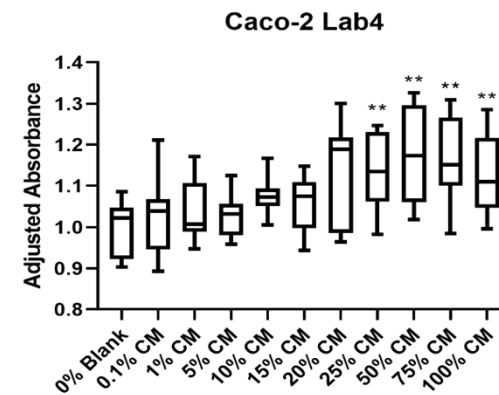
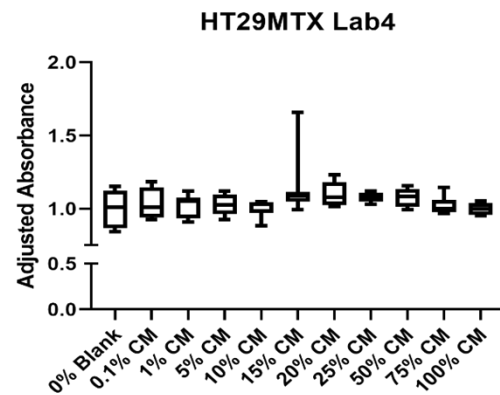


Figure 4-2: Glycoprotein production in cell lines Caco-2 and HT29MTX following 48-hour exposure to Lab4 and Lab4B probiotic-conditioned media, measured via the qAlcian blue assay. HT29MTX and Caco-2 cells exposed to either Lab4 or Lab4B conditioned medium of various concentrations for 48 hours were assessed for glycoprotein production using the qAlcian blue glycoprotein assay. The data represent the mean \pm standard deviation (SD) of 4 independent experiments (containing duplicate samples of each condition) and are presented as fold-change compared to the blank control that has been arbitrarily set as 1. Statistical analysis was performed using the unpaired t-test where * $p < 0.05$, ** $p < 0.01$.

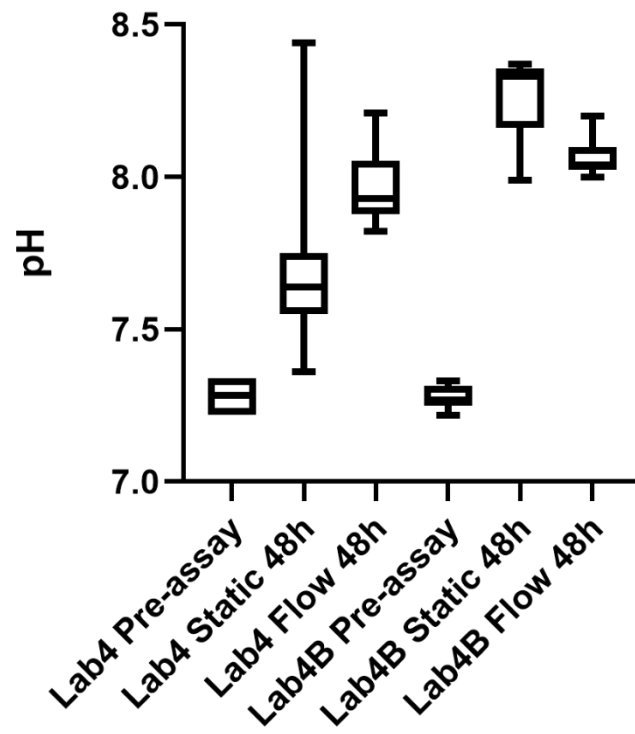


Figure 4-3: The impact of flow on the pH of media supplemented with Lab4 and Lab4B products. Cell culture medium was exposed to static or flow conditions for 48 hours and assessed using a pH probe. The data represent 3 independent experiments (containing triplicate samples of each condition). Statistical analysis was performed using the unpaired t-test.

4.3.5 Assessing the impact of pH on cellular viability via LDH assay

To confirm the proposition that the selected acid used to alter pH would not induce any cross-reactivity, a preliminary control assay was performed using a 1:100 dilution of acetic acid diluted using dPBS. In all instances, no significant signal was observed in the acetic acid samples compared to the blank control.

In the instance of both Caco-2 and HT29MTX, reduced pH was noted as inducing a significant change in cellular behaviour when compared to the pH 7.4 medium base, and these changes were observed to be time dependent and somewhat condition dependent.

4.3.5.1 Monitoring the LDH production of Caco-2 cells exposed to pH adjusted medium

When observing the Caco-2 cells exposed, between the 1-hour and 4-hour timepoints, no significant differences were observed at pH 6.5 (Figure 4-4). However, at 24 hours' and 48 hours' exposure, LDH was significantly increased under static conditions (24 hours: $p < 0.01$; 48 hours: $p < 0.001$). A similar trend was observed in flow, although this change in LDH production was noted earlier at 4 hours ($p < 0.01$) and 24 hours ($p < 0.001$), with no significant increase or decrease noted at 48 hours' exposure. When comparing static- and flow-exposed samples, at both 4 hours' and 48 hours' exposure, LDH production was significantly reduced in flow samples.

Similar to that seen at pH 6.5, static-exposed cells displayed an increased production of LDH over time, with significant increases noted at 4 hours', 24 hours' ($p < 0.05$) and 48 hours' exposure ($p < 0.01$). Flow-exposed samples yet again displayed a similar trend, albeit to a lesser extent, with all timepoints, with the exception of 48 hours' exposure, returning significant increases in LDH compared to 1 hour post-exposure (2 hours: $p < 0.01$; 4 hours: $p < 0.05$; 24 hours: $p < 0.001$). Again, at a pH of 7.0, flow-exposed cells were noted as having significantly reduced LDH production compared to the static equivalent, particularly at

timepoints 1 hour, 4 hours and 24 hours ($p < 0.05$), and 48 hours having the most significant reduction in LDH compared to the static equivalent ($p < 0.01$).

At pH 7.4, the pH that corresponds to that seen in the cell culture medium of choice for this study, almost identical trends were observed compared to the somewhat more acidic pH seen in the other assays. Static-exposed cells once again displayed a near-identical trend to that seen across the other pH with elevated LDH production over time, with significant increases observed at 4 hours' ($p < 0.01$), 24 hours' and 48 hours' exposure ($p < 0.001$).

Additionally, flow samples displayed a general trend of increased LDH production over time, although only at 4 hours' exposure was this noted as being significant ($p < 0.01$).

Additionally, while flow samples did return LDH values that were somewhat lower than the static equivalents, only 24 hours' exposure was noted as being significant ($p < 0.05$). The continued trend of flow exposure returning lower LDH values than the static equivalent could suggest that exposure to flow may act as a mitigating factor to the impact of a potentially stressful pH for Caco-2 cells.

4.3.5.2 Monitoring the LDH production of HT29MTX cells exposed to pH adjusted medium

Unlike with Caco-2, HT29MTX displays a somewhat more varied response to changes in pH. Static-exposed cells at pH 6.5 display an increase in LDH production until 4 hours, following which the LDH began to decrease (Figure 4-5). Significant increases can be noted at 4 hours' and 24 hours' exposure ($p < 0.001$), with a somewhat less significant increase observed at 48 hours ($p < 0.01$). Flow samples exhibited a consistent increase in LDH production over time, with significant increases noted between hours 4 and 48 hours (4 hours: $p < 0.01$; 24 and 48 hours: $p < 0.001$). Interestingly, flow samples at pH 6.5 were noted as having increased LDH levels in the cell line HT29MTX compared to static, with significant increases noted at 1 hour, 24 hours and 48 hours (1 hour and 24 hours: $p < 0.01$; 48 hours: $p < 0.001$).

Static-exposed cells at pH 7.0 showed a significantly increased LDH production over time, particularly at 4, 24 and 48 hours ($p < 0.01$). However, unlike the trends seen at pH 6.5, flow-

exposed samples only show an increase in LDH production between hours 1 and 24, following which LDH production appears to stabilise. Significant increases in LDH were observed in flow-exposed samples at 4 hours' ($p < 0.01$) 24 and 48 hours' ($p < 0.001$) exposure. All flow samples at pH 7.0 were notable in that there was a significant reduction in LDH produced at all timepoints in flow compared to static equivalents, with 1 and 2 hours having the least significant reduction ($p < 0.05$), whereas all other timepoints showed a highly significant reduction in LDH ($p < 0.001$).

At pH 7.4, HT29MTX cells showcase similar trends to those seen at pH 6.5, in that both flow- and static-exposed samples show an increase in LDH production over time. While static only had a significant LDH increase at 24 and 48 hours' exposure ($p < 0.05$), flow had significant increases in LDH release at 4 hours', 24 hours' and 48 hours' exposure (4 and 24 hours: $p < 0.01$; 48 hours: $p < 0.001$). Interestingly, when comparing both static and flow conditions, both conditions return similar levels of LDH across all timepoints with only 4 hours' flow exposure showing significantly higher LDH production compared to the static counterpart ($p < 0.05$), potentially suggesting that at this pH, flow has little impact on the stress response of cells, and that nutrient deprivation or other stress factors may be at work rather than LDH production being a result of either pH or dynamic flow.

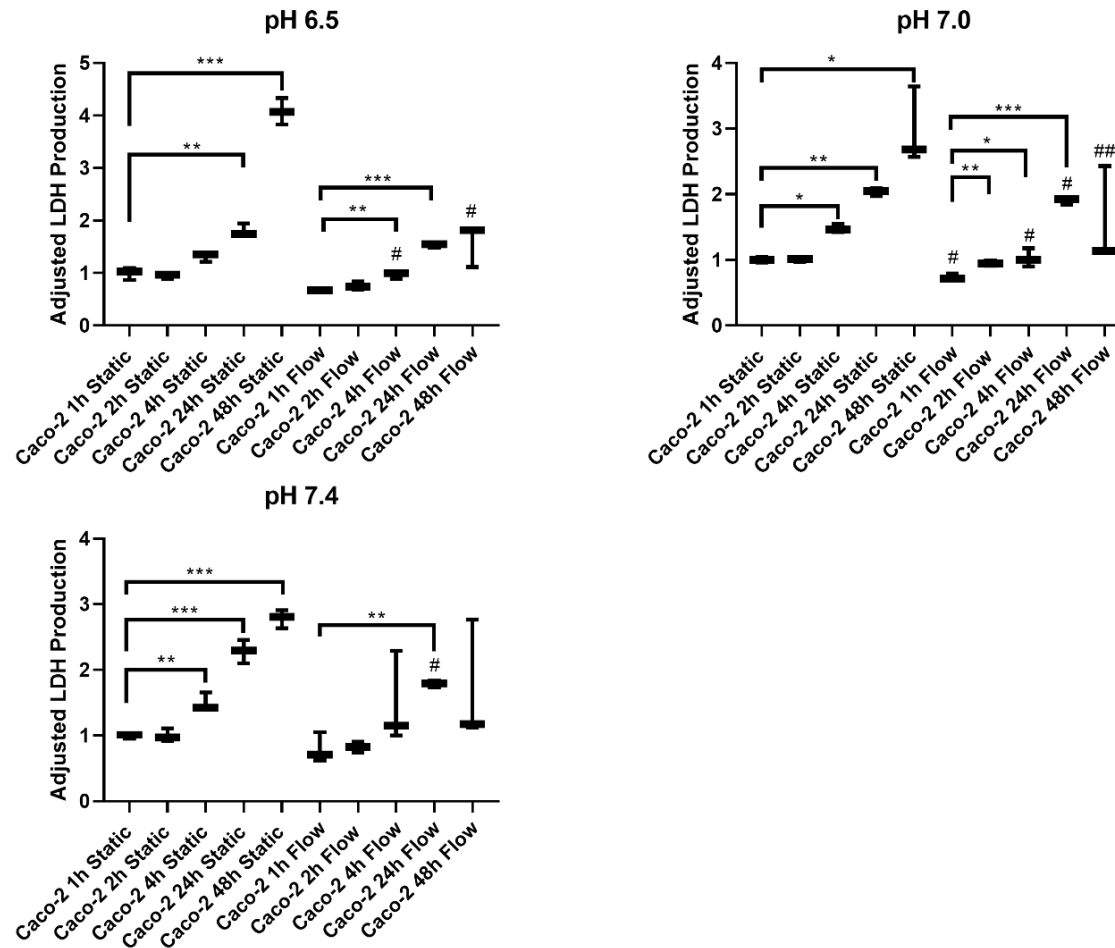


Figure 4-4: LDH production in Caco-2 cells exposed to static and flow conditions at pH 6.5, 7.0 and 7.4 monitored over a 48-hour period. Caco-2 cells under static or flow conditions were exposed to pH 6.0, pH 7.0 or pH 7.4 for varying durations and viability was assessed using the LDH-Glo™ assay. The data represent the mean ± standard deviation (SD) of 3 independent experiments (containing triplicate samples of each condition) and are presented as fold-change compared to the 1 hour static control that has been arbitrarily set as 1. Statistical analysis was performed using either the paired or unpaired t-test where * $p < 0.05$, ** $p < 0.01$, *** $p < 0.001$ as indicated, or # $p < 0.05$, ## $p < 0.01$ when comparing time-matched static and flow conditions.

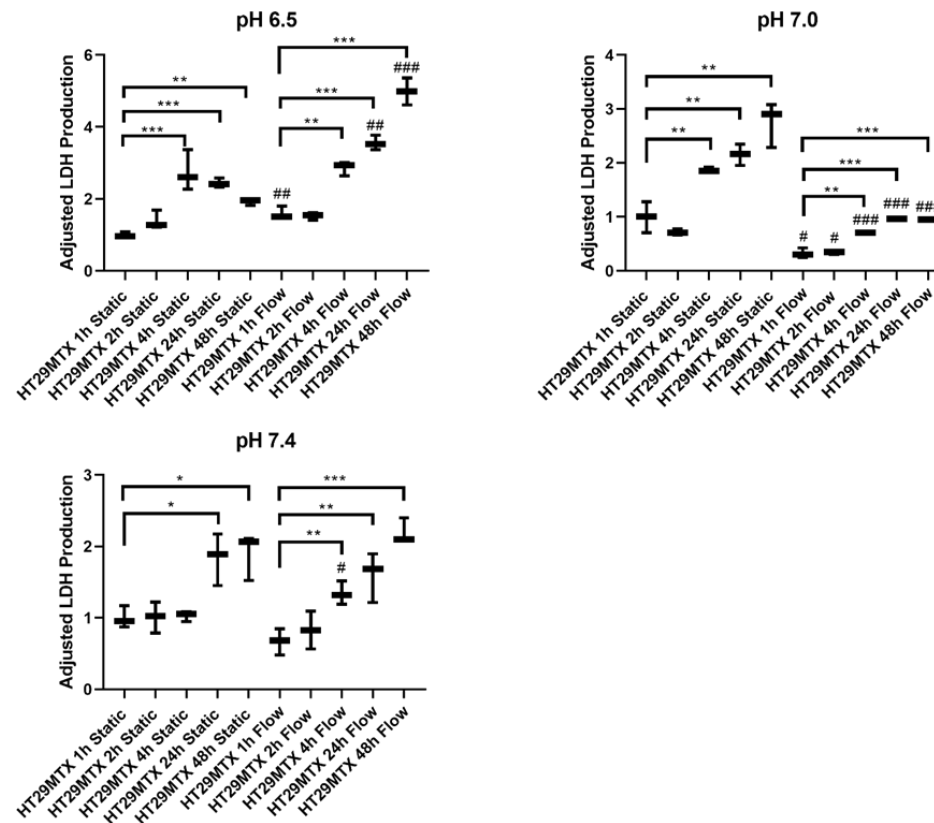


Figure 4-5: LDH production in HT29MTX cells exposed to static and flow conditions at pH 6.5, 7.0 and 7.4 monitored over a 48-hour period. HT29MTX cells under static or flow conditions were exposed to pH 6.0, pH 7.0 or pH 7.4 for varying durations and viability was assessed using the LDH-Glo™ assay. The data represent the mean±standard deviation (SD) of 3 independent experiments (containing triplicate samples of each condition) and are presented as fold-change compared to the 1-hour static control that has been arbitrarily set as 1. Statistical analysis was performed using either the paired or unpaired t-test where * $p < 0.05$, ** $p < 0.01$, *** $p < 0.001$ as indicated, or # $p < 0.05$, ## $p < 0.01$, ### $p < 0.001$ when comparing time-matched static and flow conditions.

4.3.6 The impact of dynamic flow on the production of pro-inflammatory cytokines and chemokines

Since an aim of this study was to identify the potential advantages presented by dynamic flow in cell culture, in addition to the overall impact of probiotic products under these novel conditions, the production of pro-inflammatory cytokines and chemokines by the cell lines Caco-2 and HT29MTX were of particular interest. Prior to the introduction of bacterial compounds into the flow environment, it was first important to assess the impact of dynamic flow on the production of IL-8, RANTES and TNF- α . This baseline assessment would identify whether prolonged exposure to the QV500 resulted in the production immunological markers, as previous data in the LDH assay suggested that cells may become somewhat stressed under flow. A complete summary of the results found in section 4.3.6 can be seen in Table 4-3.

Both Caco-2 and HT29MTX exhibited similar trends, although no significant alterations in inflammatory markers could be noted in Caco-2 samples (Figure 4-6).

When examining the production of IL-8, an increase was observed in both cell lines under flow conditions compared to the static equivalents, although the only significant difference was recorded in the HT29MTX cells ($p < 0.001$). However, while the inflammatory marker IL-8 was decidedly pronounced in its increase under flow, it was notable that, in both cell lines, a reduction in both RANTES and TNF- α was observed in flow-exposed samples, with a significant reduction in RANTES production ($p < 0.001$) and in TNF- α production ($p < 0.01$) observed in HT29MTX cells.

These observations in cellular behaviour across both cell lines under flow conditions further strengthen the hypothesis that dynamic flow influences cellular parameters *in vitro*. The recorded data additionally aids in emphasising the importance of selecting appropriate conditions for *in vitro* studies, as in all instances (the exception being in the production of IL-8 in Caco-2 samples), flow induced significant alterations in cellular behaviour compared to the static counterpart.

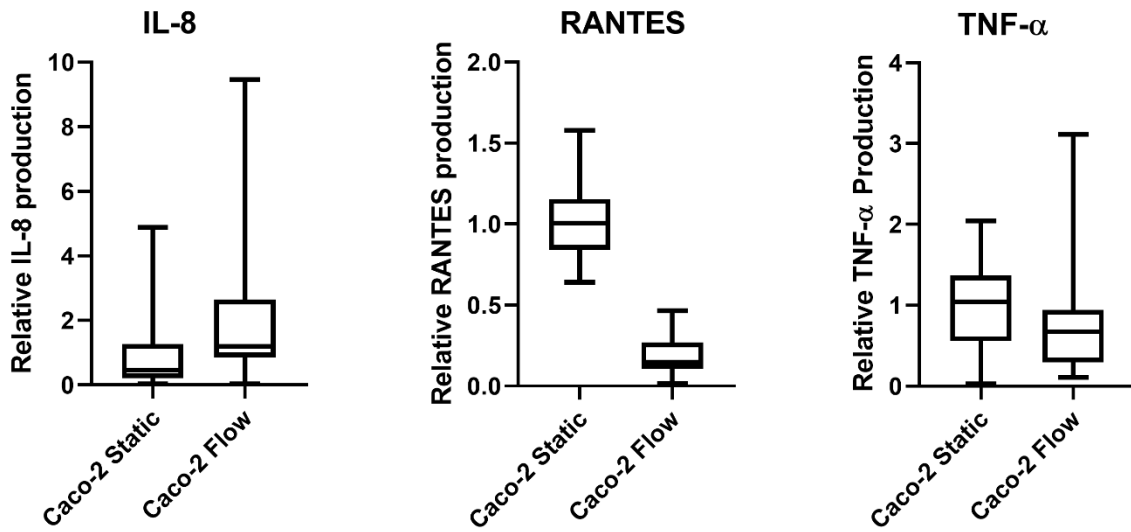
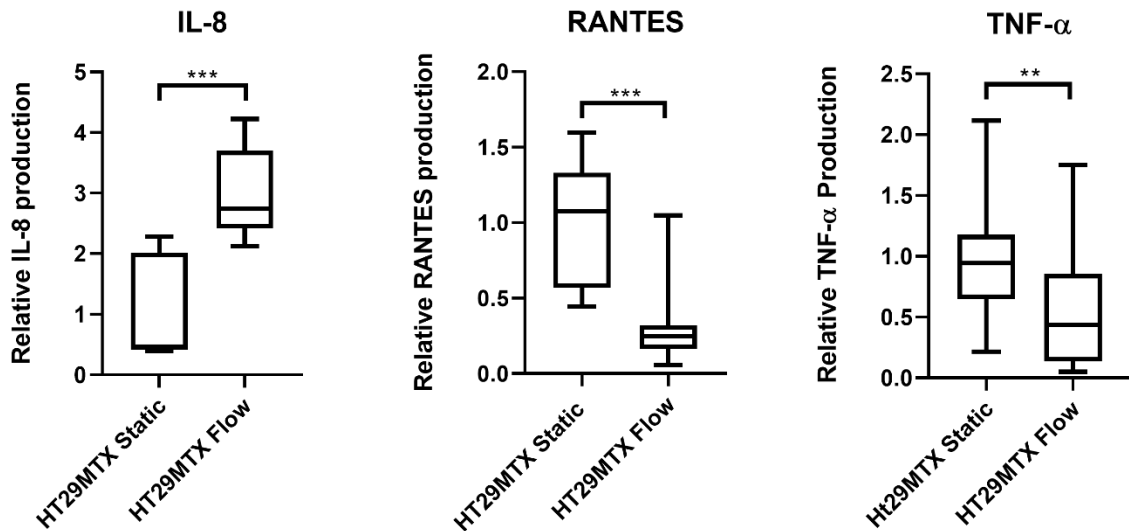
A**B**

Figure 4-6: Monitoring the inflammatory response of Caco-2 and HT29MTX following exposure to static and flow conditions. Cell culture medium from coverslips seeded with either Caco-2 (A) and HT29MTX (B) cells exposed to either static or flow conditions for 48 hours was collected and assessed for the presence of pro-inflammatory markers IL-8, RANTES and TNF- α via ABTS- and TMB-based ELISA. The data represent the mean \pm standard deviation (SD) of 9 independent experiments (containing triplicate samples of each condition) and are presented as fold-change compared to the static control that has been arbitrarily set as 1. Statistical analysis was performed using the unpaired t-test where ** $p < 0.01$, *** $p < 0.001$.

4.3.6.1 Monitoring the production of IL-8, RANTES and TNF- α in Caco-2 cells stimulated with Lab4 and Lab4B

When exposed to Lab4 or Lab4B products under static conditions, Caco-2 displayed a significant increase in IL-8 production in all groups (conditioned medium and live bacterial exposure) compared to the bacteria-free control ($p < 0.001$) (Figure 4-7). Notably, IL-8 production was most increased in those test groups exposed to Lab4 products, in which IL-8 production was approximately 3 – 4 times that seen in Lab4B-exposed samples, with a further minor trend observed where IL-8 production in conditioned medium-exposed samples were somewhat increased compared to live bacteria-exposed samples, although this was not statistically significant in any instance.

Additionally, when exposed to flow conditions, Caco-2 samples exposed to either conditioned medium or live bacteria displayed no significant changes in IL-8 production compared to the bacteria-free control (Figure 4-7). When comparing the flow samples to the equivalent static experiment, all flow samples exposed to either Lab4 or Lab4B showed significantly lower IL-8 values than their static counterparts ($p < 0.001$).

When examining RANTES production, it should first be noted that the RANTES production in the flow-exposed Lab4 conditioned medium test group and flow-exposed Lab4B live bacteria test groups were below the limit of detection in all instances and, as such, are not recorded here. Under static conditions, Caco-2 cells exposed to Lab4 and Lab4B, both conditioned medium and live bacteria, showed significantly reduced RANTES levels compared to the static conditions – the opposite trend to that seen in both the IL-8 and TNF- α test groups, with the sole non-significant change seen in those samples exposed to Lab4B live bacteria under static conditions (Lab4B (CM): $p < 0.01$; Lab4 live bacteria and conditioned medium: $p < 0.001$) (Figure 4-7). Additionally, no significant changes were noted in the flow-exposed samples compared to the bacteria-free control. Flow-exposed Lab4 live bacteria samples, however, showed a highly significant reduction in RANTES production compared to the static equivalent ($p < 0.001$).

With TNF- α production in Caco-2, static-exposed samples displayed a similar trend to that seen in the IL-8 test group, with a general trend of increased TNF- α production when cells are exposed to Lab4 and Lab4B products, with significant increases in both the live bacteria and conditioned medium Lab4 test groups ($p < 0.001$) and the Lab4B conditioned medium test group ($p < 0.05$). In the RANTES test group, those samples exposed to live Lab4B bacteria were below the limit of detection and, as such, are not included here. A general trend of increased TNF- α across all probiotic-exposed samples was again seen under flow, although significant increases were only recorded from the Lab4B conditioned medium ($p < 0.05$) and the Lab4 live bacteria-exposed samples (Figure 4-7). Only the Lab4 conditioned medium-exposed samples displayed any significant differences between static and flow conditions, with a significant decrease in TNF- α production in flow ($p < 0.001$).

4.3.6.2 Monitoring the production of IL-8, RANTES and TNF- α in HT29MTX cells stimulated with Lab4 and Lab4B

Assays for IL-8 showed that no distinct trend could be observed, and no significant changes in IL-8 production could be seen in any treatment group under both static and flow conditions compared to the bacteria-free controls (Figure 4-8).

RANTES production was observed as being significantly reduced in all bacterially exposed static samples compared to the bacteria-free control in both Lab4 and Lab4B test groups ($p < 0.001$) (Figure 4-8). Flow-exposed samples showed reduced RANTES production in bacteria-exposed samples compared to the bacteria-free control, with significantly decreased levels noted in Lab4B-conditioned media, Lab4 live bacteria ($p < 0.01$) and Lab4B live bacteria-exposed samples ($p < 0.05$). Additionally, under both static and flow conditions, Lab4-conditioned media samples showed a significantly increased RANTES production compared to the live bacteria-exposed sample (static: $p < 0.05$; flow: $p < 0.01$).

TNF- α production was unique in that similar changes were seen in both static and flow, with significant increases noted in the same treatment groups across both static and flow conditions. While static conditions generally displayed greater TNF- α levels than their flow

equivalent, Lab4B-conditioned medium-exposed and both Lab4 and Lab4B live bacteria-exposed samples showed significant increases in TNF- α compared to their static equivalents (Figure 4-8). Additionally, both static and flow Lab4 samples were noted as having elevated TNF- α production in live exposed samples compared to the conditioned medium equivalent ($p < 0.001$). When comparing static and flow, TNF- α levels were generally observed as being lower in flow exposed samples, with significant reductions only noted in Lab4B-conditioned medium- and Lab4 live bacteria-exposed samples compared to the static equivalents ($p < 0.001$).

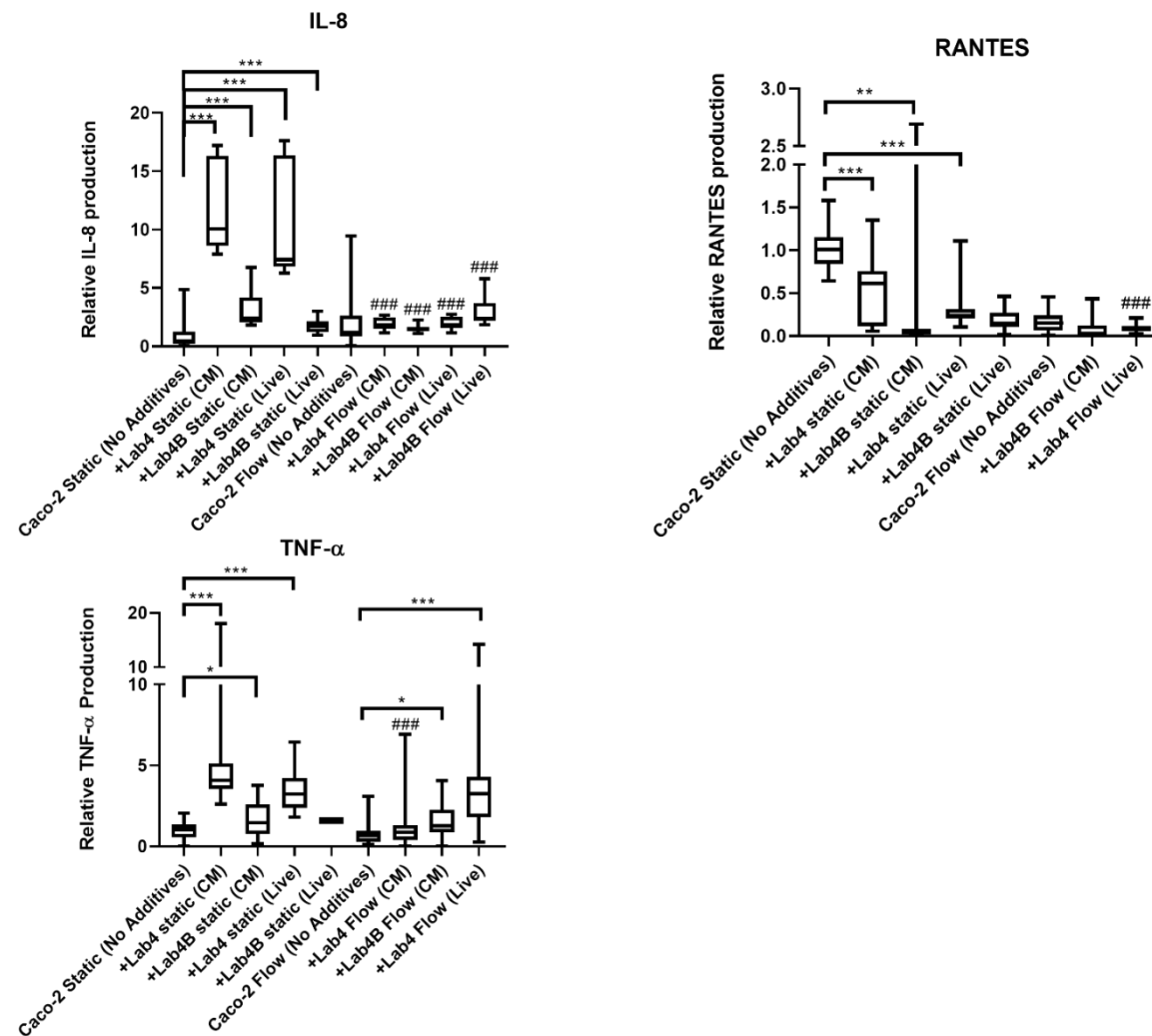


Figure 4-7: Monitoring the production of pro-inflammatory molecules IL-8, RANTES and TNF- α in Caco-2 cells following exposure to Lab4 and Lab4B probiotics under flow and static conditions. Cell culture medium from coverslips seeded with Caco-2 cells exposed to bacteria-conditioned medium or live Lab4/Lab4B-supplemented medium under static and flow conditions for 48 hours was collected and assessed for the presence of pro-inflammatory markers IL-8, RANTES and TNF- α via ABTS- and TMB-based ELISA. The data represent the mean \pm standard deviation (SD) of 9 independent experiments (containing triplicate samples of each condition) and are presented as fold-change compared to the no-additive static control that has been arbitrarily set as 1. Statistical analysis was performed using the unpaired t-test where * $p < 0.05$, ** $p < 0.01$, *** $p < 0.001$ as indicated, or ### $p < 0.001$ when comparing matched static and flow conditions.

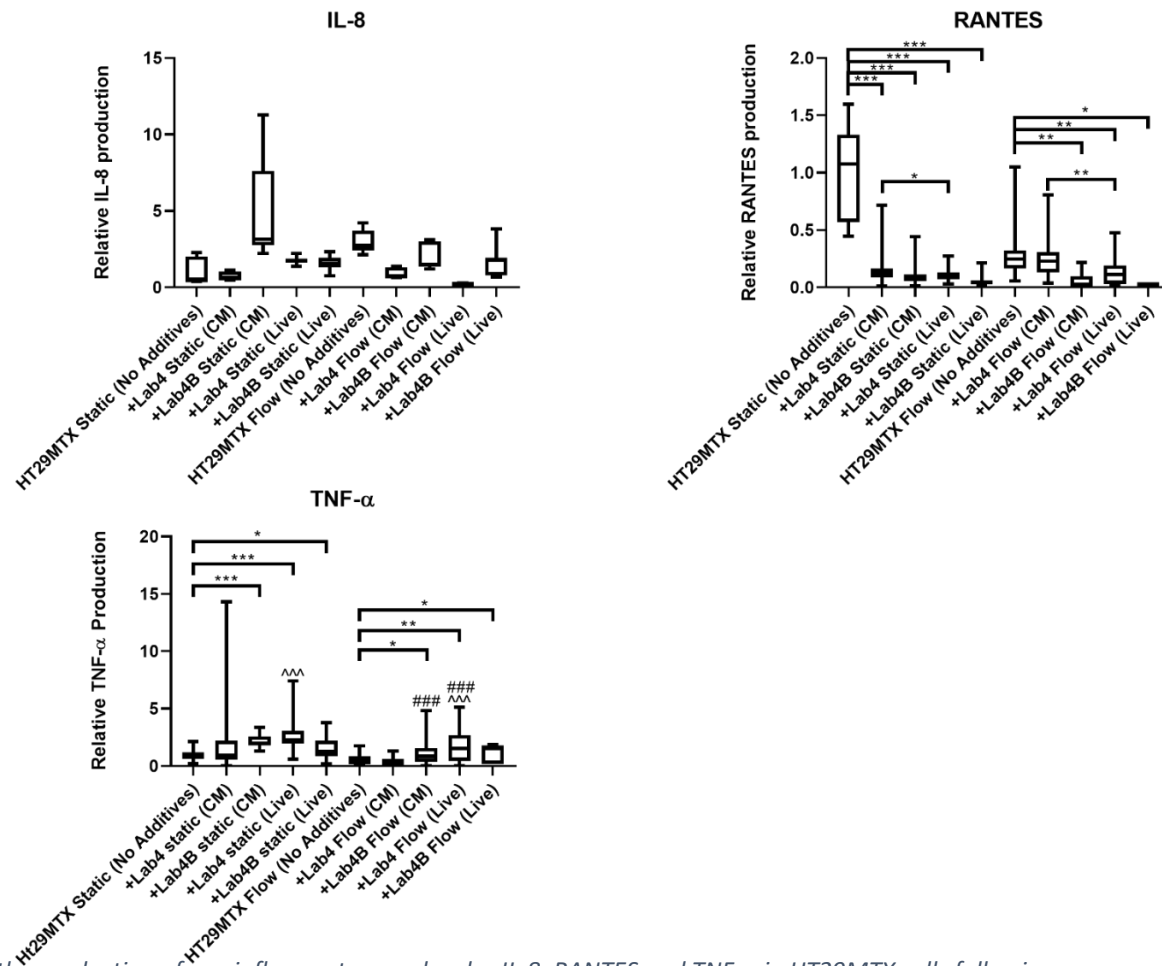


Figure 4-8: Monitoring the production of pro-inflammatory molecules IL-8, RANTES and TNF- α in HT29MTX cells following exposure to Lab4 and Lab4B under flow and static conditions for a 48-hour period. Cell culture medium from coverslips seeded with HT29MTX cells exposed to bacteria-conditioned medium or live Lab4/Lab4B-supplemented medium under static and flow conditions for 48 hours was collected and assessed for the presence of pro-inflammatory markers IL-8, RANTES and TNF- α via ABTS- and TMB-based ELISA. The data represent the mean \pm standard deviation (SD) of 9 independent experiments (containing triplicate samples of each condition) and are presented as fold-change compared to the no-additive static control that has been arbitrarily set as 1. Statistical analysis was performed using the unpaired t-test where * $p < 0.05$, ** $p < 0.01$, *** $p < 0.001$ as indicated, ### $p < 0.001$ when comparing matched static and flow conditions or ^^ $p < 0.001$ when comparing conditioned medium and equivalent live bacteria treatment groups within a given condition (static or flow).

4.3.6.3 The impact of *E. coli* strains E69, MP1 and Nissle 1917 on the production of pro-inflammatory cytokines

No Caco-2 samples assessed for TNF- α following bacterial exposure showed results that were above the limit of detection. As such, TNF- α production will only be discussed in the context of HT29MTX cells and, additionally, no values no TNF- α will be found in the following section for the cell line Caco-2.

4.3.6.3.1 The impact of *E.coli* exposure on the production of IL-8 and RANTES in Caco-2 cultures

In the case of Caco-2 cells exposed to the pathogenic *E. coli* E69, a variable trend was observed in a treatment-dependent manner (Figure 4-9). With regard to IL-8 production, no significant induction of IL-8 was observed in any static E69-exposed samples, be that conditioned medium, or those samples exposed to live bacteria, although in flow-exposed samples, a significant reduction in IL-8 production was observed compared to the bacteria-free control ($p < 0.05$). When comparing the IL-8 production across static- and flow-exposed samples, a highly significant increase in IL-8 was observed in flow-exposed E69-conditioned medium samples compared to the static equivalent ($p < 0.01$). A similar trend was not observed in the live bacteria samples, as no significant changes in IL-8 production were seen under flow at this time. Regarding the infected flow samples, neither static- nor flow-exposed infected cells were found to produce IL-8 in this study and, as such, were deemed as below the limit of detection and therefore are not recorded here.

MP1- and Nissle 1917-exposed cells showed no significant changes in the conditioned medium static samples, only returning a significant reduction in IL-8 when exposed to live bacteria. Additionally, Nissle 1917-exposed samples were shown to return a significantly reduced IL-8 response with live bacteria compared to conditioned medium. Flow-exposed samples treated with MP1- and Nissle 1917-conditioned media were generally observed as having reduced IL-8 compared to the non-bacterial exposed controls. Significant reductions in IL-8 were observed in the Nissle 1917-conditioned medium samples ($p < 0.001$) and both

the MP1 and Nissle 1917 live bacteria-exposed samples ($p < 0.01$). A highly significant induction of IL-8 was observed in the flow-exposed Nissle 1917 and MP1 live bacteria samples compared to the static equivalents, a trend that was not mirrored in the EPEC, suggesting an altered behaviour when in the presence of mutualistic and probiotic *E. coli*.

Samples examined for RANTES production in Caco-2 cells exhibited a consistently significant reduction in all bacteria-exposed samples ($p < 0.001$), with the exception of E69-conditioned medium samples (static), which showed RANTES values that were below the limit of detection and are thus absent from Figure 4-9, and all E69-exposed cells under flow conditions. Regarding the static-exposed samples, RANTES values were not significantly altered compared to the bacteria-free control. Additionally, there were no significant changes in RANTES expression in Caco-2 samples when comparing static- and flow-exposed samples, with the exception being the Nissle 1917- and MP1-conditioned medium samples, where it was shown that a significant induction of RANTES had occurred in flow compared to the static equivalent.

4.3.6.3.2 The impact of *E.coli* exposure on the production of IL-8, RANTES and TNF- α in HT29MTX cultures

Similar to those results recorded in the Caco-2 samples, HT29MTX displayed a trend of suppressed production of pro-inflammatory molecules in those samples in the *E. coli* treatment groups compared to a bacteria-free control, although this trend was not mirrored across all inflammatory markers.

As seen in Figure 4-10, IL-8 production was significantly reduced in all bacteria-exposed samples compared to the bacteria-free control ($p < 0.001$), both in static- and flow-exposed samples. Additionally, a further mitigation of the production of pro-inflammatory molecules in HT29MTX cells could be observed in static-exposed samples compared to the equivalent flow experiment, with both live *E. coli* and conditioned medium test groups' flow-exposed samples returning significantly increased levels of IL-8 ($p < 0.001$).

In a similar manner, reduced levels of RANTES could be seen in all test groups exposed to the *E. coli* strains ($p < 0.001$). However, while the trend of reduced RANTES production can be observed across both static- and flow-exposed samples, no statistically significant changes were observed when comparing static and flow equivalent experiments, and while the bacteria-free controls did exhibit heightened levels of RANTES compared to the *E. coli*-exposed samples, in no instance was this difference statistically significant (Figure 4-10).

However, IL-8, RANTES and TNF- α production in HT29MTX was notably increased in the EPEC-exposed samples compared to the bacteria-free control. In static-exposed samples, minor changes were seen in the conditioned medium and infected samples, with a significant increase in TNF- α following exposure to live bacterial cells. This trend was further emphasised when examining the flow-exposed samples, with both the conditioned medium- and live bacteria-exposed samples returning significantly increased levels of TNF- α compared to the bacteria-free control. It should be noted that, in the flow-exposed infection samples, all returned values were below the limit of detection and are, as such, absent from Figure 4-10. Unlike the changes observed in both RANTES and IL-8 assessed samples, TNF- α examined samples had no significant changes in TNF- α production in flow samples compared to the static equivalent.

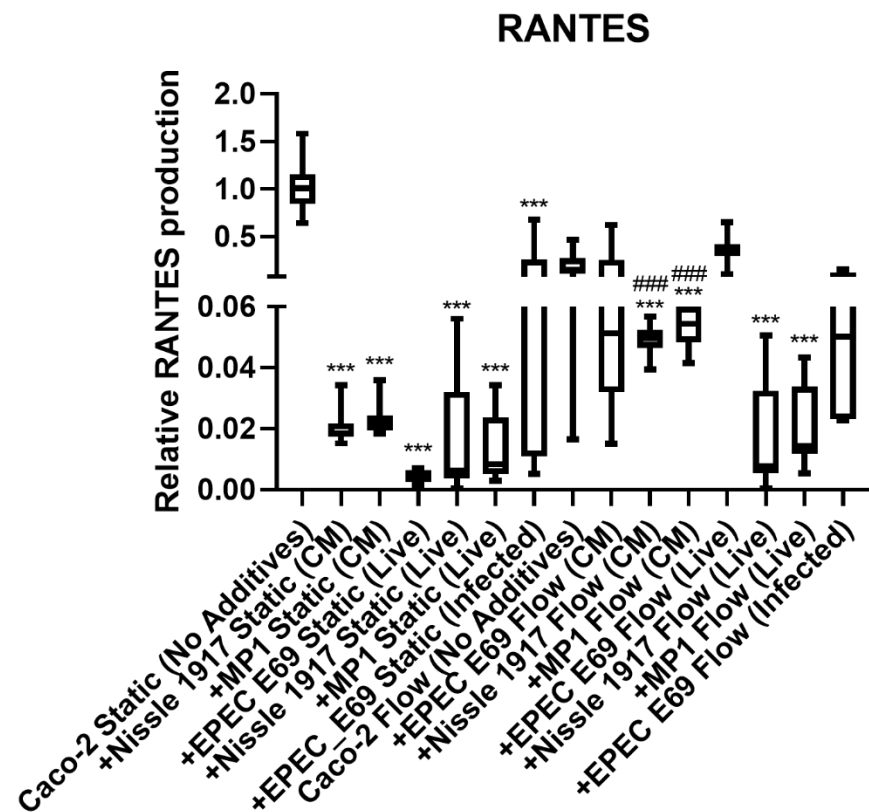
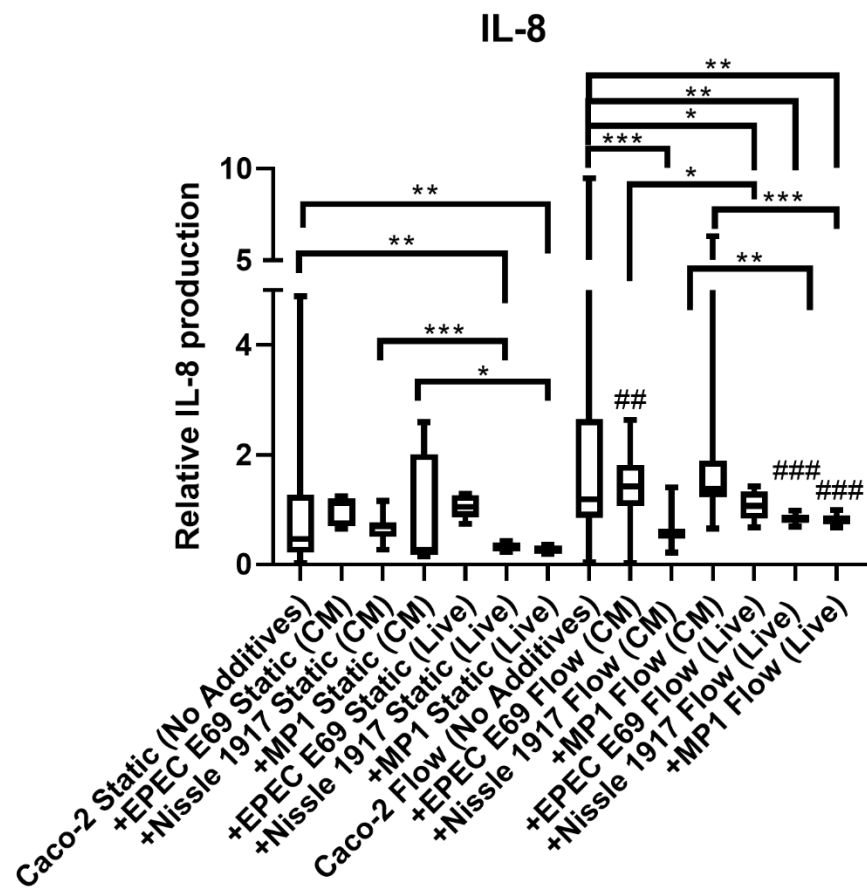


Figure 4-9: The impact of *E. coli* strains E69, Nissle 1917 and MP1 on the production of IL-8 and RANTES in Caco-2 cells exposed to flow and static conditions for 48 hours. Cell culture medium from coverslips seeded with Caco-2 cells exposed to bacteria-conditioned medium or live *E. coli* supplemented medium under static and flow conditions for 48 hours was collected and assessed for the presence of pro-inflammatory markers IL-8, RANTES via ABTS- and TMB-based ELISA. The data represent the mean \pm standard deviation (SD) of 9 independent experiments (containing triplicate samples of each condition) and are presented as fold-change compared to the no-additive static control that has been arbitrarily set as 1. Statistical analysis was performed using the unpaired t-test where * $p < 0.05$, ** $p < 0.01$, *** $p < 0.001$ as indicated or, ## $p < 0.01$, ### $p < 0.001$ when comparing matched static and flow conditions. (***) in RANTES data indicates significance between a given condition and the no additive control).

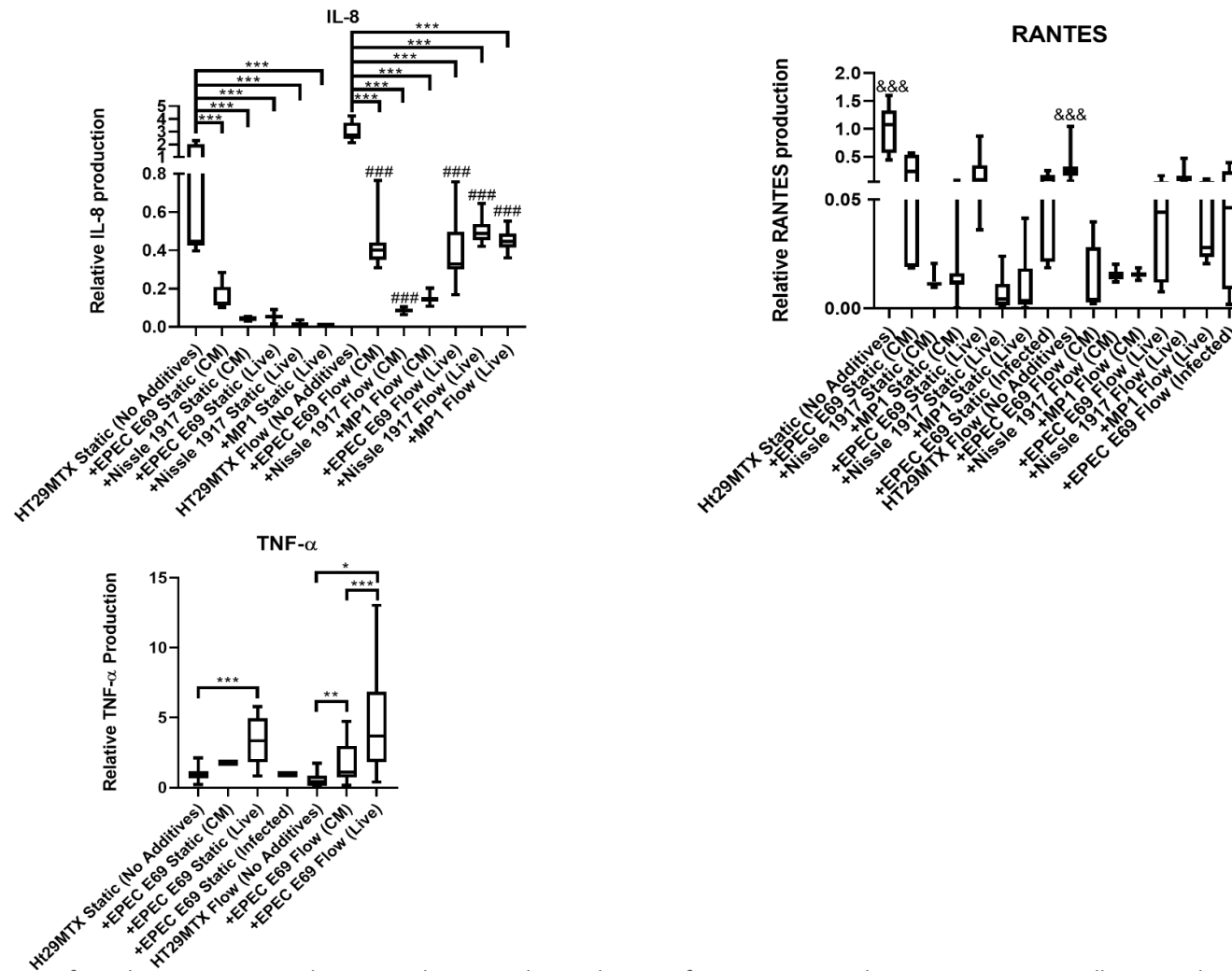


Figure 4-10: The impact of E. coli strains E69, Nissle 1917 and MP1 on the production of IL-8, RANTES and TNF- α in HT29MTX cells exposed to flow and static conditions for 48 hours. Cell culture medium from coverslips seeded with Caco-2 cells exposed to bacteria-conditioned medium or live E. coli supplemented medium under static and flow conditions for 48 hours was collected and assessed for the presence of pro-inflammatory markers IL-8, RANTES and TNF- α via ABTS- and TMB-based ELISA. The data represent the mean \pm standard deviation (SD) of 9 independent experiments (containing triplicate samples of each condition) and are presented as fold-change compared to the no-additive static control that has been arbitrarily set as 1. Statistical analysis was performed using the unpaired t-test where * $p < 0.05$, ** $p < 0.01$, *** $p < 0.001$ as indicated, ### $p < 0.001$ when comparing matched static and flow conditions, or &&& $p < 0.001$ when all assessed conditions are significantly different to the additive-free blank control. 4

4.3.6.4 Modelling the prophylactic effect of probiotic communities Lab4 and Lab4B in response to bacterial endotoxin alone and in the presence of a gastrointestinal pathogen

4.3.6.4.1 Assessing the role of LPS and LTA in the stimulation of pro-inflammatory cytokines

To reiterate a previous point, this assay was performed with IL-8 as the sole target due to the consistently significant responses observed across multiple assays in this study.

Caco-2 showed negligible IL-8 induction under the assessed conditions in the presence of LPS (Figure 4-11). LTA exposure, however, resulted in a significant increase in IL-8 production under static conditions ($p < 0.001$), while the addition of flow resulted in reduction of this response ($p < 0.001$).

In a similar manner, static 15 mL HT29MTX samples produced significant amounts of IL-8 compared to the flow exposure equivalent, in which the production of IL-8 was reduced ($p < 0.001$).

4.3.6.4.2 Pre-treatment of cell lines with the Lab4 and Lab4B probiotics and the subsequent effect on the response to the bacterial endotoxin LPS

Following the initial pre-treatment with Lab4 and Lab4B probiotics, followed by LPS exposure under static or flow conditions, a distinct trend was observed in both cell lines. Caco-2 exhibited a significant increase in IL-8 production in flow-exposed cells pre-treated with Lab4 compared to both the bacteria-free control ($p < 0.001$) and the equivalent static experiment ($p < 0.001$). Furthermore, it was noted that a significant increase in IL-8 production was observed in Caco-2 cells pre-treated with Lab4 under flow and static conditions and Lab4B under static conditions compared to those samples exposed to LPS only ($p < 0.001$). However, in the case of the Caco-2 cells treated with Lab4B, a complete mitigation of the production of pro-inflammatory molecules was observed in flow samples

compared to their static counterpart, as all values were below the limit of detection (Figure 4-11).

A similar trend in IL-8 production was observed in the HT29MTX flow samples treated with Lab4, as a significant increase in IL-8 was observed in flow-exposed samples compared to the bacteria-free control ($p < 0.001$) and the static equivalent ($p < 0.001$). However, an inverse trend was observed in static samples, in which significant reduction in IL-8 was observed in samples pre-treated with Lab4 compared to the bacteria-free control ($p < 0.001$). However, unlike that which was seen with Caco-2, when pre-treated with Lab4B, the IL-8 response of all HT29MTX samples was mitigated, as all samples in the flow and static exposure groups were below the limit of detection.

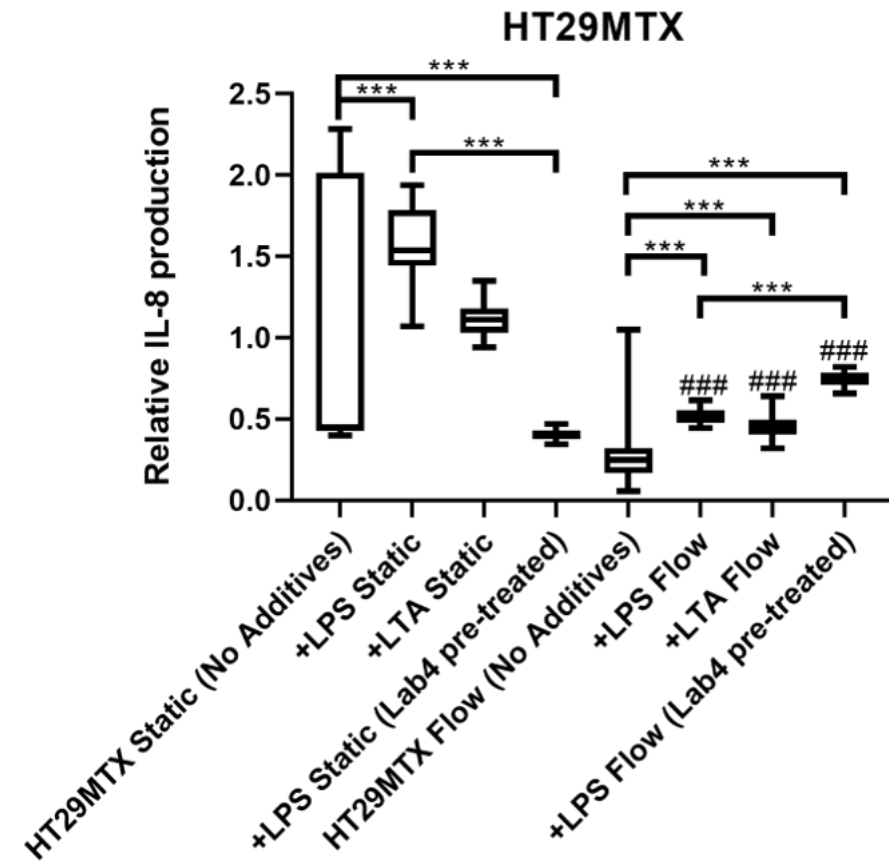
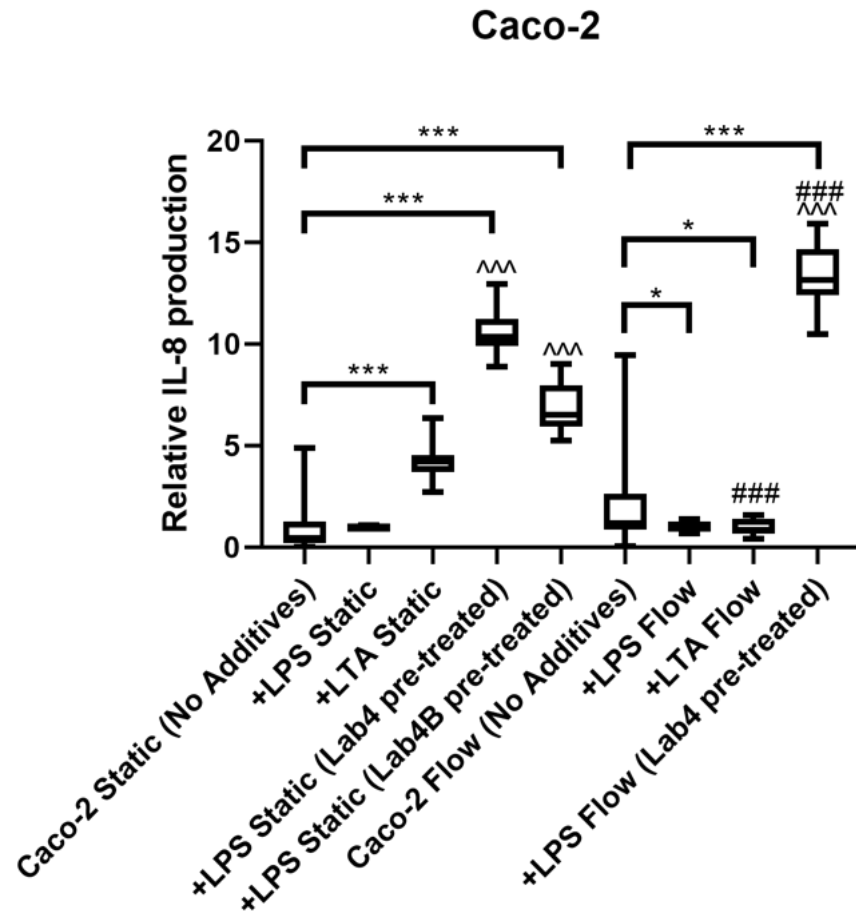


Figure 4-11: The impact of LPS and LTA on the production of IL-8, and subsequent impact of probiotic pre-treatment on the production of IL-8 in cell lines Caco-2 and HT29MTX. Cell culture medium from coverslips seeded with either Caco-2 or HT29MTX cells exposed to LPS, LTA or pre-treated with live Lab4 or Lab4B supplemented medium before exposure to LPS under static and flow conditions for 48 hours was collected and assessed for the presence of the pro-inflammatory marker IL-8 ABTS-ELISA. The data represent the mean±standard deviation (SD) of 9 independent experiments (containing triplicate samples of each condition) and are presented as fold-change compared to the no-additive static control that has been arbitrarily set as 1. Statistical analysis was performed using the unpaired t-test where * $p < 0.05$, *** $p < 0.001$ as indicated, ### $p < 0.001$ when comparing matched static and flow conditions, or ^^ $p < 0.001$ when comparing the LPS only control with the probiotic pre-treatment samples.

4.3.6.5 Pre-treatment and post-pathogen exposure of Caco-2 cells to Lab4 and Lab4B probiotics and the impact on the production of IL-8

Caco-2 cells in both the pre-treatment and post-pathogen treatment groups under static conditions display a significant reduction in IL-8 expression ($p < 0.05$), the exception of which being the samples in the post-pathogen treatment group in which Lab4B was used (Figure 4-12). Under static conditions, post-pathogen Lab4B samples displayed an increase in IL-8 compared to the pre-exposure group under static conditions ($p < 0.001$).

Under flow conditions, however, several trends were altered when comparing pre-treatment and post-pathogen treatment groups. Similarly to the static-exposed samples, all treated samples showed significantly reduced IL-8 production compared to the bacteria-free control, with significance being observed in those samples pre-treated with Lab4 ($p < 0.05$) and the post-pathogen samples exposed to both Lab4 ($p < 0.001$) and Lab4B ($p < 0.01$).

Both pre-treatment groups, and the post-pathogen Lab4B-treated samples conducted under flow conditions, showed significantly elevated IL-8 levels compared to their static counterparts ($p < 0.001$). The perceived trend of an altered cellular response following probiotic treatment is further emphasised by the significantly increased IL-8 production in the pre-treatment groups under flow compared to the post-pathogen treatment groups, which was consistently elevated in both probiotic treatment groups.

4.3.6.6 Pre-treatment and post-pathogen exposure of HT29MTX to Lab4 and Lab4B probiotics and the impact on the production of IL-8

Cells under static conditions exhibited a highly significant reduction in IL-8 production when exposed to either Lab4 or Lab4B bacterial products, regardless of treatment type, as seen in Figure 4-13 ($p < 0.001$). Additionally, no alterations in IL-8 levels were observed between treatment groups.

Similar to static conditions, IL-8 levels were significantly reduced under flow conditions when comparing a bacteria-free control to both treatment groups containing both Lab4 and Lab4B with EPEC E69 ($p < 0.001$). Additionally, when comparing the pre- and post-treatment groups under flow conditions, it was shown that a pre-treatment with either Lab4 or Lab4B resulted in a significant increase in IL-8 compared to the post-exposure group. Interestingly, when comparing the static and flow pre-treatment samples exposed to both Lab4 and Lab4B, significant increases in IL-8 can be seen between static and flow ($p < 0.001$), leading to the conclusion that, when under flow conditions, pre-treatment with probiotic products acts to stimulate the production of pro-inflammatory molecules in HT29MTX cells in response to gastrointestinal pathogens, such as with pathogenic *E. coli* strain E69.

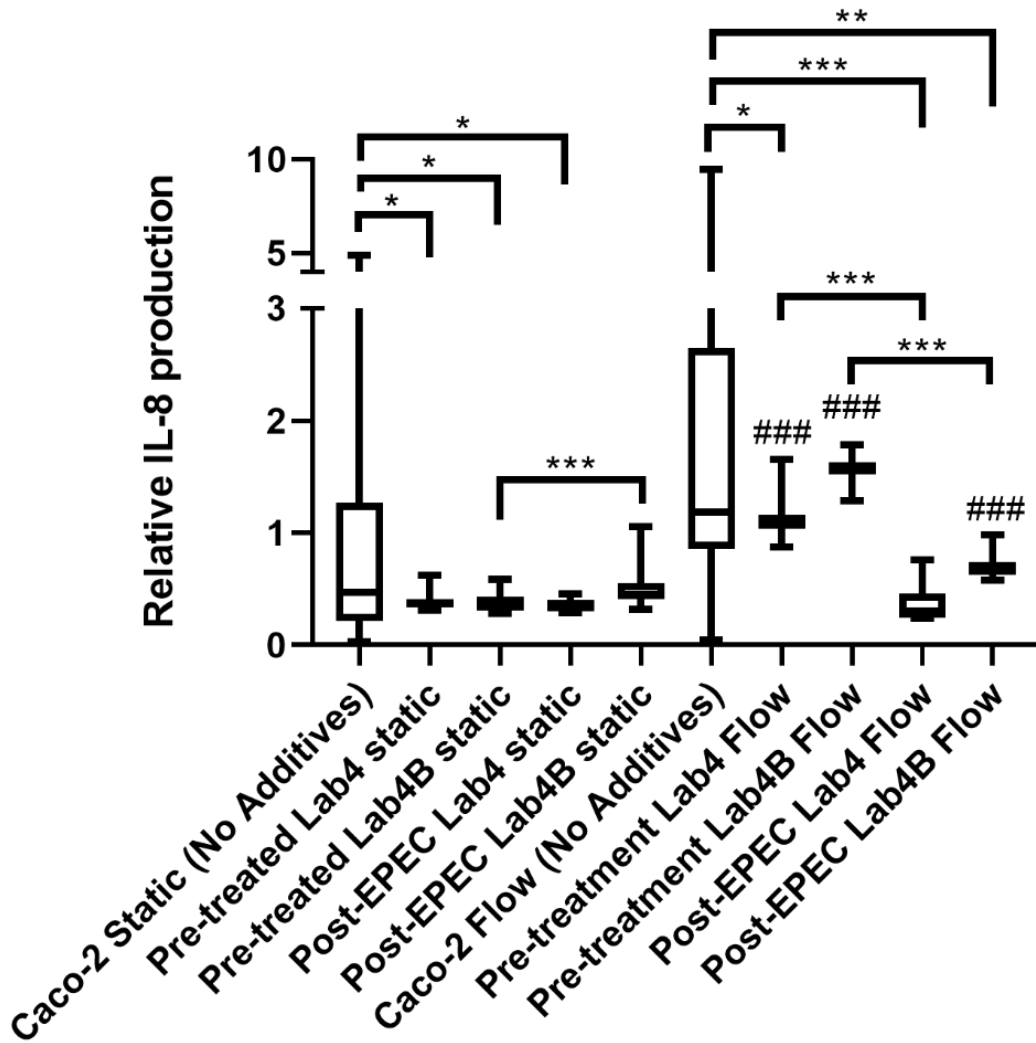


Figure 4-12: IL-8 production in Lab4- and Lab4B-treated Caco-2 cells exposed to EPEC E69 under flow and static conditions. Cell culture medium from coverslips seeded with Caco-2 cells treated with live Lab4- or Lab4B-supplemented medium either before or following exposure to E. coli E69 under static and flow conditions was collected and assessed for the presence of the pro-inflammatory marker IL-8 ABTS-ELISA. The data represent the mean ± standard deviation (SD) of 9 independent experiments (containing triplicate samples of each condition) and are presented as fold-change compared to the no-additive static control that has been arbitrarily set as 1. Statistical analysis was performed using the unpaired t-test where * $p < 0.05$, ** $p < 0.01$, *** $p < 0.001$ as indicated, or ### $p < 0.001$ when comparing matched static and flow conditions. Pre-treated refers to cells treated with the probiotic strain Lab4 or Lab4B for 24 hours prior to being exposed to the pathogenic EPEC E69 for a 24-hour period. Post-EPEC refers to cells first treated with EPEC for 24 hours, followed by a post-treatment exposure to either Lab4 or Lab4B for a further 24-hour period.

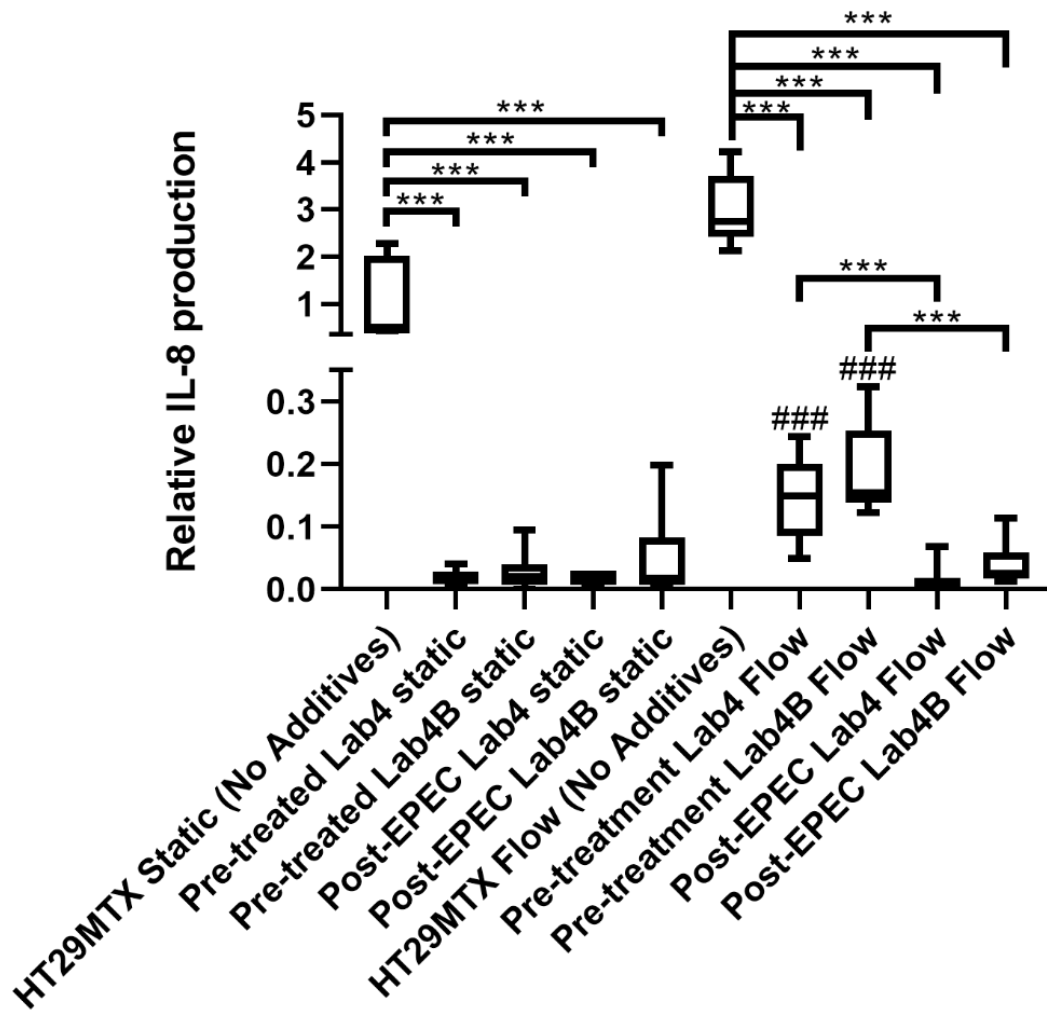


Figure 4-13: IL-8 production in Lab4- and Lab4B-treated HT29MTX cells exposed to EPEC E69 under flow and static conditions. Cell culture medium from coverslips seeded with HT29MTX cells treated with live Lab4- or Lab4B-supplemented medium either before or following exposure to E. coli E69 under static and flow conditions was collected and assessed for the presence of the pro-inflammatory marker IL-8 ABTS-ELISA. The data represent the mean \pm standard deviation (SD) of 9 independent experiments (containing triplicate samples of each condition) and are presented as fold-change compared to the no-additive static control that has been arbitrarily set as 1. Statistical analysis was performed using the unpaired t-test where *** $p < 0.001$ as indicated, or ### $p < 0.001$ when comparing matched static and flow conditions. Pre-treated refers to cells treated with the probiotic strain Lab4 or Lab4B for 24 hours prior to being exposed to the pathogenic E. coli strain E69 for a 24-hour period. Post-EPEC refers to cells first treated with E. coli strain E69 for 24 hours, followed by a post-treatment exposure to either Lab4 or Lab4B for a further 24-hour period.

Table 4-3: Summary of results from sections 4.3.6

Cell line	Condition	Exposure	Measurement	Significance ⁶	Figure
HT29MTX	Flow ¹	N/A	IL-8	***	4-6
HT29MTX	Flow ¹	N/A	RANTES	***	4-6
HT29MTX	Flow ¹	N/A	TNF- α	**	4-6
Caco-2	Static ²	Lab4 CM	IL-8	***	4-7
Caco-2	Static ²	Lab4B CM	IL-8	***	4-7
Caco-2	Static ²	Lab4 Live	IL-8	***	4-7
Caco-2	Static ²	Lab4B Live	IL-8	***	4-7
Caco-2	Flow ¹	Lab4 CM	IL-8	***	4-7
Caco-2	Flow ¹	Lab4B CM	IL-8	***	4-7
Caco-2	Flow ¹	Lab4 Live	IL-8	***	4-7
Caco-2	Flow ¹	Lab4B Live	IL-8	***	4-7
Caco-2	Static ²	Lab4 CM	RANTES	***	4-7
Caco-2	Static ²	Lab4B CM	RANTES	**	4-7
Caco-2	Static ²	Lab4 Live	RANTES	***	4-7
Caco-2	Flow ¹	Lab4 Live	RANTES	***	4-7
Caco-2	Static ²	Lab4 CM	TNF- α	***	4-7
Caco-2	Static ²	Lab4B CM	TNF- α	*	4-7
Caco-2	Static ²	Lab4 Live	TNF- α	***	4-7
Caco-2	Flow ²	Lab4B CM	TNF- α	*	4-7
Caco-2	Flow ²	Lab4 Live	TNF- α	***	4-7
Caco-2	Flow ¹	Lab4 CM	TNF- α	***	4-7
HT29MTX	Static ²	Lab4 CM	RANTES	***	4-8
HT29MTX	Static ²	Lab4B CM	RANTES	***	4-8
HT29MTX	Static ²	Lab4 Live	RANTES	***	4-8
HT29MTX	Static ²	Lab4B Live	RANTES	***	4-8
HT29MTX	Static ³	Lab4	RANTES	*	4-8
HT29MTX	Flow ²	Lab4B CM	RANTES	**	4-8
HT29MTX	Flow ²	Lab4 Live	RANTES	**	4-8
HT29MTX	Flow ²	Lab4B Live	RANTES	*	4-8
HT29MTX	Flow ³	Lab4	RANTES	**	4-8
HT29MTX	Static ²	Lab4B CM	TNF- α	***	4-8
HT29MTX	Static ²	Lab4 Live	TNF- α	***	4-8
HT29MTX	Static ²	Lab4B Live	TNF- α	*	4-8
HT29MTX	Static ³	Lab4	TNF- α	***	4-8
HT29MTX	Flow ²	Lab4B CM	TNF- α	*	4-8
HT29MTX	Flow ²	Lab4 Live	TNF- α	**	4-8
HT29MTX	Flow ²	Lab4B Live	TNF- α	*	4-8
HT29MTX	Flow ³	Lab4	TNF- α	***	4-8
HT29MTX	Flow ¹	Lab4B CM	TNF- α	***	4-8
HT29MTX	Flow ¹	Lab4 Live	TNF- α	***	4-8
Caco-2	Static ²	Nissle 1917 Live	IL-8	**	4-9
Caco-2	Static ²	MP1 Live	IL-8	**	4-9
Caco-2	Static ³	Nissle 1917	IL-8	***	4-9
Caco-2	Static ³	MP1	IL-8	*	4-9

Caco-2	Flow ²	Nissle 1917 CM	IL-8	***	4-9
Caco-2	Flow ²	EPEC E69 Live	IL-8	*	4-9
Caco-2	Flow ²	Nissle 1917 Live	IL-8	**	4-9
Caco-2	Flow ²	MP1 Live	IL-8	**	4-9
Caco-2	Flow ³	EPEC E69	IL-8	*	4-9
Caco-2	Flow ³	Nissle 1917	IL-8	**	4-9
Caco-2	Flow ³	MP1	IL-8	***	4-9
Caco-2	Flow ¹	EPEC E69 CM	IL-8	**	4-9
Caco-2	Flow ¹	Nissle 1917 Live	IL-8	***	4-9
Caco-2	Flow ¹	MP1 Live	IL-8	***	4-9
Caco-2	Static ²	Nissle 1917 CM	RANTES	***	4-9
Caco-2	Static ²	MP1 CM	RANTES	***	4-9
Caco-2	Static ²	EPEC E69 Live	RANTES	***	4-9
Caco-2	Static ²	Nissle 1917 Live	RANTES	***	4-9
Caco-2	Static ²	MP1 Live	RANTES	***	4-9
Caco-2	Static ²	EPEC E69 Infected	RANTES	***	4-9
Caco-2	Flow ²	Nissle 1917 CM	RANTES	***	4-9
Caco-2	Flow ²	MP1 CM	RANTES	***	4-9
Caco-2	Flow ²	Nissle 1917 Live	RANTES	***	4-9
Caco-2	Flow ²	MP1 Live	RANTES	***	4-9
Caco-2	Flow ¹	Nissle 1917 CM	RANTES	***	4-9
Caco-2	Flow ¹	MP1 CM	RANTES	***	4-9
HT29MTX	Static ²	EPEC E69 CM	IL-8	***	4-10
HT29MTX	Static ²	Nissle 1917 CM	IL-8	***	4-10
HT29MTX	Static ²	EPEC E69 Live	IL-8	***	4-10
HT29MTX	Static ²	Nissle 1917 Live	IL-8	***	4-10
HT29MTX	Static ²	MP1 Live	IL-8	***	4-10
HT29MTX	Flow ²	EPEC E69 CM	IL-8	***	4-10
HT29MTX	Flow ²	Nissle 1917 CM	IL-8	***	4-10
HT29MTX	Flow ²	MP1 CM	IL-8	***	4-10
HT29MTX	Flow ²	EPEC E69 Live	IL-8	***	4-10
HT29MTX	Flow ²	Nissle 1917 Live	IL-8	***	4-10
HT29MTX	Flow ²	MP1 Live	IL-8	***	4-10

HT29MTX	Flow ¹	EPEC E69 CM	IL-8	***	4-10
HT29MTX	Flow ¹	Nissle 1917 CM	IL-8	***	4-10
HT29MTX	Flow ¹	EPEC E69 Live	IL-8	***	4-10
HT29MTX	Flow ¹	Nissle 1917 Live	IL-8	***	4-10
HT29MTX	Flow ¹	MP1 Live	IL-8	***	4-10
HT29MTX	Static ²	EPEC E69 CM	RANTES	***	4-10
HT29MTX	Static ²	Nissle 1917 CM	RANTES	***	4-10
HT29MTX	Static ²	MP1 CM	RANTES	***	4-10
HT29MTX	Static ²	EPEC E69 Live	RANTES	***	4-10
HT29MTX	Static ²	Nissle 1917 Live	RANTES	***	4-10
HT29MTX	Static ²	MP1 Live	RANTES	***	4-10
HT29MTX	Static ²	EPEC E69 Infected	RANTES	***	4-10
HT29MTX	Flow ²	EPEC E69 CM	RANTES	***	4-10
HT29MTX	Flow ²	Nissle 1917 CM	RANTES	***	4-10
HT29MTX	Flow ²	MP1 CM	RANTES	***	4-10
HT29MTX	Flow ²	EPEC E69 Live	RANTES	***	4-10
HT29MTX	Flow ²	Nissle 1917 Live	RANTES	***	4-10
HT29MTX	Flow ²	MP1 Live	RANTES	***	4-10
HT29MTX	Flow ²	EPEC E69 Infected	RANTES	***	4-10
HT29MTX	Static ²	EPEC E69 Live	TNF- α	***	4-10
HT29MTX	Flow ²	EPEC E69 CM	TNF- α	**	4-10
HT29MTX	Flow ²	EPEC E69 Live	TNF- α	*	4-10
HT29MTX	Flow ³	EPEC E69	TNF- α	***	4-10
Caco-2	Static ²	LTA	IL-8	***	4-11
Caco-2	Static ²	LPS + Lab4 (Pre- treatment)	IL-8	***	4-11
Caco-2	Static ²	LPS + Lab4B (Pre- treatment)	IL-8	***	4-11
Caco-2	Static ⁴	LPS + Lab4 (Pre- treatment)	IL-8	***	4-11
Caco-2	Static ⁴	LPS + Lab4B (Pre- treatment)	IL-8	***	4-11
Caco-2	Flow ²	LPS	IL-8	*	4-11

Caco-2	Flow ²	LTA	IL-8	*	4-11
Caco-2	Flow ²	LPS + Lab4 (Pre-treatment)	IL-8	***	4-11
Caco-2	Flow ⁴	LPS + Lab4 (Pre-treatment)	IL-8	***	4-11
Caco-2	Flow ¹	LTA	IL-8	***	4-11
Caco-2	Flow ¹	LPS + Lab4 (Pre-treatment)	IL-8	***	4-11
HT29MTX	Static ²	LPS	IL-8	***	4-11
HT29MTX	Static ²	LPS + Lab4 (Pre-treatment)	IL-8	***	4-11
HT29MTX	Static ⁴	LPS + Lab4 (Pre-treatment)	IL-8	***	4-11
HT29MTX	Flow ²	LPS	IL-8	***	4-11
HT29MTX	Flow ²	LTA	IL-8	***	4-11
HT29MTX	Flow ²	LPS + Lab4 (Pre-treatment)	IL-8	***	4-11
HT29MTX	Flow ⁴	LPS + Lab4 (Pre-treatment)	IL-8	***	4-11
HT29MTX	Flow ¹	LPS	IL-8	***	4-11
HT29MTX	Flow ¹	LTA	IL-8	***	4-11
HT29MTX	Flow ¹	LPS + Lab4 (Pre-treatment)	IL-8	***	4-11
Caco-2	Static ²	Pre-treated with Lab4	IL-8	*	4-12
Caco-2	Static ²	Pre-treated with Lab4B	IL-8	*	4-12
Caco-2	Static ²	Lab4 treated following exposure to EPEC E69	IL-8	*	4-12
Caco-2	Static ⁵	Lab4B	IL-8	***	4-12
Caco-2	Flow ²	Pre-treated with Lab4	IL-8	*	4-12
Caco-2	Flow ²	Lab4 treated following exposure to EPEC E69	IL-8	***	4-12
Caco-2	Flow ²	Lab4B treated following exposure to EPEC E69	IL-8	**	4-12

Caco-2	Flow ⁵	Lab4	IL-8	***	4-12
Caco-2	Flow ⁵	Lab4B	IL-8	***	4-12
Caco-2	Flow ¹	Pre-treated with Lab4	IL-8	***	4-12
Caco-2	Flow ¹	Pre-treated with Lab4B	IL-8	***	4-12
Caco-2	Flow ¹	Lab4B treated following exposure to EPEC E69	IL-8	***	4-12
HT29MTX	Static ²	Pre-treated with Lab4	IL-8	***	4-13
HT29MTX	Static ²	Pre-treated with Lab4B	IL-8	***	4-13
HT29MTX	Static ²	Lab4 treated following exposure to EPEC E69	IL-8	***	4-13
HT29MTX	Static ²	Lab4B treated following exposure to EPEC E69	IL-8	***	4-13
HT29MTX	Flow ²	Pre-treated with Lab4	IL-8	***	4-13
HT29MTX	Flow ²	Pre-treated with Lab4B	IL-8	***	4-13
HT29MTX	Flow ²	Lab4 treated following exposure to EPEC E69	IL-8	***	4-13
HT29MTX	Flow ²	Lab4B treated following exposure to EPEC E69	IL-8	***	4-13
HT29MTX	Flow ⁵	Lab4	IL-8	***	4-13
HT29MTX	Flow ⁵	Lab4B	IL-8	***	4-13
HT29MTX	Flow ¹	Pre-treated with Lab4	IL-8	***	4-13
HT29MTX	Flow ¹	Pre-treated with Lab4B	IL-8	***	4-13

¹ Assay compares identical experimental exposure across static and flow conditions; ² Assay compares exposure condition against the equivalent additive free control; ³ Assay compares CM and Live bacteria samples within the same experimental condition; ⁴ Assay compares LPS (+ probiotic) to the LPS only exposure control; ⁵ Assay compares pre-exposure and post-pathogen exposure groups within the same experimental condition; ⁶ * P < 0.05; ** P < 0.01 and *** P < 0.005.

4.3.6.7 RT-qPCR analysis of cytokine IL-8 in HT29MTX cells exposed to varying concentrations of probiotic conditioned medium

Following an exposure period of 48 hours to Lab4- and Lab4B-supplemented media, it was noted that, in the case Lab4- and Lab4B-conditioned media, similar trends were observed via qPCR-based methodologies at each concentration of conditioned medium. It should also be stated that the observed trends were comparable to those seen in the ELISA-based analyses, further strengthening those results obtained through ELISA-based methodologies.

Exposure to the Lab4 consortium showed no significant changes in IL-8 levels at 48 hours' exposure, with only minor increases in IL-8 production noted in the 50% conditioned medium samples at 48 hours. When evaluating the production of IL-8 in Lab4B-exposed samples, HT29MTX noted a highly significant expression of the IL-8 amplicon, in which a 10 – 15-fold increase can be noted compared to the non-supplemented medium control ($p < 0.001$) (Figure 4-14). These findings support those observed in the preliminary ELISA-based analysis of both conditioned media generated from Lab4- and Lab4B-based products. Additionally, these findings further exemplify the dose-dependent responses observed in the preliminary toxicity assays, in which both 25% and 50% conditioned medium formulations induce an elevated IL-8 response from the cell line.

A second set of experiments was performed to assess the individual constituents of the probiotics to clarify which bacterial strains influence the inflammatory response. When exposed to either *B. bifidum* or *B. animalis* sub sp. *lactis*, present in both the Lab4 and Lab4B consortium, no significant changes in gene expression of IL-8 were observed (Figure 4-14). Those samples exposed to the *L. acidophilus* strains present in the Lab4 consortium displayed a significant increase in IL-8, although the single strain CUL60 was shown to induce a more significant response ($p < 0.01$) than the dual-strain mix of CUL21 and CUL60 ($p < 0.05$). However, when the Lab4B lactobacilli *L. salivarius* and *L. paracasei* were exposed to cells, all concentrations of conditioned medium displayed a highly significant increase in IL-8 expression ($p < 0.001$). It should also be noted that the IL-8 production in these samples was observed to be dose-dependent (Figure 4-14).

The recorded upregulation observed in both the ELISA-based analyses and the RT-qPCR performed were primarily induced as a result of the Lab4B lactobacilli, although without understanding the complexity of the community-based interactions, the exact cause of this behavioural change cannot be fully ascertained.

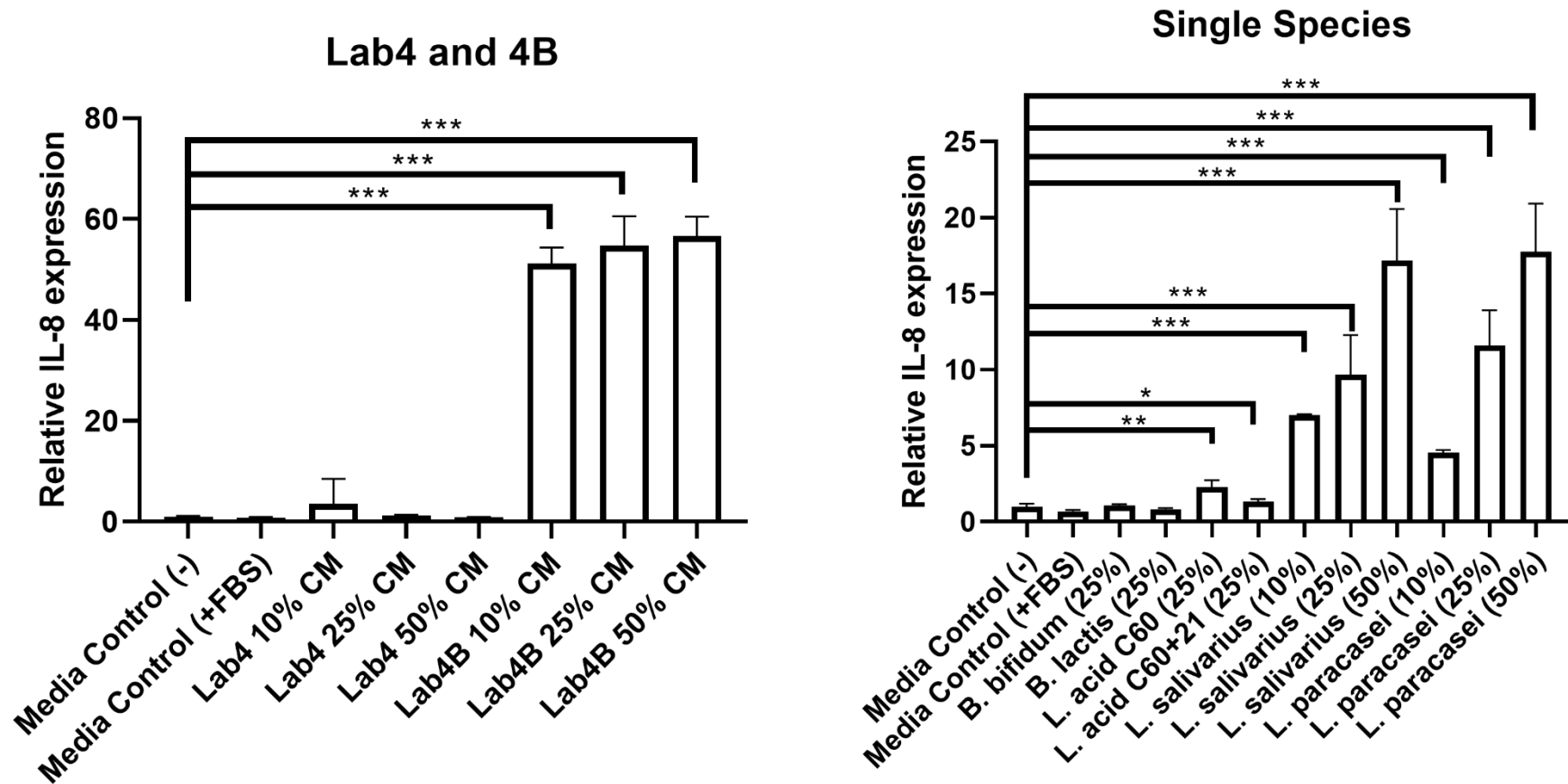


Figure 4-14: IL-8 gene expression in HT29MTX cells exposed to various concentrations of Lab4- and Lab4B-conditioned media, and conditioned media generated from single-species bacteria under static conditions as measured via qPCR. HT29MTX cells exposed to various concentrations of either Lab4, Lab4B or the constituent bacteria of the Lab4/Lab4B consortium under static conditions was assessed via qPCR for IL-8 gene expression. The data represent the mean±standard deviation (SD) of 2 independent experiments (containing duplicate samples of each condition) and are presented as fold-change compared to the blank medium control that has been arbitrarily set as 1. Statistical analysis was performed using the unpaired t-test where * $p < 0.05$, ** $p < 0.01$, *** $p < 0.001$.

4.4 Discussion

Whilst the positive implications of probiotic therapies have been indicated thanks to studies such as those examining the immune-system-modulating effector molecules present in the cell walls of probiotic bacteria (Wells 2011), and those that suggest that probiotics are capable of inducing a modulatory effect on the immune system (Yan and Polk 2011), many of these studies were conducted using *in vitro* methodologies or via the use of animal models, and, as such, could lack the desired insight for use *in vivo*. In spite of these findings the introduction of probiotics to the QV500 yielded some unexpected findings.

In this study, it was observed that, in certain instances, colonocytes treated with probiotics showed elevated levels of IL-8, RANTES or TNF- α . However, this production of pro-inflammatory cytokines to the probiotic compounds could be perceived as a proxy measure of priming of the host immune system, a behaviour that might prove invaluable in the clearing of pathogens, whose mode of infection involves suppressing the host immunological response.

During the course of this chapter, a number of possible explanations for the elevated levels of proinflammatory cytokines from the selected cell lines were examined, including the concept that reduced pH following probiotic fermentation might generate a stressful microenvironment to which the intestinal cells were not acclimatised. Additionally, it was revealed that the pre-treatment of cells with probiotics resulted in an increase in IL-8 production, which may suggest that *in situ*, the increase in cytokine production may promote pathogen clearing, due to an increased production of inflammatory markers compared to those cells exposed to either pathogenic bacteria or the bacterial endotoxin LPS only. This concept is of particular interest due to the gut having been implicated in an immune cell-/T-cell-modulated immune response and production of killer T-cells – a variety of T-cell known for their innate ability to combat and destroy cells that could be considered abnormal, including infected cells and cancer cells (Cook et al. 2014). It must be stated, while the immune response was not modelled in this study, instead focusing on the production of pro-inflammatory molecules, these findings present a promising potential

avenue of future research to identify the immune-priming potential of the Lab4 and Lab4B probiotics in flow, and if combined with other methodologies, such as the QV600, which allows for multiple cell lines to be cultured simultaneously, it could be possible to observe the impact of these cells and their produced pro-inflammatory cytokines on the behaviour of immune cells.

One of the initial aims of this chapter focused on the potential of pH in cell culture, and it was shown that pH generally exerts a significant impact on the behaviour of cells, particularly under flow. Previous studies have indicated that even minor fluctuations in biological parameters, including oxygen concentration and pH, can have a highly significant impact on cellular behaviour (Al-Ani et al. 2018), and the results observed throughout this study further corroborate this statement as, under cell culture conditions, fluctuations in ambient pH levels impact cells in a significant manner, with significantly increased LDH production at the higher pH. However, despite the observed impact of pH on cells, the observed changes were not as deleterious as would be expected, and when exposed to physiologically relevant biological parameters, such as flow, cells displayed an increased aptitude for enduring stressful environments for small periods of time in these instances.

What also must remain in the forefront with this work is that, while previous cell culture-centred studies have utilised static methodologies, the inclusion of flow adds a further layer of biological relevance with particular emphasis on improving gut modelling methodologies, enabling some additional hypotheses to be formed as to the true importance of flow within gut modelling. Dynamic flow, when introduced to cell culture, was repeatedly seen as causing an altered cellular behaviour compared to static methodologies, with particularly significant impacts observed regarding the viability of the cell lines examined. Upon examination of the responsiveness of intestinal cell lines to pH, the initial introduction of flow was once again displayed as elevating LDH production, further strengthening the concept explored in this study that initial exposure of static acclimatised cell lines to a biological stimulus, such as flow, might induce a short-term stress response. While this further strengthens the concept proposed in the previous chapter, that when assessing the response of a cell line to a given stimulus, the experimental microenvironment and presence of biological factors assist in providing a more *in situ*-like environment, while remaining

conscious of the limitations of immortalised cell lines, one must additionally take into account any potential influence the newly introduced biologically relevant condition might induce, as failing to account for the initial impact of a given condition might otherwise impede the accuracy and application of a given experiment.

While a potentially detrimental response in short-term studies, the stimulation of cell lines via flow was ultimately considered as an overall positive addition to the model with regard to the general health and behaviour of the cell lines, as noted in Chapter 3, in which LDH and MTT were assessed. However, while a mild period of stress may not initially seem beneficial in the context of improving gastrointestinal modelling, the LDH secretion identified in this chapter should not be discarded as a limiting factor, and instead could be seen as an indicator that under flow conditions, the responsiveness of cell lines to external stimuli increased, thus enabling immortalised cell lines to provide an intermediate system that could be perceived as more relevant to the *in situ* environment, in spite of their limitations.

This alteration in response to external stimuli was further expanded upon in those assays exploring the response of both Caco-2 and HT29MTX to bacterial exposure. Caco-2 and HT29MTX have previously been reported as being non-responsive cell lines to several bacterial antigens such as LPS (Böcker et al. 2003; Huang et al. 2003). In the case of Caco-2, the poor immunological potential of this cell line could be attributed to the under-expression of the TLR4 transmembrane receptor protein, a protein associated with the induction of an inflammatory response to LPS. However, in the case of HT29MTX, a lowered response could be attributed to an increased production of mucin, a parameter associated with the HT29MTX cell line (Gouyer et al. 2001) and that may act as a physiological barrier to endotoxins reaching the cell, which might subsequently trigger an inflammatory response.

When considering the results observed in the preceding chapter, where glycoprotein production was upregulated under flow conditions, the modulation of pro-inflammatory markers under flow conditions poses an interesting question: is the ability of a given cell line

to produce pro-inflammatory cytokines dependent solely on the cell line, or is it directly correlated with and influenced by the microenvironment in which the cells are found?

The significant reduction in pro-inflammatory cytokine production seen in probiotic-exposed Caco-2 and HT29MTX cells under flow further corroborated the concept that dynamic flow is impacting on intestinal cell line behaviour compared to existing static models. The variation in pro-inflammatory cytokine production by cell line and the link to glycoprotein production could, in part, be described by the combined works of Beaurivage and colleagues and Cornick and colleagues. These studies explored the impact of flow and mucin respectively on cellular behaviour and inflammation. Similarly to the results shown in this study, Beaurivage and colleagues revealed that the mucin production was typically modulated under flow conditions, with increases noted in MUC2 production within the microfluidic model, while MUC5AC was reduced (Beaurivage et al. 2020). To expand further upon these findings, the results of Cornick and colleagues showcased that the presence of MUC2 acted to suppress the immunological response of cell lines by binding bacterial antigens, thus selectively suppressing the immune response of the assessed dendritic cells in the presence of MUC2 (Cornick et al. 2015). While the observed trends in mucin production did not completely align with the trends seen in glycoprotein production, further conclusion can be drawn from this, that being that the increased glycoprotein observed in the cells assessed in Chapter 3 contributes to the protective mucin layer for the cells when faced with pro-inflammatory stimulation. However, it should be noted that, while the above statement goes some way in explaining the importance of flow in providing a more applicable gut environment for *in vitro* cell culture systems, there are likely other mechanisms that were not explored in this study influencing the cellular response when faced with external stimuli, as despite a common trend being observed across cell lines, a completely different set of responses was observed following the addition of probiotics. Furthermore, despite examining three distinct inflammatory markers, whose biological functions have been well described within the context of inflammation and beyond, the addition of both probiotics and pathogenic organisms resulted in distinct modulation to each of the selected markers. Interestingly, these behaviours, while similar across cell lines, were ultimately cell line- and condition-dependent.

As such, the addition of flow in this instance could be noted as both a stimulatory element and a suppressor simultaneously, the stimulatory nature being dependent on the marker of interest. This concept is one of note as it was explored by Kulthong and colleagues in their 2021 study using their gut on a chip system (Kulthong et al. 2021). In their study, transcriptomic analysis was conducted on Caco-2 cells under flow conditions, with 5927 genes being differentially expressed, both upregulated and downregulated. The variation of response in cells under flow could further strengthen the concepts explored throughout the study until now: that the increased importance of biologically relevant factors in cell culture research, as well as how the implementation of multiple cell lines is essential in understanding the role of a specific stimulus *in vitro*.

These concepts could be further strengthened when considering the observed trends in both Caco-2 and HT29MTX exposed to the pathogenic *E. coli* strain E69. When exposed to this strain, the production of pro-inflammatory molecules from both cell lines under both conditions was not significantly influenced, with flow generally resulting in reduced production of pro-inflammatory cytokines, IL-8, TNF- α and RANTES, particularly when compared to those results observed in the bacteria-free control samples. While the discrepancy between the observed inflammatory responses could be seen as unexpected, when considering the previously observed mild inflammatory nature of EPEC infections (Ruchaud-Sparagano et al. 2007), this response simultaneously supports the general behaviour of the pathogen. In instances of E69 infection, the bacterium is known to use effector molecules to form an actin pedestal structure to facilitate cellular infection (Wong et al. 2012). Therefore, if this bacterium were to induce a rapid host immune response, it would be unable to establish the infection due to rapid clearing of the pathogenic organism. Therefore, a dampened immune response would be characteristic of that which would be expected *in situ*.

With the addition of the RT-qPCR analysis, it was possible to identify some potential contributing organisms responsible for the observed changes in pro-inflammatory cytokine production. While this research was only conducted using static methodologies on this occasion, the key effector bacteria within the different consortia provide significant insight

into the key contributors to which organisms might be of key interest in future studies aiming to understand the true nature of probiotics in impacting on both pro-inflammatory, and potentially, anti-inflammatory cytokine production.

However, one of the less expected results reported in this chapter is the variable impact of both probiotic exposure methods, those being bacterial metabolites, represented here by the conditioned medium, and direct bacterial exposure to the cell lines. While similar trends were observed when comparing those samples exposed to conditioned medium or live bacterial cells, interestingly, in the case of the probiotic organisms, conditioned medium was generally observed as having the most potential to induce cellular production of IL-8, potentially mimicking the setting *in situ*.

The increased inflammatory response of the cells to high concentrations of conditioned medium indicates that bacterial-epithelial contact, may not contribute directly to any benefits observed following the ingestion of probiotics. Instead, it could be surmised that the combination of the metabolites produced by these species, combined with some as yet unexplored factor present in the live bacterial cells that interacts directly with the host system, could assist in the understanding of probiotics and their impact within the gut, and assist in moulding current cell culture-based methodologies. While this study focused exclusively on the implication of *E. coli* within the gut, future studies could adopt common gastrointestinal pathogens, including *Salmonella enterica*, which has previously been shown to exert a significantly negative impact on the gut during infection (Bratburd et al. 2018), to further analyse the potential of this system.

As the use and implementation of heat-killed bacterial cells was not possible within the timeframe of this study, the incorporation of such methods in a future study might allow for further insight and clarify the true effector agent(s) within probiotic studies. Additionally, transcriptomic analysis of the human cells exposed to flow and static conditions in addition to the flow-exposed bacteria, both probiotic and pathogenic, may be an avenue of interest for future research, as the transcriptome of both human and bacterial cells under flow remains an area of considerable interest with great potential, and may further unravel the impact of dynamic flow in cell culture modelling methodologies.

Focusing on the ELISA-based analyses, it could be said that to summarise the impact of probiotics on human cell lines is not a trivial matter, particularly following additional stimulation with a biological flow element. This was particularly emphasised in this study when considering the various means by which the cells were exposed to the bacteria, both probiotic and pathogenic, which influenced both cell lines in a distinct manner, with conditioned medium, infection and prolonged live bacterial cell exposure resulting in significantly different responses. Therefore, when undertaking gut research, the conditions and experimental conditions selected for such a study heavily influence the overall findings, potentially adding bias into a given study.

Once again, the research reported in this chapter was successful in addressing the aims outlined in section 4.1.5, as it was noted that conditioned media exerted a series of behavioural changes that were distinct to each cell line, to each conditioned medium, and varied by experimental condition (i.e. static or flow), further strengthening the implied importance of both cell line selection and experimental setup with regard to the inclusion of physiologically relevant conditions. Furthermore, the impact of *E coli* strain E69 on both Caco-2 and HT29MTX was ultimately distinct from that of the assessed probiotics, with a diminished production of pro-inflammatory cytokines seen in the pathogenic-exposed samples compared to probiotic-exposed samples, which, while unexpected, would in theory align with the suppression of the host immune response that would be expected *in situ*. Finally, it was shown that the administration of probiotics to cell lines prior to exposure with a pathogenic organism resulted in an increased production of pro-inflammatory cytokines under flow conditions, which aligns with the current belief that the regular consumption of probiotics acts as a preventative measure with regard to the colonisation and establishment of gastrointestinal pathogens.

This chapter and those results indicating an increased cellular response to bacteria-conditioned medium resulted in a further question that this study wished to address. If the bacterial metabolites present in the conditioned media were so influential on the cell lines HT29MTX and Caco-2, what metabolites were present in the conditioned media, and furthermore, would the metabolome of these bacteria vary depending on the

environmental factors under which they were grown? Ultimately combining these ideas, the question remained: what could the metabolites produced by the Lab4 and Lab4B probiotics mean, both in the context of this study, and beyond, when considering the development of novel means of modelling the human gut and in understanding the role of probiotics within the human gut?

5 Metabolite analysis of probiotic and pathogenic bacteria-conditioned media

5.1 Introduction

5.1.1 The importance of bacterial metabolites

As already discussed in the previous chapters (chapters 3 and 4), the host microbiota exerts a considerable impact on the general wellbeing of the host, with host predisposition to disease states often being influenced by the composition of microbes in a host's microbiome (Durack and Lynch 2019). As such, it could be stated that an individual is also subject to the influence of the bacterial metabolites produced by the constituents of the gut microbiome, which, in turn, would contribute towards the overall health status of an individual, although the mechanisms would be metabolite-specific.

Metabolomic studies focusing on the gut microbiome and its bacteria have already received considerable focus, as the gut has already been implicated in influencing the susceptibility of a host to numerous disease states, including Alzheimer's disease (Saji et al. 2020) and diabetes (Vangipurapu et al. 2020) – to name only two – be that in a positive or negative manner. Additionally, while research into the gut has focused quite extensively on the metabolic profiles of bacteria inhabiting the GI tract, many such studies are performed via stool-based, urine-based or other designated host-supplied sample analyses, where an individual has their stool, urine or other biological sample analysed for the presence of a specific metabolite or all metabolites (Jain et al. 2019). While such methodologies might provide invaluable insight into the potential mechanisms underpinning disease states that negatively impact a large community, they also are somewhat hindered by a complex bacterial community and are subject to interference from metabolites introduced from external sources, including food intake, that can, in turn, make further analysis both time consuming and difficult.

By assessing samples extracted only from a given site within the body or, more specifically, waste-based samples, it should be acknowledged that such analyses may provide only a limited insight into the samples examined, as these methodologies contain input from the entirety of the microbial inhabitants from the GI tract, in addition to any ingested compounds. Additionally, these end-point analyses might be lacking those metabolites utilised in biological processes and, as such, would lack a level of accuracy and biological insight. It should also be noted that much of the metabolic cross-feeding within the gut cannot be accounted for when utilising such methods, while those metabolites that translocate to other sites within the body, rather than being expelled as waste products, also remain unaccounted for. As such, while end-point analysis methods are invaluable for assessing a system, allowing for ease of collection and analysis, the true complexity of those interactions is often left unexplored without making use of alternative invasive analysis and sampling procedures.

While lacking the biological insight present in stool- and urine-based analyses, alternative methodologies have been proposed whereby simplified communities are utilised in cell culture media. While the issue of understanding the specific functionality of a given microorganism and their metabolic profiles is one that cannot be addressed without adapting a reductionist approach, much research has been undertaken using a single-species or polymicrobial consortium that is metabolically analysed in isolation, rather than being analysed from a biological sample. To further understand the complexity of the system at hand, this reductionist approach is understandable, and, as such, this is a concept that this chapter utilises as its primary goal in an attempt to unravel the impact of the bacterial communities used throughout this study.

5.1.2 Understanding the impact of growth medium on the metabolic profiles of the Lab4 and Lab4B probiotic consortia

The use of bacterial metabolites in the form of conditioned medium is common practice within cell culture research (Leidal et al. 2001) due to the difficulty of incubating anaerobic bacteria with human cell lines that require oxygen. Furthermore, flexibility afforded by the methodology allows an improved understanding of the impact of bacterial metabolites on human cells. This approach has proven invaluable, as it allows for investigatory analysis of bacteria via a metabolite-infused proxy, without the potentially detrimental impact of direct bacterial exposure, which might further hinder experiments due to the acidification of cell culture media (Sánchez-Clemente et al. 2018). However, little research has been performed on the impact that different cell culture medium variations and their unique compositions have on the metabolites produced by a given bacteria or consortium of interest.

As probiotic- and pathogenic-conditioned media were utilised extensively throughout numerous aspects of this study, it was of particular interest to assess what impact, if any, different cell culture media would have on the metabolite composition of conditioned media if utilised in the generation of conditioned medium. Additionally, due to the results observed in earlier chapters, in which it was identified that specific probiotic formulations often result in cell line-specific responses, including increased production of pro-inflammatory stimuli, it was important to examine the metabolic profiles of those bacteria selected for use in the study to identify those metabolites that might contribute to those results seen in previous chapters, and potentially assist in aligning those findings to published data from studies *in vitro* and human intervention studies.

Unfortunately, while understanding the potential variations between pathogenic, mutualistic and probiotic *E. coli* from within the same phylogenetic group was an avenue of interest for this study, the analysis of the probiotic and mutualistic strains (*E. coli* strains Nissle 1917 and MP1) was not possible to complete within the confines of this study due to the restrictions imposed by the COVID-19 pandemic.

Furthermore, examining the metabolic profiles of the individual bacterial species comprising the Lab4 and Lab4B consortia was of particular interest since the impact of these commercial products has been examined in considerable depth, and following discussions with staff at Cultech Ltd., it was revealed that the metabolite profiles of individual species remained unexplored. When comparing those profiles generated from single species to those generated from a multispecies consortium, it was proposed that variations in metabolic profiles might provide further insight into the observed interactions in Chapters 3 and 4..

Additionally, through comparing probiotic species with the full Lab4/Lab4B consortia, it was proposed that some insight might be provided as to which species within these consortia contribute most to the results recorded in the previous chapters. Ultimately, it was of considerable interest to identify whether these commercially available probiotic compositions used extensively within this study, result in the production unique metabolites when compared, and which species contributed more or less of its metabolites to the overall metabolite profiles

It must be noted that this chapter does not seek to fully profile the bacteria metabolically, nor assign function to those metabolites whose functions remain, as yet, unassigned. These goals lie far beyond the scope of this project, and while these remain a series of interesting concepts, they were not the ultimate aim of this chapter and, as such, are not discussed here. Rather, the aims of this chapter are to further expand on the work performed in Chapter 4, focusing on the impact of bacterial products and compounds by identifying those metabolic functions and pathways influenced by the Lab4 and Lab4B range of probiotics in addition to the small selection of *E. coli* strains selected for use in the study, while simultaneously identifying the impact of growth medium on the metabolic profiles of a given bacterial consortium and if any of these factors might have otherwise impacted the assays performed.

5.1.3 The aims of the chapter

1. To assess the metabolite profiles of Lab4 and Lab4B probiotics and whether the metabolite composition varies in accordance with the cell culture medium selected when generating a conditioned medium.
2. To assess the metabolites produced by the individual bacterial constituents of the Lab4 and Lab4B probiotics, the dual-strain bacterial mixes and the pathogenic *E. coli* strain E69.
3. To identify the metabolic pathways influenced by each bacteria-conditioned medium.
4. To identify any unique metabolites found in the assessed conditioned media, and any unique metabolic pathways influenced by a given bacterium.

5.2 Materials and methods

5.2.1 Preparing conditioned medium

Conditioned medium was generated for each bacterial species following the protocol previously outlined in section 4.2.7, with a few slight variations as follows. All bacterial strains were first grown in their specific growth medium, those being LB for the *E. coli* strain E69 and MRS broth for the Lab4 and Lab4B commercial mixes/single species. Following this pre-growth, the bacteria were pelleted by centrifuging the bacterial suspensions at 1638 rcf for 10 minutes at 4 °C. The spent growth medium was removed from the pellet, ensuring that the pellet remained undisturbed, and aliquoted into 10 mL aliquots before being frozen at -20 °C for downstream metabolite analysis at a later date. The bacterial pellet was subsequently resuspended in 10 mL of an appropriate cell culture medium, and returned to anaerobic conditions as noted in section 4.2.7 to allow for a secondary growth cycle. Following this secondary growth phase, the conditioned medium was centrifuged at 1638 rcf for 10 minutes at 4 °C to generate a pellet, and the media collected.

Having been filtered through a 0.2 µm filter, the conditioned medium was aliquoted into 10 mL aliquots and frozen at -20 °C, and unlike the conditioned media used in previous experiments, in this instance, the conditioned media generated for metabolite analysis were

not pH adjusted. For preliminary assays to assess the impact of cell culture medium on the metabolite production of Lab4 and Lab4B probiotics, conditioned medium was generated using McCoy's 5A, RPMI 1640, low glucose DMEM and high glucose DMEM, and each sample was stored at -20 °C. Additionally, blank medium controls for all growth media and cell culture media bases were frozen prior to analysis.

5.2.2 Nuclear magnetic resonance (NMR) analysis of conditioned medium for metabolite identification

NMR and multivariate analyses noted in sections 5.2.2.1 and 5.2.2.2 were performed by staff at Imperial College, London. Frozen samples were transported to Imperial College on ice to preserve metabolite integrity. Sample preparation, analysis and metabolite identification are outlined below.

5.2.2.1 Preparing samples for NMR analysis

Samples were defrosted and brought to room temperature before being centrifuged in a temperature-controlled centrifuge for 10 minutes at 20,000 rcf and 4 °C, ensuring that the entire sample was homogenised prior to performing the NMR. Following centrifugation, 540 µL of the sample was added to 60 µL of a specified NMR buffer containing trisodium phosphate (TSP), potassium dihydrogen phosphate (KH₂PO) and sodium azide (NaN₃). pH was subsequently adjusted to 7.4. Samples containing the buffer were once again centrifuged at 20,000 rcf for 10 minutes at 4 °C, following which 580 µL was transferred to a fresh 5 mm glass NMR tube.

NMR was performed in accordance with a standardised protocol using a Bruker BMM NH270718 spectrometer (McDonald et al. 2018). Data was curated, and multivariate analysis was performed via the MATLAB software prior to metabolite analysis.

5.2.2.2 Identification of metabolites in conditioned medium samples via multivariate analysis and the use of metabolite identification software

Metabolite profiles were analysed using the Chenomx online database and the TopSpin NMR software for manual identification of specific metabolites from NMR profiles that appeared potentially significant and that were of particular interest for encapsulating the complexity of the metabolite profiles produced by each bacterial species or consortium. Following Chenomx- and TopSpin-based analyses, metabolite profiles for each conditioned medium sample, including relative abundance or exact concentrations, were transferred and stored using Microsoft Excel 2013 for subsequent analysis.

5.2.3 Analysis of Lab4- and Lab4B-conditioned medium metabolite profiles in four distinct cell culture media

Preliminary datasets for the Lab4 and Lab4B consortia in multiple cell culture media bases were provided with no exact metabolite concentrations – only relative abundance within a given sample. As such, the data presented and analysed in the following section represents relative concentrations as opposed to exact values.

Metabolite datasets were formatted using Microsoft Excel, and, due to the absence of exact numeric values, samples were assigned a colour representative of the relative metabolite abundance within the sample to allow for immediate visualisation of abundance similar to that seen in a heatmap. The colour red was utilised to indicate high abundance of a metabolite within a sample, while white was used to represent low abundance of a given metabolite within the sample. Metabolites for each experimental sample were subsequently sorted alphabetically using Microsoft Excel 365 A – Z function, and all samples of a given bacterial consortium, either Lab4 or Lab4B, were aligned to allow for metabolite presence-absence analysis

5.2.4 Metabolite presence-absence analysis and function identification in Lab4 and Lab4B consortia-conditioned, single-species-conditioned and *E. coli*-conditioned medium

5.2.4.1 Metabolite presence-absence analysis

Data for each bacteria-conditioned medium was firstly formatted to allow for subsequent analysis. Samples were compared with the metabolite profile of a blank control to identify any changes in the metabolite concentrations and any metabolites used by the bacteria during growth or those produced by the bacteria as part of their metabolism. Samples were compared with a conditioned MRS medium to identify if any specific metabolites were present or absent in either medium formulation. Finally, single-species-conditioned medium samples were analysed in comparison to the Lab4 or Lab4B consortia to which they belong to identify which bacteria are responsible for the production of any unique metabolites and whether a specific compound was present or absent in the single-species metabolite profiles that might suggest metabolic cross-feeding.

E. coli samples were additionally analysed in a similar manner, comparing a blank medium and conditioned LB medium to identify any metabolites that were produced following incubation with bacteria. Samples were additionally compared against probiotic species to enable presence-absence analysis of any unique metabolites that might aid in suppressing the immune response or that might act as a marker of disease.

5.2.4.2 Identifying metabolite functions, and metabolic pathways influenced

Metabolites were analysed utilising the KEGG metabolic pathways and KEGG compound analysis tools (Kyoto Encyclopedia of Genes and Genomes 2020). Metabolite names were entered into the search function of the KEGG website with the “COMPOUND” filter applied. Once identified, the appropriate compound was selected, and the pathways that the metabolite in question has been reported as influencing (as displayed within the compound database) were recorded for downstream analysis. This process was repeated for each

compound. Additional functionality and context for each metabolite was compiled using the PubChem online database. Each metabolite was manually identified, functions identified, and the information stored utilising Microsoft Excel.

When it was not possible to identify the functions of a given metabolite due to an exceptional number of potential hits on the KEGG compound database, and in instances where the available information on the metabolite at hand was not sufficient regarding the chemical structure of a given metabolite, including the presence of ligands, chemical orientation or configuration, these metabolites were excluded from the metadata to avoid erroneous conclusions.

5.2.5 Data visualisation

Data visualisation was primarily performed using R version 3.4.3 and RStudio version 1.1.423, utilising the R packages noted in section 2.12. In instances where numeric values were not available, data was sorted according to concentration and, using a colour gradient ranging from red (high concentration) to white (low concentration), denoted relative metabolite abundance within a given sample. Metabolite data was subsequently sorted alphabetically by using the A – Z function in Microsoft Excel to generate a heatmap-like plot to enable immediate visual analysis. Samples were subsequently aligned to enable cross-sample comparisons, noting which metabolites were absent from a sample and inserting a textured cell to indicate metabolite absence from a given sample.

5.3 Results

5.3.1 The importance of medium selection in the production of bacterial metabolites in conditioned medium assays

5.3.1.1 Metabolite variations in Lab4-conditioned cell culture media

The analysis of the Lab4 consortium in the 4 selected cell culture media showed 75 unique metabolites, and not all metabolites were produced by the probiotic species across all growth media selected for the study (Figure 5-1). In all instances, lactate was the most abundant metabolite regardless of the medium base selected. All metabolites that are produced by the Lab4 consortium can be noted in Figure 5-1.

Additionally, it should be noted that, when grown in specific cell culture media, a number of unique metabolites are produced, with 1, 3, 6 and 10 unique metabolites present in conditioned RPMI 1640, McCoy's 5A, low glucose DMEM and high glucose DMEM medium samples respectively.

5.3.1.2 Metabolite variations in Lab4B-conditioned cell culture media

A total of 80 unique metabolites were identified in the conditioned media generated from the Lab4B consortia when grown in the 4 selected cell culture media bases (Figure 5-2). Similarly to the trend observed in the Lab4 samples, lactate was the most abundant metabolite in every analysed sample, which coincides with what was expected due to the fermentative growth characteristically observed in lactic acid-fermenting bacteria, to which the probiotic species comprising the Lab4 and Lab4B consortia belong.

The comprehensive list of all metabolites identified within these conditioned medium formulations can be seen in Figure 5-2. With regard to the unique metabolites present only in a single conditioned medium formulation, conditioned RPMI 1640 medium had no

metabolites unique to that medium formulation. However, in the case of McCoy's 5A and low glucose DMEM, both conditioned medium formulations contained 4 metabolites each that were unique to each formulation, while high glucose DMEM had a total of 26 unique metabolites not found in other medium formulations.

	Lab4 RPMI 1640	Lab4 McCoy's 5A	Lab 4 Low Glucose DMEM	Lab4 High Glucose DMEM
2-Aminoadipate	Red	Red	Red	Red
2-Aminobutyrate	Red	Red	Red	Red
2-Hydroisobutyrate	Red	Red	Red	Red
2-Hydroisocaproate	Red	Red	Red	Red
2-Hydroxybutyrate	Red	Red	Red	Red
2-Hydroxyvalerate	Red	Red	Red	Red
2-Phosphoglycerate	Red	Red	Red	Red
3-Hydrobutyrate	Red	Red	Red	Red
3-Hydroxy-3-methylglutarate	Red	Red	Red	Red
3-Hydroxyisobutyrate	Red	Red	Red	Red
Acetate	Red	Red	Red	Red
Agmatine	Red	Red	Red	Red
Alanine	Red	Red	Red	Red
Alloisoleucine	Red	Red	Red	Red
Arginine	Red	Red	Red	Red
Asparagine	Red	Red	Red	Red
Azelate	Red	Red	Red	Red
Betaine	Red	Red	Red	Red
Cadaverine	Red	Red	Red	Red
Citrulline	Red	Red	Red	Red
Creatine	Red	Red	Red	Red
Creatine phosphate	Red	Red	Red	Red
D-Threitol	Red	Red	Red	Red
Erythritol	Red	Red	Red	Red
Ethanol	Red	Red	Red	Red
Fructose	Red	Red	Red	Red
Galactarate	Red	Red	Red	Red
Galactonate	Red	Red	Red	Red
Glucarate	Red	Red	Red	Red
Glucitol	Red	Red	Red	Red
Gluconate	Red	Red	Red	Red
Glucuronate	Red	Red	Red	Red
Glutamate	Red	Red	Red	Red
Glutamine	Red	Red	Red	Red
Glycerate	Red	Red	Red	Red
Glycine	Red	Red	Red	Red
Glycylproline	Red	Red	Red	Red
Guanidoacetate	Red	Red	Red	Red
Histidine	Red	Red	Red	Red
Homoserine	Red	Red	Red	Red
Isobutyrate	Red	Red	Red	Red
Isoleucine	Red	Red	Red	Red
Lactate	Red	Red	Red	Red
Leucine	Red	Red	Red	Red
Lysine	Red	Red	Red	Red
Mannitol	Red	Red	Red	Red
Methionine	Red	Red	Red	Red
Methylmalonate	Red	Red	Red	Red
N-Acetylglycine	Red	Red	Red	Red
N-Isovaleroylglycine	Red	Red	Red	Red
O-Phosphoserine	Red	Red	Red	Red
Oxypurinol	Red	Red	Red	Red
Phenylalanine	Red	Red	Red	Red
Proline	Red	Red	Red	Red
Protocatechuate	Red	Red	Red	Red
Putrescine	Red	Red	Red	Red
Pyroglutamate	Red	Red	Red	Red
Pyruvate	Red	Red	Red	Red
Ribose	Red	Red	Red	Red
S-Sulfocysteine	Red	Red	Red	Red
Saccharopine	Red	Red	Red	Red
Serine	Red	Red	Red	Red
Suberate	Red	Red	Red	Red
Succinate	Red	Red	Red	Red
Threonate	Red	Red	Red	Red
Threonine	Red	Red	Red	Red
trans-4-Hydroxy-L-proline	Red	Red	Red	Red
Tyrosine	Red	Red	Red	Red
Urea	Red	Red	Red	Red
Valine	Red	Red	Red	Red
Xanthine	Red	Red	Red	Red
Xanthurenate	Red	Red	Red	Red
Xylitol	Red	Red	Red	Red
π -Methylhistidine	Red	Red	Red	Red

Figure 5-1: Identified metabolites and relative concentration profile of Lab4 probiotic-conditioned medium made from four distinct cell culture medium bases (McCoy's 5A, RPMI 1640, low glucose DMEM and high glucose DMEM). Metabolites were identified using the Chenomx online database and TopSpin NMR software. Colour gradient represents the relative concentration of a metabolite within a given conditioned medium with a more vivid colour representing greater metabolite abundance. Red: High abundance. White: Low abundance. Textured: Metabolite not present.

	Lab4B RPMI 1640	Lab4B McCoy's 5a	Lab 4B Low Glucose DMEM	Lab4B High Glucose DMEM
2-Amino adipate				
2-Aminobutyrate				
2-Hydroisobutyrate				
2-Hydroisocaproate				
2-Hydroxy-3-ethylvalerate				
2-Hydroxy-3-methylvalerate				
2-Hydroxybutyrate				
2-Hydroxyglutarate				
2-Hydroxyisocaproate				
2-Hydroxyvalerate				
2-Phosphoglycerate				
3-Hydroisobutyrate				
3-Hydroxy-3-methylglutarate				
Acetate				
Agmatine				
Alanine				
Allisoleucine				
Arabinitol				
Arginine				
Azelate				
Cadaverine				
Citrulline				
Creatine				
D-Threitol				
Erythritol				
Ethanol				
Formate				
Fructose				
Galactonate				
Glucarate				
Glucitol				
Gluconate				
Glucose				
Glucose-6-phosphate				
Glucuronate				
Glutamate				
Glutamine				
Glutarate				
Glycerate				
Glycerol				
Glycine				
Glycolate				
Glycylproline				
Guanidoacetate				
Homoserine				
Imidazole				
Isobutyrate				
Isoleucine				
Lactate				
Leucine				
Lysine				
Mannitol				
Methionine				
Methylmalonate				
myo-Insitol				
O-Phosphoserine				
Ornithine				
Oxypurinol				
Phenylalanine				
Proline				
Protocatechuete				
Putrescine				
Pyruvate				
Pyroglutamate				
Pyruvate				
Saccharopine				
Serine				
S-Sulfocysteine				
Suberate				
Succinate				
Taurine				
Threonate				
Threonine				
trans-4-Hydroxy-L-proline				
Urea				
Valerate				
Valine				
Xanthurenate				
Xylitol				

Figure 5-2: Identified metabolites and relative concentration profile of Lab4B probiotic-conditioned medium made from four distinct cell culture medium bases (McCoy's 5A, RPMI 1640, low glucose DMEM and high glucose DMEM). Metabolites were identified using the Chemomx online database and TopSpin NMR software. Colour gradient represents the relative concentration of a metabolite within a given conditioned medium with a more vivid colour representing greater metabolite abundance. Red: High abundance. White: Low abundance. Textured: Metabolite not present.

5.3.2 Impact of glucose levels on metabolite production in conditioned media

It was initially proposed that, due to the variable glucose concentrations present in the cell culture media, any variation in glucose levels may, in turn, have influenced the production of metabolites due to variable availability of nutrients across each conditioned medium, contributing to either an increased or decreased metabolic activity from the probiotic bacteria. In the case of both Lab4 and Lab4B, conditioned high glucose DMEM medium boasted the largest number of metabolites from among the four selected medium bases, potentially due to the high nutrient availability acting as a contributing factor to the variety of metabolites produced by the Lab4 and Lab4B consortia when generating conditioned media. Due to time limitations, not all conditioned media were analysed; therefore, some of this work remains speculation at this stage.

5.3.3 Bacterial metabolite composition following growth in MRS and high glucose DMEM

Blank MRS broth and high glucose DMEM metabolite profiles were generated using the methods applied for conditioned medium analysis. The values generated for the blank medium were compared with the corresponding conditioned medium and notable changes in metabolite concentrations can be seen in Appendix 2.

MRS-based conditioned medium metabolite analysis was performed to identify any potential trends that occur when the probiotic species are grown in their optimal growth medium. The analysis of primary growth medium was of particular interest as, by doing so, it would be possible to identify whether any metabolites of particular interest are lost following the initial reconstitution and growth in MRS and the subsequent secondary growth cycle in high glucose DMEM.

The results of the metabolite analysis performed on both MRS and the corresponding conditioned high glucose DMEM medium can be seen in Figure 5-3. Notably, analysed MRS samples contained elevated levels of acetate and glycine when compared to the conditioned high glucose DMEM media. Additionally, alanine was exclusively identified in

MRS samples, while lactate was observed at lower concentrations in MRS medium compared to those seen in the conditioned high glucose DMEM media, and it is absent from both *Bifidobacterium* single-species MRS samples. Additionally, glucose was also identified as occurring at elevated concentrations in the analysed MRS samples, possibly as a result of the initial reconstitution and acclimatisation to the growth medium.

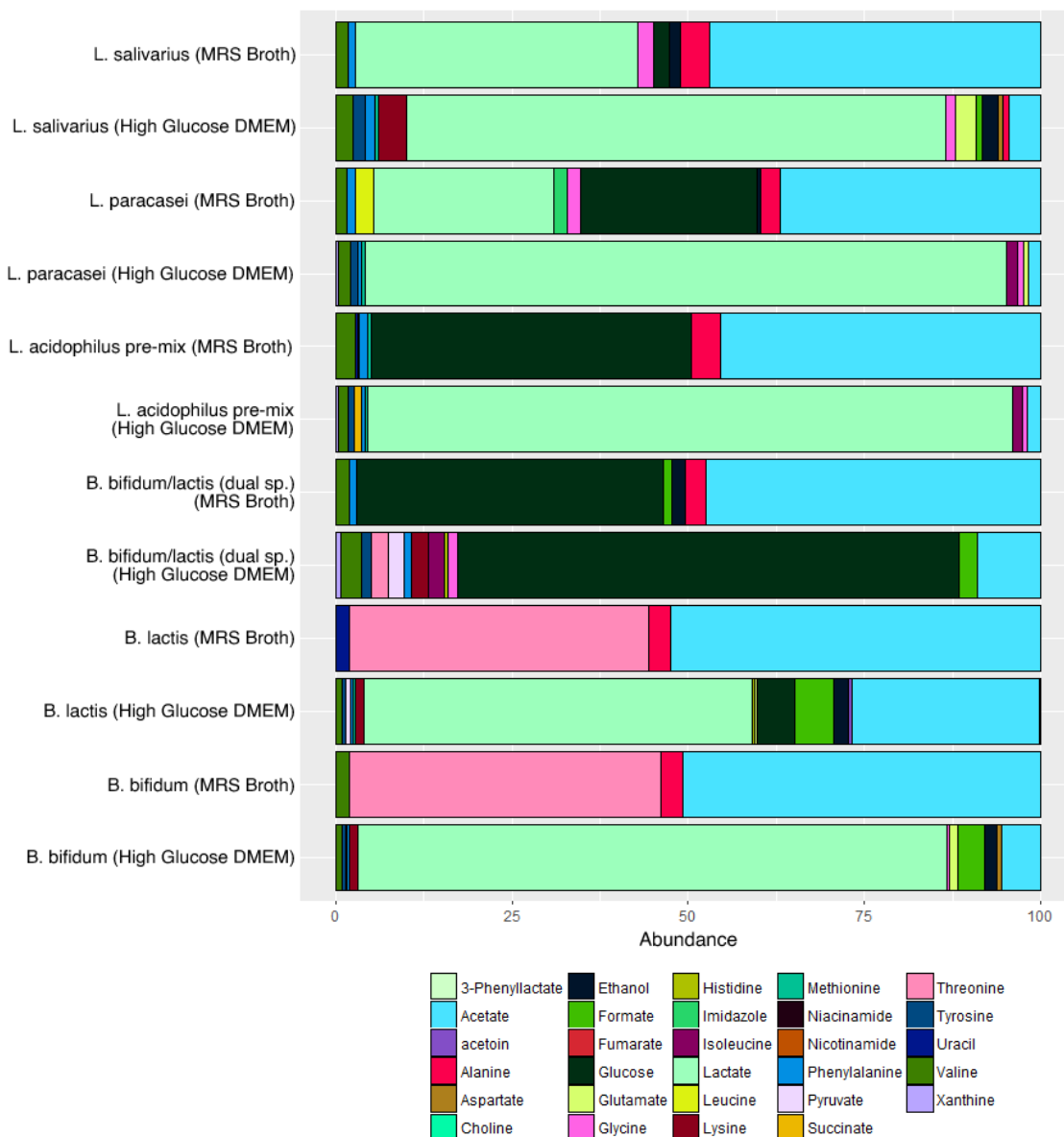


Figure 5-3: Metabolite profiles of the individual bacteria that comprise the Lab4 and Lab4B probiotics prepared using both MRS Broth and high glucose DMEM. Metabolites were identified using the Chemomx online database and TopSpin NMR software.

5.3.4 Metabolite production in single-species- and dual-species-conditioned medium

Lactate was observed as being the dominant metabolite in five of the six analysed probiotic-conditioned media, with lactate accounting for over 50% of the detected metabolites within said samples (Figure 5-4(A)). However, in the case of the dual-cultured *Bifidobacterium* (containing both *B. bifidum* and *B. animalis* sub sp. *lactis*), it can be noted that lactate was absent from this conditioned medium sample, meaning that lactic acid fermentation did not occur when both species were combined for the purposes of generating a conditioned medium. Such a trend was not observed in either the *B. bifidum* or *B. animalis* sub sp. *lactis* conditioned medium, thus suggesting an interspecies interaction that alters the overall behaviour of both species, possibly contributing to the improved viability of the species seen in the growth curves conducted in which dual species were noted as having improved O₂ tolerance compared to single species.

A secondary analysis was performed by removing lactate values from the data samples to allow for greater clarity and ease in identifying unique metabolites and can be seen in Figure 5-4(B). From among the 25 metabolites identified across the 6 conditioned media assayed (including the lactate data removed from the analysis), 6 metabolites were identified that only occurred in a single conditioned medium formulation, those being: alanine found in the *L. salivarius*-conditioned medium, fumarate produced by the *L. acidophilus* dual mix, threonine produced exclusively in the *B. bifidum* and *B. animalis* sub sp. *lactis* dual-species mix, and, finally, nicotinamide, phenyllactate and acetoin that were noted as only occurring in the conditioned medium generated from the single species *B. animalis* sub sp. *lactis*.

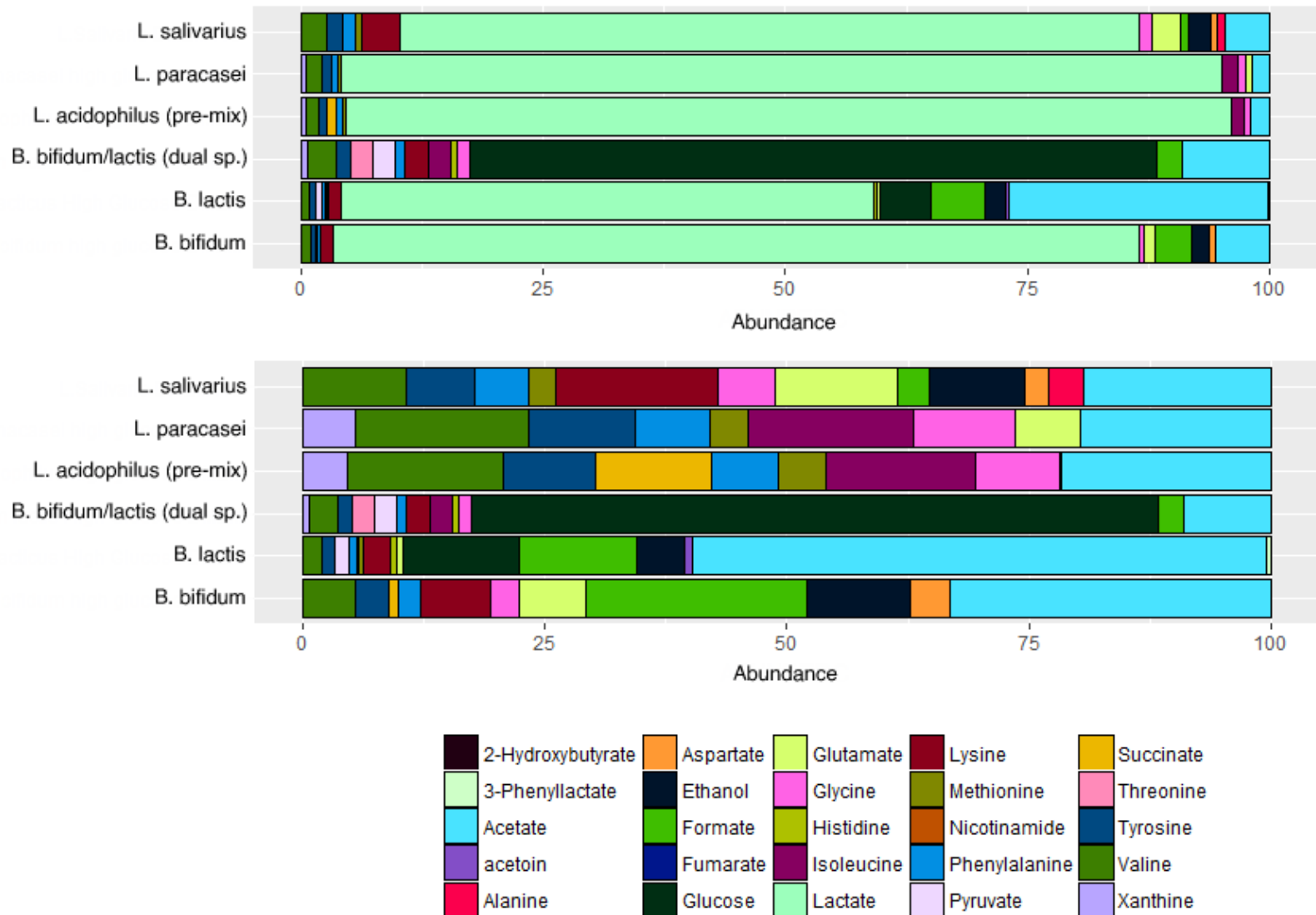


Figure 5-4: Metabolite profiles of the constituent bacteria found in the Lab4 and Lab4B probiotics, generated using high glucose DMEM. A) Relative concentration profile of all metabolites present in the original conditioned media. B) Relative concentration profile of the metabolites present in the conditioned media with the omission of lactate. Metabolites were identified using the Chemomx online database and TopSpin NMR software.

5.3.5 Metabolic analysis of enteropathogenic *E. coli* E69-conditioned media generated using both LB broth and high glucose DMEM

EPEC E69 analysis was conducted in an identical manner to the methodologies used in the analysis of the Lab4 and Lab4B consortia. The results of the metabolite analysis for the conditioned media based on both the LB and high glucose DMEM can be seen in Figure 5-5.

Analysis of LB broth revealed a considerable diversity of metabolites when compared to the conditioned high glucose DMEM medium. This loss of metabolic diversity could, in part, be due to the relatively simplified composition of the cell culture medium compared to the initial growth medium. Conditioned medium generated in high glucose DMEM is notably dominated by formate, glucose and acetate. Three unique compounds could be identified in the final conditioned medium that were not found in the initial growth medium, those being a small amount of lactate, formate and 2-hydroxybutyrate.

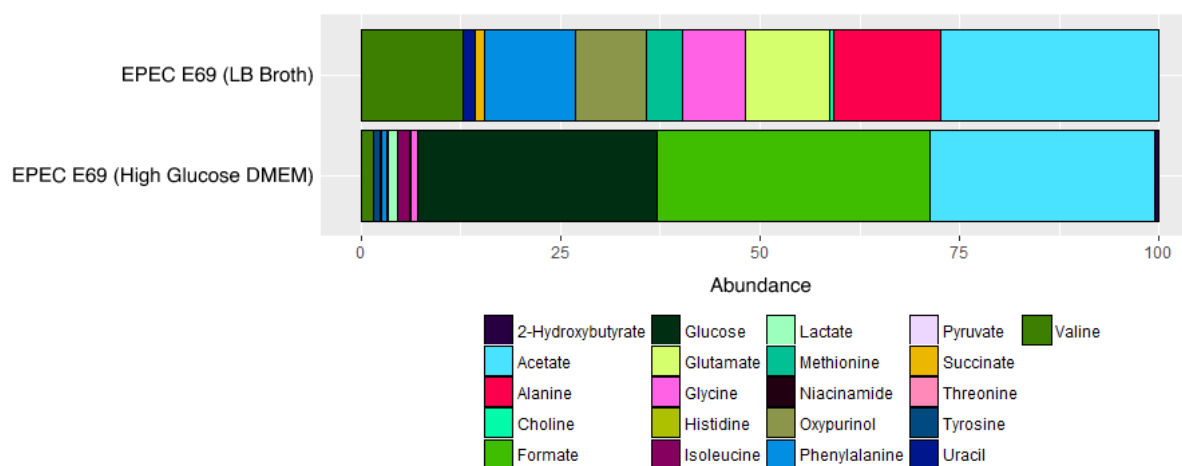


Figure 5-5: Metabolite profiles of enteropathogenic *E. coli* strain E69 (EPEC E69)-conditioned medium generated using both LB broth and high glucose DMEM. Metabolites were identified using the Chenomx online database and TopSpin NMR software.

5.3.6 The metabolic pathways influenced by the Lab4 and Lab4B probiotics and the pathogenic *E. coli* EPEC E69

Due to a lack of quantifiable data from the metabolite analysis performed using various cell culture medium bases, the following analysis was performed using only single-species-/dual-species-conditioned medium as applicable. A comprehensive breakdown of all metabolic pathways influenced by each metabolite found in all conditioned medium formulations can be found in Appendices 3 – 8, while the total number of metabolic pathways influenced by a given conditioned medium can be seen in Table 5-1. Unique metabolic pathways that were influenced within each conditioned medium profile were compiled, and the final total pathway count can be seen in Table 5-1. Across the six assessed probiotic conditioned media, *L. paracasei* and *L. acidophilus* were the sole conditioned media capable of influencing a unique metabolic pathway, with *L. acidophilus* having metabolites identified as influencing pathways relating to cancer, and renal cell carcinoma (fumarate), whereas *L. paracasei* possesses a metabolite known for its role in mTOR signalling pathways (leucine).

The metabolite profile for *E. coli* strain E69 was noted as having the potential to influence only a single unique metabolic pathway when compared to the probiotic Lab4 and Lab4 strains, that being a pathway linked to the peroxisome. Interestingly, the analysed conditioned medium profiles generated from the dual-species *B. bifidum* and *B. animalis* sub sp. *lactis* mix and dual-strain *L. acidophilus* mix influenced fewer metabolic pathways than the single-strain and consortium-conditioned media. This is particularly noticeable with the *Bifidobacterium* dual-species mix, as, individually, both these bacteria are capable of influencing 139 metabolic pathways as opposed to the 113 when combined.

Table 5-1: Metabolic pathways influenced by both probiotic and pathogenic single-species/dual-species-conditioned media.

Conditioned medium	Unique metabolic pathways influenced
<i>L. acidophilus</i> (high glucose DMEM) – Dual-strain mix	119
<i>L. paracasei</i> (high glucose DMEM)	135
<i>L. salivarius</i> (high glucose DMEM)	137
<i>B. bifidum</i> (high glucose DMEM)	139
<i>B. animalis</i> sub sp. <i>lactis</i> (high glucose DMEM)	139
<i>B. bifidum</i> and <i>B. animalis</i> sub sp. <i>lactis</i> (high glucose DMEM) – Dual-species mix	113
<i>E. coli</i> E69 (high glucose DMEM)	137

5.4 Discussion

When attempting to comprehend the importance of the metabolic profiles generated in the above experiments, one aspect is undeniable: single-species-conditioned media and multi-species conditioned media, while similar in their composition, do contain a number of unique metabolites that distinguish conditioned media from one another, thus reinforcing the idea that community composition and selected medium is highly influential on the final metabolite profile of a conditioned medium. This is further exemplified when examining the experiments in which medium composition resulted in considerable variations when generating conditioned medium, leading to distinct metabolomes depending on the medium selected. While it is possible to hypothesise that nutrient availability and amino acid variations in the cell culture medium influence the production of these metabolites, the degree to which each factor influences metabolite production remains unknown at this stage and would require additional validation.

One of the objectives of this chapter was to identify whether, any immediate variations between conditioned media could be observed that may, in turn, contribute to those inflammatory responses observed in section 4.3.6.

As such, the common theme seen throughout this study remains of equal importance here, that being that greater selectivity is required when incorporating biological stimuli into cell culture assays, as minor variations in methodologies can significantly impact the final result. This was particularly exemplified when comparing the variations in the metabolic profiles of conditioned medium generated using different cell culture medium bases, and as such it could be said that certain considerations should be given to the initial selection of cell line, as subsequent selection of medium for use in generating of conditioned medium will be dependent on the cells being used. What should be noted, however, is that in this study, cells were only exposed to the conditioned medium generated from High Glucose DMEM, and without having exposed the cell lines used in this study to the other conditioned medium formulations, the exact impact of the conditioned medium profiles cannot be noted here but does provide an interesting prospect for future studies to explore.

Lactate was unsurprisingly identified as the predominant molecule in almost all conditioned media generated using the constituents of the Lab4 and Lab4B probiotic consortia. This production of lactate is promising, as lactate is a characteristic metabolite produced by all the Lab4 and Lab4B bacteria, due to fermentation being a key aspect of all the probiotic species used in this study's life cycle, thus suggesting that the majority of species examined are behaving as expected under anaerobic conditions. While *Bifidobacterium* have not been ascribed the nomenclature of lactic acid-producing bacteria, it has been documented that these species additionally produce lactic acid in large quantities as a part of their life cycle and as a by-product of their metabolism (Bintsis 2018). Furthermore, these findings are of particular interest as it has been suggested that lactate provides additional health benefits when ingested, particularly during disease states, including for inflammatory diseases of the gut such as UC and CD, as consumption of probiotics containing lactic acid-producing bacteria has aided in maintaining and prolonging remission periods following surgical intervention (Saez-Lara et al. 2015). Furthermore, lactate has additional benefits in regions external to the gut – it has previously been identified as one of the key metabolites that

translocate to the brain following ingestion of the Lab4 consortium (O'Hagan et al. 2017), a significant finding considering the importance of lactate in the brain (Riske et al. 2017). However, when analysing the conditioned media conditioned with the dual-species mix of *B. bifidum* and *B. animalis* sub sp. *lactis*, no lactate was identified in these samples. Lactate is a molecule that is produced in large quantities in anaerobic metabolism, and contributes a key function, even in aerobic metabolism. It has been noted in numerous studies that under aerobic conditions, the consumption of sugars and subsequent fermentation and production of alcohol is considerably reduced compared to that seen in anaerobic environments due to the abundance of oxygen negating the need for fermentation to occur, and yet it has been reported that lactate is always produced as a by-product in glycolysis (Rogatzki et al. 2015), functioning as an intermediary molecule linking both glycolysis and oxidative phosphorylation. As such, a lack of lactate from this dual-species-conditioned medium raises the question as to why lactate is not produced under these conditions. Potential solutions to this question include sub-optimal growth of the bacteria and the use of lactate as an alternative energy source, among others. However, without further examination, these questions remain unanswered, thus presenting possible topics for future research.

When examining the metabolite profiles of the single- or dual-species-conditioned media, where the lactate data had been removed, it was possible to identify a small number of possible trends, many of which are conserved to the bacterial genera used in the study. Those conditioned media generated using the different *Lactobacillus* species were noted as possessing higher concentrations of the amino acids valine, tyrosine, isoleucine and phenylalanine, whose roles in the human body are highly varied and generally noted as being beneficial in nature, although, interestingly, tyrosine has been noted as a key component of catecholamine synthesis in the brain – a series of neurotransmitters that include dopamine and both epinephrine and norepinephrine (Fernstrom and Fernstrom 2007). However, the medium conditioned with the *Bifidobacterium* held higher percentages of acetate, which has been implicated in beneficial energy and substrate metabolism (Hernández et al. 2019), ethanol and lysine. Interestingly, despite the high initial concentration of glucose present in high glucose DMEM (4500 mg/L), glucose was only present in the *B. lactis* and *Bifidobacterium* dual-mix conditioned medium, potentially suggesting a low metabolic rate from these bacteria. It could also be proposed that the

remaining glucose was a result of these bacteria conducting metabolic cross-feeding or utilising alternative nutrient sources preferentially to glucose. Without conducting further experiments into the behaviour of these bacteria, however, this concept remains as speculation only.

Additionally, when examining the data acquired from the KEGG database it is possible to note that mTOR is influenced by leucine, which is found exclusively in the conditioned medium produced by *L. paracasei*, a finding of particular interest. Pathways relating to mTOR have been shown to hold a key role in human metabolism, with mTOR-related pathways typically being dysregulated during certain disease states (Saxton and Sabatini 2017), including, but not limited to, cancer (Alayev and Holz 2013), depression (Ignácio et al. 2016) and even diabetes (Mao and Zhang 2018). While the exact impact this metabolite would have on the mTOR signalling cascade is unknown, the presence of a metabolite capable of influencing a major signalling pathway highlights this as potential bacterium of interest for future metabolic studies, even if this information is only speculative at this stage.

A pair of interesting findings were identified in the conditioned medium generated from *E. coli* strain E69, those being the single uniquely influenced metabolic pathway compared to the assessed probiotic bacteria, and the elevated production of formate. *E. coli* strain E69 was shown to be the sole bacterium within this study whose metabolites could influence the peroxisome. Given the biological importance of the peroxisome in a number of metabolic interactions, in addition to its role in oxidation and catalysis (Titorenko and Terlecky 2011), the potential influence of this bacterium on the peroxisome is a notable one, although the nature of this influence, be that positive or negative, cannot be ascertained from this data and would require further investigation to truly understand the impact of this bacteria on the peroxisome. When considering the formate abundance within the *E. coli* E69-conditioned medium, a notable difference in the quantity of formate was seen, with quantities that totalled over 33% of the total metabolites in that formulation. Formate is a precursor molecule for the production of purines and the production of thymidylate (Pietzke et al. 2020) and has already been identified as having a key role in both health and disease progression, often resulting in improved disease outcomes for cancer patients and those

patients with either cardiovascular or neurological disorders (Pietzke et al. 2020). As such, the high percentage of formate present in the conditioned medium presents an interesting question: could the metabolites produced by *E. coli* as a species be relatively conserved, in a manner similar to what was observed with the probiotics, where metabolites displayed only minor species-specific variations? Furthermore, despite there being a comprehensive collection of data discussing the influence of gut derived metabolites on disease states, this concept raises the question as to whether it is the effector molecules and pathogenicity elements that contribute primarily to the development of a disease phenotype and impact on human cells are majorly variable between strains of a given bacterium, with only minor variations in metabolite production occurring between strains. This was something initially pursued in this study with the use and analysis of the *E. coli* strains Nissle 1917 and MP1. While the subsequent generation of conditioned medium of both species was prepared for metabolite profiling and analysis, unfortunately, this analysis could not be performed within the confines of the study due to time limitations.

Ultimately, the results presented in this study suggests that other factors such as effector molecules, secreted proteins or cell wall composition play a larger role in the pathogenesis of E69 than the produced metabolites. However, interestingly, the results of this chapter identifying the production of beneficial metabolites by *E. coli* E69 propose a potential means of offsetting the self-limiting nature of E69 during infection, a result of further note, particularly when considering that “healthy”, non-compromised individuals are typically capable of clearing the bacteria in a comparatively short time frame, although the mechanism of action and efficacy of pathogen clearance is subject to external influence by the host’s biological factors (Pearson and Frankel 2016).

While the diversity of metabolites identified across the multiple conditioned media is relatively consistent across all assessed samples, 25 unique metabolites were identified across all conditioned medium formulations. However, due to these metabolites occurring in comparatively low concentrations (with all non-lactate/high-abundance metabolites accounting for approximately 30% – 45% in total in each individual conditioned medium), identifying any potential pro-inflammatory or anti-inflammatory molecules in these conditioned media was not possible at this stage. It should also be stated that the overall

impact of these metabolites was not assessed in this study, so the overall impact of these metabolites in a biological context remains unknown, and as such, it could be speculated that the comparatively low abundance metabolites may, in truth, be responsible for the observed behavioural changes seen in Chapter 4. However, the generated conditioned medium profiles provide a key insight into the variation in bacterial metabolite composition, while also providing some potential targets for individual metabolite exposure assays to understand the impact of a given metabolite under cell culture conditions, with particular interest for the impact of these metabolites under physiologically relevant conditions (such as flow) and whether these physiological conditions affect the cellular response to said metabolites.

6 General discussion

This study aimed to explore the impact of the Lab4 and Lab4B ranges, produced by Cultech Ltd., and dynamic flow, induced by the Kirkstall Quasi Vivo® QV500 system, on cell culture systems, with particular emphasis given to the impact of these factors combined on the cellular parameters of viability, glycoprotein production and the production of pro-inflammatory cytokines. Furthermore, it was initially proposed that through examining these systems, with the addition of a few biological parameters, some insight might be provided as to the importance of physiological relevance *in situ*, although it should be noted that without additional research, no definitive conclusions can be drawn at this stage. Ultimately, as the research into these factors progressed, it was noted that two key themes were applicable to multiple experiments discussed throughout this project. While somewhat broad in their scope, those two key areas were: the importance of combining bacteria and flow in cell culture and the impact of physiological flow and potential of the QV500 as a method of improving the biological relevance of cell culture modelling.

Current cell culture studies that use probiotics as a key component of their research may make use of these products in a manner that lacks biological relevance. In the 2002 study from Mattar and colleagues (Mattar et al. 2002), it was reported that the cell line Caco-2, when exposed to the probiotic species *Lactobacillus casei*, reported an increased expression of mucin gene MUC2, a result that was not mirrored in this study following exposure to the Lab4 or Lab4B consortia under static or flow conditions. While the study showcased the impact and variation in response between cell lines in flow and static conditions when exposed to probiotics, simultaneously, it should be noted that Mattar and colleagues employed static cell line monocultures only during their research. While this study has revealed that adding flow to cell culture can act as an invaluable tool for cell culture methodologies *in vitro*, simultaneously the use of 2D culture should not be dismissed as antiquated, as both methodologies provide unique applications that may outweigh the benefits of the other, depending on the research at hand.

Probiotics have typically been observed as being useful in preventing the establishment of gastrointestinal pathogens via the production of anti-microbial agents or through inter-species competition for adhesion sites (Fuller 1991), and has been found to displace pathogenic bacteria from mucin when bound to prevent colonisation (Collado et al. 2007). Furthermore, it has been noted that the ingestion and administration of probiotics results in the modulation of pathogen-induced inflammatory responses, in which the inflammatory response is typically diminished (Vanderpool et al. 2008). However, despite the potential benefits of probiotic bacteria, while some probiotics show limited inflammatory potential, resulting in a weaker cytokine production response from epithelial cells compared to a pathogenic bacterium, not all species act in an identical manner. This was particularly notable with the works of Monteros and colleagues, in which it was noted that exposure to probiotics resulted in an increase in interleukin production, but a diminished oxidative stress response to indomethacin, an anti-inflammatory drug, known to induce an inflammatory side effects in patients (Monteros et al. 2021), a finding that somewhat coincides with what was shown in this study with an increase in interleukin production from a non-pathogenic bacterium. Additionally, it has been suggested in prior studies that the production of pro-inflammatory cytokines could be due to the features of a given epithelial cell line (Ng et al. 2009). This would coincide with the findings reported in this study, as the increase in inflammatory markers in this study, while somewhat contradictory to those stated in previous works, suggests that, while the initial response of the cells is to increase production of pro-inflammatory cytokines, it is not an inherently negative finding, and could instead be viewed that the ingestion of probiotic bacteria may result in the induction of a mild inflammatory response, thus priming the immune system to face and clear invading pathogens.

Unfortunately, this project did face certain challenges as a result of the COVID-19 pandemic, as certain experiments that were initially deemed of interest had to be discarded or otherwise adjusted to account for the restrictions imposed. The chapter most affected by the pandemic was Chapter 5, as this simultaneously impacted on unravelling the effects of bacterial agents on cell lines under flow conditions. A minor limitation within this chapter stemmed from the fact that the metabolite analysis could not be performed on site and, therefore, was prepared and transported to Imperial College (London) for analysis by staff.

As such, the need for an altered approach to conducting research further compounded this issue by preventing analysis and metabolite identification in time for project completion. This was primarily an issue as a number of samples prepared for metabolite analysis remained un-analysed, including the bacteria-conditioned media and corresponding LB growth broths for the non-pathogenic *E. coli* strains Nissle 1917 and MP1. These two strains were selected as they are members of the same phylogenetic group as *E. coli* E69, that being phylogenetic group B2 (Lasaro et al. 2014; Hazen et al. 2017). Additionally, strains MP1 and Nissle 1917 are non-pathogenic, and Nissle 1917 is a probiotic (Grozdanov et al. 2004). The analysis of these conditioned media was proposed to provide further insight regarding the influential factors inherent in non-pathogenic *E. coli*, and how these compare to the assessed Lab4 and Lab4B probiotic species used extensively throughout this study. It has been previously noted that EPEC, when exposed to gastrointestinal epithelia, induces a suppression of the inflammatory response – a response that has been theorised as playing a key role in the prevention of pathogen clearing *in situ*, thus promoting the pathogenesis of the species (Yen et al. 2010; Edwards et al. 2011).

Previous studies that made use of the QV500 system, whether exposed to probiotic bacteria or not, have displayed the considerable potential of this system. These studies have modelled the impact of flow on various cell types, including hepatocytes (Rashidi et al. 2016), fibroblasts (Nithiananthan et al. 2017) and cardiac tissue (Pagliari et al. 2014), while also revealing further insight on the infection rate of specific gastrointestinal pathogens, including the GI parasite *Leishmania major* (O’Keeffe et al. 2019). In all instances, the system has displayed considerable potential. However, the efficacy of the QV500 system has been shown to depend on the flow speed setting of the system, requiring bespoke flow limiters or an accurate measure of flow rates within the system prior to experimental challenging, as the efficacy of a given assay often hinges on the QV500 system and the use of a biologically relevant flow rate.

It has been mentioned on numerous occasions in this study that cell culture has made use of the individual traits of immortalised cell lines isolated from regions of interest within the body, taking full advantage of the individual biological traits of each cell line (Obinata 2007) and the large volume of cells that can be generated rapidly for use in experiments.

However, as has been noted throughout this study, when attempting to introduce cells typically cultured *in vitro* to physiologically relevant environments, in reality, this exposure can severely hinder the efficacy of the cells, and in some instances to a degree that will render a given cell line useless through impacting the biological functions of a cell line. While this does somewhat align with current research, where the introduction of flow can be observed as inducing a cellular response in real time, the negative response recorded from the cell line HT29 was a novel finding within this study, as this presented the concept of a “poor responding” cell line to physiological flow.

The observed alteration in cell line behaviour under physiological flow was not restricted only to the cell line HT29, however, as all cell lines displayed altered behavioural traits under dynamic flow compared to a static counterpart in almost all experimental conditions. While both Caco-2 and HT29MTX were examined, the parameters that were observed in each cell line were prone to considerable variation depending on the environment in which the cells found themselves, in addition to the assay being performed. While both cell lines displayed heightened viability and general wellbeing, as noted by the LDH, MTT and glycoprotein production assays, interestingly, the response of each cell line was subject to varying degrees of response when faced with the probiotic and pathogenic bacteria used in this study.

Many individuals have begun to shift research methodologies towards systems that improve biological relevance, as was the aim with this study, through the incorporation of biological factors such as those used in this study, or through altering culture methods for cell culture, often favouring 3D cell culture, primarily featuring the use of organoids or other complex multi-cellular systems (Jensen and Teng 2020) thus allowing cell culture to encapsulate a greater degree of biological complexity, through the addition of *in situ*-like factors.

However, it should be stated that, at present, the means by which cell lines are selected for use in research lacks an important step to firstly ensure that cell lines are suitable for use in physiological assays. Cell repositories typically list the genetic characteristics in addition to several key behavioural characteristics found in each cell line (ATCC 2020). While current research utilising 3D culture and studies employing physiologically relevant factors is

increasing, the overall availability of information regarding the impact of flow on specific cell lines is not as easily accessible.

As the use of 3D and flow-based methodologies increases, it is likely that other cell lines will be recorded as responding poorly to these physiological factors. With this consideration in mind, cell line databases and repositories might consider the inclusion of cell line-specific information with regard to the response of a cell under physiological conditions, as this could be of considerable importance for those cell lines that express a particularly poor response when faced with flow, like HT29, and for researchers aiming to utilise them.

One of the major limitations encountered throughout the study was with the physical limitations of the QV500 system. The QV500 system requires a compatible pump system to function, and it is this pump system that somewhat limits the ability to utilise this system effectively under a myriad of experimental conditions. Given the relative bulk of the system, in addition to requiring an external power supply, methodologies utilised in the emulation of biological parameters – including oxygen level and pressure modulation – are typically incompatible with the QV500 system due either to the size of the system, meaning that a given apparatus is unable to accommodate the QV500, or due to the external power supply required for the QV500 system to function, which would compromise the gas-impervious seals essential for ensuring a given atmosphere or pressure, thus limiting the use of the system in conjunction with alternative biological parameters.

Despite the observed limitations of the QV500, as this study aimed to understand the implications of dynamic flow in conjunction with probiotic bacteria, the issues with the QV500 system could be circumvented in most instances. However, it must be noted that, in cases where an individual might seek to perform flow-based cell culture assays, alternative flow models may provide a more desirable prospect in those instances, and particular focus should be given to the size and system requirements of a given flow model. Ultimately, the conclusion can be drawn that, while the QV500 dynamic flow system used in this study has been integral in implementing an effective biological flow element into cell culture assays, thus furthering the understanding of interactions that occur between cell lines and a myriad

of bacterial species, it does have its own set of limitations that must be considered in order to take full advantage of its benefits. Simultaneously, the QV500 system remains a comparatively accessible flow model for those seeking to incorporate flow into their cell culture research. However, while small-scale proof-of-concept studies may choose to utilise these systems, studies aiming to unravel the intricacies of such interactions through the implementation of high cell volume, rapidly implemented experiments, may instead choose alternative methodologies, as these may provide a more attractive prospect given the current limitations of the QV500 system. Regardless of the system selected for use, however, the potential limitations should be considered when approaching the design of such studies in future. It has been demonstrated that flow in this study has an important role in further understanding the behaviour of cell lines, particularly when in the presence of bacterial agents, and, as such, should be noted as a key resource in further improving current gut modelling methodologies.

6.1 Future work

The most promising aspect to come from this study is the scope for future research making use of either the QV500 system or, more broadly, dynamic flow in cell culture.

Unfortunately, as previously mentioned, the size, comparative bulk and configuration of the QV500 system led to some challenging moments, and may prove undesirable for studies aiming to utilise the system within other biological control systems, such as hypoxic chambers. However, while the QV500 may prove incompatible with other systems, the concept of incorporating flow systems with other biological parameters, such as biologically relevant oxygen levels, is one that might provide some invaluable insight into the impact of biological oxygen levels when combined with biological flow rates, such as those used in this study.

Additionally, while not possible within the scope of this study, transcriptomic assays would be a concept of considerable interest for future studies making use of dynamic flow. As mentioned in chapter 3, previous studies that employ similar systems to the QV500 have already revealed that the inclusion of flow in cell culture results in the differential activation

and suppression of many genes. While this study revealed that cellular behaviour is modulated with the inclusion of flow, there was a number of elements present within the study that may suggest a stressful environment. Combining the results in this study with that of Kulthong and colleagues, the use of transcriptomics may enable future studies to identify all genes influenced by flow, and assist in understanding whether these changes are beneficial or detrimental to the overall health and efficacy of a given cell line.

Following on from above, while it was not performed during this study, analysis of the bacterial transcriptome under flow would be of considerable interest. The focus of this study was the impact of dynamic flow and probiotics on a selection of biological parameters, and, as such, the impact of dynamic flow on the bacteria was not examined at this time. While the impact of probiotic bacteria was revealed to impact the production of pro-inflammatory cytokines in cell lines treated with probiotics, resulting in an altered response from cells subsequently treated with the pathogen of choice for this study, *E. coli* strain E69, the wider impact of pathogenic bacteria within flow centred cell culture was not extensively explored in depth, despite becoming a key component in later experiments of the study. Interestingly, flow experiments using the *E. coli* strain E69 reported minimal variation in inflammatory response, showing little in the way of variation from static assays, apart from those co-treated with probiotic species. To further examine this impact, it would be of great interest to incorporate other key pathogenic bacteria known to influence the GI tract and examine whether this flow impact is species specific, or a general trend observed in pathogenic bacteria of the GI tract.

6.2 Conclusion

The scientific rationale behind this thesis was to explore the overall impact of two distinct factors – physiological flow and probiotics – on a select number of biological parameters across four distinct cell lines. While this initial proposal was adjusted at select intervals throughout the study, the fact remains that dynamic flow was shown to be an effective means of moderating cellular behaviour, often in a manner that coincides with behaviours expected from that seen *in situ*. While base behaviours seen in cells grown in static culture

remain consistent with that which has been observed in other studies, several changes can be seen in the behaviours of all assessed cells when under flow conditions. These changes are particularly exemplified with experiments that make use of probiotic and pathogenic bacteria and their related conditioned media.

While many of these impacts could be interpreted as positive, particularly when considering the need for improved cell culture modelling methods – a concept discussed at length throughout this thesis – there remains a level of ambiguity when interpreting certain findings in this study. Whether it is the nature of increased glycoprotein produced by cell lines Caco-2 and HT29MTX, or the fluctuations in inflammatory markers following exposure to both flow and probiotic products, it remains an undeniable fact that this study has highlighted the potential for these methodologies, and, subsequently, the importance of incorporating biologically relevant factors into future cell culture studies.

Further investigation is required to unravel the true impact of the findings outlined in this study. However, throughout the chapters of this thesis, a solid foundation has been prepared from which future studies might springboard.

References

- Adegbola, S. O., Sahnan, K., Warusavitarne, J., Hart, A. and Tozer, P. 2018. Anti-TNF therapy in Crohn's disease. *International Journal of Molecular Sciences* 19(8), doi: 10.3390/ijms19082244
- Al-Ani, A., Toms, D., Kondro, D., Thundathil, J., Yu, Y. and Ungrin, M. 2018. Oxygenation in cell culture: Critical parameters for reproducibility are routinely not reported. *PLoS ONE* 13(10), doi: 10.1371/journal.pone.0204269
- Alayev, A. and Holz, M. K. 2013. mTOR signaling for biological control and cancer. *Journal of Cellular Physiology* 228(8), pp. 1658-1664. doi: 10.1002/jcp.24351
- Andersen, M. L. and Winter, L. M. F. 2019. Animal models in biological and biomedical research - experimental and ethical concerns. *Anais da Academia Brasileira de Ciencias* 91, p. e20170238. doi: 10.1590/0001-3765201720170238
- Arnoldini, M., Cremer, J. and Hwa, T. 2018. Bacterial growth, flow, and mixing shape human gut microbiota density and composition. *Gut microbes* 9(6), pp. 559-566. doi: 10.1080/19490976.2018.1448741
- Arora, M. 2013. Cell Culture Media: A Review. *Materials and Methods* 3(75), doi: //dx.doi.org/10.13070/mm.en.3.175
- Astashkina, A., Mann, B. and Grainger, D. W. 2012. A critical evaluation of in vitro cell culture models for high-throughput drug screening and toxicity. *Pharmacology and Therapeutics* 134(1), pp. 82-106. doi: 10.1016/j.pharmthera.2012.01.001
- ATCC. 2019. *Cell Lines*. American Type Culture Collection. Available at: http://www.lgcstandards-atcc.org/Products/Cells_and_Microorganisms/Cell_Lines.aspx [Accessed: 10th May].
- ATCC. 2020. *Caco-2 [Caco-2] (ATCC® HTB-37™)*. Available at: <https://www.lgcstandards-atcc.org/en/Products/All/HTB-37.aspx#characteristics> [Accessed: 19 December 2020].
- Australian Government. 1990. Therapeutic Goods Regulations 1990.
- Australian Government. 2013. *An overview of the regulation of complementary medicines in Australia*. Available at: [Accessed].

Australian Government. 2021a. Therapeutic Goods Act 1989.

Australian Government. 2021b. Therapeutic Goods Regulations 1990.

Bahari, L., Bein, A., Yashunsky, V. and Braslavsky, I. 2018. Directional freezing for the cryopreservation of adherent mammalian cells on a substrate. *PLoS ONE* 13(2), doi: 10.1371/journal.pone.0192265

Barré-Sinoussi, F. and Montagutelli, X. 2015. Animal models are essential to biological research: issues and perspectives. *Future Sci. OA* 1(4),

Bassotti, G., Antonelli, E., Villanacci, V., Salemme, M., Coppola, M. and Annese, V. 2014. Gastrointestinal motility disorders in inflammatory bowel diseases. *World Journal of Gastroenterology* 20(1), pp. 37-44. doi: 10.3748/wjg.v20.i1.37

Beaurivage, C., Kanapeckaitė, A., Loomans, C., Erdmann, K. S., Stallen, J. and Janssen, R. A. J. 2020. Development of a human primary gut-on-a-chip to model inflammatory processes. *Scientific Reports* 10(1), doi: 10.1038/s41598-020-78359-2

Berger, E. et al. 2018. Millifluidic culture improves human midbrain organoid vitality and differentiation. *Lab on a Chip* 18(20), pp. 3172-3183. doi: 10.1039/c8lc00206a

Bintsis, T. 2018. Lactic acid bacteria: Their applications in foods. *Journal of Bacteriology and Mycology* 6(2), pp. 89-94.

Blagoev, K. B. 2009. Cell proliferation in the presence of telomerase. *PLoS ONE* 4(2), doi: 10.1371/journal.pone.0004622

Bratburd, J. R., Keller, C., Vivas, E., Gemperline, E., Li, L., Rey, F. E. and Currie, C. R. 2018. Gut microbial and metabolic responses to salmonella enterica serovar typhimurium and candida albicans. *mBio* 9(6), doi: 10.1128/mBio.02032-18

Burge, M. N. 1988. *Fungi in biological control systems*. Manchester University Press.

Bury, S., Soundararajan, M., Bharti, R., Büna, R., Förstner, K. U. and Oelschlaeger, T. A. 2018. The probiotic Escherichia coli Strain nissle 1917 combats lambda Bacteriophages stx and lambda. *Frontiers in Microbiology* 9(MAY), doi: 10.3389/fmicb.2018.00929

Buttó, L. F. and Haller, D. 2016. Dysbiosis in intestinal inflammation: Cause or consequence. *International Journal of Medical Microbiology* 306(5), pp. 302-309. doi: 10.1016/j.ijmm.2016.02.010

Böcker, U. et al. 2003. Responsiveness of intestinal epithelial cell lines to lipopolysaccharide is correlated with Toll-like receptor 4 but not Toll-like receptor 2 or CD14 expression. *International Journal of Colorectal Disease* 18(1), pp. 25-32. doi: 10.1007/s00384-002-0415-6

Carrera, S., Senra, J., Acosta, M. I., Althubiti, M., Hammond, E. M., De Verdier, P. J. and Macip, S. 2014. The role of the HIF-1 α transcription factor in increased cell division at physiological oxygen tensions. *PLoS ONE* 9(5), doi: 10.1371/journal.pone.0097938

Cencič, A. and Langerholc, T. 2010. Functional cell models of the gut and their applications in food microbiology - A review. *International Journal of Food Microbiology* 141(SUPPL.), p. S4. doi: 10.1016/j.ijfoodmicro.2010.03.026

Chen, X. M., Elisia, I. and Kitts, D. D. 2010. Defining conditions for the co-culture of Caco-2 and HT29-MTX cells using Taguchi design. *Journal of Pharmacological and Toxicological Methods* 61(3), pp. 334-342. doi: 10.1016/j.vascn.2010.02.004

Cheung, C. and Gonzalez, F. J. 2008. Humanized mouse lines and their application for prediction of human drug metabolism and toxicological risk assessment. *Journal of Pharmacology and Experimental Therapeutics* 327(2), pp. 288-299. doi: 10.1124/jpet.108.141242

Cobo, E. R., Kisson-Singh, V., Moreau, F., Holani, R. and Chadee, K. 2017. MUC2 mucin and butyrate contribute to the synthesis of the antimicrobial peptide cathelicidin in response to entamoeba histolytica- and dextran sodium sulfate-induced colitis. *Infection and Immunity* 85(3), doi: 10.1128/IAI.00905-16

Collado, M. C., Meriluoto, J. and Salminen, S. 2007. Role of commercial probiotic strains against human pathogen adhesion to intestinal mucus. *Letters in Applied Microbiology* 45(4), pp. 454-460. doi: 10.1111/j.1472-765X.2007.02212.x

Conlon, M. A. and Bird, A. R. 2015. The impact of diet and lifestyle on gut microbiota and human health. *Nutrients* 7(1), pp. 17-44. doi: 10.3390/nu7010017

Cook, K. D., Waggoner, S. N. and Whitmire, J. K. 2014. NK cells and their ability to modulate T cells during virus infections. *Critical Reviews in Immunology* 34(5), pp. 359-388. doi: 10.1615/CritRevImmunol.2014010604

Corfield, A. P. 2018. The interaction of the gut microbiota with the mucus barrier in health and disease in human. *Microorganisms* 6(3), p. 78.

Cornick, S., Tawiah, A. and Chadee, K. 2015. Roles and regulation of the mucus barrier in the gut. *Tissue Barriers* 3(1), doi: 10.4161/21688370.2014.982426

Costa, J. and Ahluwalia, A. 2019. Advances and Current Challenges in Intestinal in vitro Model Engineering: A Digest. *Frontiers in Bioengineering and Biotechnology* 7(JUN), doi: 10.3389/fbioe.2019.00144

Cremer, J., Arnoldini, M. and Hwa, T. 2017. Effect of water flow and chemical environment on microbiota growth and composition in the human colon. *Proceedings of the National Academy of Sciences of the United States of America* 114(25), pp. 6438-6443. doi: 10.1073/pnas.1619598114

Cremer, J. et al. 2016. Effect of flow and peristaltic mixing on bacterial growth in a gut-like channel. *Proceedings of the National Academy of Sciences of the United States of America* 113(41), pp. 11414-11419. doi: 10.1073/pnas.1601306113

Dale, H. F., Rasmussen, S. H., Asiller, Ö. Ö. and Lied, G. A. 2019. Probiotics in irritable bowel syndrome: An up-to-date systematic review. *Nutrients* 11(9), doi: 10.3390/nu11092048

Davies, T., Plummer, S., Jack, A., Allen, M. and Michael, D. 2018. Lactobacillus and bifidobacterium promote antibacterial and antiviral immune response in human macrophages. *Journal of Probiotics and Health* 6, pp. 195-202.

de Simone, C. 2019. The Unregulated Probiotic Market. *Clinical Gastroenterology and Hepatology* 17(5), pp. 809-817. doi: 10.1016/j.cgh.2018.01.018

Draper, K., Ley, C. and Parsonnet, J. 2017. Probiotic guidelines and physician practice: A cross-sectional survey and overview of the literature. *Beneficial Microbes* 8(4), pp. 507-519. doi: 10.3920/BM2016.0146

Durack, J. and Lynch, S. V. 2019. The gut microbiome: Relationships with disease and opportunities for therapy. *Journal of Experimental Medicine* 216(1), pp. 20-40. doi: 10.1084/jem.20180448

Eckardt, K. U. and Kurtz, A. 2005. Regulation of erythropoietin production. *European Journal of Clinical Investigation, Supplement* 35(3), pp. 13-19. doi: 10.1111/j.1365-2362.2005.01525.x

Edwards, L. A., Bajaj-Elliott, M., Klein, N. J., Murch, S. H. and Phillips, A. D. 2011. Bacterial-epithelial contact is a key determinant of host innate immune responses to enteropathogenic and enteroaggregative *Escherichia coli*. *PLoS ONE* 6(10), doi: 10.1371/journal.pone.0027030

Elmore, S. 2007. Apoptosis: A Review of Programmed Cell Death. *Toxicologic pathology* 35(4), pp. 495-516. doi: 10.1080/01926230701320337

Evans, D. F., Pye, G., Bramley, R., Clark, A. G., Dyson, T. J. and Hardcastle, J. D. 1988. Measurement of gastrointestinal pH profiles in normal ambulant human subjects. *Gut* 29(8), pp. 1035-1041. doi: 10.1136/gut.29.8.1035

Fenwick, N., Griffin, G. and Gauthier, C. 2009. The welfare of animals used in science: How the "Three Rs" ethic guides improvements. *Canadian Veterinary Journal* 50(5), pp. 523-530.

Fernstrom, J. D. and Fernstrom, M. H. 2007. Tyrosine, phenylalanine, and catecholamine synthesis and function in the brain. *Journal of Nutrition* 137(6), pp. 1539S-1547S. doi: 10.1093/jn/137.6.1539s

Frenkel, E. S. and Ribbeck, K. 2015. Salivary mucins in host defense and disease prevention. *J Oral Microbiol* 7(1),

Fuller, R. 1991. Probiotics in human medicine. *Gut* 32(4), pp. 439-442. doi: 10.1136/gut.32.4.439

Fábrega, M. J. et al. 2017. Intestinal anti-inflammatory effects of outer membrane vesicles from *Escherichia coli* Nissle 1917 in DSS-experimental colitis in mice. *Frontiers in Microbiology* 8(JUL), doi: 10.3389/fmicb.2017.01274

Geraghty, R. J. et al. 2014. Guidelines for the use of cell lines in biomedical research. *British journal of cancer* 111(6), pp. 1021-1046. doi: 10.1038/bjc.2014.166

Gong, D., Gong, X., Wang, L., Yu, X. and Dong, Q. 2016. Involvement of Reduced Microbial Diversity in Inflammatory Bowel Disease. *Gastroenterology Research and Practice* 2016, doi: 10.1155/2016/6951091

Gouyer, V. et al. 2001. Specific secretion of gel-forming mucins and TFF peptides in HT-29 cells of mucin-secreting phenotype. *Biochimica et Biophysica Acta- Molecular Cell Research* 1539(1-2), pp. 71-84. doi: 10.1016/S0167-4889(01)00092-1

Grondin, J. A., Kwon, Y. H., Far, P. M., Haq, S. and Khan, W. I. 2020. Mucins in Intestinal Mucosal Defense and Inflammation: Learning From Clinical and Experimental Studies. *Frontiers in Immunology* 11, doi: 10.3389/fimmu.2020.02054

Grozdanov, L., Raasch, C., Schulze, J., Sonnenborn, U., Gottschalk, G., Hacker, J. and Dobrindt, U. 2004. Analysis of the genome structure of the nonpathogenic probiotic *Escherichia coli* strain Nissle 1917. *Journal of Bacteriology* 186(16), pp. 5432-5441. doi: 10.1128/JB.186.16.5432-5441.2004

Hansen, T. H. et al. 2018. The effect of drinking water pH on the human gut microbiota and glucose regulation: results of a randomized controlled cross-over intervention. *Scientific Reports* 8(1), doi: 10.1038/s41598-018-34761-5

Hazen, T. H., Daugherty, S. C., Shetty, A. C., Nataro, J. P. and Rasko, D. A. 2017. Transcriptional variation of diverse enteropathogenic *Escherichia coli* isolates under virulence-inducing conditions. *mSystems* 2(4), doi: 10.1128/mSystems.00024-17

He, X., Zhao, S. and Li, Y. 2021. Faecalibacterium prausnitzii: A Next-Generation Probiotic in Gut Disease Improvement. *Canadian Journal of Infectious Diseases and Medical Microbiology* 2021, doi: 10.1155/2021/6666114

Hendrickson, B. A., Gokhale, R. and Cho, J. H. 2002. Clinical aspects and pathophysiology of inflammatory bowel disease. *Clinical Microbiology Reviews* 15(1), pp. 79-94. doi: 10.1128/CMR.15.1.79-94.2002

Hernández, M. A. G., Canfora, E. E., Jocken, J. W. E. and Blaak, E. E. 2019. The Short-Chain Fatty Acid Acetate in Body Weight Control and Insulin Sensitivity. *Nutrients* 11(8), p. 1943. doi: 10.3390/nu11081943

Hong, H. A. et al. 2009. *Bacillus subtilis* isolated from the human gastrointestinal tract. *Research in Microbiology* 160(2), pp. 134-143. doi: 10.1016/j.resmic.2008.11.002

Hu, F. B., Manson, J. E., Stampfer, M. J., Colditz, G., Liu, S., Solomon, C. G. and Willett, W. C. 2001. Diet, lifestyle, and the risk of type 2 diabetes mellitus in women. *New England Journal of Medicine* 345(11), pp. 790-797. doi: 10.1056/NEJMoa010492

Hu, N., Yu, J. T., Tan, L., Wang, Y. L. and Sun, L. 2013. Nutrition and the risk of alzheimer's disease. *BioMed Research International* 2013, doi: 10.1155/2013/524820

Huang, Y., Li, N., Liboni, K. and Neu, J. 2003. Glutamine decreases lipopolysaccharide-induced IL-8 production in Caco-2 cells through a non-NF- κ B p50 mechanism. *Cytokine* 22(3), pp. 77-83. doi: [https://doi.org/10.1016/S1043-4666\(03\)00115-7](https://doi.org/10.1016/S1043-4666(03)00115-7)

Huh, D., Hamilton, G. A. and Ingber, D. E. 2011. From 3D cell culture to organs-on-chips. *Trends in Cell Biology* 21(12), pp. 745-754. doi: 10.1016/j.tcb.2011.09.005

Ignácio, Z. M., Réus, G. Z., Arent, C. O., Abelaira, H. M., Pitcher, M. R. and Quevedo, J. 2016. New perspectives on the involvement of mTOR in depression as well as in the action of antidepressant drugs. *British Journal of Clinical Pharmacology*, pp. 1280-1290. doi: 10.1111/bcp.12845

Ilhan, Z. E., Marcus, A. K., Kang, D. W., Rittmann, B. E. and Krajmalnik-Brown, R. 2017. pH-Mediated microbial and metabolic interactions in fecal enrichment cultures. *mSphere* 2(3), doi: 10.1128/mSphere.00047-17

Itzkowitz, S. H. and Yio, X. 2004. Inflammation and Cancer IV. Colorectal cancer in inflammatory bowel disease: the role of inflammation. *American Journal of Physiology-Gastrointestinal and Liver Physiology* 287(1), pp. G7-G17. doi: 10.1152/ajpgi.00079.2004

Jain, A., Li, X. H. and Chen, W. N. 2019. An untargeted fecal and urine metabolomics analysis of the interplay between the gut microbiome, diet and human metabolism in Indian and Chinese adults. *Scientific Reports* 9(1), doi: 10.1038/s41598-019-45640-y

Janssen, P. W. M., Lentle, R. G., Asvarujanon, P., Chambers, P., Stafford, K. J. and Hemar, Y. 2007. Characterization of flow and mixing regimes within the ileum of the brushtail possum using residence time distribution analysis with simultaneous spatio-temporal mapping. *Journal of Physiology* 582(3), pp. 1239-1248. doi: 10.1113/jphysiol.2007.134403

Jensen, C. and Teng, Y. 2020. Is It Time to Start Transitioning From 2D to 3D Cell Culture? *Frontiers in molecular biosciences* 7, pp. 33-33. doi: 10.3389/fmolb.2020.00033

Justiz Vaillant, A. A. and Qurie, A. 2019. Interleukin. *StatPearls [Internet]*. Treasure Island (FL): StatPearls Publishing.

Kallioliias, G. D. and Ivashkiv, L. B. 2016. TNF biology, pathogenic mechanisms and emerging therapeutic strategies. *Nature Reviews Rheumatology* 12(1), pp. 49-62. doi: 10.1038/nrrheum.2015.169

Kapałczyńska, M. et al. 2018. 2D and 3D cell cultures – a comparison of different types of cancer cell cultures. *Archives of Medical Science* 14(4), pp. 910-919. doi: 10.5114/aoms.2016.63743

Kaur, G. and Dufour, J. M. 2012. Cell lines: Valuable tools or useless artifacts. *Spermatogenesis* 2(1), pp. 1-5. doi: 10.4161/spmg.19885

KDE Community. 2020. Krita.

Kiela, P. R. and Ghishan, F. K. 2016. Physiology of intestinal absorption and secretion. *Best Practice and Research: Clinical Gastroenterology* 30(2), pp. 145-159. doi: 10.1016/j.bpg.2016.02.007

Kim, J. J. and Khan, W. I. 2013. Goblet cells and mucins: Role in innate defense in enteric infections. *Pathogens* 2(1), pp. 55-70. doi: 10.3390/pathogens2010055

Kleiveland, C. R. 2015. Co-cultivation of caco-2 and HT-29MTX. *The Impact of Food Bioactives on Health: In Vitro and Ex Vivo Models*. pp. 135-140.

Knight, E. and Przyborski, S. 2015. Advances in 3D cell culture technologies enabling tissue-like structures to be created in vitro. *Journal of Anatomy* 227(6), pp. 746-756. doi: 10.1111/joa.12257

Koh, C. M. and Lorsch, J. 2013. Chapter Seventeen - Preparation of Cells for Microscopy using Chamber Slides and Coverslips. *Methods in Enzymology*. Vol. 533. Academic Press, pp. 241-247.

Kulthong, K., Hooiveld, G. J. E. J., Duivenvoorde, L., Miro Estruch, I., Marin, V., van der Zande, M. and Bouwmeester, H. 2021. Transcriptome comparisons of in vitro intestinal epithelia grown under static and microfluidic gut-on-chip conditions with in vivo human epithelia. *Scientific Reports* 11(1), doi: 10.1038/s41598-021-82853-6

Kumar, J., Kumar, M., Gupta, S., Ahmed, V., Bhambi, M., Pandey, R. and Chauhan, N. S. 2016. An Improved Methodology to Overcome Key Issues in Human Fecal Metagenomic DNA Extraction. *Genomics, Proteomics and Bioinformatics* 14(6), pp. 371-378. doi: 10.1016/j.gpb.2016.06.002

Kuna, P., Reddigari, S. R., Schall, T. J., Rucinski, D., Viksman, M. Y. and Kaplan, A. P. 2002. Rantes, a monocyte and T lymphocyte chemotactic cytokine releases histamine from human basophils. *Journal of Immunology* 149(2), pp. 636-642.

Lasaro, M. et al. 2014. Escherichia coli isolate for studying colonization of the mouse intestine and its application to two-component signaling knockouts. *Journal of Bacteriology* 196(9), pp. 1723-1732. doi: 10.1128/JB.01296-13

Lea, T. 2015a. Caco-2 cell line. *The Impact of Food Bioactives on Health: In Vitro and Ex Vivo Models*. pp. 103-111.

Lea, T. 2015b. Epithelial cell models; general introduction. *The Impact of Food Bioactives on Health: In Vitro and Ex Vivo Models*. pp. 95-102.

Lee, W. Y., Hong, H. K., Ham, S. K., Kim, C. I. N. and Cho, Y. B. 2014. Comparison of colorectal cancer in differentially established liver metastasis models. *Anticancer Research* 34(7), pp. 3321-3328.

Leidal, K. G., Munson, K. L. and Denning, G. M. 2001. Small molecular weight secretory factors from *Pseudomonas aeruginosa* have opposite effects on IL-8 and RANTES expression by human airway epithelial cells. *American Journal of Respiratory Cell and Molecular Biology* 25(2), pp. 186-195. doi: 10.1165/ajrcmb.25.2.4273

Lesuffleur, T., Barbat, A., Dussaulx, E. and Zweibaum, A. 1990. Growth Adaptation to Methotrexate of HT-29 Human Colon Carcinoma Cells Is Associated with Their Ability to Differentiate into Columnar Absorptive and Mucus-secreting Cells. *Cancer Research* 50(19), pp. 6334-6343.

Li, W., Zhou, Y., Shang, C., Sang, H. and Zhu, H. 2020. Effects of Environmental pH on the Growth of Gastric Cancer Cells. *Gastroenterology Research and Practice* 2020, doi: 10.1155/2020/3245359

Li, Y., Chi, L., Stechschulte, D. J. and Dileepan, K. N. 2001. Histamine-induced production of interleukin-6 and interleukin-8 by human coronary artery endothelial cells is enhanced by endotoxin and tumor necrosis factor- α . *Microvascular Research* 61(3), pp. 253-262. doi: 10.1006/mvre.2001.2304

Liao, T. N. and Hsieh, K. H. 1992. Characterization of histamine-releasing activity: Role of cytokines and IgE heterogeneity. *Journal of Clinical Immunology* 12(4), pp. 248-258. doi: 10.1007/BF00918148

Lightfoot, Y. L. and Mohamadzadeh, M. 2013. Tailoring gut immune responses with lipoteichoic acid-deficient *Lactobacillus acidophilus*. *Frontiers in Immunology* 4(FRB), doi: 10.3389/fimmu.2013.00025

Lin, C. S. et al. 2014. Impact of the gut microbiota, prebiotics, and probiotics on human health and disease. *Biomedical Journal* 37(5), pp. 259-268. doi: 10.4103/2319-4170.138314

Lindner, M., Laporte, A., Block, S., Elomaa, L. and Weinhart, M. 2021. Physiological shear stress enhances differentiation, mucus-formation and structural 3d organization of intestinal epithelial cells in vitro. *Cells* 10(8), doi: 10.3390/cells10082062

Liu, S., Tao, R., Wang, M., Tian, J., Genin, G. M., Lu, T. J. and Xu, F. 2019. Regulation of cell behavior by hydrostatic pressure. *Applied Mechanics Reviews* 71(4), doi: 10.1115/1.4043947

- Luo, T., Fan, L., Zhu, R. and Sun, D. 2019. Microfluidic single-cell manipulation and analysis: Methods and applications. *Micromachines* 10(2), doi: 10.3390/mi10020104
- Lustri, B. C., Sperandio, V. and Moreira, C. G. 2017. Bacterial chat: Intestinal metabolites and signals in host-microbiota-pathogen interactions. *Infection and Immunity* 85(12), doi: 10.1128/IAI.00476-17
- Maeyashiki, C. et al. 2020. Activation of pH-Sensing Receptor OGR1 (GPR68) Induces ER Stress Via the IRE1 α /JNK Pathway in an Intestinal Epithelial Cell Model. *Scientific Reports* 10(1), doi: 10.1038/s41598-020-57657-9
- Maier, L. et al. 2018. Extensive impact of non-antibiotic drugs on human gut bacteria. *Nature* 555(7698), pp. 623-628. doi: 10.1038/nature25979
- Mao, Z. and Zhang, W. 2018. Role of mTOR in glucose and lipid metabolism. *International Journal of Molecular Sciences* 19(7), doi: 10.3390/ijms19072043
- Markets, M. a. 2019. *Probiotics Market worth \$69.3 billion by 2023*. Markets and Markets: Available at: <https://www.marketsandmarkets.com/PressReleases/probiotics.asp> [Accessed: 10th May].
- Martin, A. M., Sun, E. W., Rogers, G. B. and Keating, D. J. 2019. The influence of the gut microbiome on host metabolism through the regulation of gut hormone release. *Frontiers in Physiology* 10(MAR), doi: 10.3389/fphys.2019.00428
- Martín, R. et al. 2017. Functional characterization of novel *Faecalibacterium prausnitzii* strains isolated from healthy volunteers: A step forward in the use of *F. prausnitzii* as a next-generation probiotic. *Frontiers in Microbiology* 8(JUN), doi: 10.3389/fmicb.2017.01226
- Martínez-Maqueda, D., Miralles, B. and Recio, I. 2015. HT29 Cell Line. *The Impact of Food Bioactives on Health: in vitro and ex vivo models*. Cham: Springer International Publishing, pp. 113-124.
- Masters, J. R. and Stacey, G. N. 2007. Changing medium and passaging cell lines. *Nature Protocols* 2(9), pp. 2276-2284. doi: 10.1038/nprot.2007.319
- Mattar, A. F., Teitelbaum, D. H., Drongowski, R. A., Yongyi, F., Harmon, C. M. and Coran, A. G. 2002. Probiotics up-regulate MUC-2 mucin gene expression in a Caco-2 cell-culture model. *Pediatric Surgery International* 18(7), pp. 586-590. doi: 10.1007/s00383-002-0855-7

Mattei, G., Gusti, S. and Ahluwalia, A. 2014. Design Criteria for Generating Physiologically Relevant *In Vitro* Models in Bioreactors. *Processes* 2, pp. 548-569.

Matull, W. R. et al. 2008. MUC4 and MUC5AC are highly specific tumour-associated mucins in biliary tract cancer. *British Journal of Cancer* 98(10), pp. 1675-1681. doi: 10.1038/sj.bjc.6604364

Mazzei, D., Guzzardi, M. A., Giusti, S. and Ahluwalia, A. 2010. A low shear stress modular bioreactor for connected cell culture under high flow rates. *Biotechnology and Bioengineering* 106(1), pp. 127-137. doi: 10.1002/bit.22671

McDonald, J. A. K. et al. 2018. Inhibiting Growth of *Clostridioides difficile* by Restoring Valerate, Produced by the Intestinal Microbiota. *Gastroenterology* 155(5), pp. 1495-1507.e1415. doi: 10.1053/j.gastro.2018.07.014

McGinty, S., Hyndman, L., Mottram, N., McKee, S. and Webb, S. 2017. In-Silico Characterisation of the Kirkstall QV900 In-Vitro System for Advanced Cell Culture. In: P. Nithiarasu, A.M.R. ed. *5th International Conference on Computational and Mathematical Biomedical Engineering - CMBE2017*. United States.

Merck. 2020. *Specification Sheet*. Available at: <https://www.sigmaaldrich.com/catalog/DataSheetPage.do?brandKey=SIGMA&symbol=D6429> [Accessed: 19 December 2020].

Michael, D. R. et al. 2021. Daily supplementation with the Lab4P probiotic consortium induces significant weight loss in overweight adults. *Scientific Reports* 11(1), p. 5. doi: 10.1038/s41598-020-78285-3

Michael, D. R., Davies, T. S., Loxley, K. E., Allen, M. D., Good, M. A., Hughes, T. R. and Plummer, S. F. 2019. In vitro neuroprotective activities of two distinct probiotic consortia. *Beneficial Microbes* 10(4), pp. 437-447. doi: 10.3920/BM2018.0105

Michael, D. R. et al. 2017. The anti-cholesterolaemic effect of a consortium of probiotics: An acute study in C57BL/6J mice. *Scientific Reports* 7(1), doi: 10.1038/s41598-017-02889-5

Michael, D. R., Moss, J. W. E., Lama Calvente, D., Garaiova, I., Plummer, S. F. and Ramji, D. P. 2016. *Lactobacillus plantarum* CUL66 can impact cholesterol homeostasis in Caco-2 enterocytes. *Beneficial Microbes* 7(3), pp. 443-451. doi: 10.3920/BM2015.0146

Mimetas. 2020. *Technology*. Available at: <https://mimetas.com/page/technology> [Accessed: 19 December 2020].

Miranda-Azpiazu, P., Panagiotou, S., Jose, G. and Saha, S. 2018. A novel dynamic multicellular co-culture system for studying individual blood-brain barrier cell types in brain diseases and cytotoxicity testing. *Scientific Reports* 8(1), doi: 10.1038/s41598-018-26480-8

Monaco, C., Nanchahal, J., Taylor, P. and Feldmann, M. 2015. Anti-TNF therapy: Past, present and future. *International Immunology* 27(1), pp. 55-62. doi: 10.1093/intimm/dxu102

Monteros, M. J. M., Galdeano, C. M., Balcells, M. F., Weill, R., De Paula, J. A., Perdigón, G. and Cazorla, S. I. 2021. Probiotic lactobacilli as a promising strategy to ameliorate disorders associated with intestinal inflammation induced by a non-steroidal anti-inflammatory drug. *Scientific Reports* 11(1), doi: 10.1038/s41598-020-80482-z

Motevaseli, E., Dianatpour, A. and Ghafouri-Fard, S. 2017. The role of probiotics in cancer treatment: Emphasis on their in vivo and in vitro anti-metastatic effects. *International Journal of Molecular and Cellular Medicine* 6(2), pp. 1-11.

Mouriaux, F. et al. 2016. Effects of long-term serial passaging on the characteristics and properties of cell lines derived from uveal melanoma primary tumors. *Investigative Ophthalmology and Visual Science* 57(13), pp. 5288-5301. doi: 10.1167/iovs.16-19317

MyAssays Ltd. 2020. *Four Parameter Logistic Curve*. Available at: <https://www.myassays.com/four-parameter-logistic-curve.assay> [Accessed: 19 December 2020].

NC3R. *The 3 Rs*. The National Centre for the Replacement, Refinement and Reduction of Animals in Research (NC3R): Available at: <https://nc3rs.org.uk/the-3rs> [Accessed: 10th May].

NCBI. 2020. *Primer-BLAST: A tool for finding specific primers*. Available at: <https://www.ncbi.nlm.nih.gov/tools/primer-blast/index.cgi> [Accessed: 19 December 2020].

Ng, S. C., Hart, A. L., Kamm, M. A., Stagg, A. J. and Knight, S. C. 2009. Mechanisms of action of probiotics: Recent advances. *Inflammatory Bowel Diseases* 15(2), pp. 300-310. doi: 10.1002/ibd.20602

NHS. 2018. *Probiotics*. NHS. Available at: <https://www.nhs.uk/conditions/probiotics/> [Accessed: 9th May 2019].

Nithiananthan, S., Crawford, A., Knock, J. C., Lambert, D. W. and Whawell, S. A. 2017. Physiological Fluid Flow Moderates Fibroblast Responses to TGF- β 1. *Journal of Cellular Biochemistry* 118(4), pp. 878-890. doi: 10.1002/jcb.25767

Nouri, Z. et al. 2016. Dual anti-metastatic and anti-proliferative activity assessment of two probiotics on HeLa and HT-29 cell lines. *Cell Journal* 18(2), pp. 127-134.

Nugent, S. G., Kumar, D., Rampton, D. S. and Evans, D. F. 2001. Intestinal luminal pH in inflammatory bowel disease: Possible determinants and implications for therapy with aminosaliculates and other drugs. *Gut* 48(4), pp. 571-577. doi: 10.1136/gut.48.4.571

O'Hagan, C., Li, J. V., Marchesi, J. R., Plummer, S., Garaiova, I. and Good, M. A. 2017. Long-term multi-species Lactobacillus and Bifidobacterium dietary supplement enhances memory and changes regional brain metabolites in middle-aged rats. *Neurobiology of Learning and Memory* 144, pp. 36-47. doi: 10.1016/j.nlm.2017.05.015

Obinata, M. 2007. The immortalized cell lines with differentiation potentials: Their establishment and possible application. *Cancer science* 98, pp. 275-283. doi: 10.1111/j.1349-7006.2007.00399.x

Olesen, S. W. and Alm, E. J. 2016. Dysbiosis is not an answer. *Nature Microbiology* 1, pp. 1-2. doi: 10.1038/nmicrobiol.2016.228

oliGO! 2018. Available at: https://oligo.co/result/homosapiens/NM_002046.5/primers [Accessed: 6 June 2018].

O'Keeffe, A., Hyndman, L., McGinty, S., Riezk, A., Murdan, S. and Croft, S. L. 2019. Development of an in vitro media perfusion model of Leishmania major macrophage infection. *PLoS ONE* 14(7), doi: 10.1371/journal.pone.0219985

Pagliari, S., Tirella, A., Ahluwalia, A., Duim, S., Goumans, M. J., Aoyagi, T. and Forte, G. 2014. A multistep procedure to prepare pre-vascularized cardiac tissue constructs using adult stem cells, dynamic cell cultures, and porous scaffolds. *Frontiers in Physiology* 5 JUN, doi: 10.3389/fphys.2014.00210

Paone, P. and Cani, P. D. 2020. Mucus barrier, mucins and gut microbiota: The expected slimy partners? *Gut* 69(12), pp. 2232-2243. doi: 10.1136/gutjnl-2020-322260

Pastor, D. M. et al. 2010. Primary cell lines: false representation or model system? a comparison of four human colorectal tumors and their coordinately established cell lines. *International journal of clinical and experimental medicine* 3(1), pp. 69-83.

Pavlacky, J. and Polak, J. 2020. Technical Feasibility and Physiological Relevance of Hypoxic Cell Culture Models. *Frontiers in Endocrinology* 11, doi: 10.3389/fendo.2020.00057

Pearson, J. S. and Frankel, G. 2016. Immunity to Enteropathogenic Escherichia coli. *Encyclopedia of Immunobiology*. Vol. 4. pp. 43-51.

Petersen, C. and Round, J. L. 2014. Defining dysbiosis and its influence on host immunity and disease. *Cellular Microbiology* 16(7), pp. 1024-1033. doi: 10.1111/cmi.12308

Philippeos, C., Hughes, R. D., Dhawan, A. and Mitry, R. R. 2012. Introduction to cell culture. *Methods in Molecular Biology*.

Pietzke, M., Meiser, J. and Vazquez, A. 2020. Formate metabolism in health and disease. *Molecular Metabolism* 33, pp. 23-37. doi: 10.1016/j.molmet.2019.05.012

Pizzino, G. et al. 2017. Oxidative Stress: Harms and Benefits for Human Health. *Oxidative Medicine and Cellular Longevity* 2017, doi: 10.1155/2017/8416763

Pound, P., Ebrahim, S., Sandercock, P., Bracken, M. B. and Roberts, I. 2004. Where is the evidence that animal research benefits humans? *British Medical Journal* 328(7438), pp. 514-517.

Public Health England. 2018. *Culture Collections*. Available at: <https://www.phe-culturecollections.org.uk/collections/ecacc.aspx> [Accessed: 6 June 2018].

Public Health England. 2020. *ECACC General Cell Collection: HT29-MTX-E12*. Available at: https://www.phe-culturecollections.org.uk/products/celllines/generalcell/detail.jsp?refId=12040401&collection=ecacc_gc [Accessed: 19 December 2020].

Public Health England. 2021a. *ECACC General Cell Collection: CACO-2* Available at: https://www.phe-culturecollections.org.uk/products/celllines/generalcell/detail.jsp?refId=09042001&collection=ecacc_gc [Accessed: 8 May 2021].

Public Health England. 2021b. *ECACC General Cell Collection: HCT 116* Available at: https://www.phe-culturecollections.org.uk/products/celllines/generalcell/detail.jsp?refId=91091005&collection=ecacc_gc [Accessed: 8 May 2021].

Public Health England. 2021c. *ECACC General Cell Collection: HT29*. Available at: https://www.phe-culturecollections.org.uk/products/celllines/generalcell/detail.jsp?refId=91072201&collection=ecacc_gc [Accessed: 8 May 2021].

Quante, M. and Wang, T. C. 2009. Stem cells in gastroenterology and hepatology. *Nature Reviews Gastroenterology and Hepatology* 6(12), pp. 724-737. doi: 10.1038/nrgastro.2009.195

Rashidi, H., Alhaque, S., Szkolnicka, D., Flint, O. and Hay, D. C. 2016. Fluid shear stress modulation of hepatocyte-like cell function. *Archives of Toxicology* 90(7), pp. 1757-1761. doi: 10.1007/s00204-016-1689-8

Redondo, N., Gheorghe, A., Serrano, R., Nova, E. and Marcos, A. 2015. Hydragut study: influence of hydration status on the gut microbiota and their impact on the immune system. *Federation of American Societies for Experimental Biology Journal* 29, p. 593.

Riske, L., Thomas, R. K., Baker, G. B. and Dursun, S. M. 2017. Lactate in the brain: an update on its relevance to brain energy, neurons, glia and panic disorder. *Therapeutic advances in psychopharmacology* 7(2), pp. 85-89. doi: 10.1177/2045125316675579

Rogatzki, M. J., Ferguson, B. S., Goodwin, M. L. and Gladden, L. B. 2015. Lactate is always the end product of glycolysis. *Frontiers in Neuroscience* 9(FEB), doi: 10.3389/fnins.2015.00022

Ruchaud-Sparagano, M. H., Maresca, M. and Kenny, B. 2007. Enteropathogenic *Escherichia coli* (EPEC) inactivate innate immune responses prior to compromising epithelial barrier function. *Cellular Microbiology* 9(8), pp. 1909-1921. doi: 10.1111/j.1462-5822.2007.00923.x

Ryan, J. A. 2008. *Evolution of cell culture surfaces*.

Saez-Lara, M. J., Gomez-Llorente, C., Plaza-Diaz, J. and Gil, A. 2015. The role of probiotic lactic acid bacteria and bifidobacteria in the prevention and treatment of inflammatory bowel disease and other related diseases: A systematic review of randomized human clinical trials. *BioMed Research International* 2015, doi: 10.1155/2015/505878

Saji, N. et al. 2020. Relationship between dementia and gut microbiome-associated metabolites: a cross-sectional study in Japan. *Scientific Reports* 10(1), doi: 10.1038/s41598-020-65196-6

Sanchez-Muñoz, F., Dominguez-Lopez, A. and Yamamoto-Furusho, J. K. 2008. Role of cytokines in inflammatory bowel disease. *World Journal of Gastroenterology* 14(27), pp. 4280-4288. doi: 10.3748/wjg.14.4280

- Sanders, M. E. and Klaenhammer, T. R. 2001. Invited review. The scientific basis of *Lactobacillus acidophilus* NCFM functionality as a probiotic. *Journal of Dairy Science* 84(2), pp. 319-331. doi: 10.3168/jds.S0022-0302(01)74481-5
- Saxton, R. A. and Sabatini, D. M. 2017. mTOR Signaling in Growth, Metabolism, and Disease. *Cell* 168(6), pp. 960-976. doi: 10.1016/j.cell.2017.02.004
- Scholz, W. K. 2010. Cell Adhesion and Growth on Coated or Modified Glass or Plastic Surfaces. *Technical Bulletin* 13, pp. pp. 1-12.
- Shah, P. et al. 2016. A microfluidics-based in vitro model of the gastrointestinal human-microbe interface. *Nature Communications* 7, doi: 10.1038/ncomms11535
- Shaheen, S., Ahmed, M., Lorenzi, F. and Nateri, A. S. 2016. Spheroid-Formation (Colonosphere) Assay for in Vitro Assessment and Expansion of Stem Cells in Colon Cancer. *Stem Cell Reviews and Reports* 12(4), pp. 492-499. doi: 10.1007/s12015-016-9664-6
- Smith, T. D. H., Watt, H., Gunn, L., Car, J. and Boyle, R. J. 2016. Recommending oral probiotics to reduce winter antibiotic prescriptions in people with asthma: A pragmatic randomized controlled trial. *Annals of Family Medicine* 14(5), pp. 422-430. doi: 10.1370/afm.1970
- Smuda, C. and Bryce, P. J. 2011. New developments in the use of histamine and histamine receptors. *Current allergy and asthma reports* 11(2), pp. 94-100. doi: 10.1007/s11882-010-0163-6
- Sodhi, C. P. et al. 2012. Intestinal epithelial toll-like receptor 4 regulates goblet cell development and is required for necrotizing enterocolitis in mice. *Gastroenterology* 143(3), pp. 708-718.e705. doi: 10.1053/j.gastro.2012.05.053
- Stacey, G. 2006. Primary Cell Cultures and Immortal Cell Lines.
- Subramanian, S. et al. 2008. Characterization of epithelial IL-8 response to inflammatory bowel disease mucosal *E. coli* and its inhibition by mesalamine. *Inflammatory Bowel Diseases* 14(2), pp. 162-175. doi: 10.1002/ibd.20296
- Syngai, G. G., Gopi, R., Bharali, R., Dey, S., Lakshmanan, G. M. A. and Ahmed, G. 2016. Probiotics - the versatile functional food ingredients. *Journal of Food Science and Technology* 53(2), pp. 921-933. doi: 10.1007/s13197-015-2011-0

Sánchez-Clemente, R., Igeño, M. I., Población, A. G., Guijo, M. I., Merchán, F. and Blasco, R. 2018. Study of pH changes in media during bacterial growth of several environmental strains. *Proceedings* 2(20), p. 1297.

Tawiah, A., Cornick, S., Moreau, F., Gorman, H., Kumar, M., Tiwari, S. and Chadee, K. 2018. High MUC2 Mucin Expression and Misfolding Induce Cellular Stress, Reactive Oxygen Production, and Apoptosis in Goblet Cells. *American Journal of Pathology* 188(6), pp. 1354-1373. doi: 10.1016/j.ajpath.2018.02.007

Thornton, D. J. and Sheehan, J. K. 2004. From mucins to mucus: toward a more coherent understanding of this essential barrier. *Proceedings of the American Thoracic Society* 1(1), pp. 54-61. doi: 10.1513/pats.2306016

Titorenko, V. I. and Terlecky, S. R. 2011. Peroxisome Metabolism and Cellular Aging. *Traffic* 12(3), pp. 252-259. doi: 10.1111/j.1600-0854.2010.01144.x

Tworkoski, E., Glucksberg, M. R. and Johnson, M. 2018. The effect of the rate of hydrostatic pressure depressurization on cells in culture. *PLoS ONE* 13(1), doi: 10.1371/journal.pone.0189890

Ubeda, C., Djukovic, A. and Isaac, S. 2017. Roles of the intestinal microbiota in pathogen protection. *Clin Transl Immunol* 6(2),

Ursell, L. K., Metcalf, J. L., Parfrey, L. W. and Knight, R. 2012. Defining the human microbiome. *Nutrition Reviews* 70(SUPPL. 1), pp. S38-S44. doi: 10.1111/j.1753-4887.2012.00493.x

Valdes, A. M., Walter, J., Segal, E. and Spector, T. D. 2018. Role of the gut microbiota in nutrition and health. *BMJ* 361, p. k2179. doi: 10.1136/bmj.k2179

Vandamme, T. 2014. Use of rodents as models of human diseases. *Journal of Pharmacy and Bioallied Sciences* 6(1), pp. 2-9. doi: 10.4103/0975-7406.124301

Vanderpool, C., Yan, F. and Polk, D. B. 2008. Mechanisms of probiotic action: Implications for therapeutic applications in inflammatory bowel diseases. *Inflammatory Bowel Diseases* 14(11), pp. 1585-1596. doi: 10.1002/ibd.20525

Vangipurapu, J., Silva, L. F., Kuulasmaa, T., Smith, U. and Laakso, M. 2020. Microbiota-related metabolites and the risk of type 2 diabetes. *Diabetes Care* 43(6), pp. 1319-1325. doi: 10.2337/dc19-2533

Varankovich, N. V., Nickerson, M. T. and Korber, D. R. 2015. Probiotic-based strategies for therapeutic and prophylactic use against multiple gastrointestinal diseases. *Frontiers in Microbiology* 6(JUN), doi: 10.3389/fmicb.2015.00685

Verna, E. C. and Lucak, S. 2010. Use of probiotics in gastrointestinal disorders: what to recommend? *Therapeutic advances in gastroenterology* 3(5), pp. 307-319. doi: 10.1177/1756283X10373814

Wells, J. M. 2011. Immunomodulatory mechanisms of lactobacilli. *Microbial Cell Factories* 10(SUPPL. 1), doi: 10.1186/1475-2859-10-S1-S17

WHOCC. 2018. *Structure and Principles*. Available at: https://www.whooc.no/atc/structure_and_principles/ [Accessed: 18 December 2020].

Williams, E. A., Stimpson, J., Wang, D., Plummer, S., Garaiova, I., Barker, M. E. and Corfe, B. M. 2009. Clinical trial: A multistrain probiotic preparation significantly reduces symptoms of irritable bowel syndrome in a double-blind placebo-controlled study. *Alimentary Pharmacology and Therapeutics* 29(1), pp. 97-103. doi: 10.1111/j.1365-2036.2008.03848.x

Wong, A. R. C., Raymond, B., Collins, J. W., Crepin, V. F. and Frankel, G. 2012. The enteropathogenic *E. coli* effector EspH promotes actin pedestal formation and elongation via WASP-interacting protein (WIP). *Cellular Microbiology* 14(7), pp. 1051-1070. doi: 10.1111/j.1462-5822.2012.01778.x

Wu, Q. et al. 2020. Organ-on-a-chip: Recent breakthroughs and future prospects. *BioMedical Engineering Online* 19(1), doi: 10.1186/s12938-020-0752-0

Yan, F. and Polk, D. B. 2011. Probiotics and immune health. *Current Opinion in Gastroenterology* 27(6), pp. 496-501. doi: 10.1097/MOG.0b013e32834baa4d

Yen, H., Ooka, T., Iguchi, A., Hayashi, T., Sugimoto, N. and Tobe, T. 2010. NleC, a Type III Secretion Protease, Compromises NF- κ B Activation by Targeting p65/RelA. *PLOS Pathogens* 6(12), p. e1001231.

Yeung, T. M., Gandhi, S. C., Wilding, J. L., Muschel, R. and Bodmer, W. F. 2010. Cancer stem cells from colorectal cancer-derived cell lines. *Proceedings of the National Academy of Sciences of the United States of America* 107(8), pp. 3722-3727. doi: 10.1073/pnas.0915135107

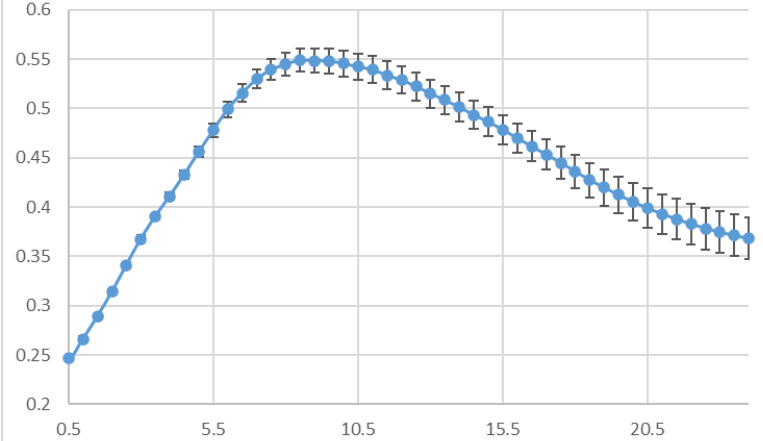
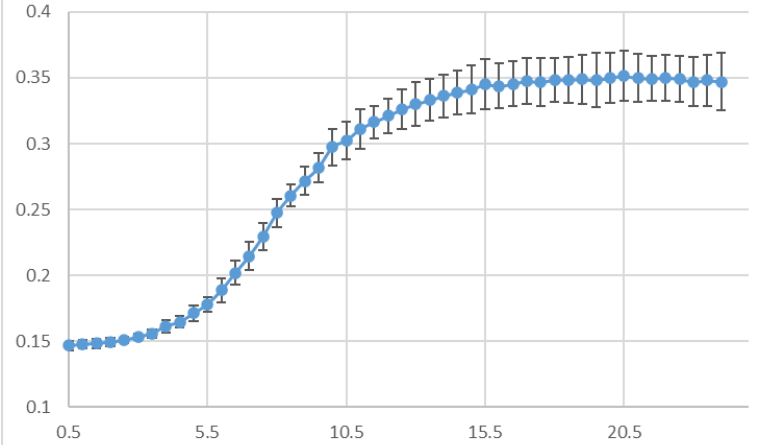
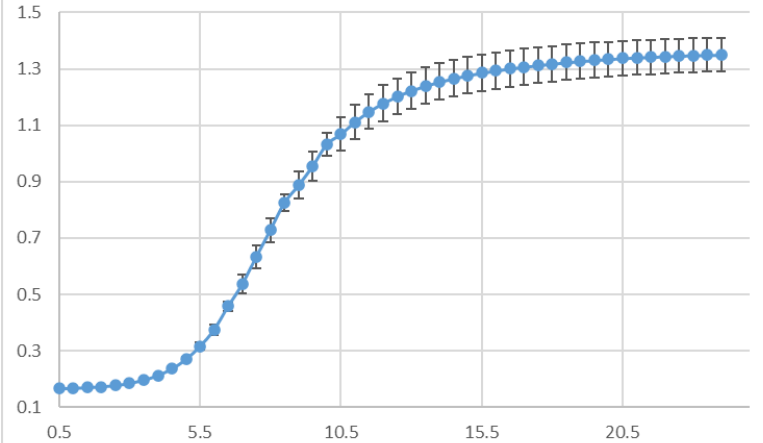
Zeitouni, N. E., Chotikatum, S., von Köckritz-Blickwede, M. and Naim, H. Y. 2016. The impact of hypoxia on intestinal epithelial cell functions: consequences for invasion by bacterial pathogens. *Molecular and Cellular Pediatrics* 3, p. 14. doi: 10.1186/s40348-016-0041-y

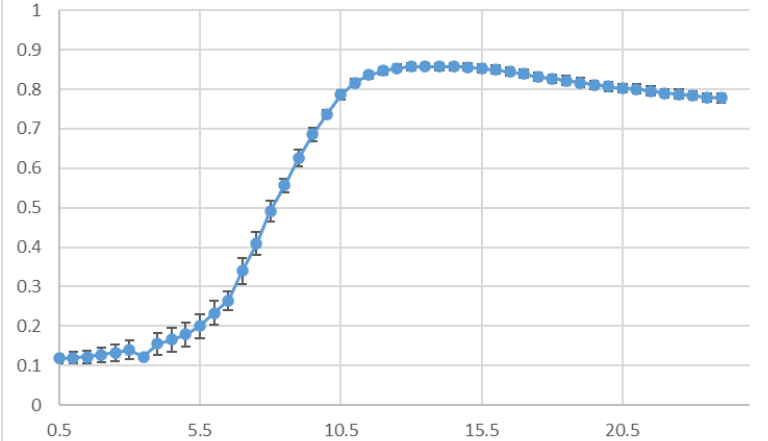
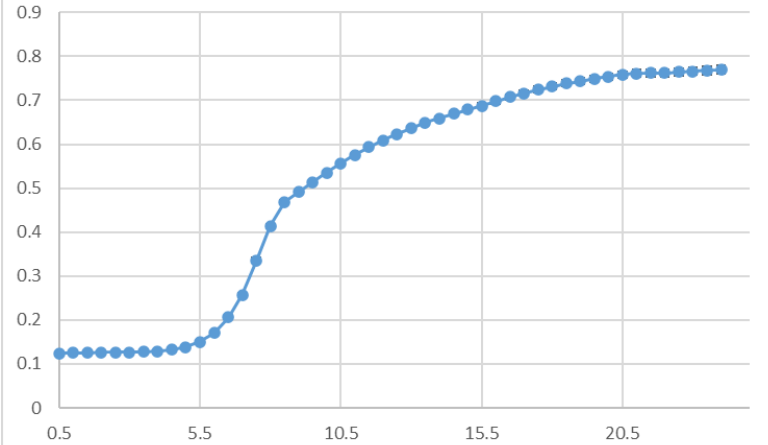
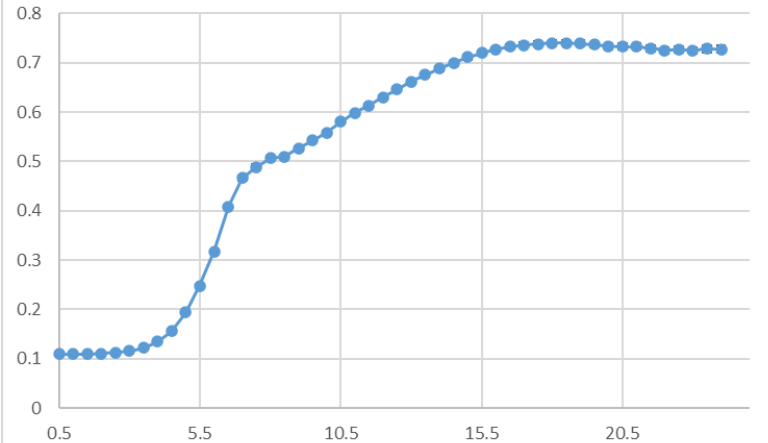
Zheng, J. et al. 2020. A taxonomic note on the genus *Lactobacillus*: Description of 23 novel genera, emended description of the genus *Lactobacillus* Beijerinck 1901, and union of *Lactobacillaceae* and *Leuconostocaceae*. *International Journal of Systematic and Evolutionary Microbiology* 70(4), pp. 2782-2858. doi: 10.1099/ijsem.0.004107

Appendices

Appendix 1: Growth curves for Lab4 and Lab4B probiotics and their constituent bacterial communities and *E. coli* strains E69, MP1 and Nissle 1917.

Species/ consortia	Growth curve	Exponential phase duration (hours)
<i>L. acidophilus</i> (dual-strain mix)	<p>Detailed description: This line graph plots optical density on the y-axis (ranging from 0.3 to 0.55) against time in hours on the x-axis (ranging from 0.5 to 24). The data points, marked with blue squares and error bars, show a rapid increase from 0.33 at 0.5 hours to a peak of approximately 0.52 at 5.5 hours. Following the peak, the optical density gradually decreases to about 0.49 by 10.5 hours and remains relatively stable with minor fluctuations until 24 hours.</p>	0.5 – 5
<i>L. paracasei</i>	<p>Detailed description: This line graph plots optical density on the y-axis (ranging from 0 to 1.6) against time in hours on the x-axis (ranging from 0.5 to 24). The data points, marked with blue circles and error bars, show a steady, nearly linear increase from 0.28 at 0.5 hours to a plateau of approximately 1.4 starting at 15.5 hours, which continues until 24 hours.</p>	1.5 – 8
<i>L. salivarius</i>	<p>Detailed description: This line graph plots optical density on the y-axis (ranging from 0 to 1.6) against time in hours on the x-axis (ranging from 0.5 to 24). The data points, marked with blue squares and error bars, show a steady, nearly linear increase from 0.28 at 0.5 hours to a plateau of approximately 1.4 starting at 15.5 hours, which continues until 24 hours.</p>	1.5 – 8

<p><i>B. animalis</i> sub sp. <i>lactis</i> and <i>B. bifidum</i> (dual-species mix)</p>		<p>0.5 – 8</p>
<p>Lab4 consortia (Bioacidophilus powder)</p>		<p>5.5 – 10</p>
<p>Lab4B consortia (Proven Baby Breastfed)</p>		<p>5.5 – 10</p>

<p><i>E. coli</i> strain E96</p>	 <p>The graph shows the growth of <i>E. coli</i> strain E96. The y-axis represents a normalized value from 0 to 1.0, and the x-axis represents time from 0.5 to 24 hours. The curve starts at approximately 0.12 at 0.5 hours, remains relatively flat until 4 hours, then rises sharply between 5 and 10 hours, reaching a plateau of about 0.85 by 12 hours, and slightly declines thereafter.</p>	<p>5.5 – 10.5</p>
<p><i>E. coli</i> strain MP1</p>	 <p>The graph shows the growth of <i>E. coli</i> strain MP1. The y-axis represents a normalized value from 0 to 0.9, and the x-axis represents time from 0.5 to 24 hours. The curve starts at approximately 0.12 at 0.5 hours, remains flat until 4 hours, then rises between 5 and 10 hours, reaching a plateau of about 0.75 by 15 hours, and remains stable until 24 hours.</p>	<p>5.5 – 8.5</p>
<p><i>E. coli</i> strain Nissle 1917</p>	 <p>The graph shows the growth of <i>E. coli</i> strain Nissle 1917. The y-axis represents a normalized value from 0 to 0.8, and the x-axis represents time from 0.5 to 24 hours. The curve starts at approximately 0.12 at 0.5 hours, remains flat until 4 hours, then rises between 5 and 10 hours, reaching a plateau of about 0.72 by 15 hours, and remains stable until 24 hours.</p>	<p>4.5 – 8</p>

Appendix 2: Breakdown of changes in metabolite presence in conditioned media and the unconditioned medium control.

Metabolite	Conditioned medium						
	<i>B. bifidum</i>	<i>B. animalis</i> sub <i>sp. lactis</i>	<i>Bifidobacterium</i> (dual-species mix)	<i>L. acidophilus</i> (dual-strain mix)	<i>L. paracasei</i>	<i>L. salivarius</i>	<i>E. coli</i> E69
Acetate	CM	CM	CM	CM	CM	CM	CM
Alanine	0	0	0	0	0	CM	0
Aspartate	CM	0	0	0	0	CM	0
Choline	UC-low	UC-low	UC-low	UC-low	UC-low	UC-low	UC-low
Formate	CM	CM	CM	0	0	CM	CM
Fumarate	0	0	0	CM-low	0	0	0
Glutamate	CM	CM	0	0	CM	CM	0
Glycine	UC > CM	UC	UC > CM	UC > CM	UC > CM	UC > CM	UC > CM
Histidine	UC	UC > CM	UC > CM	UC	UC	UC	UC > CM
Isoleucine	UC	UC	UC > CM	UC > CM	UC > CM	UC	UC > CM
Lactate	CM	CM	0	CM	CM	CM	CM
Lysine	CM	CM	CM	0	0	CM	0
Methionine	UC	UC > CM	UC	UC > CM	UC > CM	UC > CM	UC > CM
Nicotinamide	0	CM-low	0	0	0	0	0
Phenylalanine	UC > CM	UC > CM	UC > CM	UC > CM	UC > CM	UC > CM	UC > CM
Succinate	CM	CM-low	0	CM	0	0	CM
Tyrosine	UC > CM	UC > CM	UC > CM	UC > CM	UC > CM	UC > CM	UC > CM
Valine	UC > CM	UC > CM	UC > CM	UC > CM	UC > CM	UC > CM	UC > CM
Xanthine	0	0	CM	CM	CM	0	0
acetoin	0	CM	0	0	0	0	0
Ethanol	CM	CM	0	0	0	CM	0
Threonine	UC	UC	UC > CM	UC	UC	UC	UC
Glucose	UC	UC > CM	UC > CM	UC	UC	UC	UC > CM
Pyruvate	UC	UC > CM	UC > CM	UC	UC	UC	UC
Niacinamide	UC	UC	UC	UC	UC	UC	UC
2-Hydroxybutyrate	0	0	0	0	0	0	CM
3-Phenyllactate	0	CM	0	0	0	0	0

CM = present in the conditioned medium only; UC = present in the un-inoculated control; UC > CM = present in both the blank and conditioned media, but in lower quantities in the conditioned medium, CM-low = present in the conditioned medium only, but at very low levels (≤ 0.02 mM); UC-low = present in the un-inoculated control only, but at very low levels (≤ 0.02 mM); 0 = not present in the specified conditioned medium.

Appendix 3: Metabolic profile of the *L. acidophilus* dual-strain mix assessed in this study, including those metabolic pathways influenced by each metabolite.

Metabolite	Pathway Influenced
Acetate	Biosynthesis of secondary metabolites; C5-Branched dibasic acid metabolism; Carbohydrate digestion and absorption; Carbon fixation pathways in prokaryotes; Carbon metabolism; Cholinergic synapse; Degradation of aromatic compounds; Glycolysis / Gluconeogenesis; Glycosaminoglycan biosynthesis - heparan sulfate / heparin; Glyoxylate and dicarboxylate metabolism; Metabolic pathways; Methane metabolism; Microbial metabolism in diverse environments; Phosphonate and phosphinate metabolism; Propanoate metabolism; Protein digestion and absorption; Pyruvate metabolism; Sulfur metabolism; Taurine and hypotaurine metabolism; Zeatin biosynthesis
Alanine	ABC transporters; Alanine, aspartate and glutamate metabolism; Aminoacyl-tRNA biosynthesis; Biosynthesis of amino acids; Biosynthesis of plant secondary metabolites; Biosynthesis of secondary metabolites; Biosynthesis of various secondary metabolites - part 2; Carbon fixation in photosynthetic organisms; Carbon metabolism; Central carbon metabolism in cancer; Cysteine and methionine metabolism; D-Alanine metabolism; Metabolic pathways; Microbial metabolism in diverse environments; Mineral absorption; Protein digestion and absorption; Selenocompound metabolism; Sulfur relay system; Taurine and hypotaurine metabolism; Vancomycin resistance
Choline	ABC transporters; Bile secretion; Choline metabolism in cancer; Cholinergic synapse; Glycerophospholipid metabolism; Glycine, serine and threonine metabolism; Metabolic pathways
Fumerate	Alanine, aspartate and glutamate metabolism; Arginine biosynthesis; Biosynthesis of alkaloids derived from histidine and purine; Biosynthesis of alkaloids derived from ornithine, lysine and nicotinic acid; Biosynthesis of alkaloids derived from shikimate pathway; Biosynthesis of alkaloids derived from terpenoid and polyketide; Biosynthesis of phenylpropanoids; Biosynthesis of plant hormones; Biosynthesis of plant secondary metabolites; Biosynthesis of secondary metabolites; Biosynthesis of terpenoids and steroids; Butanoate metabolism; Carbon fixation pathways in prokaryotes; Carbon metabolism; Central carbon metabolism in cancer; Citrate cycle (TCA cycle); Degradation of aromatic compounds; Glucagon signaling pathway; Metabolic pathways; Microbial metabolism in diverse environments; Nicotinate and nicotinamide metabolism; Oxidative phosphorylation; Pathways in cancer; Phenylalanine metabolism; Pyruvate metabolism; Renal cell carcinoma; Styrene degradation; Two-component system; Tyrosine metabolism
Glycine	ABC transporters; Aminoacyl-tRNA biosynthesis; Biofilm formation - Escherichia coli; Biosynthesis of amino acids; Biosynthesis of plant secondary metabolites; Biosynthesis of secondary metabolites; Biosynthesis of various secondary metabolites - part 3; Carbon metabolism; Central carbon metabolism in cancer; Cyanoamino acid metabolism; Glutathione metabolism; Glycine, serine and threonine metabolism; Glyoxylate and dicarboxylate metabolism; Lysine degradation; Metabolic pathways; Methane metabolism; Microbial metabolism in diverse environments; Mineral absorption; Neuroactive ligand-receptor interaction; Phosphonate and phosphinate metabolism; Porphyrin and chlorophyll metabolism; Primary bile acid biosynthesis; Protein digestion and absorption; Purine metabolism; Synaptic vesicle cycle; Thiamine metabolism; Vancomycin resistance;

Histidine	ABC transporters; Aminoacyl-tRNA biosynthesis; beta-Alanine metabolism; Biosynthesis of alkaloids derived from histidine and purine; Biosynthesis of amino acids; Biosynthesis of plant secondary metabolites; Biosynthesis of secondary metabolites; Central carbon metabolism in cancer; Histidine metabolism; Metabolic pathways; Protein digestion and absorption; Staurosporine biosynthesis
Isoleucine	2-Oxocarboxylic acid metabolism; ABC transporters; Aminoacyl-tRNA biosynthesis; Biosynthesis of alkaloids derived from ornithine, lysine and nicotinic acid; Biosynthesis of amino acids; Biosynthesis of plant secondary metabolites; Biosynthesis of secondary metabolites; Central carbon metabolism in cancer; Cyanoamino acid metabolism; Glucosinolate biosynthesis; Metabolic pathways; Mineral absorption; Protein digestion and absorption; Shigellosis; Tropane, piperidine and pyridine alkaloid biosynthesis; Valine, leucine and isoleucine biosynthesis; Valine, leucine and isoleucine degradation
Lactate	Biosynthesis of secondary metabolites; cAMP signaling pathway; Central carbon metabolism in cancer; Fructose and mannose metabolism; Glucagon signaling pathway; Glycolysis / Gluconeogenesis; HIF-1 signaling pathway; Metabolic pathways; Microbial metabolism in diverse environments; Propanoate metabolism; Pyruvate metabolism; Styrene degradation;
Methionine	2-Oxocarboxylic acid metabolism; Aminoacyl-tRNA biosynthesis; Antifolate resistance; Biosynthesis of amino acids; Biosynthesis of plant hormones; Biosynthesis of plant secondary metabolites; Biosynthesis of secondary metabolites; Central carbon metabolism in cancer; Cysteine and methionine metabolism; Glucosinolate biosynthesis; Metabolic pathways; Mineral absorption; Protein digestion and absorption
Phenylalanine	2-Oxocarboxylic acid metabolism; ABC transporters; Aminoacyl-tRNA biosynthesis; Biosynthesis of alkaloids derived from ornithine, lysine and nicotinic acid; Biosynthesis of alkaloids derived from shikimate pathway; Biosynthesis of amino acids; Biosynthesis of phenylpropanoids; Biosynthesis of plant hormones; Biosynthesis of plant secondary metabolites; Biosynthesis of secondary metabolites; Biosynthesis of various secondary metabolites - part 2; Central carbon metabolism in cancer; Cyanoamino acid metabolism; Glucosinolate biosynthesis; Metabolic pathways; Mineral absorption; Phenylalanine metabolism; Phenylalanine, tyrosine and tryptophan biosynthesis; Phenylpropanoid biosynthesis; Protein digestion and absorption; Tropane, piperidine and pyridine alkaloid biosynthesis
Succinate	Alanine, aspartate and glutamate metabolism; Biosynthesis of alkaloids derived from histidine and purine; Biosynthesis of alkaloids derived from ornithine, lysine and nicotinic acid; Biosynthesis of alkaloids derived from shikimate pathway; Biosynthesis of alkaloids derived from terpenoid and polyketide; Biosynthesis of phenylpropanoids; Biosynthesis of plant hormones; Biosynthesis of plant secondary metabolites; Biosynthesis of secondary metabolites; Biosynthesis of terpenoids and steroids; Butanoate metabolism; cAMP signaling pathway; Carbon fixation pathways in prokaryotes; Carbon metabolism; Central carbon metabolism in cancer; Chlorocyclohexane and chlorobenzene degradation; Citrate cycle (TCA cycle); Degradation of aromatic compounds; GABAergic synapse; Glucagon signaling pathway; Glyoxylate and dicarboxylate metabolism; Lysine degradation; Metabolic pathways; Microbial metabolism in diverse environments; Nicotinate and nicotinamide metabolism; Oxidative phosphorylation; Phenylalanine metabolism; Propanoate metabolism; Pyruvate metabolism; Sulfur metabolism; Two-component system; Tyrosine metabolism

Tyrosine	2-Oxocarboxylic acid metabolism; Alcoholism; Aminoacyl-tRNA biosynthesis; Amphetamine addiction; Betalain biosynthesis; Biosynthesis of alkaloids derived from shikimate pathway; Biosynthesis of amino acids; Biosynthesis of enediyne antibiotics; Biosynthesis of plant secondary metabolites; Biosynthesis of secondary metabolites; Biosynthesis of vancomycin group antibiotics; Biosynthesis of various secondary metabolites - part 2; Central carbon metabolism in cancer; Cocaine addiction; Cyanoamino acid metabolism; Dopaminergic synapse; Glucosinolate biosynthesis; Isoquinoline alkaloid biosynthesis; Melanogenesis; Metabolic pathways; Methane metabolism; Monobactam biosynthesis; Novobiocin biosynthesis; Parkinson disease; Phenylalanine metabolism; Phenylalanine, tyrosine and tryptophan biosynthesis; Phenylpropanoid biosynthesis; Prolactin signaling pathway; Protein digestion and absorption; Thiamine metabolism; Tyrosine metabolism; Ubiquinone and other terpenoid-quinone biosynthesis
Uracil	beta-Alanine metabolism; Metabolic pathways; Pantothenate and CoA biosynthesis; Pyrimidine metabolism
Valine	2-Oxocarboxylic acid metabolism; ABC transporters; Aminoacyl-tRNA biosynthesis; Biosynthesis of alkaloids derived from shikimate pathway; Biosynthesis of amino acids; Biosynthesis of plant secondary metabolites; Biosynthesis of secondary metabolites; Central carbon metabolism in cancer; Cyanoamino acid metabolism; Glucosinolate biosynthesis; Metabolic pathways; Mineral absorption; Pantothenate and CoA biosynthesis; Penicillin and cephalosporin biosynthesis; Protein digestion and absorption; Valine, leucine and isoleucine biosynthesis; Valine, leucine and isoleucine degradation
Xanthine	Biosynthesis of alkaloids derived from histidine and purine; Biosynthesis of plant secondary metabolites; Biosynthesis of secondary metabolites; Caffeine metabolism; Metabolic pathways; Microbial metabolism in diverse environments; Purine metabolism
Threonine	ABC transporters; Aminoacyl-tRNA biosynthesis; Biosynthesis of amino acids; Biosynthesis of plant secondary metabolites; Biosynthesis of secondary metabolites; Biosynthesis of various secondary metabolites - part 3; Glycine, serine and threonine metabolism; Metabolic pathways; Microbial metabolism in diverse environments; Mineral absorption; Monobactam biosynthesis; Porphyrin and chlorophyll metabolism; Protein digestion and absorption; Valine, leucine and isoleucine biosynthesis
Pyruvate	2-Oxocarboxylic acid metabolism; Alanine, aspartate and glutamate metabolism; AMPK signaling pathway; Arginine and proline metabolism; Ascorbate and aldarate metabolism; Benzoate degradation; Biosynthesis of alkaloids derived from histidine and purine; Biosynthesis of alkaloids derived from ornithine, lysine and nicotinic acid; Biosynthesis of alkaloids derived from shikimate pathway; Biosynthesis of alkaloids derived from terpenoid and polyketide; Biosynthesis of amino acids; Biosynthesis of phenylpropanoids; Biosynthesis of plant hormones; Biosynthesis of plant secondary metabolites; Biosynthesis of secondary metabolites; Biosynthesis of terpenoids and steroids; Biosynthesis of various secondary metabolites - part 1; Biosynthesis of various secondary metabolites - part 3; Butanoate metabolism; C5-Branched dibasic acid metabolism; Carbon fixation in photosynthetic organisms; Carbon fixation pathways in prokaryotes; Carbon metabolism; Central carbon metabolism in cancer; Citrate cycle (TCA cycle); Cysteine and methionine metabolism; D-Alanine metabolism; Degradation of aromatic compounds; Dioxin degradation; Glucagon signaling pathway; Glycine, serine and threonine metabolism; Glycolysis /

	Gluconeogenesis; Glyoxylate and dicarboxylate metabolism; HIF-1 signaling pathway; Insulin resistance; Insulin secretion; Metabolic pathways; Methane metabolism; Microbial metabolism in diverse environments; Monobactam biosynthesis; Nicotinate and nicotinamide metabolism; Pantothenate and CoA biosynthesis; Pentose and glucuronate interconversions; Pentose phosphate pathway; Phenylalanine metabolism; Phosphonate and phosphinate metabolism; Phosphotransferase system (PTS); Pyruvate metabolism; Taurine and hypotaurine metabolism; Terpenoid backbone biosynthesis; Thiamine metabolism; Type II diabetes mellitus; Tyrosine metabolism; Valine, leucine and isoleucine biosynthesis; Vancomycin resistance; Xylene degradation
Niacinamide	Longevity regulating pathway – worm; Metabolic pathways; Nicotinate and nicotinamide metabolism; Vitamin digestion and absorption

Appendix 4: Metabolic profile of the species *L. paracasei* assessed in this study, including those metabolic pathways influenced by each metabolite. * For full breakdown of the metabolic pathways influenced by this metabolite, see Appendix 4.

Metabolite	Pathway influenced
Acetate	*
Alanine	*
Choline	*
Glutamate	2-Oxocarboxylic acid metabolism; ABC transporters; Alanine, aspartate and glutamate metabolism; Alcoholism; Aminoacyl-tRNA biosynthesis; Amphetamine addiction; Amyotrophic lateral sclerosis (ALS); Arginine and proline metabolism; Arginine biosynthesis; Biosynthesis of alkaloids derived from ornithine, lysine and nicotinic acid; Biosynthesis of amino acids; Biosynthesis of plant secondary metabolites; Biosynthesis of secondary metabolites; Biosynthesis of various secondary metabolites - part 3; Butanoate metabolism; C5-Branched dibasic acid metabolism; Carbapenem biosynthesis; Carbon metabolism; Central carbon metabolism in cancer; Circadian entrainment; Cocaine addiction; D-Glutamine and D-glutamate metabolism; Ferroptosis; FoxO signaling pathway; GABAergic synapse; Gap junction; Glutamatergic synapse; Glutathione metabolism; Glyoxylate and dicarboxylate metabolism; Histidine metabolism; Huntington disease; Long-term depression; Long-term potentiation; Metabolic pathways; Microbial metabolism in diverse environments; Neomycin, kanamycin and gentamicin biosynthesis; Neuroactive ligand-receptor interaction; Nicotine addiction; Nitrogen metabolism; Phospholipase D signaling pathway; Porphyrin and chlorophyll metabolism; Protein digestion and absorption; Proximal tubule bicarbonate reclamation; Retrograde endocannabinoid signaling; Spinocerebellar ataxia; Synaptic vesicle cycle; Taste transduction; Taurine and hypotaurine metabolism; Two-component system
Glycine	*
Histidine	*
Isoleucine	*
Lactate	*
Leucine	2-Oxocarboxylic acid metabolism; ABC transporters; Aminoacyl-tRNA biosynthesis; Biosynthesis of alkaloids derived from histidine and purine; Biosynthesis of amino acids; Biosynthesis of plant secondary metabolites; Biosynthesis of secondary metabolites; Central carbon metabolism in cancer; Glucosinolate biosynthesis; Metabolic pathways; Mineral absorption; mTOR signaling pathway; Protein digestion and absorption; Shigellosis; Valine, leucine and isoleucine biosynthesis; Valine, leucine and isoleucine degradation
Methionine	*
Phenylalanine	*
Tyrosine	*
Valine	*
Xanthine	*
Ethanol	Alcoholism; Biosynthesis of secondary metabolites; Glycolysis / Gluconeogenesis; Inflammatory mediator regulation of TRP channels; Metabolic pathways; Microbial metabolism in diverse environments
Imidazole ¹	
Threonine	*
Pyruvate	*
Niacinamide	*

Appendix 5: Metabolic profile of the species *L. salivarius* assessed in this study, including those metabolic pathways influenced by each metabolite. * For full breakdown of the metabolic pathways influenced by this metabolite, see Appendix 4. ** For full breakdown of the metabolic pathways influenced by this metabolite, see Appendix 5.

Metabolite	Pathway influenced
Acetate	*
Alanine	*
Aspartate	2-Oxocarboxylic acid metabolism; ABC transporters; Alanine, aspartate and glutamate metabolism; Aminoacyl-tRNA biosynthesis; Arginine biosynthesis; Bacterial chemotaxis; beta-Alanine metabolism; Biosynthesis of alkaloids derived from ornithine, lysine and nicotinic acid; Biosynthesis of amino acids; Biosynthesis of plant hormones; Biosynthesis of plant secondary metabolites; Biosynthesis of secondary metabolites; Biosynthesis of various secondary metabolites - part 3; Carbon fixation in photosynthetic organisms; Carbon metabolism; Central carbon metabolism in cancer; Cyanoamino acid metabolism; Cysteine and methionine metabolism; Glycine, serine and threonine metabolism; Histidine metabolism; Lysine biosynthesis; Metabolic pathways; Microbial metabolism in diverse environments; Monobactam biosynthesis; Neuroactive ligand-receptor interaction; Nicotinate and nicotinamide metabolism; Pantothenate and CoA biosynthesis; Protein digestion and absorption; Two-component system
Choline	*
Formate	Carbon fixation pathways in prokaryotes; Carbon metabolism; Chloroalkane and chloroalkene degradation; Degradation of aromatic compounds; Glyoxylate and dicarboxylate metabolism; Metabolic pathways; Methane metabolism; Microbial metabolism in diverse environments; Nitrogen metabolism; Phosphonate and phosphinate metabolism; Pyruvate metabolism
Glutamate	**
Glycine	*
Histidine	*
Isoleucine	*
Lactate	*
Lysine	2-Oxocarboxylic acid metabolism; ABC transporters; Aminoacyl-tRNA biosynthesis; Biosynthesis of alkaloids derived from ornithine, lysine and nicotinic acid; Biosynthesis of amino acids; Biosynthesis of plant secondary metabolites; Biosynthesis of secondary metabolites; Biosynthesis of various secondary metabolites - part 3; Biotin metabolism; Lysine biosynthesis; Lysine degradation; Metabolic pathways; Microbial metabolism in diverse environments; Protein digestion and absorption; Tropane, piperidine and pyridine alkaloid biosynthesis
Methionine	*
Phenylalanine	*
Tyrosine	*
Valine	*
Ethanol	**
Threonine	*
Pyruvate	*
Niacinamide	*+

Appendix 6: Metabolic profile of the species *B. bifidum* assessed in this study, including those metabolic pathways influenced by each metabolite. * For full breakdown of the metabolic pathways influenced by this metabolite, see Appendix 4. ** For full breakdown of the metabolic pathways influenced by this metabolite, see Appendix 5. *** For full breakdown of the metabolic pathways influenced by this metabolite, see Appendix 6

Metabolite	Pathway Influenced
Acetate	*
Alanine	*
Aspartate	***
Choline	*
Formate	***
Glutamate	**
Glycine	*
Histidine	*
Isoleucine	*
Lactate	*
Lysine	***
Methionine	*
Phenylalanine	*
Succinate	*
Tyrosine	*
Valine	*
Ethanol	**
Threonine	*
Pyruvate	*
Niacinamide	*

Appendix 7: Metabolic profile of the species *B. animalis sub sp. lactis* assessed in this study, including those metabolic pathways influenced by each metabolite. * For full breakdown of the metabolic pathways influenced by this metabolite, see Appendix 4. ** For full breakdown of the metabolic pathways influenced by this metabolite, see Appendix 5. *** For full breakdown of the metabolic pathways influenced by this metabolite, see Appendix 6.

Metabolite	Pathway influenced
Acetate	*
Alanine	*
Choline	*
Formate	***
Glutamate	**
Glycine	*
Histidine	*
Isoleucine	*
Lactate	*
Lysine	***
Methionine	*
Nicotinamide	Nicotinate and nicotinamide metabolism; Metabolic pathways; Longevity regulating pathway – worm; Vitamin digestion and absorption
Phenylalanine	*
Succinate	*
Tyrosine	*
Uracil	*
Valine	*
Acetoin	Butanoate metabolism; C5-Branched dibasic acid metabolism
Ethanol	**
Threonine	*
Pyruvate	*
Niacinamide	*
Phenyllactate	Biosynthesis of alkaloids derived from ornithine, lysine and nicotinic acid; Metabolic pathways; Phenylalanine metabolism; Tropane, piperidine and pyridine alkaloid biosynthesis

Appendix 8: Metabolic profile of the Bifidobacterium dual-species mix assessed in this study, including those metabolic pathways influenced by each metabolite * For full breakdown of the metabolic pathways influenced by this metabolite, see Appendix 4. ** For full breakdown of the metabolic pathways influenced by this metabolite, see Appendix 5. *** For full breakdown of the metabolic pathways influenced by this metabolite, see Appendix 6.

Metabolite	Pathways influenced
Acetate	*
Alanine	*
Choline	*
Formate	***
Glycine	*
Histidine	*
Isoleucine	*
Lysine	***
Methionine	*
Phenylalanine	*
Tyrosine	*
Valine	*
Xanthine	*
Ethanol	**
Threonine	*
Pyruvate	*
Niacinamide	*